High-throughput discovery of inhibitors for DNA gyrase and DNA topoisomerase VI

James Taylor

Department of Biological Chemistry

John Innes Centre

Norwich

September 2011

This thesis is submitted in partial fulfillment of the requirements of the degree of Doctor of Philosophy at the University of East Anglia

Statement

The work submitted within this thesis is entirely my own, except where due reference has been paid, and has not be submitted to this or any other university as part of any degree.

High-throughput discovery of inhibitors for DNA gyrase and DNA topoisomerase VI

James Andrew Taylor

DNA topoisomerases are important drug targets that have been successfully exploited to produce effective anticancer and antimicrobial agents. Unfortunately the increasing level of antibiotic resistance amongst pathogen strains has diminished the potency of existing antimicrobials. The discovery of novel inhibitors which target DNA topoisomerase would provide the basis for new antimicrobials effective against these resistant strains. However, such research has been limited by the low-throughput nature of traditional assays. Using a novel high-throughput assay I have screened a library of 960 compounds against *Escherichia coli* DNA gyrase and *Methanosarcina mazei* topoisomerase VI. The two novel hits produced from the *E. coli* DNA gyrase screen, mitoxanthrone and suramin, were tested for bactericidal activity against Gram-negative and Gram-positive bacteria. Mitoxanthrone was found to inhibit the growth of the Gram-positive bacteria *Mycobacterium smegmatis* in liquid cultures. Their modes of inhibition were also investigated *in vitro*. Suramin was found to inhibit the enzyme by preventing it from binding to DNA, whilst mitoxanthrone was shown to stabilize enzyme-mediated double-strand breaks (the "cleavage complex"). The screen against *M. mazei* topo VI produced six hits, five of which were novel. The mechanism of these compounds was explored *in vitro* against both *M. mazei* topo VI and *S. shibatae* topo VI, although the exact details proved elusive. The hits from the *M. mazei* screen were tested against *Arbadopsis thaliana* topo VI *in planta* using a morphological screen. One hit, hexylresorcinol, exhibited herbicidal activity and produced a morphology similar to topoisomerase VI knock-out mutations in *Arbadopsis.* In addition, the mechanism of *M. mazei* topo VI was explored revealing that the enzyme strongly binds to DNA in the presence of ATP. It was found that the *M. mazei* enzyme complex is unusually robust; with the subunits remaining associated despite harsh buffer conditions, and appears to be resistant to proteinase K digest. Additionally, the limits of the traditional gel-based topoisomerase assay and the microtitre plate-assay were explored, and the potential for triplex-affinity purification of DNA plasmids was investigated.

Acknowledgments

First and foremost I would like to thank my supervisor Prof. Tony Maxwell for all the support, advice and insight he has provided over the course of this project (as well as generally putting up with me!). I'd also like to thank my co-supervisor Prof. Rob Field for his helpful and down-to-earth comments and advice on the more chemical aspects of the project. I've learned so much from both of you.

I'd like to thank my family, especially my parents, for their continued love and support over the years. You've always believed in me, and that means so much.

Next I would like to thank all my collaborators and those who have contributed towards this work including: Daniel Mitrovic for his assistance with the triplex-affinity purification of DNA; Dr Kevin Corbett and Prof. James Berger for supplying the clones for the *M. mazei* topo VI enzyme (University of California Berkley); Danielle Gadelle and Patrick Forterre for providing the *S. shibatae* topoisomerase VI (University of Paris XI, Orsay); August Johansson and Dr Neil Thompson for the AFM imaging (University of Leeds); and Dr Mark Thompson for providing experimental antimalarial compounds (University of Sheffield).

I'd like to thank all the mentors I've had over the years. In particular I'd like to thank Lesley Mitchenall for her exceptional experimental know-how, Dr Nick Burton for his insights into the microtitre plate assay and baculovirus expression (amongst other things), Martin Stocks for his practical outlook and being on my supervisory committee, Nicola Stacey for training and advice with the *Arabidopsis* work, Dr Matthew Burrell for initial training on the microtitre plate-based assay, Dr Richard Bowater and Prof. Julea Butt for early encouragement, Dr Martin Rejzek for help with the Microsource Library and Dr Sandra Grieve for her inspirational pep-talks. In addition I'd like to thank all members of the Maxwell Group and Inspiralis Ltd., past and present, for help and insights.

Lastly I'd like to thank all my friends who have stood by during this time. In particular I'd like to thank Daniel Mitrovic and Stacey Price for being exceptional house-mates, Grant Howitt and Mary Hamilton, Fay Ikin and Hannah Powell-Smith, Lauran Wheaton, and Lizzy Townsend. I'd also like to thank the other denizens of the student office: Stuart King, Tracey Holley, Dr Karl Syson, Dr Fredric Collin, Dr Marcus Edwards and Farzana Miah for fruitful conversations and generating a positive working environment.

Abbreviations

ADP	Adenosine 5'-diphosphate
ADPNP	5’-Adenylyl β,γ-imidodiphosphate
ATP	Adenosine 5'-triphosphate
bp	Base pairs
BSA	Bovine serum albumin
CARE	Continuous affinity recycle extraction
DMSO	Dimethyl sulfoxide
DNA	Deoxyribonucleic acid
dsDNA	Double stranded DNA
dNTP	Deoxyribonucleoside 5'-triphosphate
DTT	Dithiothreitol
EDTA	Ethylenediaminetetraacetic acid
FCS	Foetal calf serum
G segment	DNA gate segment
GyrA	Gyrase subunit A
GyrB	Gyrase subunit B
IPTG	Isopropyl-β-D-thiogalactopyranoside
kb	Kilobases
kDa	KiloDaltons
LDH	Lactate dehydrogenase
Lin.	Linear DNA plasmid
M	Molar
MRSA	Methicillin resistant *Staphylococcus aureus*
NADH	Nicotinamide adenine dinucleotide
MmT6	*Methanosarcina Mazei* topoisomerase VI
MOI	Multiplicity of Infection

OAc	Acetate
OC	Open-circular DNA plasmid
P1/P2	Viral titre from passage 1 or 2
PCR	Polymerase chain reaction
PEP	phosphoenolpyruvate
PfTopo6A1	Hypothetical *Plasmodium falciparum* topoisomerse VI subunit A (*PF10_0412*)
PfTopo6A2	Hypothetical *Plasmodium falciparum* topoisomerse VI subunit A (*PFL0825c*)
PfTopo6B	Hypothetical *Plasmodium falciparum* topoisomerse VI subunit B (*MAL13P1.328*)
PK	pyruvate kinase
RNA	Ribonucleic acid
SC	Supercoiled DNA plasmid
SEM	Scanning electron microscopy
SDS	Sodium dodecyl sulphate
PAGE	Polyacrylamide gel electrophoresis
Tm	DNA melting point
TF buffer	Triplex Forming buffer
T segment	DNA transfer segment
Topo	Topoisomerase
Tris	Tris(hydroxymethyl)aminomethane
U	Units of enzyme
v/v	Volume per volume
w/v	Weight per volume

Table of Contents

List of Figures

List of Tables

List of Equations

This thesis is dedicated to my parents.

Your faith in me is what has made this all possible.

"Nothing in life is to be feared. It is only to be understood."

Attributed to Marie Curie (1867-1934)

Chapter 1

General Introduction

1.1 Infectious diseases, antibiotics and the problem of antibiotic resistance

The development of antibiotics is one of the greatest achievements of medical science, responsible for saving the lives of countless people over the last sixty years. When penicillin was first manufactured in 1944 its speed and efficiency at curing previously fatal infections caused people to view it with awe and led to it being termed a "wonder drug". Even though it is disputed that Dr. William H. Stewart, the US Surgeon General 1965-1969, actually made his now infamous pronouncement that "It is time to close the book on infectious diseases, and declare the war against pestilence won" the statement certainly captured the attitude of the times (Spellberg, 2008).

This level of optimism seems absurd these days with antibiotic resistant strains of bacteria such as *Staphylococcus aureus* generating apocalyptic headlines about the rise of "superbugs". Although these articles are laden with hyperbole, the emergence of these resistant strains is a significant threat to public health. The emergence of *S. aureus* strains resistant to the penicillin derivative methicillin (MRSA) was reported soon after the introduction of the drug in 1960 (Eriksen, 1961). By the late 1960s strains resistant to multiple antibiotics had evolved (Grundmann et al, 2006). It has been demonstrated that patients infected with these resistant strains have significantly increased mortality and morbidity rates than those afflicted with antibiotic susceptible strains (Kock et al, 2010). In the last two decades the number of infections reported to be caused by MRSA has increased rapidly, although has begun to drop in recent years (Figure 1.1). This is most likely due to improved awareness and hygiene (although a more sceptical view is that the disease is now being under-reported to

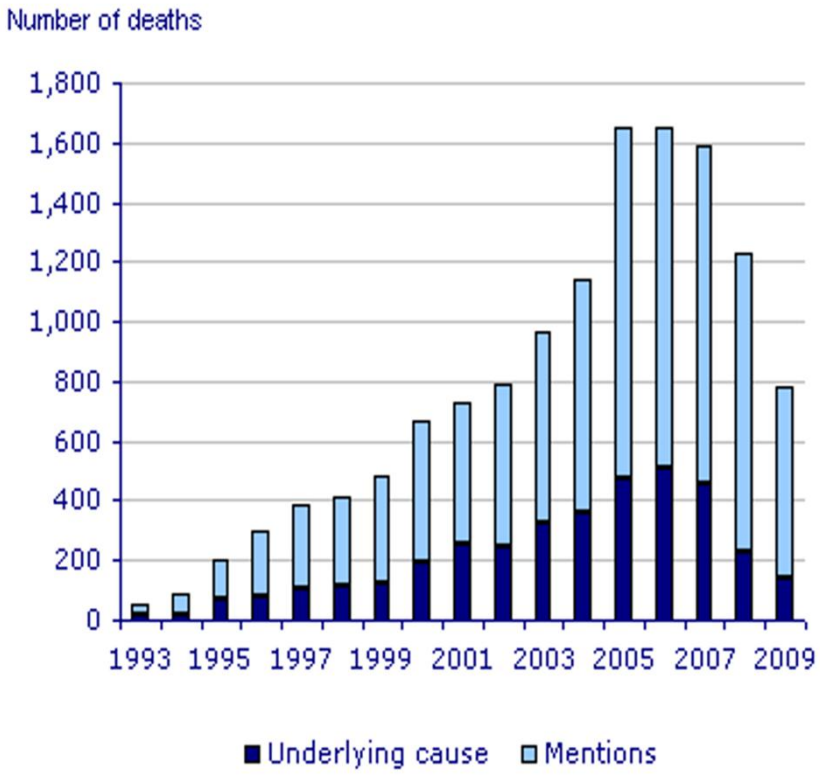

Figure 1.1 The number of deaths attributable to MRSA in the UK. Figure from the National Statistics Department website (www. statistics.gov.uk).

improve hospital statistics). Although *S. aureus* has been focused on here antibiotic resistance is also a problem for arguably more threatening diseases such as tuberculosis, which was thought to have infected a third of the world's population and been responsible for around 2 million deaths in 2009 (WHO 2010 report). The evolution of both multidrug-resistant *Mycobacterium tuberculosis* (resistant to one of two potent front line drugs) and extremely-drug resistant *M. tuberculosis* (resistant to several front-line and second-line drugs) is causing significant difficulties in treating this highly lethal disease. Nor is the development of drug resistance restricted to bacterial diseases, with the emergence of drug resistant strains of the malaria causing protozoa *Plasmodium falciparum*. Malaria was thought to infect around 200 million people and kill approximately one million in 2009 (WHO 2010 report). Unfortunately several parasite strains have evolved which are resistant to some of the most commonly used and potent antimalarials (Farooq & Mahajan, 2004).

The public and professional misuse of antibiotics has been pivotal to the evolution and spread of these resistant strains of these pathogens (Rice, 2003). Self-prescription, mis-prescription and over-prescription have exposed various human pathogens to sub-lethal levels of antibiotics. This has generated the selective pressure necessary for the evolution of resistant strains. Resistance puts its own fitness burden on strains bearing it, which in turn selects for compensatory mutations. The end result of these processes is the rapid evolution of stable resistant strains which will persist long after the misuse of antibiotics is curtailed (Andersson, 2003; Levy, 1998; Projan, 2007). It is clear that although better management of how antibiotics are used and improving public awareness are very important they will do very little to help against existing resistant strains.

New antibiotics with novel modes of action to which these strains are susceptible are necessary if we wish to keep our lead in the "war on pestilence". However the number of new antimicrobials has been decreasing steadily over the last few decades (Figure 1.2). This is due to a number of

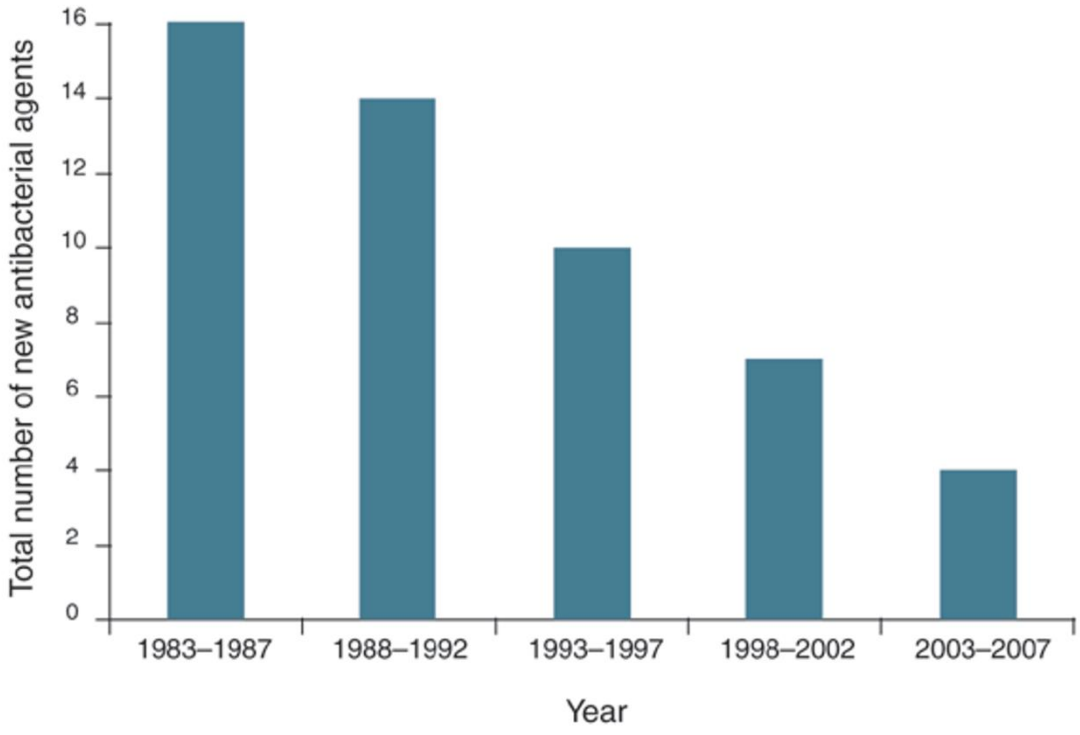

Figure 1.2 The number of antibacterial agents approved by the USA FDA. Figure from Fox, 2006 and Spellberg et al, 2004.

factors including the high attrition rate for antimicrobial drugs in high-throughput screens (which are about five-fold higher than similar screens for other diseases) and the lack of financial incentive for pharmaceutical companies (high attrition rates, the emergence of resistance, extensive clinical trials and short treatment courses all play their part here) (Payne et al, 2007). This vacuum caused by the withdrawal of the pharmaceutical companies from antibiotic research means that academic institutions and non-profit organisations must rise to meet the challenge of developing new antibacterial agents, preferably in coalition with the remaining industrial researchers in the area.

1.2 Drug screening strategies

The current paradigm for drug discovery is that of high-throughput biochemical or cell-based screening of rational targets, although the benefits of this approach over traditional pharmacological approaches are still debatable due to high attrition rates (Kola & Landis, 2004). This is partly due to increasing restrictions placed on the development of new drugs, but also due to the efficiency of the screening process itself. The overall performance of the screen is determined by the quality of the technology used, the assay optimisation, the data processing and the screened materials (Fischer, 2007).

When screening for anti-infective agents one can either start with a specific target enzyme in mind which you are aiming to inhibit or assay compounds for their ability to kill the pathogen in cell-based assays. If the second approach is used it is common to then identify the target for any hits so that rational improvements can be easily made. Each of these two approaches has their own strengths and weaknesses, and there is no clearly superior strategy (Moore & Rees, 2001). The cell-based approach has pragmatism on its side: compounds which kill the pathogen will be selected by the screen. However there are a host of logistical issues including the maintenance and handling of the pathogen. Unless a non-pathogenic relative is used in the screen then a containment laboratory of the appropriate level is required. Cell-based assays also tend to have high

variability and report more false positives than target based screens. This is due to the difficulty in maintaining consistency of the reagents (i.e. the cells) over the course of the screen, the complexity of the cellular environment and the low level cytotoxic effects of solvents such as DMSO (especially after the extended exposure necessary in many cell-based assays) (Moore & Rees, 2001). Since the success of a screen is as much about statistics as it is about biochemistry this is a significant factor to consider when designing a screen.

Target-based screening on the other hand is much simpler from a logistical stand point: large quantities of reagents can be produced and frozen to ensure consistency over the screen. Furthermore there are significantly fewer variables in a biochemical assay which results in a higher level of consistency. On the other hand there is no guarantee that a powerful *in vitro* inhibitor of a good target will make a successful antimicrobial. This can be for a range of reasons, including the compound not being able to enter the pathogen or the pathogen already possessing export or degradation pathways that target the compound. Target-based screening is simply impossible in some cases where the target cannot be successfully expressed and purified to the quantity and quality needed for screening. In short, neither of these screening strategies are perfect and in reality they are often used in concert (with hits from a cell-based screen being sub-screened against various targets or visa versa).

Until 1996 80% of all medical drugs were derived from or inspired by natural products (Harvey, 2007). Despite this, there has been an increasing aversion to the use of natural products in screening for new drugs (Harvey, 2007). This is because natural products are thought to be too structurally complex to make good drugs (Fischer, 2007). Also, the extensive extraction and purification procedures that are necessary to access natural products is thought not to be compatible with a high-throughput approach (Lam, 2007).

However the success of natural products as leads for drug development cannot be denied and they offer a wealth of screening opportunities. They are highly structurally diverse, have been put under evolutionary pressures to acquire biological activity and often have activity

in a range of species due to protein homology (Harvey, 2007). Most of the natural products discovered thus far have not have had their biological activity tested, and new sources of compounds are constantly being discovered and catalogued (such as from marine organisms and exotic plants) (Harvey, 2007).

Once a natural product with the desired activity has been identified, a combinatorial approach can be taken to further improve effectiveness. This can be rational, such as the addition of nitrogen groups to make the compound more "drug-like" (Lopez et al, 2007) or random to generate a new library which can be screened (Pelish et al, 2001).

An alternative approach to screen novel natural products is to screen existing drugs against new targets. This is appealing for a number of reasons (Chong & Sullivan, 2007): the pharmacokinetics and safety profiles of existing drugs are usually already well understood, and they have often already been approved for use by the regulatory authorities. This bypasses much of the time-consuming clinical trials as well as the much of the toxicological and pharmacokinetic evaluation, which is predicted to reduce the overall cost of production by 40% (DiMasi et al, 2003). Also existing drugs are known to have bioactivity, which greatly increases the chance of finding a biologically relevant inhibitor. This process of finding "new uses for old drugs" has proven successful in the past, as demonstrated by the successful rebranding of the breast cancer drug miltefosine to treat visceral leishmaniasis (Sundar et al, 2002).

1.3 Antimicrobial targets

When screening for antimicrobial agents with a target lead approach one must first choose a target enzyme to screen against. A good target for antimicrobial drugs: is essential for pathogen viability, is present with high homology in several pathogens, has no or low homology to any human enzymes and occurs only as a single copy (Payne et al, 2007). The range of cellular processes that the currently successfully exploited antibacterial targets participate in is relatively limited (Table 1.1). This means that there are only a handful of these well validated targets. Attempts to discern new

targets via a genomic approach have had very little success, which is attributable in part to the difficulty in establishing the link between *in vitro* inhibition of a target and its ability to kill cells *in vivo* (Payne et al, 2007).

As such it is much better to seek out compounds which inhibit a well validated target in novel ways. DNA topoisomerases, in particularly DNA gyrase, have been proven to be incredibly good targets for antimicrobial agents with a wide range of drugs targeting them now in clinical use. This is due in part to them satisfying the criteria for a good target as well as their unique mode of action (as discussed below).

1.4 DNA Topology

DNA topoisomerases are enzymes which are responsible for maintaining the topological state of DNA in the cell (Bates & Maxwell, 2005). As such a brief explanation of DNA topology is necessary before a detailed discussion on their mechanisms can take place.

In relaxed B-form DNA the two strands of the double helix twist around their helical axis once per 10.5 base pairs. By dividing the number of base pairs in a DNA molecule by this value, the number of helical "twists" can be determined. Interactions between proteins and DNA which require unwinding of the helix (such as during replication), can alter this value, which introduces stress into the molecule. In an unrestrained DNA molecule the mobility of the free ends allows this stress to easily dissipate. However

Cellular process	Example target	Example antibiotic
DNA replication	DNA gyrase	Ciprofloxacin
	Topoisomerase IV	
Cell wall synthesis	Lipid II	Ramoplanin
Transcription	RNA polymerase	Rifampicin
Translation	16S rRNA A site	Tetracycline
Fatty acid synthesis	2-*trans*-Enoyl ACP reductase	Triclosan
Cofactor synthesis	Dihydrofolate reductase	Trimethoprim

Table 1.1 Successfully exploited targets for antimicrobials. Adapted from Bumann, 2008.

if the DNA is constrained at either end by existing in a closed-circular form, or by interactions with proteins such as nucleosomes, then the DNA must find another way to relieve strain. It does so by contorting into superhelical turns (also called supercoils or writhe) (Bates & Maxwell, 2005).

This relationship can be described mathematically using the concept of linking number (Lk) (Crick, 1976; Fuller, 1971), which represents the number of times the two strands of closed circular DNA are linked. The linking number of a hypothetical closed circular DNA molecule with no writhe (Lk°) can be calculated with the following equation:

$$Lk^{\circ} = \frac{bp\ length\ of\ DNA}{helical\ turn\ (10.5\ bp)}$$

Equation 1.1 Calculating the theoretical linking number of closed circular DNA.

This number does not have to be an integer, but it is clear that fractional links do not exist in reality. The observed linking number Lk can be obtained by simply rounding of the Lk°. The difference between the hypothetical and observed linking numbers gives an indication of the intrinsic strain inside the molecule:

$$\Delta Lk = Lk - Lk^{\circ}$$

Equation 1.2 Calculating the difference between the theoretical an observed linking number.

Since smaller DNA molecules are less able to distribute this stress than larger ones, ΔLk is often scaled to the size of the DNA by dividing by Lk^{o} (which is determined by the number of base pairs). This gives the specific linking difference or superhelical density (σ):

$$\sigma = \frac{\Delta Lk}{Lk^{\circ}}$$

Equation 1.3 Calculating the specific superhelical density.

The level of superhelical density can be used as an indication of the level of torsional strain, and hence the level of supercoiling, in a molecule. The sign of σ can be either negative or positive which indicates whether the DNA is negatively or positively supercoiled. Referring to the above observations,

the Lk can be related to the number of helical twists (Tw) and the superhelical writhes (Wr) with the following equation:

$$Lk = Tw + Wr$$

Equation 1.4 The relationship between twist, writhe and linking number.

Since Lk is an intrinsic property of restrained DNA, a change in either twist or writhe must result in an equal and opposite change in the other. This also implies that if Lk was to change, then both the twist and the writhe would change to compensate (Figure 1.3). This process can occur if the DNA molecule is broken, and either one or more strands passed through the break or if one strand is broken and rotated about the intact strand. In the cell, these processes are co-ordinated by DNA topoisomerases.

1.5 DNA topoisomerases

1.5.1 Overview

Proper maintenance of a cell's DNA is crucial to the stability of its genome, and hence its survival (Zhivotovsky & Kroemer, 2004). As a result of this a vast array of proteins and enzymes exist to package, repair, and replicate DNA. DNA topoisomerases are a class of enzymes whose function bridges all these processes, as they are responsible for managing the topological state

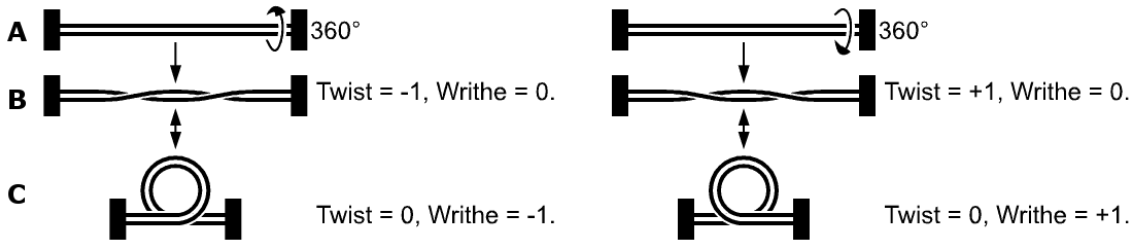

Figure 1.3 The effect in a change in Lk upon the twist and writhe of a restrained DNA molecule. Note the double helix structure of the DNA has been simplified for clarity. The black boxes represent constraints placed upon the DNA, such as those imposed by chromatin or being in a closed-circular form. *A*. A break is formed in one strand and that strand rotated around the intact strand 360°. *B*. Either a negative or positive twist is introduced into the DNA, depending on whether the initial rotation was right-handed or left-handed. *C*. Change in twist converted into an opposite change in writhe. This increases the level of supercoiling in the DNA, and forms either a negative node (writhe -1) or a positive node (writhe +1). Figure adapted from Wheeler, R., 2007, Wikimedia commons.

of DNA. By covalently binding active site tyrosine residues to the phosphodiester backbone of either one or two strands of a DNA helix they produce controlled breaks in the DNA. They then utilise these breaks to unknot, decatenate or alter the supercoiling state of the helix via either strand passage or rotation (Figure 1.4). Topoisomerases are categorised by their mechanism, with type I topoisomerases nicking a single strand whilst type II topoisomerases form double-strand nicks (Bates & Maxwell, 1997). Which of these mechanisms a topoisomerase utilises dictates the range of reactions it can catalyse, for example a type I topoisomerase can only decatenate plasmids if a nick is present in one of the double-strands. As a general rule type I topoisomerases tend to be monomeric, whilst type II topoisomerases are either homodimers (A_2) or heterotetramers (A_2B_2). These categories are further subdivided based on structure and mechanism: IA, IB or IC for type I topoisomerases and IIA or IIB for type II topoisomerase. A summary of the reactions catalysed by specific topoisomerase can be found in Figure 1.5. The specific enzymes used in this study can be found in Table 1.2.

Type	Example enzyme	Ortholog in this study
IA	Bacterial topoisomerase I	N/A
IB	Eukaryotic topoisomerase I	Wheat germ
IIA	DNA gyrase	*Escherichia coli*
IIB	Topoisomerase VI	• *Methanosarcina mazei* • *Sulfolobus shibatae* • *Plasmodium falciparum*

Table 1.2 Examples of each class of topoisomerase and the specific orthologs in this study.

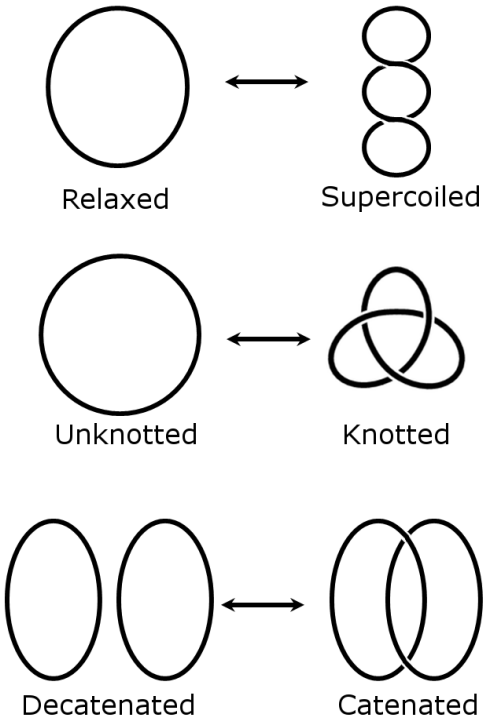

Figure 1.4 DNA topoisomers interconvertible by DNA topoisomerases. The DNA double helix has been simplified to a single line in this diagram.

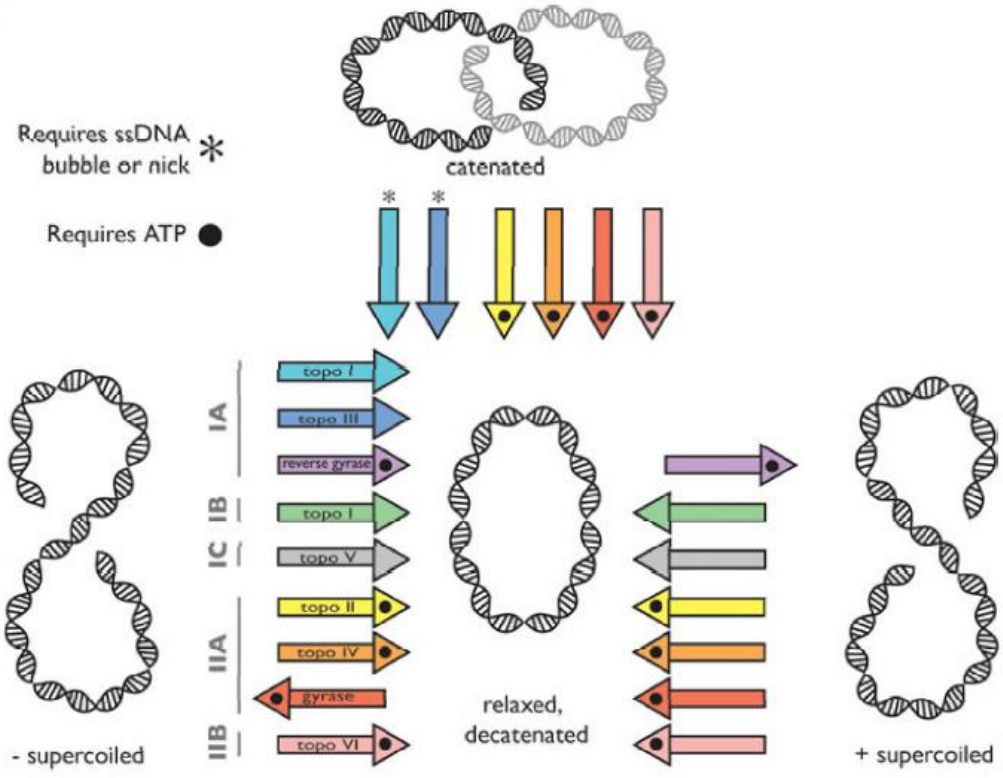

Figure 1.5 Summary of reactions catalysed by specific topoisomerases. Figure from Schoeffler & Berger, 2008.

1.5.2 Type I topoisomerases

Type I topoisomerases can be further subdivided into types IA, IB and IC based on the specifics of their structure and mechanism.

1.5.2.1 Type IA topoisomerases

Type IA topoisomerases have been found in both bacteria and eukaryotes. The majority of type IA topoisomerases are monomeric (Champoux, 2001) and require a divalent magnesium ion as a cofactor for carrying out relaxation (Domanico & Tse-Dinh, 1991). The binding of type IA topoisomerases to a double-stranded piece of DNA results in partial melting of the helix to form a short stretch of single-stranded DNA (Wang, 2002) (Figure 1.6). The topoisomerase then introduces a break into one of the single strands by catalysing reversible transesterfication between its active site tyrosine and the 5'-phosphate of the DNA. The less negatively supercoiled the DNA, the harder it is for the enzyme to unpair the bases to form this single-stranded region (Wang, 2002). This means that the enzyme can only relax the DNA to a certain level. After the nick has been generated the complementary strand is passed through the break into the interior of the enzyme. The nicked strand is then ligated, and the enzyme unbinds. This alters the linking number of the DNA by one (Bates & Maxwell, 2005). If a nick is already present in one of the two strands of a piece of double-stranded DNA it is possible for a type IA topoisomerase to instead pass another double-stranded DNA molecule through the break, allowing it to catenate/decatenate or knot/unknot double-stranded DNA (Wang, 2002).

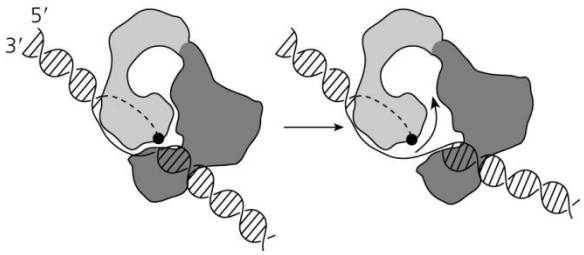

Figure 1.6 The mechanism of action for type IA topoisomerases. The enzyme generates a single strand break by forming a covalent bond between its active site tyrosine and the 5'-phosphate of the DNA backbone. The intact strand is then passed through the break into the central cavity of the enzyme. This results in relaxation of the DNA by a linking number of one. Figure from Bates & Maxwell, 2005.

Interestingly type IA enzymes cannot relax positively supercoiled DNA since they are unable to unpair the helix to produce a single-stranded region. However relaxation of positively supercoiled DNA can occur if a single-stranded loop is present in the molecule (Kirkegaard & Wang, 1985)

Reverse gyrase is an unusual member of this class of enzymes. It is found in hyperthermophilic eubacteria and archaea such as *Sulfolobus acidocaldarius*, in which it was first discovered (Forterre et al, 1985; Kikuchi & Asai, 1984; Nakasu & Kikuchi, 1985), and is the only topoisomerases currently known to introduce positively supercoils into DNA in an ATP-dependent manner (Forterre et al, 1985; Krah et al, 1996; Shibata et al, 1987). It has been proposed that controlled unwinding by a helicase domain present in the enzyme is the cause of the enzymes supercoiling activity (Rodriguez, 2003). The introduction of positive supercoils into the genomes of hyperthermophilic archaea may help stabilize the DNA under the high temperatures at which they live.

Type IA topoisomerase have been found in bacteria but not in humans, fulfilling one of the criteria for a good drug target. However so far they have proven poor targets for antimicrobials. This may be due to redundancy of function within the bacterial cell which typically contains several different type IA topoisomerases and one or more type IIA topoisomerases capable of carrying out similar reactions. This is demonstrated by the fact that bacteria in which the genes for topoisomerase I (topo I), the most prevalent type IA topoisomerase in bacteria, has been knocked out are still viable when grown at 37°C without the need for compensatory mutations (Stupina & Wang, 2005). Since they are not essential for survival one can predict them to be poor antimicrobial targets, a hypothesis reinforced by the historic absence of drugs targeting them. Current research into type IA topoisomerases as drug targets focuses on stabilizing the covalent protein—DNA intermediate otherwise known as the "cleavage complex", an aim which will be assisted by the recent crystal structure of the intact complex (Zhang et al, 2011). Bacteria containing mutations which lead to the accumulation of topo I cleavage complexes have been shown to have reduced viability, displaying SOS responses and

cell death (Tse-Dinh, 2009). Whether compounds can be found to replicate the effects of these mutations remains to be seen.

1.5.2.2 Type IB topoisomerases

Type IB topoisomerases are distinct from type IA topoisomerases in both their structure and mechanism. They are largely found in eukaryotes but have also been observed in viruses and archaea. Unlike type 1A, type 1B topoisomerases form a covalent bond between their active site tyrosine and the 3'-phosphate of the DNA (Wang, 2002). Unlike the type IAs they do not need to melt the DNA duplex in order to relax it, and as such their activity is not dependent on the supercoiling state of their substrate (Champoux, 2001). Furthermore they do not require magnesium ions to cleave DNA and can relax both negative and positive supercoils (Champoux, 2001). The reason for these dramatic differences is that they do not facilitate relaxation by strand passage but by a "controlled rotation" mechanism (Stewart et al, 1998) (Figure 1.7). The two domains of the enzyme form a clamp around the DNA, completely encircling it (Champoux, 2001). After generating a single strand break by the formation of a covalent bond between its active site tyrosine and a phosphate in the DNA backbone the enzyme loosens its "grip" on the 5'-OH end of the broken strand. The broken strand is then free to rotate around the intact strand before being religated.

Since the type IB topoisomerases are found in humans and not bacteria they are useless as antimicrobial targets. They may have some mileage as an antiviral or antiprotozoal target, but it would be expected that any such compounds would have significant cross-reactivity with the human

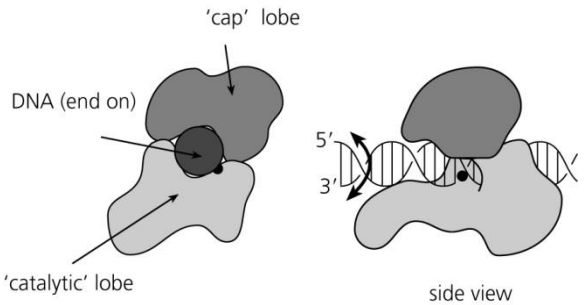

Figure 1.7 The mechanism of action for type IB topoisomerases. The enzyme clamps around the DNA double helix and makes a single-strand break by forming a covalent bond between its active site tyrosine and the 3'-phosphate of the DNA backbone. It then allows "controlled rotation" of the 5'–hydroxyl side of the break before religation, resulting in relaxation. Figure from Bates & Maxwell, 2005.

enzyme. Currently human topo IB is used as a target for anticancer drugs such as camptothecin (Ulukan & Swaan, 2002; Wethington et al, 2008).

1.5.2.3 Type IC topoisomerases

Currently the only member of the type IC class of topoisomerases is topoisomerase V from the hyperthermophilic archaea *Methanopyrus kandleri* (Slesarev et al, 1993). Its mode of action is thought to be similar to that of the type IB topoisomerases. However it also possesses the ability to repair abasic regions in DNA, making it unique amongst the topoisomerases (Belova et al, 2001). Since the only reported type IC topoisomerase belongs to a non-pathogenic microbe it is not a viable target for therapeutics.

1.5.3 Type II topoisomerases

Type II topoisomerases are subdivided into type IIA and type IIB based on structural and mechanistic differences. Unlike different subtypes of the type I topoisomerases the reaction catalysed by type IIA and type IIB topoisomerases is very similar: the passage of one intact double-stranded DNA molecule through a double-strand break (Berger et al, 1996; Bergerat et al, 1994; Corbett et al, 2007; Roca & Wang, 1994). Type II topoisomerases are amongst the widest distributed class of enzyme being essential in all organisms currently known (Gadelle et al, 2003).

1.5.3.1 Type IIA topoisomerases

All type IIA topoisomerases possess two domains crucial for their activity: a DNA breakage-reunion domain and an ATPase domain. In eukaryotes these domains occur within a single subunit whilst prokaryotic enzymes split them between two subunits (A and B respectively). Eukaryotic enzymes therefore operate as symmetrical homodimers whilst the prokaryotic enzymes form symmetrical heterotetramers (A_2B_2) (Figure 1.8).

The active site tyrosines are located on the A subunit (or the equivalent region of the eukaryotic homologue) within a 5Y- catabolite activator protein-like (CAP) domain, but the DNA breakage-reunion domain itself is spread across both the A and B subunits. This means that DNA

cleavage can only take place when the whole complex is assembled (Champoux, 2001; Corbett & Berger, 2004).

The toprim (topoisomerase-primase) domain is common to types IA, IIA and IIB of topoisomerases as well as bacterial primases (Aravind et al, 1998; Corbett & Berger, 2004). The domain contains a conserved glutamate thought to be important for religation of the DNA break in topoisomerases or nucleotide polymerisation in primases, as well as two aspartates necessary for coordinating the Mg^{2+} necessary for the activity of these two classes of enzyme (Aravind et al, 1998).

The GHKL ATPase domain is located on the B subunit (or equivalent region for eukaryotic homologues) and contains an ATP-binding Bergerat fold (Bergerat et al, 1997; Dutta & Inouye, 2000). Although there appears

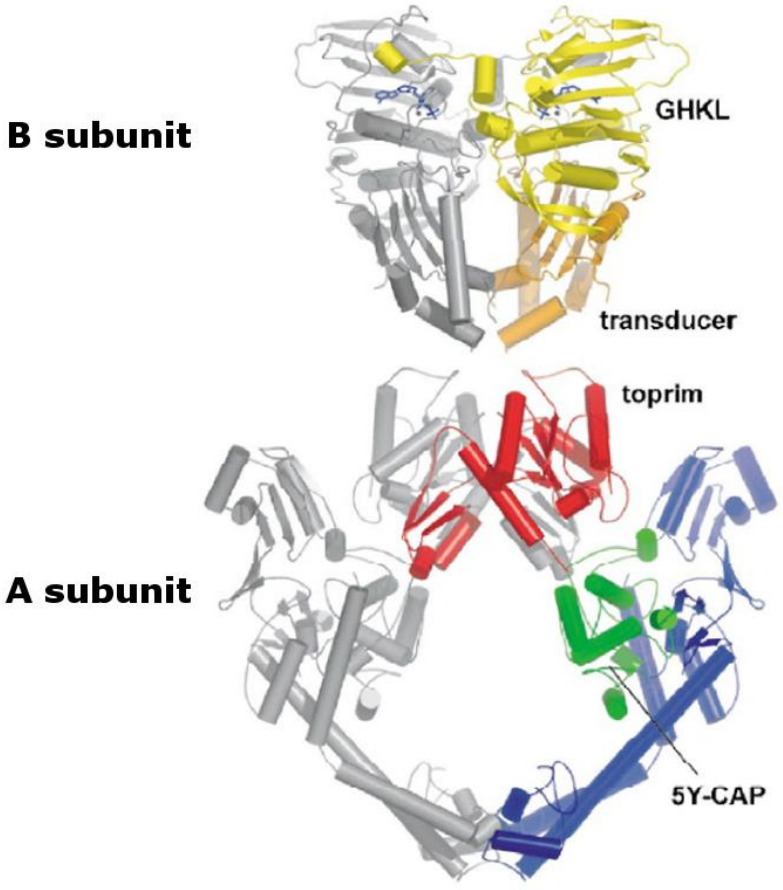

Figure 1.8 The general structure of type IIA topoisomerases. The domains which comprise the A and B subunits of bacterial enzymes are indicated. The domains are coloured as follows: *yellow*, GHKL domain; *orange*, transducer; *red*, toprim; green 5Y-CAP. Figure from Corbett & Berger, 2004.

to be a considerable degree of variation in the sequence of this region between type IIA topoisomerases there is a high degree of structural similarity, particularly in respect to the Bergerat fold (Dutta & Inouye, 2000).

The C-terminal domains of the A subunits of type IIA topoisomerases (or their equivalents in eukaryotic homologues) have little homology with one another and are believed to be important for substrate recognition, cellular targeting and interactions with other proteins (Champoux, 2001).

The activity mechanism of type IIA topoisomerases can be described as proceeding by a "three-gate" mechanism in which it binds two segments of DNA (Figure 1.9). The reaction cycle begins when the enzyme binds the first DNA segment (the G or gate segment) in its DNA breakage-reunion domain. The G segment can be acutely bent by the enzyme, with an angle

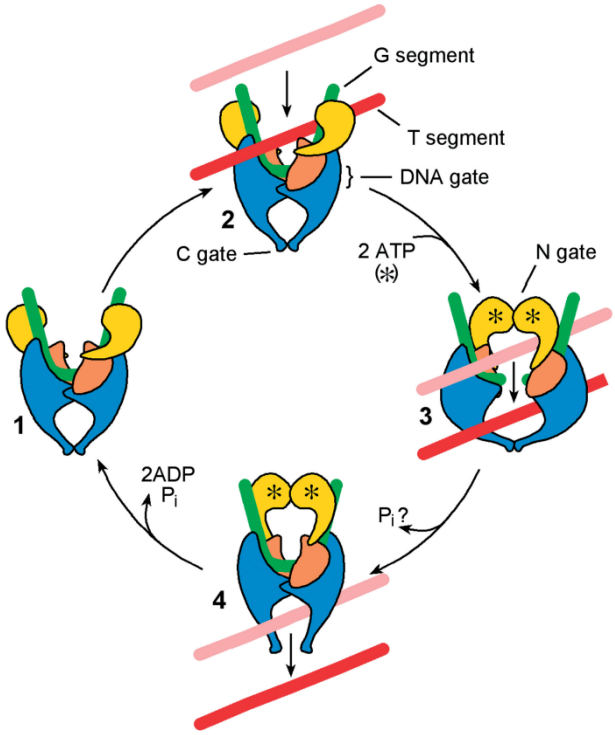

Figure 1.9 The mechanism of action for type IIA topoisomerases. The different domains of the protein are coloured as follows: *yellow*, ATPase domain (B subunit N-terminus in prokaryotic enzymes); *orange*, B subunit C-terminus (or homologous region in homodimeric eukaryotic enzymes); *blue*, A subunit N-terminal breakage-reunion domain (or homologue). The C-terminal domain of the A subunit is not shown. The G-segment (*green*), T-segment (*red*/*pink*) and the DNA, N- and C-gates are indicated. Movement of the T-segment is shown from the pink to the red position. Figure from Bates et al, 2011.

up to 150° (Dong & Berger, 2007). At this point the active site tyrosines can cleave the G segment by forming covalent bonds with the 5'-phosphate groups of the DNA backbone, generating a controlled double-strand break with a 4 base pair stagger (Sander & Hsieh, 1983). However the two ends of the break are held in close proximity, allowing for religation. The second segment (the T or transported segment) then enters the upper cavity of the enzyme. The T segment is then trapped by the ATP-induced dimerisation of the N-terminal domains of the B subunit forming the first of the three gates (the N gate). At the same time conformational changes brought about by ATP binding cause two sides of the double strand break in the G segment to be pulled apart (the DNA gate). The T segment is then passed through the open DNA gate, a process thought to be stimulated by narrowing of the upper cavity. The DNA gate then closes and the final gate formed by a protein interface of the A subunits (the C gate) opens to allow the exit of the T segment (Roca et al, 1996; Roca & Wang, 1994; Williams & Maxwell, 1999b). ATP hydrolysis allows the enzyme to reset ready for subsequent rounds of reaction. This reaction results in either the linking number of the DNA changing by two if the G- and T-segments are in the same molecule (and an increase or decrease in supercoiling), or decatenation/catenation if the G and T segments are on different DNA molecules (Bates & Maxwell, 2005).

The essential nature of the type IIA topoisomerases makes them appealing drug targets. Furthermore, the stabilization of the protein—DNA intermediate (the "cleavage complex") by compounds is exceptionally lethal in cells. This is because the stalled complexes act as "roadblocks" for replication machinery. The collision between a replication fork and a stabilized cleavage-complex results in the formation of a double-strand DNA lesion, the accumulation of which rapidly leads to cell death (Drlica & Zhao, 1997). The up-regulation of the human topoisomerase II in cancer cells has lead to its successful use as an anticancer drug target. Serendipitously, bacteria possess a unique type IIA topoisomerase which is absent in humans: DNA gyrase. DNA gyrase is one of the most successfully exploited antimicrobial targets known so far, and its structure, mechanism and inhibitors will be discussed in detail in a later section of this chapter.

1.5.3.2 Type IIB topoisomerase

Type IIB topoisomerases catalyse a very similar reaction to the type IIA topoisomerases, but have significant structural and mechanistic differences. Most strikingly they only have two gates, lacking the C gate found in type IIAs (Corbett et al, 2007). Since topoisomerase VI is the only known member of this class, the structure and mechanism of the type IIB topoisomerases will be discussed in detail in the section below.

1.6 Topoisomerase VI

Topoisomerase VI (topo VI) is the only known member of the type IIB topoisomerases and has primarily been found in archaea, which are largely thought to be non-pathogenic. Consequently there have been relatively few studies of its structure and mechanism compared to the type IIA topoisomerases. Topo VI was first characterised from the thermophilic archaea *Sulfolobus shibatae* (Bergerat et al, 1997) and the majority of studies on the mechanism and structure of topo VI have been carried out on the *S. shibatae* enzyme. The topo VI from the methanogenic archaea *Methanosarcina mazei* has also been documented, but studies on this version of the enzyme have been limited and primarily focused on its structure (Corbett et al, 2007).

Although no pathogenic archaea have been identified so far, they are present in the human body. In particular methanogenic archaea have been found in the human gut, vagina and mouth (Belay et al, 1988; Belay et al, 1990; Eckburg et al, 2005). Studies have linked methanogenic archaea with the formation of periodontal tooth cavities (Lepp et al, 2004) as well as host of intestinal diseases including: Crohn's disease, irritable bowel syndrome, colorectal cancer, diverticulosis, and obesity (Nakamura et al, 2010; Roccarina et al, 2010). Although the role of these archaea in these diseases is far from clear (and hotly disputed) the existence of pathogenic archaea is an interesting possibility. If their role in these diseases is confirmed antimicrobials targeting methanogenic archaea will suddenly become medically relevant, since topo VI appears to be the main type II

topoisomerase in many archaea (Gadelle et al, 2003) which in turn makes it a good drug target.

Topo VI has also been identified in some eukaryotes including plants, such as *Arabidopsis* thaliana (Hartung et al, 2002; Hartung & Puchta, 2000), and genes hypothetically encoding for its subunits have been discovered in the genome of the malaria parasite *Plasmodium falciparum* (Aravind et al, 2003). These include two genes with homology for the topo VI A subunit (*PF10_0412,* abbreviated to PfTopo6A1; *PFL0825c,* abbreviated to PfTopo6A2) whilst one gene had homology for the topo VI B subunit (*MAL13P1.328*, abbreviated to PfTopo6B). Since it is absent in humans, validation of its presence in *P. falciparum* could lead to topo VI being a novel target for anti-malarial drugs.

Inhibitors of the plant version of the enzyme may find uses as herbicides, as resistant strains have emerged for the most heavily used commercial herbicide glyphosate (Owen & Zelaya, 2005). One of the major reasons for the development of resistant weeds has been the lack of commercially viable alternatives to glyphosate, which is due to the lack of research and development in the area (Owen & Zelaya, 2005). Novel herbicides would provide farmers with alternatives to glyphosate and so elevate the selective pressure for resistant strains to develop. The development of herbicides has a different set of concerns compared to anti-infectives including: cost of large scale spraying, environmental impact and the development of crops resistant to the herbicide. Since knockout mutants of topo VI in *Arabidopsis thaliana* have demonstrated severe dwarfism and do not live past five weeks it is likely a good target for herbicides (Hartung et al, 2002; Sugimoto-Shirasu et al, 2002).

The potential for topo VI to serve as target for a range of medically and commercially useful compounds, as well as the relatively small body of research on it, make it an interesting candidate for inhibitor screening.

1.6.1 Biological roles of topoisomerase VI

In archaea topo VI is thought to fulfil a similar role to the type IIA topoisomerases (which they often lack) (Gadelle et al, 2003): the regulation of the global level of supercoiling within the cell and the resolution of catenated DNA molecules during replication. During the replication of constrained DNA molecules (such as plasmids or genomic DNA) it is necessary for the DNA helix to be unwound (Postow et al, 2001). This causes positive and negative supercoils to be generated either side of the replication fork, which if not resolved result in a breakdown of the replication machinery. Additionally, when two replication forks converge catenated DNA can be formed if the daughter molecules are inter-wound, which can be lethal for the cell (Figure 1.10) (Wang, 1996). In *E. coli* this problem is resolved by a type IIA topoisomerase called topoisomerase IV, which if inactivated results in an increased amount of catenated DNA (Adams et al, 1992). Although these observations have all been carried out with type IIA topoisomerases in bacteria it is likely they hold true for topo VI due to the similarities between their mechanisms and the ubiquitous nature of these problems.

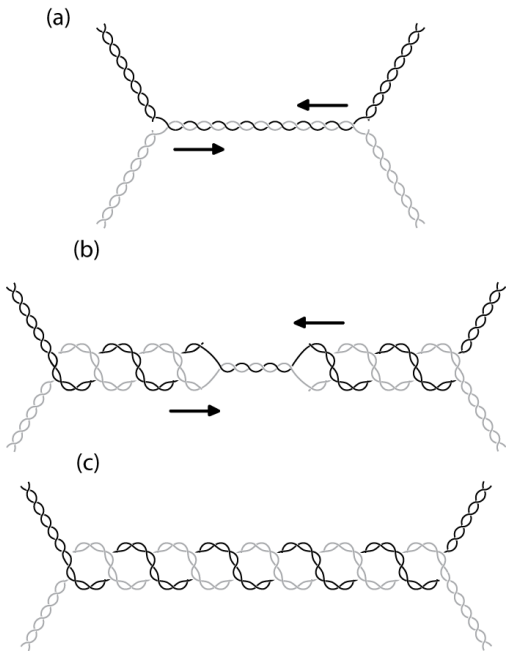

Figure 1.10 The formation of catenated DNA during termination of replication. At the terminus of replication, converging replication forks (a), lead to the interwinding of daughter molecules and the formation of pre-catenanes (b). Upon completion of replication, the products are catenated DNA circles (c). Figure from Bates & Maxwell, 2005.

The only direct evidence for the biological role of topo VI in archaea has come from the inhibition of *Haloferax volcanii* growth by the topo VI inhibitor radicicol (Gadelle et al, 2005). As well as general inhibition of growth the archaeal cells were seen to grow much larger than normal, which may be indicative of replication without cell division. This would in turn imply that the genomes of the cells were catenated, which would be expected from topo VI inhibition if decatenation was a main role of the enzyme *in vivo*.

There is considerably more evidence for the role of topo VI in plants, although the enzyme is yet to be expressed in an active, soluble form. Knock-out mutations of the genes encoding for either *Arabidopsis* topo VIA or VIB subunits (Figure 1.11) results in plants with an extreme dwarf phenotype, yellowish leaves, reduced trichome ("leaf hair") size and reduced root hair size and frequency (Hartung et al, 2002; Sugimoto-Shirasu et al, 2002). These plants die after 4-5 weeks of growth, which indicates the essential nature of topo VI in plants. The cells of these plants demonstrated an increased number of chromosome breaks, which supports the hypothesis that topo VI is involved with the resolution of catenanes during replication (Hartung et al, 2002). Furthermore, the cells demonstrated reduced cell size and a reduction in ploidy (chromosome number) (Hartung et al, 2002; Sugimoto-Shirasu et al, 2002). Plant cells are capable of adopting an alternative cell cycle called endoreduplication in which genome replication occurs but cell division does not, resulting in an increase in ploidy (Sugimoto-Shirasu & Roberts, 2003). This, through unknown mechanisms, leads to an increase in the size of the cell cytoplasm and therefore overall cell size. The inability of these mutants to induce high ploidy (above eight chromosome copies, or 8C) implies that topo VI is essential in the process of endoreduplication.

As well as the A and B subunits, three other proteins are thought to be part of the plant topo VI complex: BIN4, MIGET and RHL1 (Breuer et al, 2007; Kirik et al, 2007; Sugimoto-Shirasu et al, 2005). All three of these proteins have been shown to interact with the topo VI subunits by yeast-two-hybrid experiments and produce identical morphologies when inactivated to the subunit knock-out mutants. Furthermore, the double

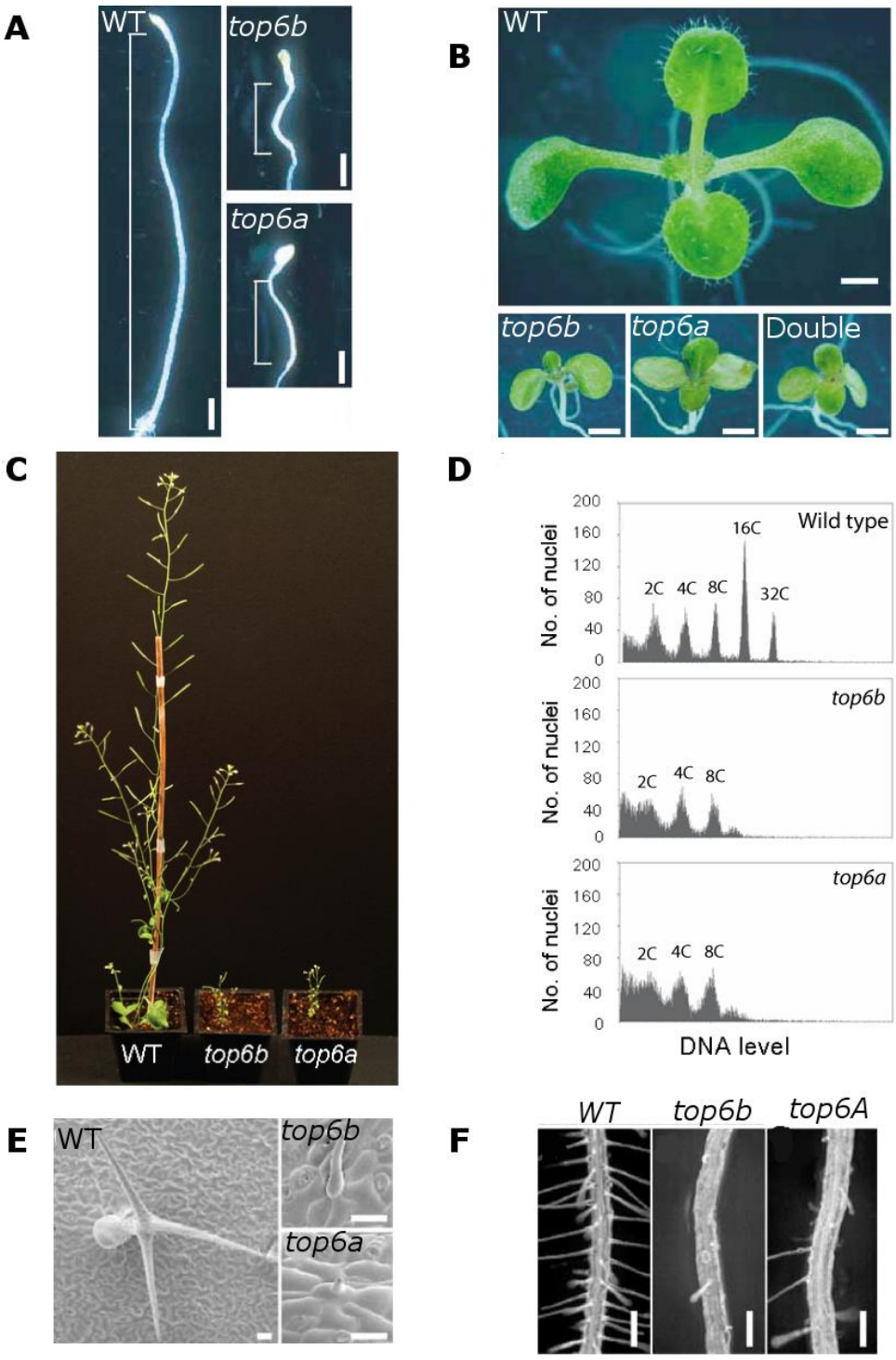

Figure 1.11 The morphology of topo VI knock-out mutants. Morphologies of wild-type (WT), topo VI A subunit knock-out (*topo6a*), topo VI B subunit knock-out (*topo6b*), or double knock-out shown. *A*. 7 day old dark-grown seedlings (hypocotyls indicated). *B*. 7 day old light-grown seedlings. *C*. 30 day old plants: mutants are only 10% of wild-type size. *D*. Mutants are unable to increase ploidy above 8C. *E*. Trichome of mutants smaller. *F*. Root hairs of mutants smaller and less frequent. Both trichomes and root hairs are single cells, so the size of these organs is directly linked to cell size. Figure adapted from Sugimoto-Shirasu et al, 2002.

knock-out mutants of the genes coding for these proteins and either of the topo VI subunits produced no additional characteristics. The role of these proteins is not known, but they are thought to play crucial roles in the regulation of topo VI activity.

Although the presence of topo VI is yet to be confirmed in *Plasmodium falciparum* the biology of the parasite lends credibility to the idea. As part of the parasite's life cycle it undergoes a process called schizogony, which bears similarities to endoreduplication in plants (Figure 1.12). During the process of schizogony the parasite replicates its genome several times without cell division before budding daughter cells (Gantt et al, 1998; Sturm & Heussler, 2007). Since this step is a crucial part of the parasite's life cycle, with several current antimalarial drugs thought to target it (Chauhan & Srivastava, 2001), it is likely that topo VI would make a good target if it was essential for this process.

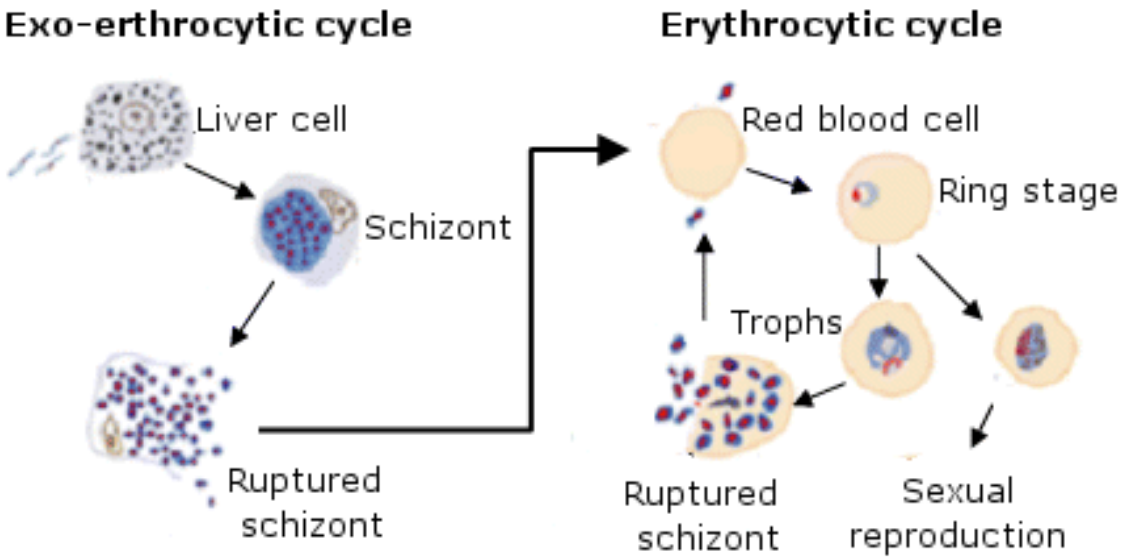

Figure 1.12 Schizogony in the *Plasmodium* life cycle. *Plasmodium* cytoplasm shown in blue and nuclei in red. Multiple rounds of genome replication occur during the schizont step without cell division. This is followed by rapid budding of mature parasites and rupturing of the host cell, leading to further proliferation of the pathogen. Figure adapted from Tuteja, 2007.

1.6.2 Topoisomerase VI structure

Topo VI has been shown to be a symmetrical heterotetramer of two A and two B subunits (Figure 1.13). The B subunits of type IIA and type IIB topoisomerases are highly structurally related, and appear to share the same function in both type II subfamilies (Corbett & Berger, 2003) whereas the A subunits are only partially homologous (Corbett et al, 2007; Nichols et al, 1999). Unlike the type IIA topoisomerases crystal structures of the entire A_2B_2 complex have been solved for the *S. shibatae* (Graille et al, 2008) and *M. mazei* (Corbett et al, 2007) orthologues of topo VI, both with a resolution of ~4 Å. These two structures appear to have captured the enzymes in different conformations, giving insight into the motions of topo VI during its reaction cycle (Figure 1.14 and Figure 1.15). In addition, a number of high-resolution structures have been solved for domains of the two subunits including: the DNA-binding core of the A subunit of

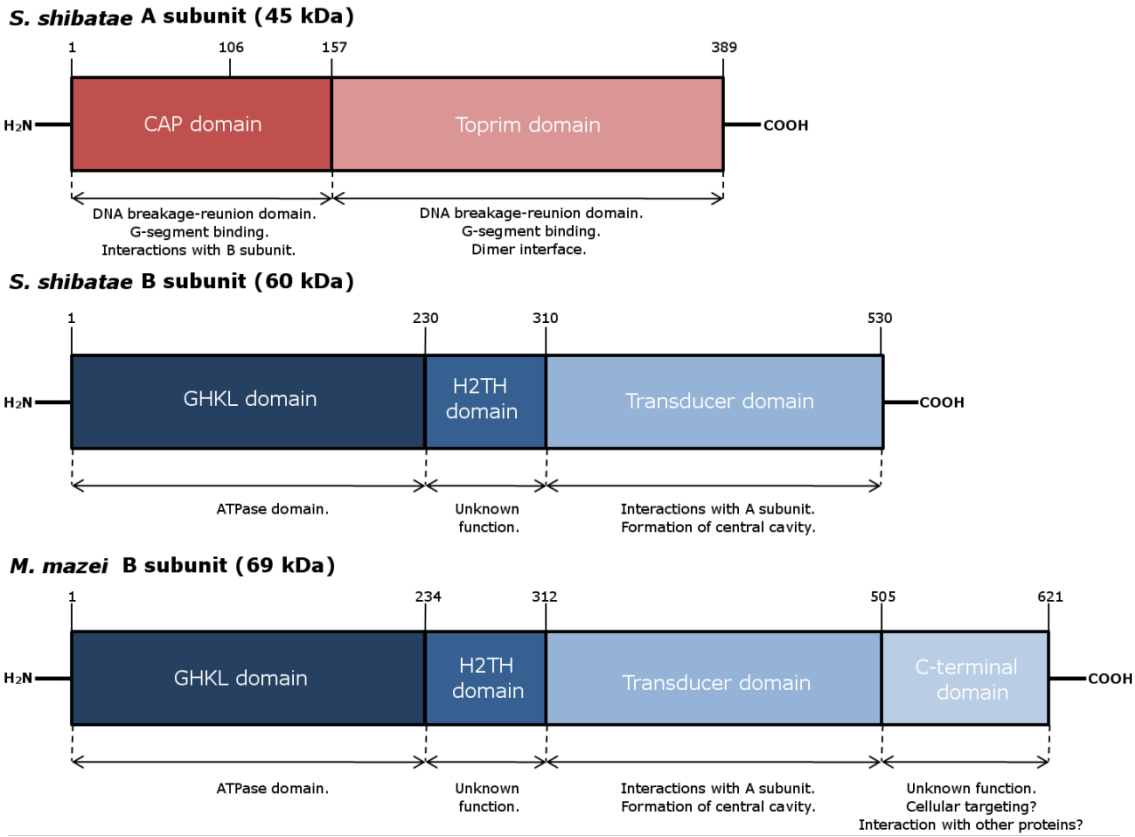

Figure 1.13 The domain structure of *S. shibatae* and *M. mazei* topo VI subunits. The A subunit consists of a CAP domain containing the active site tyrosine 106 and a toprim domain. The domain structure of the A subunit is identical for the *M. mazei* ortholog. The B subunit consists of the GHKL ATPase domain, a helix-two-turn-helix domain and a transducer domain. The *M. mazei* ortholog also has a C-terminal domain of unknown function.

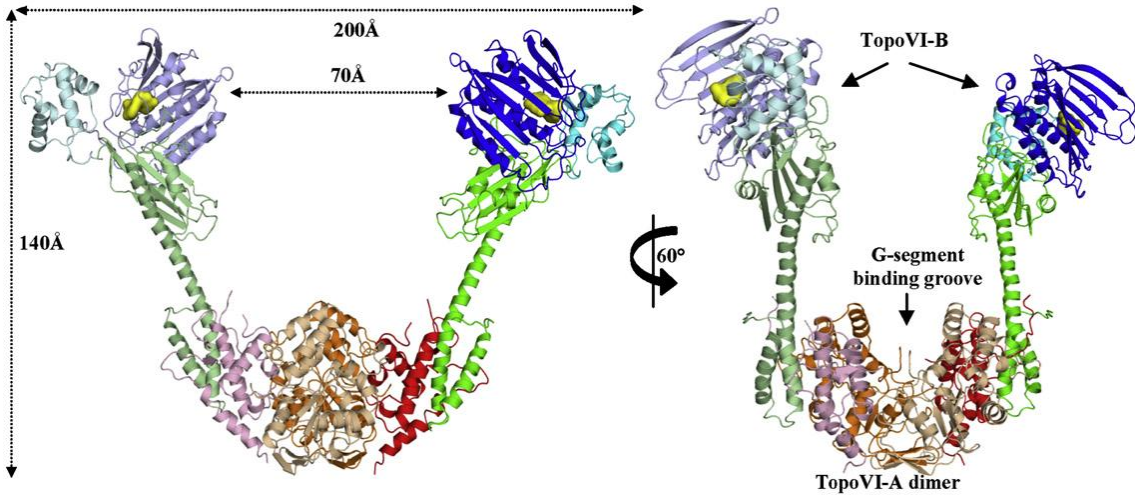

Figure 1.14 The structure of *Sulfolobus shibatae* topo VI. Two different views of the enzyme are shown. B subunit: *dark blue*, GHKL ATPase domain; *light blue*, H2TH domain; and *green*, transducer domain. A subunit: *red*, WHD/CAP; and *orange*, toprim and scaffold domain. The ATP-binding pocket of both B subunits is coloured light blue; dotted circles represent the proposed binding sights for G- and T-segment DNAs. Figure taken from Graille et al, 2008.

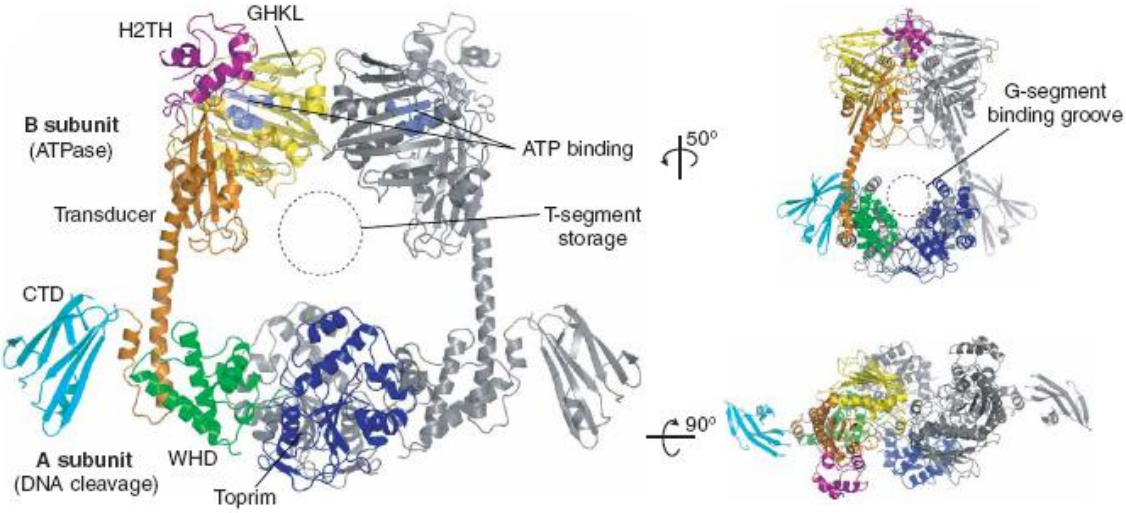

Figure 1.15 The structure of *Methanosarcina mazei* topo VI. Three different views of the enzyme are shown. One A-B dimer is shaded grey whilst the other is coloured as follows. B subunit: *yellow*, GHKL ATPase domain; *purple*, H2TH domain; *orange*, transducer domain; and *cyan*, CTD. A subunit: *green*, WHD/CAP; and *blue*, toprim and scaffold domain. The ATP-binding pocket of both B subunits is coloured light blue; dotted circles represent the proposed binding sights for G- and T-segment DNAs. Figure taken from Corbett et al, 2007.

Methanococcus jannaschii topo VI (Nichols et al, 1999) and residues 1-470 of the B subunit of *S. shibatae* topo VI (Corbett & Berger, 2003). All together these structures give an impressive level of detail about the architecture of the topo VI enzyme.

The A subunit is comprised of a CAP-like domain (also called a winged-helix domain, or WHD) and a toprim domain both of which are present in type IIA topoisomerases but in different arrangements (Nichols et al, 1999). The catalytic tyrosine is located in the CAP-like domain and forms the main point of contact with the B subunit. The toprim domain contains the conserved acidic residues necessary for the binding of Mg^{2+} which are positioned so that they form the "DNA cleavage-reunion" site with the active site tyrosine (Nichols et al, 1999). Positively charged residues in both these domains form a 20 Å DNA binding saddle when the A subunit is dimerised (Corbett et al, 2007; Graille et al, 2008). The CAP-like domain of the *M. mazei* enzyme is thought to contain a disordered loop which may reach into the saddle and interact with the G-segment (Corbett et al, 2007). The most striking difference between the A subunit of topo VI and that of the type IIA subunits is the absence of the second dimer interface which makes up the C-gate in the type IIAs and the cavity it causes.

The B subunit is comprised of three core domains: the GHKL ATPase domain, the helix-two-turn-helix (H2TH) domain and the transducer domain. The GHKL domain has a similar function as when found in the type IIA topoisomerases, causing the B subunits to dimerise upon the binding of ATP (Corbett & Berger, 2003). The H2TH domain is entirely unique to topo VI, not being observed in any other topoisomerases. Its role is not currently known, but it is thought to be tangentially involved in binding of DNA glycosylases to DNA by positioning other domains in order to form the necessary interactions (Fromme & Verdine, 2002; Gilboa et al, 2002; Serre et al, 2002; Zharkov et al, 2002). The transducer domain is thought to "transduce" signals from the GHKL ATPase site to the DNA cleavage-reunion site in the A subunit (Corbett & Berger, 2003). It is expected to be flexible as it contains a hinge region about halfway down its length (Graille et al, 2008). The *M. mazei* enzyme has been shown to contain an additional C-terminal domain absent in the *S. shibatae* enzyme. This domain is only found in a small number of archaeal topo VI orthologs and is generally found in those species which also possess a DNA gyrase (Corbett et al, 2007). It is postulated to be involved in protein—protein or protein—carbohydrate interactions which may assist in targeting or regulating the

enzyme, but there is currently no direct evidence for its function (Corbett et al, 2007).

1.6.3 Topoisomerase VI mechanism

Topo VI has shown itself to be capable of a number of reactions, including the relaxation of negative and positive supercoiled DNA, unknotting and decatenation (Bergerat et al, 1994; Corbett et al, 2007). All of these reactions require ATP and Mg^{2+} (Bergerat et al, 1997; Corbett et al, 2007). The mechanism of topo VI is basically the same as type IIA topoisomerase (Schoeffler & Berger, 2008): a G-segment of DNA is bound by the A subunits, a T-segment is captured by binding of ATP and dimerisation of the B subunits, the G-segment is cleaved by the A subunits and the T-segment passed through the gap. ATP hydrolysis allows the enzyme to reset for further rounds of reaction.

Although the general reaction is very similar to the type IIA enzymes there are a number of specifics which differ. Unlike in type IIA enzymes the cleavage of the G-segment by topo VI is tightly linked to the binding of ATP (Buhler et al, 2001). Additionally the G-segment is cut with a two base pair stagger rather than the four base pair cut of the type IIA enzymes (Buhler

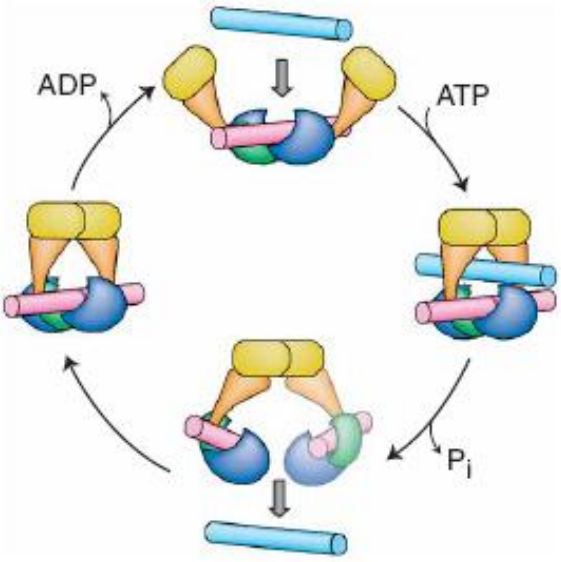

Figure 1.16 The mechanism of topo VI. The domains are coloured as follows: *yellow*, B subunit ATPase and H2TH domains; *orange*, B subunit transducer domain; *green*, A subunit CAP-like domain; and *blue*, toprim domain. The G-segment is shown in *pink* whilst the T-segment is *light blue*. From Corbett et al, 2007.

et al, 2001). Finally the absence of the C-gate is thought to alter the range of relaxed topoisomers that the enzyme produces upon relaxing supercoiled DNA compared to type IIA enzymes but this is yet to be confirmed (Stuchinskaya et al, 2009). It is thought that the absence of the C-gate is compensated for by the tight coupling of DNA cleavage with ATP binding, which helps the complex maintain stability during strand passage (Bates et al, 2011).

1.6.4 Inhibitors of topoisomerase VI

There has been relatively little work looking into specific inhibitors of topoisomerase VI since it has been considered an archaeal curiosity, and therefore not medically or commercially useful. The *S. shibatae* enzyme was tested against a range of classic topoisomerase IIA inhibitors when it was first discovered (Bergerat et al, 1994). The enzyme was found to be resistant to both the coumarin and quinolone class of compound, both of which are potent inhibitors of DNA gyrase. It was however susceptible to several inhibitors of eukaryotic topoisomerase II used as anticancer drugs including: doxorubicin, ellipticine, m-amsacrine, and to a lesser extent o-amsacrine. All these compounds inhibited *S. shibatae* topo VI at similar concentrations at which they inhibited eukaryotic topoisomerase II. The structures of these compounds can be found in Figure 1.17.

The Hsp90 inhibitor radicicol has also been shown to inhibit *S. shibatae* topo VI (Gadelle et al, 2005). The drug is a relatively weak inhibitor of the enzyme with an Inhibitory Concentration for 50% activity (IC_{50}) of 250 μM. However it has not been reported to inhibit any type IIA topoisomerases, which makes it noteworthy compared to the other inhibitors of topo VI. The drug has been shown to specifically target the ATPase activity of the enzyme and to bind in a pocket near the ATP-binding site of the enzymes B subunit (Corbett & Berger, 2006; Graille et al, 2008). The binding of the compound does not cause dimerisation of the B subunits like ATP would, and it is thought that drug binds in such a way as to prevent the binding of ATP to the enzyme (Graille et al, 2008).

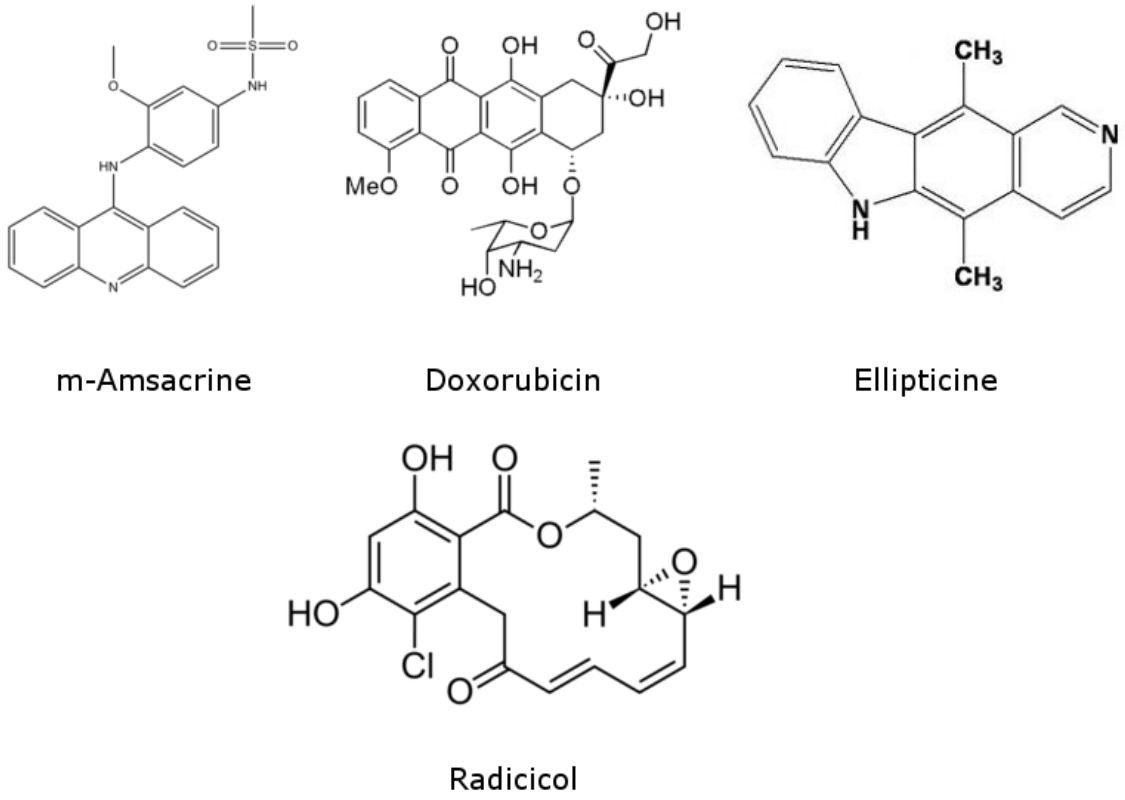

Figure 1.17 The structures of currently known *S. shibatae* topo VI inhibitors.

1.7 DNA gyrase

DNA gyrase is unique among the type IIA topoisomerases since it can introduce negative supercoils into DNA in an ATP-dependent manner as well as relax positive supercoils with high efficiency (Bates et al, 1996; Gellert et al, 1976). Initially it was thought to be found exclusively in bacteria, but genes putatively encoding for both the A (GyrA) and B (GyrB) subunits have been since identified in plants as well as the malaria parasite *Plasmodium falciparum* (Garcia-Estrada et al, 2010; Raghu Ram et al, 2007; Wall et al, 2004). The essential nature, unique mechanism amongst the type IIA topoisomerases and absence in humans have lead to DNA gyrase being an exceptional antimicrobial target.

1.7.1 The biological role of DNA gyrase

DNA gyrase is responsible for the global level of supercoiling inside the bacterial cell which is important for a number of reasons. The first is a matter of logistics: the length of a bacterial genome vastly exceeds the length of a bacterial cell. For example the *E. coli* genome is approximately 1600 μm long whilst the bacterium is only ~1 μm in diameter and ~3-5 μm in length (Zimmerman, 2006). The introduction of negative supercoils is essential for compaction of this DNA into cellular bodies called nucleoids which occupy ~25% of the cell volume (Worcel & Burgi, 1972).

The replication of bacterial plasmids requires the DNA to be negatively supercoiled to facilitate the unwinding of the target sequence (Schvartzman & Stasiak, 2004). Additionally, during DNA replication positive supercoils are generated ahead of the replication fork as it advances (Figure 1.18) (Sawitzke & Austin, 2000; Zechiedrich & Cozzarelli, 1995). Failure to remove these supercoils can result in the formation of catenanes between the daughter duplexes (Zechiedrich & Cozzarelli, 1995) and the stalling of the replication machinery.

As well as its role in the process of DNA replication, DNA gyrase is also essential for the process of transcription. The transcription of many genes has been shown to be influenced by the global level of supercoiling in the cell (Bates & Maxwell, 2005). This is because supercoiling affects the binding of RNA polymerase and various promoter or suppressor proteins (Lilley et al, 1996). In addition it is thought that the interaction of the binding of RNA polymerase to DNA causes the DNA to rotate on its axis, allowing the enzyme to follow the helical path of the DNA strands (Liu & Wang, 1987). If the DNA is topologically constrained, for example bound to regulatory proteins, positive supercoils are formed ahead of the polymerase and whilst negative supercoils form behind. These supercoils are removed by DNA gyrase and bacterial topoisomerase I respectively (Lockshon & Morris, 1983; Pruss & Drlica, 1986).

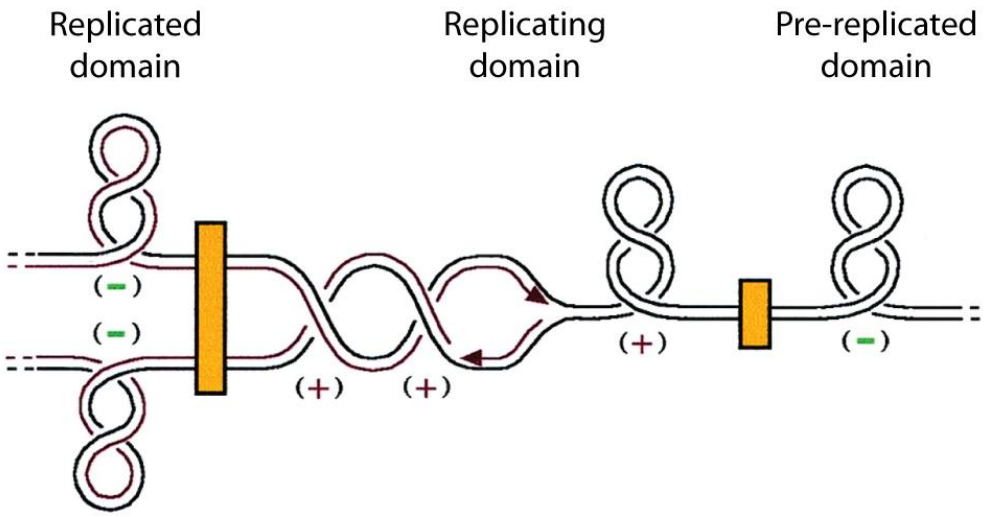

Figure 1.18 The effect of replication on the supercoiling state of DNA. The DNA has been separated into domains, indicated by the gold boxes. In the replicating domain, positive supercoils form in front of the replication fork and can diffuse behind to form pre-catenanes. Figure from Bates & Maxwell, 2005.

1.7.2 Structure of DNA gyrase

Like all bacterial type IIA topoisomerases DNA gyrases is a symmetrical heterotetramer of two GyrA and two GyrB subunits. Limited proteolysis experiments have further revealed both subunits are comprised of two domains (Kampranis & Maxwell, 1998; Reece & Maxwell, 1989) (Figure 1.19). Although there is not currently a crystal structure for complete heterotetramers, crystal structures of the constituent domains have been solved (Figure 1.20). For the sake of convenience the subunit sizes and residue numbering in this section is for *E. coli* DNA gyrase, unless otherwise stated.

The GyrA subunit is comprised of a 59 kDa N-terminal domain and a 35 kDa C-terminal domain. The N-terminal domain contains the active site tyrosine and a DNA-binding saddle for the G-segment DNA when in its dimeric form. These features have led to it being known as the "DNA breakage-reunion domain". As well as these features the structure of the N-terminal domain causes a 30 Å cavity to form in the GyrA dimer between the major dimer interaction regions that is large enough to accommodate double-stranded DNA (Berger, 1998). The C-terminal domain is comprised of a novel β-pinwheel fold (which resembles a β-propeller fold). This roughly cylindrical structure possesses a band of positive charge around its diameter

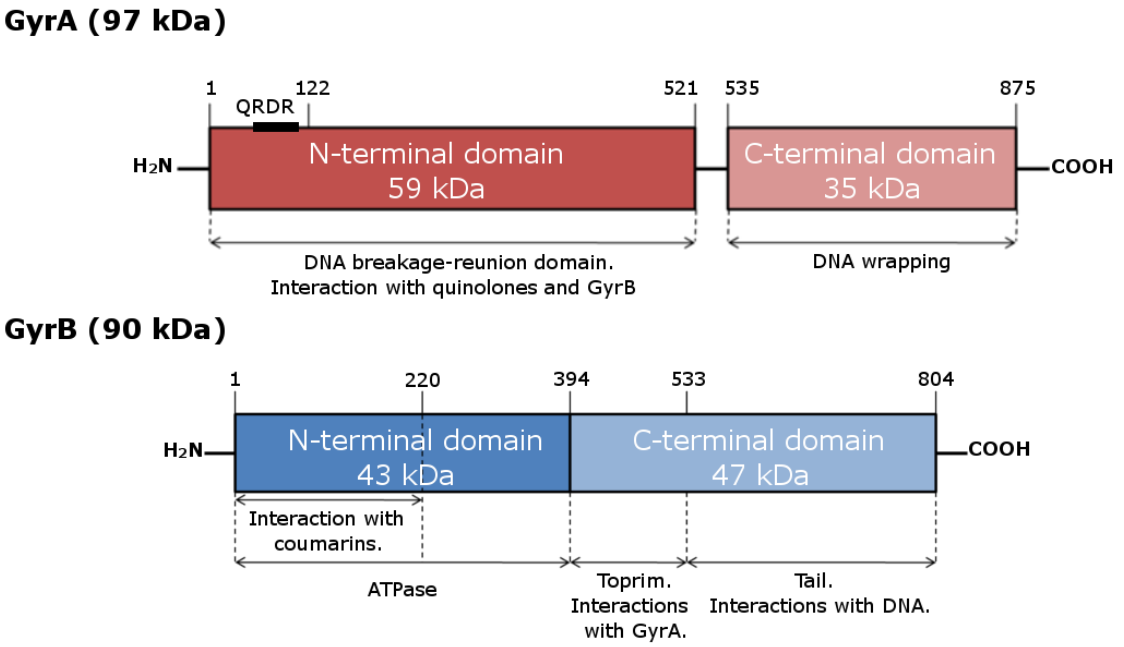

Figure 1.19 The domain structure of DNA gyrase subunits. The GyrA subunit consists of a N-terminal domain, which contains the Quinolone-Resistance Determining Region (QRDR) and the active site tyrosine 122, and a C-terminal domain responsible for DNA wrapping. The GyrB contains an N-terminal domain, containing the ATPase site, and a C-terminal domain which interacts with GyrA and DNA.

which could be used to wrap DNA (Corbett et al, 2004), a process essential for the mechanism of DNA gyrase. This is supported by the observation that mutants with the GyrA C-terminal domain deleted were no longer able to supercoil DNA, instead relaxing DNA in an ATP-dependent manner (Kampranis & Maxwell, 1998; Reece & Maxwell, 1989).

The GyrB subunit is comprised of a 43 kDa N-terminal domain and a 47 kDa C-terminal domain. The N-terminal domain contains the GHKL ATPase domain (Wigley et al, 1991). When ATP (or a non-hydrolysable analogue such as ADPNP) is bound the N-terminal domain dimerises (Wigley et al, 1991). This dimer possesses a 20 Å cavity which is large enough to accommodate a DNA duplex (Wigley et al, 1991). The C-terminal domain contains both the Toprim domain necessary for DNA cleavage-religation (Noble & Maxwell, 2002) and a "Tail" region thought to interact with DNA (Costenaro et al, 2007). Small angle x-ray scattering (SAXS) experiments suggest that the GyrB subunit is "tadpole" shaped in solution with the N-terminal domain forming the "head" and the C-terminal the "tail" (Costenaro et al, 2007).

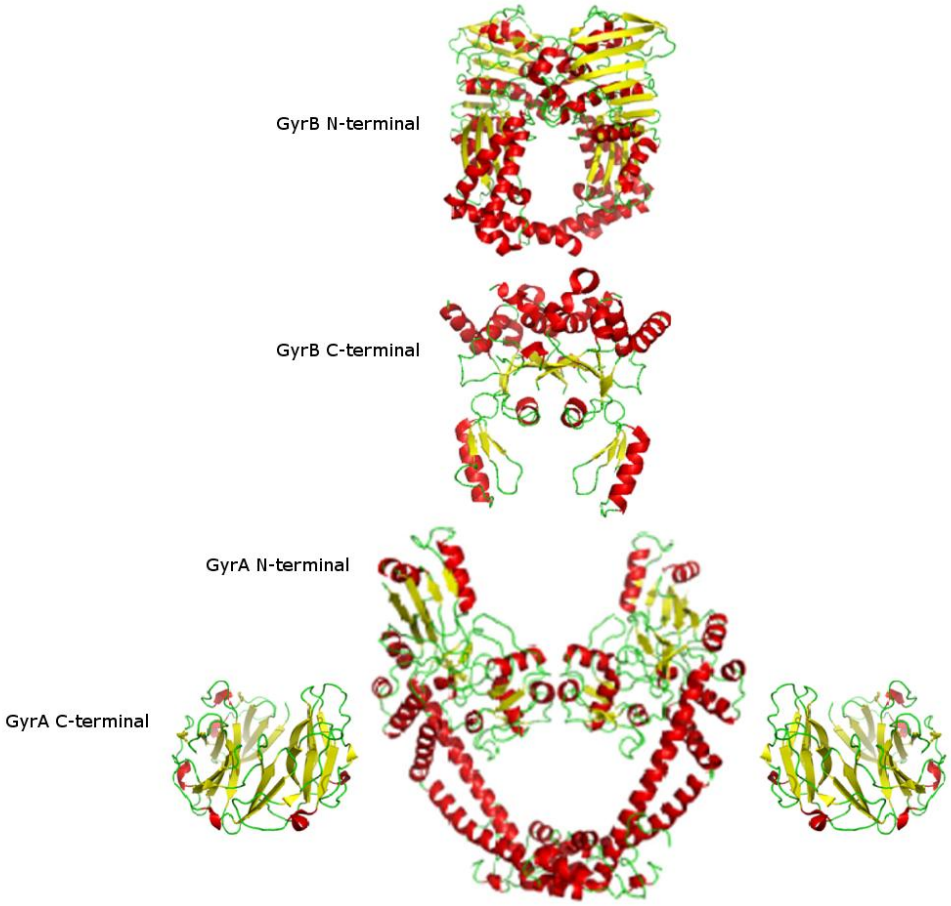

Figure 1.20 The crystal structures of DNA gyrase domains. Structures have been solved for the N-terminal (Morais Cabral et al, 1997) and C-terminal domains (Ruthenburg et al, 2005) of *E. coli* GyrA, as well as the N-terminal domain of *E. coli* GyrB (Brino et al, 2000) and the C-terminal domain of *M. tuberculosis* GyrB (Fu et al, 2009). Structures presented in their approximate location in the intact DNA gyrase complex, but have not been drawn to exact scale.

1.7.3 Mechanism of DNA gyrase

DNA gyrases follows a similar reaction cycle to other type IIA topoisomerases (Section 1.5.3.1, Figure 1.9) with one important exception: it is able to introduce negative supercoils into DNA in an ATP dependent manner. It is thought that the C-terminal domain of the GyrA subunit is crucial for the supercoiling reaction, with its removal resulting in a loss of supercoiling activity (Corbett et al, 2004; Kampranis & Maxwell, 1996). Upon binding the G-segment DNA is wrapped around this C-terminal domain in a right-handed manner, resulting in DNA looping back across itself to form the T-segment (Figure 1.21)(Corbett et al, 2004; Wang, 1998). The total amount of DNA wrapped in this manner by DNA gyrase is thought to be 120-150 bp (Champoux, 2001).

Since the introduction of supercoils is not energetically favourable ATP hydrolysis is necessary to drive the reaction. The binding of ATP to the GyrB subunits causes their N-terminal domains to dimerise, clamping the T-segment in place (Kampranis & Maxwell, 1996). It has been found that ATPase activity is stimulated by the cleavage of DNA by the GyrA subunit (Williams & Maxwell, 1999a). This G-segment is then cleaved on both its strands with a 4 bp stagger (Horowitz & Wang, 1987; Mizuuchi et al, 1980). Conformational changes occur which cause the break to widen enough to allow passage of the T-segment through this "DNA gate" into the positively charged cavity formed by the GyrA N-terminal domains (Morais Cabral et al, 1997). The T-segment can then exit the complex by the bottom gate of the GyrA N-terminal domains. Although it is not clear what drives the T-segment to do this, it is thought that the closing of the DNA gate causes the GyrA N-terminal cavity to narrow and "squeeze" T-segment out (Wang, 1998). ATP hydrolysis allows the enzyme to reset, ready do another round of activity (Sugino et al, 1978).

If ATP is replaced by a non-hydrolysable analogue such as ADPNP (5'-

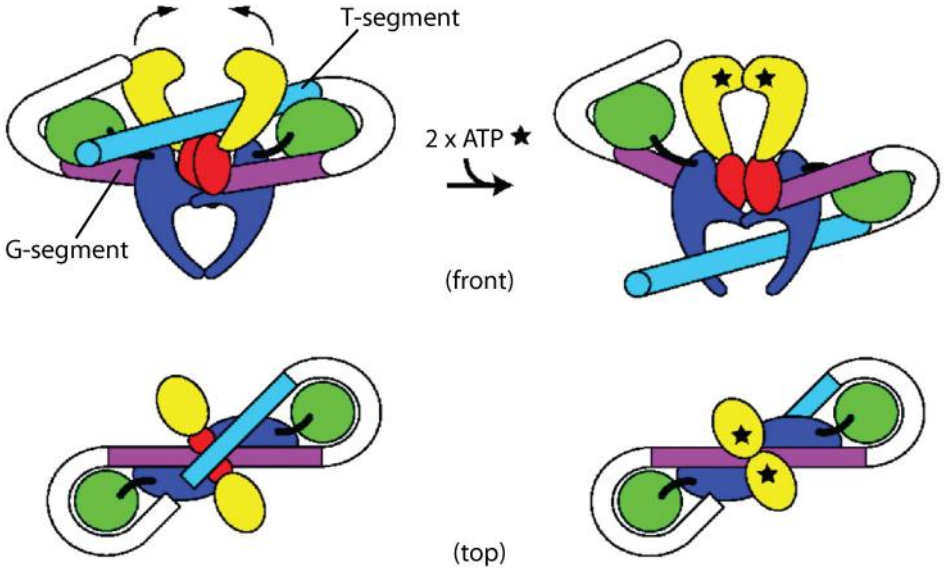

Figure 1.21 DNA wrapping and strand passage by DNA gyrase. The different domains of the protein are coloured as follows: *yellow*, GyrB N-terminal (containing the ATPase domain); *red*, GyrB C-terminus (containing toprim and tail domains); *dark blue*, GyrA subunit N-terminal (containing the "breakage-reunion" domain); *green*, GyrA C-terminal domain (responsible for DNA wrapping). The G-segment (*purple*), T-segment (*light blue*) and the DNA, N- and C-gates are indicated. Figure from Corbett et al, 2004.

adenylyl β,γ-imidodiphosphate) the T-segment can be captured by the GyrB subunits and the strand passage event can occur (Ali et al, 1993; Ali et al, 1995; Lindsley & Wang, 1993; Roca & Wang, 1992). However the enzyme is unable to religate the double strand break and is trapped in an inactive state (Roca et al, 1996).

DNA gyrase is also able to relax negatively supercoiled DNA in the absence of ATP, passing the T-segment in the opposite direction (Williams & Maxwell, 1999b). ATP is not necessary since the removal of negative supercoils is energetically favourable. This reaction is significantly less efficient than the enzyme's supercoiling activity (Gellert et al, 1979; Higgins et al, 1978). DNA gyrase is capable of relaxing positive supercoils in the presence of ATP, a reaction which has enhanced activity over the enzyme's negative supercoiling activity (Bates et al, 1996). This reaction is thought to happen in an identical manner to the negative supercoiling reaction. The catenation, decatenation and unknotting activities of DNA gyrase have all been described and are ATP-dependent (Kreuzer & Cozzarelli, 1980; Liu et al, 1980).

1.8 DNA gyrase inhibitors

Because of the essential nature of its function and its absence in humans DNA gyrase is a highly appealing drug target. A large number of antibiotics have been produced which target it (and its companion type IIA topoisomerase, topoisomerase IV) (Froelich-Ammon & Osheroff, 1995). The two biggest classes of these inhibitors are the quinolones and aminocoumarins.

1.8.1 Quinolones

The quinolones, which include the drug ciprofloxacin, are among the most successful classes of antimicrobials developed. The first quinolone, nalidixic acid, was discovered by accident as a by-product in the synthesis of the antimalarial drug chloroquine (Lesher et al, 1962). Subsequent modifications to the ring decoration have resulted in progressively more

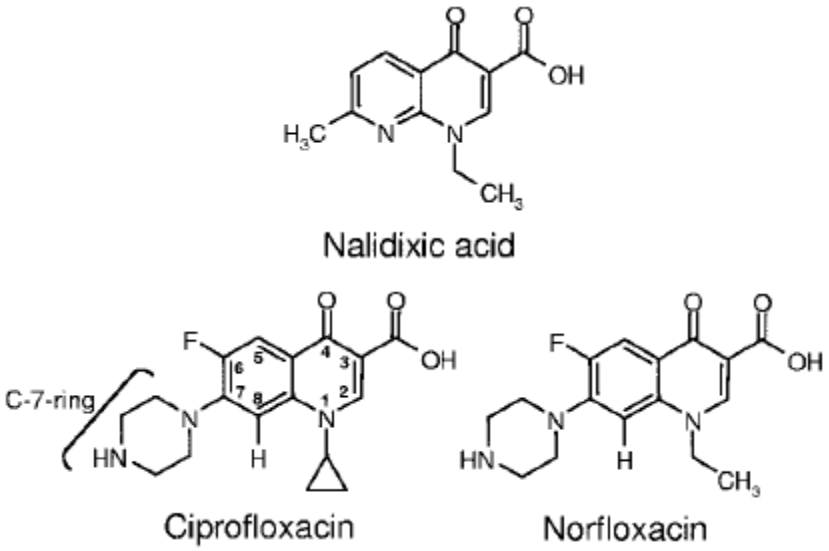

Figure 1.22 Structures of selected quinolones. Figure from Drlica et al, 2008.

potent second, third and fourth generation quinolones (Emmerson & Jones, 2003; King et al, 2000).

Quinolones are thought to operate by stabilisation of the cleavage-complex formed during the topoisomerase reaction (Heddle et al, 2000). This converts the enzymes into physiological toxins that introduce high levels of breaks into the cell's genome (Kreuzer & Cozzarelli, 1979), resulting in mutagenesis (Ripley, 1994) and cell death (Zhivotovsky & Kroemer, 2004). Their lethality is reflected in their low *in vivo* minimum inhibitory concentration for bacterial growth (MIC) compared to their *in vitro* IC_{50} values, as only a small number of breaks are required to disrupt the stability of the cell (Domagala et al, 1986; Gellert et al, 1977). What's more they are highly effective against rapidly dividing cells, such as bacteria, since the presence of replication machinery greatly increases the number of breaks formed (Hsiang et al, 1989). However, the exact details of quinolone activity and binding have remained elusive. Several low resolution crystal structures have been published which show the stabilization of DNA cleavage by various quinolones with DNA gyrase or topoisomerase IV (Figure 1.23) (Bax et al, 2010; Laponogov et al, 2010; Laponogov et al, 2009; Wohlkonig et al, 2010). In all these structures the DNA gate is closed, showing that gate opening is not necessary for quinolone binding or strand cleavage. This is consistent with previous biochemical studies

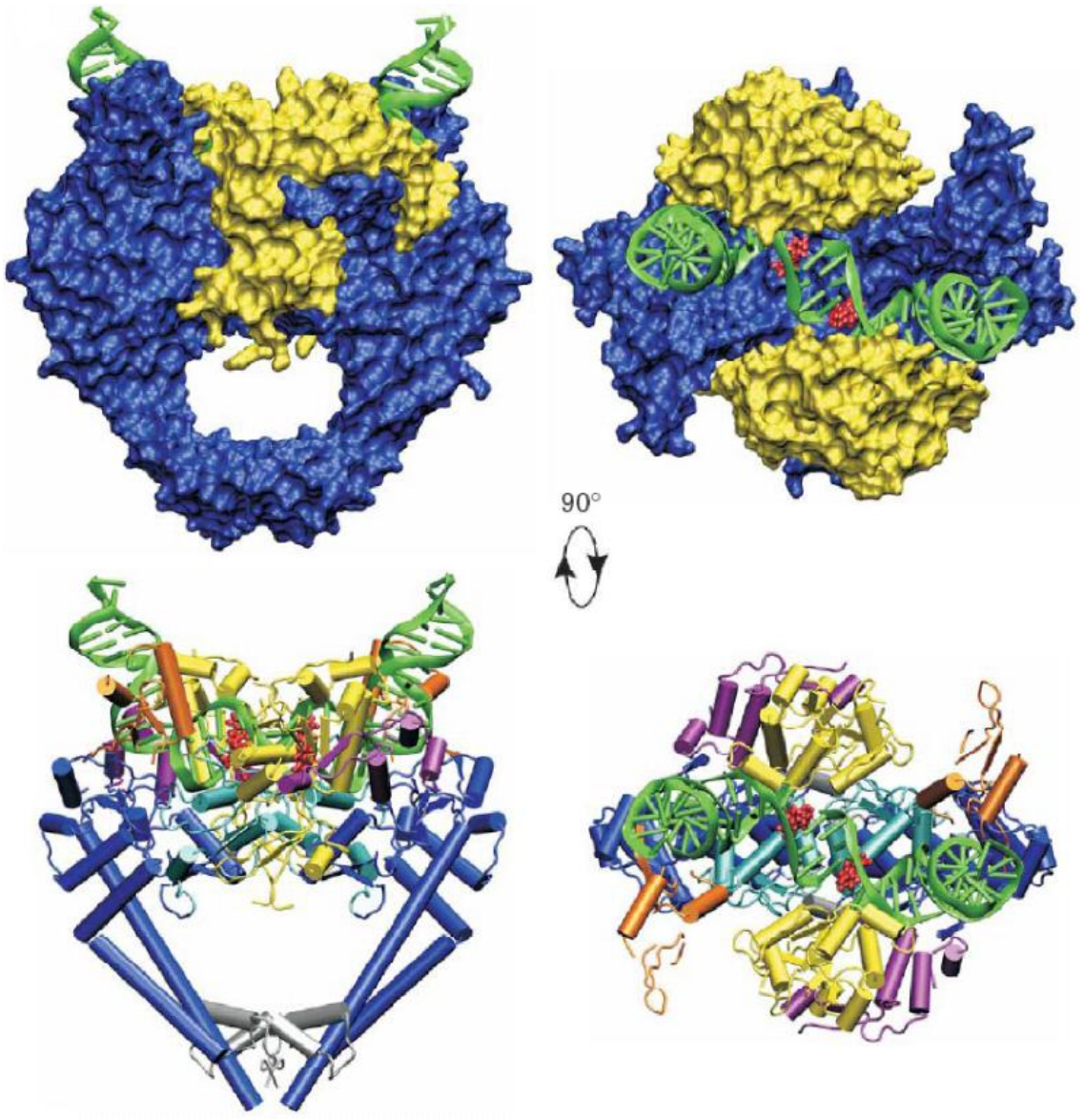

Figure 1.23 The binding of moxifloxacin to topo IV breakage-reunion domain. Colouring as follows: *blue*, ParC (GyrA homologue) N-terminal domain; *yellow*, ParE (GyrB homologue) toprim domain; *green*, 34 bp DNA duplex; *red*, moxifloxacin; c*yan*, WHD or CAP-like domain; *orange*, 'tower' domain; and *silver*, C-gate. The interface region between ParC and ParE subunits is in *purple*. Figure from Laponogov et al, 2009.

(Williams & Maxwell, 1999a). Although these structures show approximately where the binding sites for the quinolones are in this enzyme, low resolution and discrepancies between the structures means drawing conclusions about the exact interactions between drug, enzyme and DNA is not possible. The binding sites revealed in the crystal structures appear to overlap with the so-called Quinolone-Resistance-Determining-Region (QRDR) region of the GyrA subunit (Yoshida et al, 1990).

Despite their potency several bacterial strains which are resistant to the quinolones have emerged (Hooper, 1999). Some of these strains bear genes which prevent uptake of the drugs or encode for pumps which export them from the bacteria before they can kill the cell. Others have mutations within the gyrase genes, altering key interaction residues and preventing the drugs binding. The majority of these mutations occur in the QRDR region of the GyrA subunit, which lies near the dimer interface and active site tyrosine (Morais Cabral et al, 1997). The residues most commonly mutated in these resistant strains are Ser83 and Asp87 (Yoshida et al, 1990). The mutation of these residues is thought to reduce the binding of quinolones (Willmott & Maxwell, 1993). In addition to these resistance-conferring mutations of DNA gyrase, a plasmid-borne quinolone resistance gene has been identified in clinical isolates (Jacoby et al, 2003). The protein it encodes for, a pentapeptide repeat protein called Qnr (Bateman et al, 1998), is thought to be a DNA mimic capable of inhibiting gyrase activity by binding to the enzyme instead of the G-segment (Hegde et al, 2005). Presumably, by lowering the activity of the enzyme in this way the bacteria reduce the number of DNA lesions generated by the drugs and therefore reduce their lethality.

1.8.2 Aminocoumarins

The aminocoumarin class of natural products have been known to inhibit nucleic acid synthesis in bacteria since the 1950s. There are three naturally occurring aminocoumarins produced by *Streptomyces*: novobiocin, clorobiocin and coumermycin A1 (Figure 1.24) (Maxwell & Lawson, 2003). All three of these compounds possess a 3-amino-4, 7-dihydroxycoumarin core (referred to as a coumarin ring), a L-noviosyl sugar and an aromatic acyl component attached to the amino group of the coumarin ring (Maxwell & Lawson, 2003). They have been shown to inhibit the ATPase activity of DNA gyrase by competing with ATP for binding to GyrB (Mizuuchi et al, 1978; Sugino & Cozzarelli, 1980; Sugino et al, 1978). High resolution crystal structures (Holdgate et al, 1997; Lewis et al, 1996a; Lewis et al, 1996b; Maxwell & Lawson, 2003) and biochemical studies (Gilbert & Maxwell, 1994) have revealed that they do not bind to the ATP binding site of the enzyme but rather to an overlapping site, with the noviose sugar of

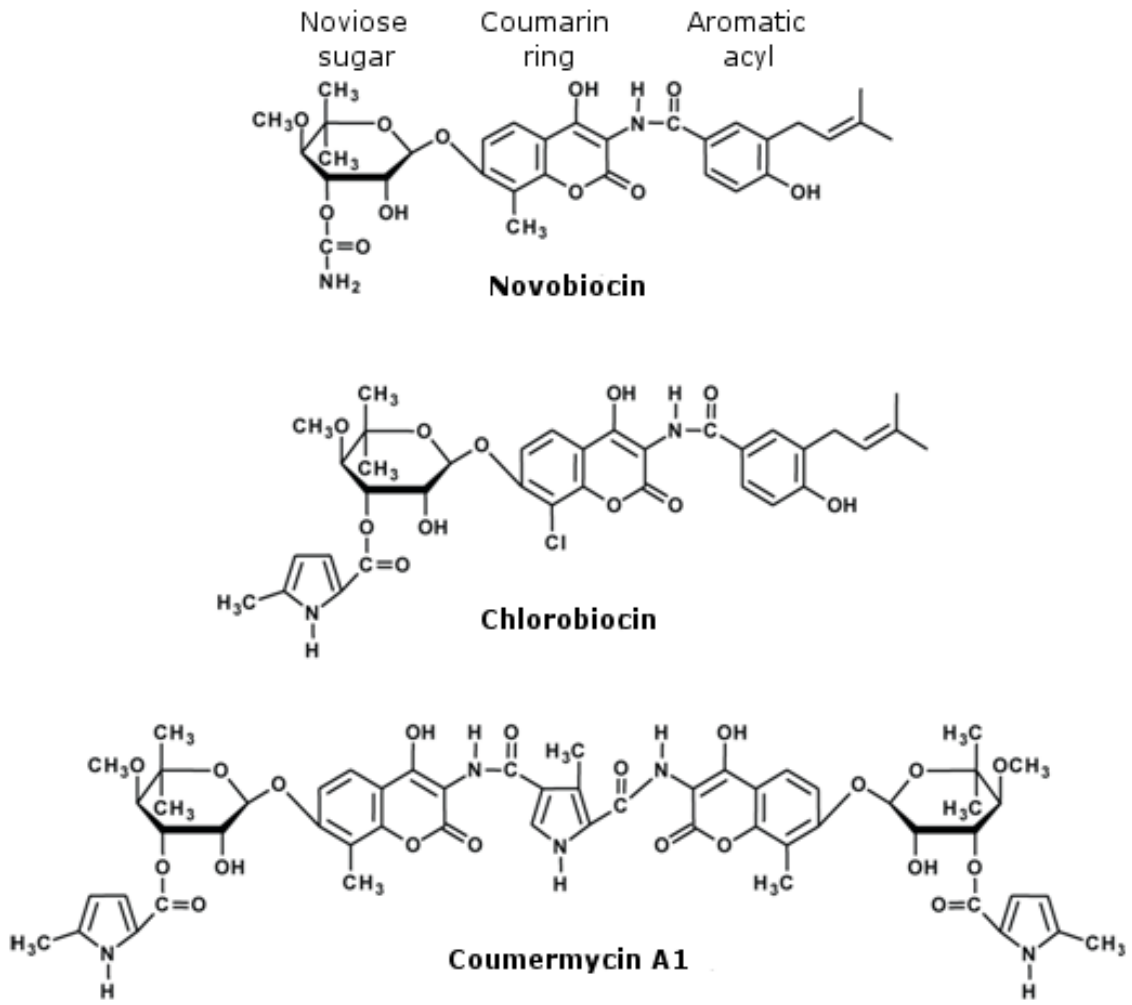

Figure 1.24 The structures of the three natural aminocoumarins. Coumermycin A1 is unusual, appearing to be a symmetrical dimer of the clorobiocin noviose sugar and coumarin ring linked by a pyrrole group.

the aminocoumarin overlapping with the adenine ring of ATP/ADPNP (Figure 1.25).

Resistance to aminocoumarins usually arises due to mutations in the GyrB subunit. The most common of these mutations involve an Arg residue critical to aminocoumarin binding (Arg136 in *E. coli*) (Contreras & Maxwell, 1992; del Castillo et al, 1991; Kampranis et al, 1999; Lewis et al, 1996a; Tsai et al, 1997). Mutations in other residues in the drug binding site have been reported such as Gly164 to Val, Asp73 to Glu, Gly77 to Ala or Ser, Ile78 to Ala or Leu and Thr165 to Ala or Val (Contreras & Maxwell, 1992; Gross et al, 2003). Some mutations have been shown to confer more selective resistance, such as Asp-89 to Gly and Ser-128 to Leu which make the enzyme resistant to novobiocin and not coumermycin A1 (Fujimoto-

Nakamura et al, 2005). Many of these mutations are detrimental to the activity of the enzyme, most likely due to their proximity to the ATPase active site (Contreras & Maxwell, 1992; Gross et al, 2003). This means that there is a possibly significant cost for the bacteria to develop resistance to these drugs, which is an appealing thought for developing clinical aminocoumarins.

However, although these compounds are potent DNA gyrase inhibitors they make poor clinical antimicrobials due to their poor solubility, high toxicity in humans and ineffectiveness against Gram-negative bacteria due to poor penetration of the bacterial cells (Maxwell & Lawson, 2003). Novobiocin has been used as a clinical antibiotic under the names albamycin and cathomycin but was withdrawn due to low potency and unpleasant side-effects such as skin rashes and liver dysfunction. The mitigation of these flaws by chemical modification is now the main challenge for producing clinically relevant aminocoumarin drugs.

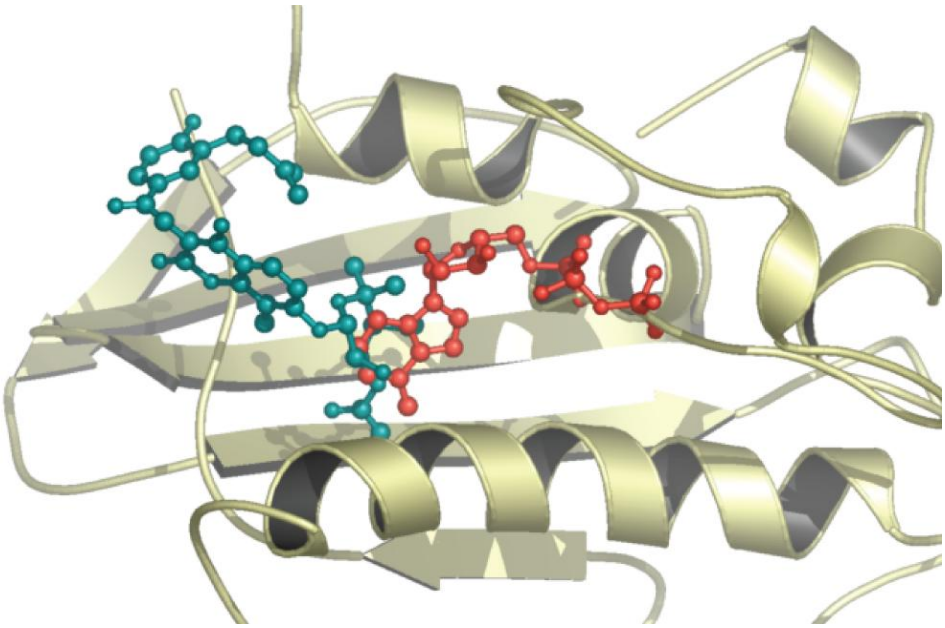

Figure 1.25 The overlapping binding sites of ADPNP and novobiocin. ADPNP is shown in *red* and novobiocin in *green*. This image was produced by aligning the structures of the ADPNP-bound GyrB fragment (Brino et al, 2000)and novobiocin-bound GyrB fragment (Holdgate et al, 1997).

1.8.3 Other small molecule inhibitors of DNA gyrase

As well as the two major classes of inhibitors above a host of other compounds have been found that inhibit DNA gyrase. Many of these compounds have only been recently identified, and their modes of action still require further exploration.

The simocyclinones are hybrid antibiotics, produced by *Streptomyces antibioticus* Tü 6040, which target DNA gyrase (Flatman et al, 2005) that are mostly intermediates of simocyclinone D8 (SD8) (Theobald et al, 2000; Trefzer et al, 2002). These antibiotics possess both aminocoumarin and polyketide moieties linked by a tetraene dicarboxylic acid–olivose sugar linker (Figure 1.26). Although the aminocoumarin and polyketide moieties can inhibit DNA gyrase individually, their potency is much less than the intact antibiotic (Edwards et al, 2009). Surprisingly, the binding site for the aminocoumarin end of the molecule is not at the ATPase site of GyrB (Edwards et al, 2009; Flatman et al, 2006). A crystal structure of SD8 bound to the GyrA N-terminal domain has revealed that both ends of the molecule bind to two different sites on the GyrA subunit at the GyrA—GyrB interface (Edwards et al, 2009). This is supported by the biochemical evidence that SD8 does not affect the ATPase activity of DNA gyrase, instead appearing to prevent the binding of the enzyme to DNA (Flatman et al, 2005). The crystal structure shows that four SD8 molecules stabilise a tetramer of GyrA subunits, with each SD8 binding one of its two heads to two different GyrA subunits. Since it is not clear if this mode of binding is physiologically relevant an alternative model, supported by mass spectrometry data, has been proposed in which one SD8 bridges the two sites on the same GyrA subunit (Edwards et al, 2011). Unfortunately SD8 does not appear to be a good candidate for clinical use, having poor bactericidal activity and cytotoxicity against human cells (Richter et al, 2010; Sadiq et al, 2010; Schimana et al, 2000).

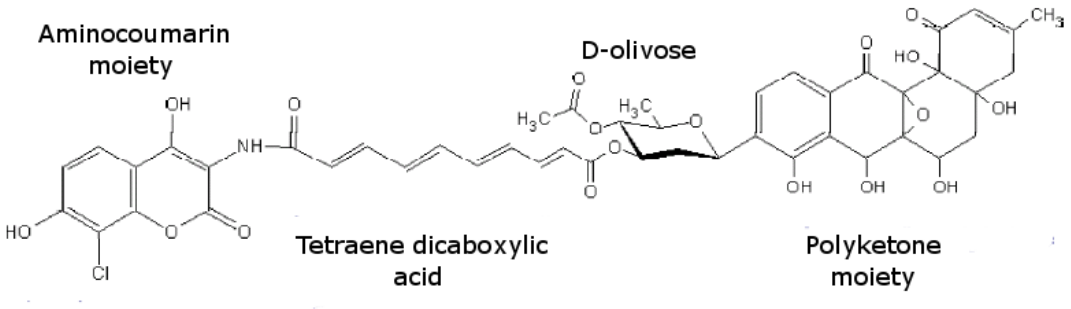

Simocyclinone D8

Figure 1.26 The structure of simocyclinone D8.

Cyclothialidine is a cyclic peptide with weak antibacterial activity produced by *Streptomyces filipinensis* (Goetschi et al, 1993; Nakada et al, 1993). It has been shown to inhibit the ATPase activity of DNA gyrase (Goetschi et al, 1993; Nakada et al, 1994; Oram et al, 1996). Several analogues have been produced with enhanced activity (Angehrn et al, 2004; Goetschi et al, 1993), and the crystal structure of one of these compounds (GR122222X) shows that they bind to a site overlapping with the ATP-binding site, like novobiocin (Nakada et al, 1995; Oram et al, 1996). These derivatives are yet to be tested clinically.

Cinodine is a natural product of the *Norcardia spp*. of bacteria that belongs to the glycocinnamoylspermidine antibiotic class (Martin et al, 1978; Tresner et al, 1978). Three different forms have been discovered: β, γ1 and γ2. Cinodine has been shown to have bactericidal activity, inhibiting bacterial DNA synthesis (Greenstein et al, 1981). It has also been shown to have activity against gyrase *in vitro* and resistant mutants have been mapped to the A subunit (Osburne, 1995; Osburne et al, 1990). Other than this, its mode of action has not been explored.

As well as these natural product inspired inhibitors many synthetic inhibitors of DNA gyrase have been devised, often referred to as new bacterial topoisomerase inhibitors (NBTIs). NBTIs are generally compounds with antibacterial activity which do not belong to the quinolone class but have the same mode of action (stabilization of the cleavage complex) whilst remaining efficient against quinolone-resistant strains (Widdowson &

Hennessy, 2010). One such compound is the potent DNA gyrase inhibitor GSK299423 which has had its structure solved bound to *Staphylococcus aureus* DNA gyrase (Bax et al, 2010). The compound binds in a site close, but distinct from, the quinolone binding site. However, the compound does not stabilize double-strand breaks, instead inducing single-strand breaks (Bax et al, 2010). This implies a novel mode of action which requires further exploration.

1.9 A high-throughput assay for topoisomerase inhibitors

All the above goes to demonstrate that DNA topoisomerases have made exceptional drug targets, and that the problem of resistance to antimicrobials targeting them necessitates the discovery of new inhibitors. However, the discovery of such novel inhibitors has been limited by the traditional assay for topoisomerase activity, which is based on the principle that different DNA topoisomers have different mobilities on an agarose gel. This assay is information-rich, but is also slow and requires intensive handling. As such it is not suitable for the high-throughput format necessary for large scale screening for novel inhibitors. To address the limitations of this assay, a microtitre plate-based assay was developed (Maxwell et al, 2006) which is based on the formation of parallel-motif DNA triplexes.

As well as its standard duplex structure DNA is capable of forming DNA triplexes under the correct conditions. The formation of DNA triplexes was first observed with polynucleotide strands in 1957 (Felsenfeld et al, 1957), and later with triplex-forming oligos (or TFOs) with polypurine-polypyrimidine sections of double-stranded DNA (Le Doan et al, 1987; Moser & Dervan, 1987) (Figure 1.27). The binding of the TFO is thought to occur in the major groove of the double-stranded DNA in either a parallel or antiparallel orientation relative to the purine strand (Fox, 2000; Vasquez & Glazer, 2002). Whether a TFO binds in one or another of these two motifs is dependent on its sequence.

The antiparallel motif has had the least study of the two binding motifs. It is characterized by the formation of A•AT, T•AT and G•GC triplets

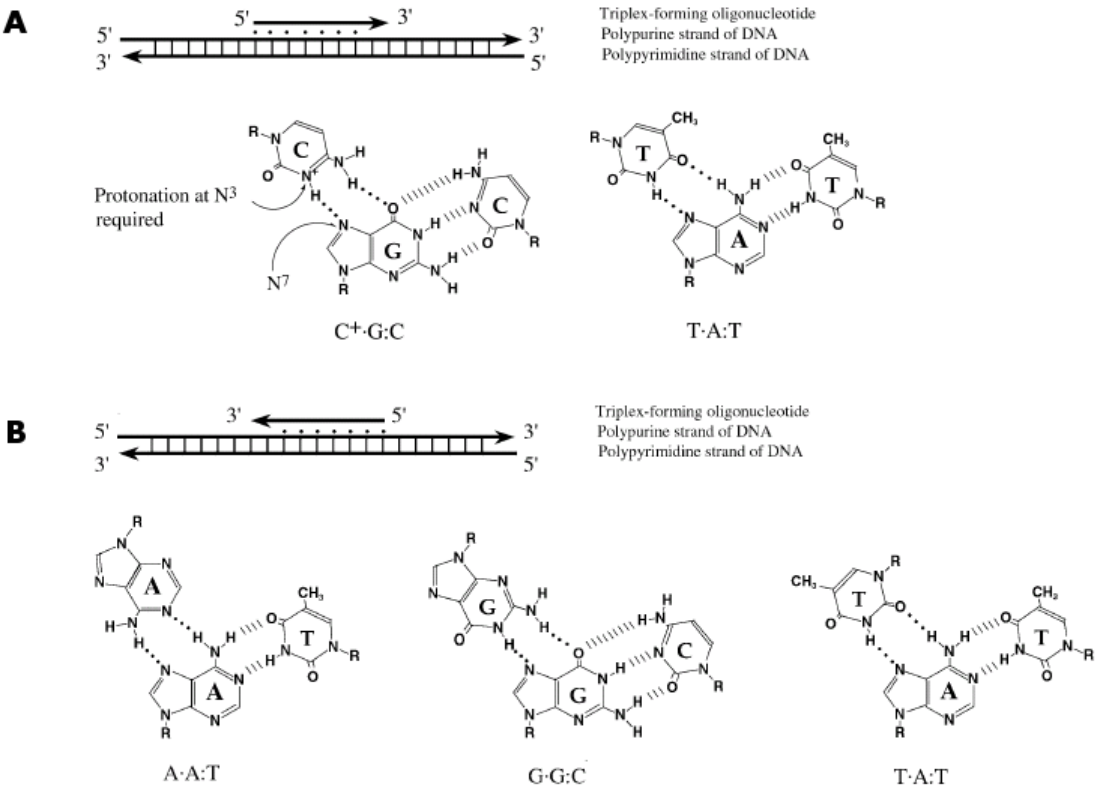

Figure 1.27 The two motifs for DNA triplex formation. Triplex formation occurs at polypurine—polypyrimidine sites in duplex DNA. At such sites a third strand (the triplex forming oligo) can bind in either a: *A*. pyrimidine motif; or *B*. purine motif. Figure from Vasquez & Glazer, 2002.

via reverse-Hoogsteen base pairing (Beal & Dervan, 1991; Chen, 1991) (DNA triplets are usually written in the form X•YZ, where the third strand base X interacts with an YZ base pair by forming hydrogen bonds to Y). The formation of antiparallel DNA triplexes is not dependent on pH (unlike the parallel motif, see below) but requires the presence of divalent metal ions (such as Mg^{2+}) (Fox, 2000). Their stability is highly sequence specific which has made them difficult to predict. This sequence specificity is thought to arise from the non-isohelical nature of the triplets as well as the formation of unusual guanine-mediated inter and intra molecular structures (Fox, 2000).

The parallel motif usually requires a TFO containing CT repeats, forming T•AT and C^+•GC triplets via two Hoogsteen hydrogen bonds. The formation of C^+•GC triplets necessitates a low pH (<6.0) to protonate the third strand cytosine (Fox, 2000; Lee et al, 1979; Vasquez & Glazer, 2002). Triplet formation is still possible without this protonation, but is much

weaker since it can form only one Hoogsteen hydrogen bond (Asensio et al, 1998). Interestingly the difference in stability between the protonated and non-protonated forms is much greater than one would expect for a single hydrogen bond (Asensio et al, 1998). It is likely electrostatic interactions with the phosphate backbone or altered stacking with neighboring bases play a role, possibly as a result of favorable interactions between the positive charge and the π systems of these bases (Fox, 2000). Although the pKa of free cytosine is around 4.5, this may vary considerably when the base forms part of a DNA triplex with internal cytosines possessing much higher pKas (i.e. being more stable) than terminal ones (Asensio et al, 1998). As well as pH a number of other factors affect the efficiency of parallel triplex formation including the valancey of cations present (Hampel et al, 1991; Rougee et al, 1992) and the ionic strength of the buffer (Rougee et al, 1992; Singleton & Dervan, 1993). Importantly for the high-throughput microtitre plate-based assay, triplex formation has been shown to be enhanced by negative supercoiling of the double-stranded DNA (Hanvey et al, 1988; Sakamoto et al, 1996).

The microtitre plate-based assay reactions are carried out in streptavidin-coated microtitre wells, which have had a single-stranded biotinylated CT-rich TFO immobilized on their surfaces. This oligo can form triplexes with a target plasmid by the addition of a low pH triplex formation buffer containing divalent metal ions, which also stops the topoisomerase reaction. Supercoiled DNA will be retained in the wells after washing, whereas relaxed, open circle and linear DNA will be removed. The amount of DNA retained can be quantified with a fluorescent dye, and directly correlates with the level of enzyme activity (Figure 1.28).

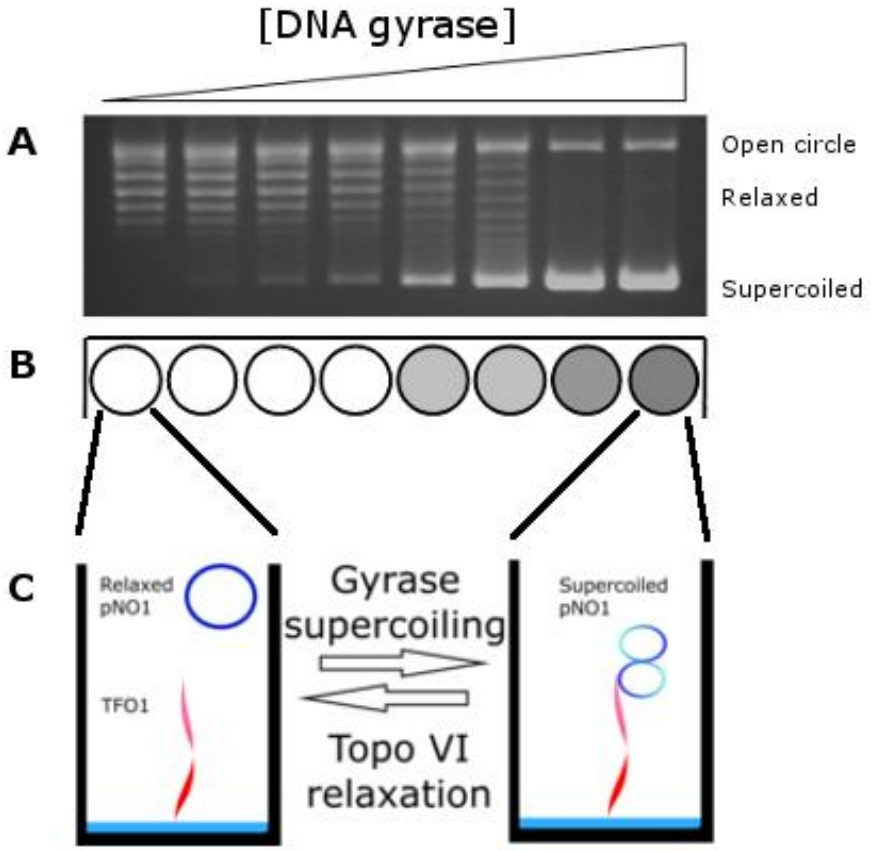

Figure 1.28 A graphical depiction of the agarose and microtitre plate-based assays. *A*. Sample agarose gel assay for increasing units of DNA gyrase with position of different topoisomers indicated. Relaxed DNA runs as a series of bands whilst supercoiled DNA runs as a single band. *B*. A cartoon representation of the equivalent experiment in the high-throughput assay. Each circle represents a well in a microtitre plate shaded to represent fluorescence intensity. *C*. Cartoon of the contents of the indicated wells (plasmid and TFO not drawn to scale). Conversion of relaxed to supercoiled DNA increases the amount of DNA retained in the well due to triplex formation and subsequently the intensity of the fluorescent signal after SBYR Gold staining. Figure adapted from Maxwell et al, 2006.

This assay has several advantages over the traditional assay for screening: it is much faster since it does not require a lengthy electrophoresis step, hundreds of reactions can be carried out simultaneously, the visualisation of DNA is quicker and simpler than the classic assay and there is less sample handling required by the operator. All these factors greatly speed up the assaying processes and open up the possibility for automation. However there are limits to the assay which need to be considered before it is used. Since the test compounds remain in the wells during the triplex formation step they may stimulate or inhibit triplex formation. This can result in the generation of false positives or negatives

(depending on whether a supercoiling or relaxing enzyme is being assayed). This is a particular concern since many topoisomerase inhibitors interact with DNA as part of their mode of inhibition.

1.10 Project aims

Since the microtitre plate-assay had yet to be tested in a high-throughput format the initial aim of this project was to demonstrate that it could be used for such a purpose. It would begin by carrying out a screen using a small library of natural products and existing drugs (the Genplus library from Microsource) against the well characterised *E. coli* DNA gyrase. It would then investigate the mode of action of any hits and test them for bactericidal activity against Gram-negative and Gram-positive bacteria.

The project would then move on to screening against the more exotic topoisomerase VI. Topo VI was chosen due to the relatively small number of studies conducted on it and the scarcity of specific inhibitors known for it. The *M. mazei* orthalogue was chosen to screen against since it is active at room temperature and is easily expressed. The the mode of action on any hits would then be explored and tested on the plant enzyme *in vivo* by carrying out a morphological screen with *Arabidopsis* hypocotyls. Towards the end of the project the possible existence of a hypothetical *Plasmodium* topo VI was discovered in the literature and an attempt was made to express the enzyme in order to test the archaeal topo VI hits against it.

Along the way the traditional and microtitre-plate assays for topoisomerase activity were explored and optimised, and the *M. mazei* enzyme was characterised.

A summary of the areas covered in the project can be found in Figure 1.29.

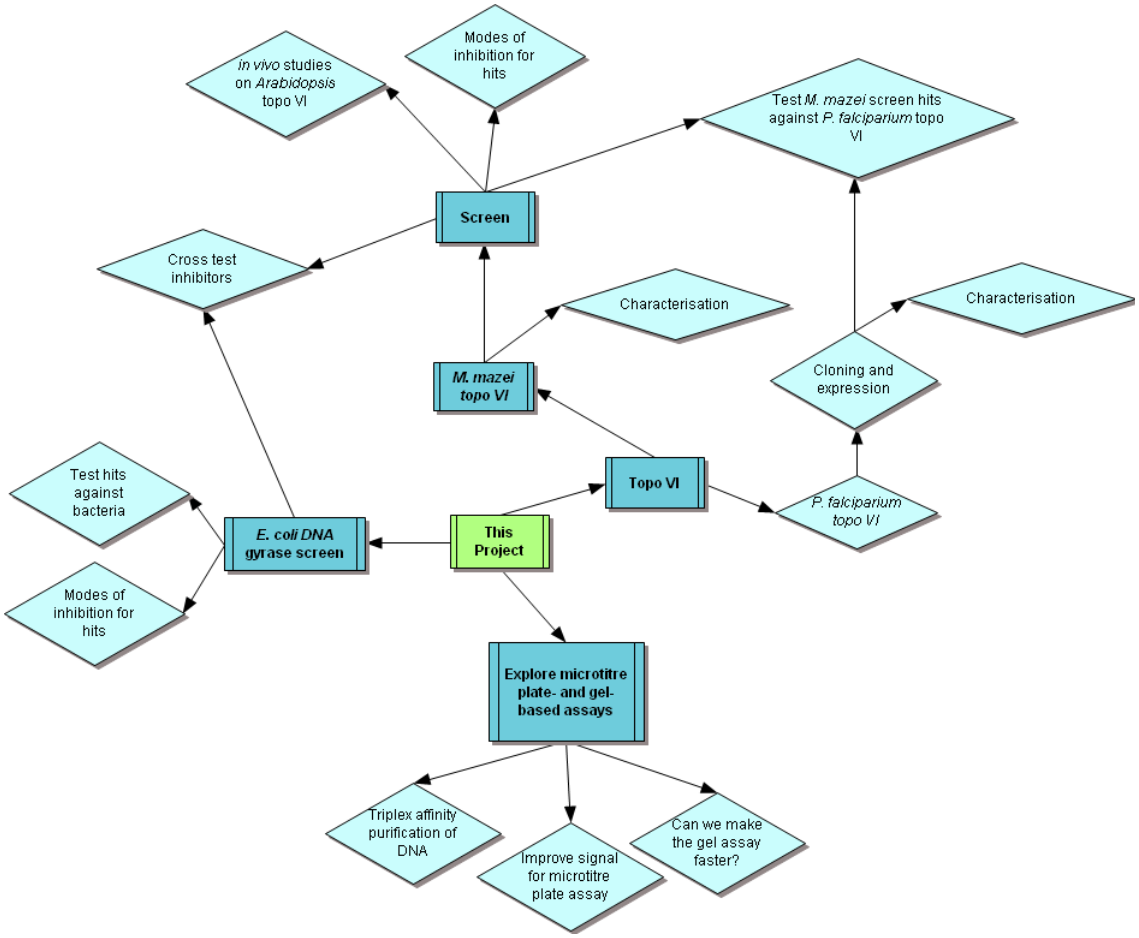

Figure 1.29 A general outline of project. *E. coli* DNA gyrase screen would be pursued first, followed by the *M. mazei* topo VI screen and the morphological screening of *M. mazei* topo VI screen hits against *Arabidopsis* seedlings. Other areas of study would be pursued as opportunity presented itself.

Chapter 2

Materials and Methods

2.1 Buffers and solutions

Buffer/solution	Details
DNA gyrase dilution buffer	50 mM Tris·HCl (pH 7.5), 100 mM KCl, 2 mM DTT, 1 mM EDTA, 10% (w/v) glycerol. Store at -20°C.
Calcium acetate	75 mM calcium acetate (pH 4.7). Filtered with 0.2 μm filter. Store at room temperature.
Chicken erythrocyte topoisomerase I dilution buffer	10 mM Tris·HCl (pH 7.5), 1 mM DTT, 1 mM EDTA, 50 % (v/v) glycerol, 100 mg/mL bovine serum albumin.
Chicken erythrocyte topoisomerase I relaxation buffer	20 mM Tris·HCl (pH 8), 200 mM NaCl, 0.25 mM EDTA, 5% glycerol. The buffer is stored as a 10× concentrate at -20°C.
DNA gyrase relaxation buffer	35 mM Tris·HCl (pH 7.5), 24 mM KCl, 4 mM $MgCl_2$, 2 mM DTT, 6.5% (w/v) glycerol, 0.1 mg/mL bovine serum albumin. The buffer is stored as a 5× concentrate at -20°C.
DNA gyrase supercoiling buffer	35 mM Tris·HCl (pH 7.5), 24 mM KCl, 4 mM $MgCl_2$, 2 mM DTT, 1.8 mM spermidine, 1 mM ATP, 6.5% (w/v) glycerol, 0.1 mg/mL bovine serum albumin. The buffer is stored as a 5× concentrate at -20°C.

Gel shift binding buffer (5x)	250 mM Tris·HCl (pH 7.5), 500 mM KCl, 25 mM $MgCl_2$, 10 mM DTT, 50% w/v glycerol).
STEB (x2)	40% sucrose, 100 mM Tris·HCl (pH 8.0), 100 mM EDTA, 0.5 mg/mL bromophenol blue.
T10E1 buffer	10 mM Tris·HCl (pH 8.0), 1 mM EDTA. Filtered with 0.2 μm filter. Store at room temperature.
TAE	40 mM Tris·Acetate (pH 8.0), 1 mM EDTA.
TBM	90 mM Tris·Borate (pH 7.5), 4 mM $MgCl_2$.
Topoisomerase VI dilution buffer	20 mM HEPES pH 7.5, 10% (v/v) glycerol. Store at -20°C.
Topoisomerase VI relaxation buffer	20 mM bis-tris propane (pH 6.5), 100 mM potassium glutamate, 10 mM $MgCl_2$, 1 mM DTT, and 1 mM ATP. The buffer is stored as a 5× concentrate at -20°C.
Triplex formation (TF) buffer	75 mM magnesium acetate (pH 4.7). Filtered with 0.2 μm filter. Store at room temperature.
Wash Buffer	20 mM Tris·HCl (pH 7.6), 137 mM NaCl, 0.01% (w/v) bovine serum albumin (acetylated), 0.05% (v/v) Tween-20. Filtered with 0.2 μm filter. Store at 4°C.
Wheat germ topoisomerase I dilution buffer	50 mM Tris·HCl (pH7.9), 1 mM EDTA, 1 mM DTT, 50% (v/v) glycerol, 500 mM NaCl
Wheat germ topoisomerase I relaxation buffer	50 mM Tris·HCl (pH7.9), 1 mM EDTA, 1 mM DTT, 20% (v/v) glycerol, 50 mM NaCl

Table 2.1 Commonly used buffers and solutions.

2.2 Antibiotics

Stock solutions of antibiotics were prepared at the concentration detailed below (Table 2.2). All antibiotics were purchased from Sigma. Stock solutions were prepared with Milli-Q water; filter sterilized and stored at minus 20°C.

2.3 Microbiology

2.3.1 Strains and species

The *Escherichia coli* strains used in this work are detailed below (Table 2.3). *Mycobacterium smegmatis* mc^2155 (wild-type) was used for the *M. smegmatis* studies.

2.3.2 Growth media

E. coli growth was carried out in a range of media as detailed below. All media was sterilized by autoclaving. When solid media was required 15 g of Bacto Agar per litre of media was added before autoclaving. Solid media was melted in a microwave prior to the pouring of plates, and allowed to cool to ~50 °C before any thermolabile substances were added (i.e. antibiotics).

Antibiotic	**Stock concentration** (mg/mL)	**Final concentration** (µg/mL)
Ampicillin*	100	100
Chloramphenicol**	35	35
Kanamycin*	50	50 or 100 (in autoinduction medium)
Neomycin*	5	5
Penicillin*	5	5
Streptomycin*	10	10
Tetracycline*	10	10
Gentamicin*	7	7

Table 2.2 Summary of antibiotic stocks and working concentrations. * in Milli-Q water. ** in 100% ethanol.

Strain	Genotype
BL21(DE3) (Studier & Moffatt, 1986)	*E. coli* B F- *dcm ompT hsdS*(r_B- m_B-) gal [malB$^+$]$_{K-12}$(λ^S)
DH5α (Invitrogen)	F$^-$ endA1 glnV44 thi-1 recA1 relA1 gyrA96 deoR nupG Φ80d*lacZ*ΔM15 Δ(*lacZYA-argF*)U169, hsdR17(r_K^- m_K^+), λ–
DH10Bac (Invitrogen)	F$^-$ *mcr*A Δ(*mrr-hsd*RMS-*mcr*BC) Φ80*lac*ZΔM15 Δ*lac*X74 *rec*A1 *end*A1 *ara*D139 Δ(*ara leu*) 7697 *gal*U *gal*K λ– *rps*L *nup*G/ pMON14272/pMON7124
JM109(pLysS) (Yanisch-Perron et al, 1985)	F´ *traD*36 *proA*$^+$*B*$^+$ *lac*I^q Δ(*lac*Z)M15/Δ(*lac-proAB*) *glnV*44 e14$^-$ *gyrA*96 *recA*1 *relA*1 *endA*1 *thi hsdR*17 pLysS (Cam^R).
MG1655 (Blattner et al, 1997)	F$^-$, lambda$^-$, rph-1
NR698 (Ruiz et al, 2005)	F$^-$ [araD139]$_{B/r}$ Δ(argF-lac)169* &lambda$^-$ e14- flhD5301 Δ(fruK-yeiR)725 (fruA25)‡ relA1 rpsL150(strR) rbsR22 Δ(fimB-fimE)632(::IS1) deoC1 imp4213
Rosetta (Novagen)	F$^-$ *ompT hsdS*$_B$(r_B^- m_B^-) *gal dcm* pRARE (Cam^R)
Rosetta 2 (Novagen)	F$^-$ *ompT hsdS*$_B$(r_B^- m_B^-) *gal dcm* pRARE2 (Cam^R)
Top10 (Invitrogen)	F$^-$ mcrA Δ(mrr-hsdRMS-mcrBC) φ80lacZΔM15 ΔlacX74 nupG recA1 araD139 Δ(ara-leu)7697 galE15 galK16 rpsL(Str^R) endA1 λ$^-$

Table 2.3 Summary of *E. coli* strains and genotypes.

Auto Induction Medium (AIM): 0.1% (w/v) Tryptone, 0.05% (w/v) yeast extract, 0.0033% $(NH_4)_2SO_4$, 0.0068% (w/v) KH_2PO_4, 0.0071% (w/v) Na_2HPO_4, 0.0005% (w/v) glucose, 0.002% (w/v) α-lactose, 0.00015%, (w/v), $MgSO_4$, 0.00003% (w/v), trace elements.

Luria-Bertani (LB) medium: 1% w/v tryptone, 0.05% w/v yeast extract, 1% w/v NaCl, adjusted to pH 7 with 10 M NaOH.

Middlebrook broth 7H9 (Difco): 0.05% (w/v) L-glutamic acid, 0.25% (w/v) Na_2HPO_4, 0.1% (w/v) NaH2PO4, 0.05% (w/v) $(NH_4)_2SO_4$, 0.01% (w/v) sodium citrate, 0.004% (w/v) ferric ammonium citrate, 0.005% (w/v) $MgSO_4$, 0.0001% (w/v) $CuSO_4$, 0.0001% (w/v) pyridoxine, 0.0001% (w/v)

$ZnSO_4$, 0.00005% (w/v) biotin, 0.000025% (w/v) malachite green, 0.00005% (w/v) CaCl. Supplement with Middlebrook ADC enrichment.

Middlebrook ADC enrichment (10x) (Difco): 5% (w/v) bovine albumin fraction V, 2% (w/v) dextrose, 0.003% (w/v) catalase.

Middlebrook 7H11 agar (Difco): 0.1% (w/v) enzymatic digest of casein, 0.15% (w/v) Na_2HPO_4, 0.15% (w/v) KH_2PO_4, 0.05% (w/v) $(NH_4)_2SO_4$, 0.05% (w/v) monosodium glutamate, 0.04% (w/v) sodium citrate, 0.004% (w/v) ferric ammonium citrate, 0.005% (w/v) $MgSO_4$, 0.0001% (w/v) $CuSO_4$, 0.0001% (w/v) pyridoxine, 0.0001% (w/v) $ZnSO_4$, 0.00005% (w/v) biotin, 0.000025% (w/v) malachite green, 1.35% (w/v) agar

Plasmid DNA medium (PDM) (Danquaha & Fordea, 2007): 0.79% tryptone, 0.44% w/v yeast extract, 0.05% w/v NH_4Cl and 0.024% w/v $MgSO_4$. After autoclaving add glucose to 1% w/v and 10x PDM phosphate buffer to 1x.

PDM phosphate buffer (10x): 12.8 % w/v $Na_2HPO_4.7H_2O$, 3% w/v KH_2PO_4.

SOC medium: 2% w/v tryptone, 0.5% w/v yeast extract, 10 mM NaCl, 2.5 mM KCl, 10 mM $MgCl_2$, 10 mM $MgS0_4$, 20 mM glucose.

2.3.3 Preparation of chemically competent cells

Competent cells were generated by a $CaCl_2$ method. *E. coli* to be made competent were grown overnight in LB media. A 4 mL inoculum was then taken and added to 50 mL LB in a 250 mL conical flask. Cells were grown until the culture had entered early mid-log phase (~ 2 hrs) then centrifuged at 3453 x g for 4 minutes at 4°C (Sorvall Legend RT centrifuge, Heraeus rotor). The supernatant was then discarded and 50 mL of ice cold $CaCl_2$ (50 mM) was added. Cells were gently resuspended and left on ice for 30 min., after which they were centrifuged at 3453 x g for 3 minutes at 4°C. The cells were quickly returned to ice and the supernatant discarded. The pellet was then resuspended in 0.5 mL 50 mM $CaCl_2$, 15% (v/v) glycerol. After a further 30 minutes on ice the cells were dispensed into 50 μL aliquots, snap-frozen in liquid nitrogen and stored at -80°C.

2.3.4 Halo assays

For *E. coli* work a 10 mL culture of *E. coli* MG1655 or NR698 was grown overnight at 37°C. Petri dishes containing LB agar were prepared aseptically and 100 μL of culture was spread across their surface. Filter disks soaked in compound were then applied to the surface and the bacteria allowed to grow at 37°C. The zone of clearing for each disk acted as an indicator of the compounds antimicrobial activity.

For work on *M. smegmatis* a 50 mL culture was grown for 48 hrs in Middlebrooks 7H9 media at 37°C. Bacterial lawns were grown on Middlebrooks 7H11 agar for 48 hrs at 37°C.

2.3.5 Slope assays

A 10 mL culture of *E. coli* MG1655 or NR698 was grown overnight at 37°C. The culture was then diluted 1:1000 and streaked on Petri dishes containing LB agar. Colonies were allowed to develop by incubation of the plates at 37°C overnight. Alternatively, 50 mL of *M. smegmatis* was grown for 48 hrs at 37°C, spread on Middlebrooks 7H11 agar and grown for 48 hrs at 37°C.

The following day 50 mL of molten LB or Middlebrooks 7H11 agar was prepared and the desired concentration of test compound added. A 100 mm square Petri dish was propped at ~45^{o} to horizontal and the agar poured in. After the agar had set the dish was returned to horizontal and another 50 mL of molten agar (this time lacking compound) was added. This resulted in a gradient of compound concentration across the plate. Colonies from both strains were then streaked with a toothpick across the gradient and the plates incubated at 37°C overnight.

2.3.6 Liquid-culture growth assays

For *E. coli* work, a 10 mL culture of *E. coli* MG1655 or NR698 was grown overnight at 37°C. A 100 μL aliquot of the overnight culture was then added to 10 mL LB containing the desired concentration of compound. The culture was then allowed to grow at 37°C for 5 hours and its OD_{600} measured every hour.

For work on *M. smegmatis* a 50 mL culture was grown for 48 hrs in Middlebrooks 7H11 media at 37°C. A 100 μL of the overnight culture was then added to 10 mL Middlebrooks 7H11 containing the desired concentration of compound. The culture was then allowed to grow at 37°C for 9 hours and its OD_{600} measured every three hours.

2.3.7 Colony counting assays

A 50 mL culture of *M. smegmatis* was grown for 48 hrs in Middlebrooks 7H9 media at 37°C. Cultures of 10 mL Middlebrooks 7H9 media containing the desired concentration of each compound were then inoculated with 100 μL and allowed to grow at 37°C overnight. After 16 hours, 20 μL samples were taken from the cultures and diluted 1 in 10, 000 with Middlebrooks 7H9 media. Petri dishes containing Middlebrooks 7H11 agar were prepared and 100 μL of each diluted culture was spread out. The plates were subsequently stored at 4°C. This was repeated every three hours for six hours, after which the plates were transferred to 37°C for 48 hrs. The numbers of colonies for each time point were counted manually.

2.4 Arabidopsis Methods

2.4.1 Arabidopsis lines used

All experiments in this work were carried out on the *Arabidopsis thaliana columbia* (Col-0) line.

2.4.2 Seed sterilization

Seeds were surface sterilized with 5% bleach for 10 mins immediately prior to use. The seeds were then washed three times with sterile water under a laminar flow hood.

2.4.3 Hypocotyl extension assays

MS Salts medium (Murashige & Skoog, 1962) (micro and macro elements including vitamins, pH 5.8) was supplemented with 1 g/L sucrose and 0.7g/L phytagel (Sigma) before autoclaving. After the medium cooled to ~50°C it was divided into 50 mL aliquots and compounds to be tested (or

an equivalent amount of appropriate solvent for the controls) then added to the desired concentration under aseptic conditions. The media were then poured into separate 100 mm square Petri dishes and allowed to cool to room temperature in a laminar flow hood. Surface sterilized seeds were then planted in a grid pattern (32 seeds per dish) and the dishes sealed with surgical tape.

The plates were transferred to 4°C and left for 64 hrs in the dark to vernalise, after which they were transferred to a 22°C growth cabinet. After 2 hrs of light exposure the plates were stacked vertically in the dark at 22°C to allow for hypocotyl extension along the agar's surface. After 4-5 days the hypocotyls were observed using an optical microscope and their length measured.

2.4.4 Flow cytometry experiments

Flow cytometry experiments were carried out using a Partec PAS flow cytometer. Samples (either rosettes or hypocotyls) were finely chopped with a sharp razor blade in 1 mL nuclear extraction buffer (Partec) and passed through a 30 μM CellTric filter (Partec). A 1 mL solution of DAPI (4', 6-diamidino-2-phenylindole) staining buffer (CyStain UV Precise P, Partec) was then added. After approximately 30 seconds the sample was loaded into the cytometer. Samples were excited with a HBO mercury lamp (filters KG1, BG38, UG1) and their emission detected (FL-4, filter GG435) to an average of 20, 000 stained particle counts.

2.4.5 Cryo- Scanning Electron Microscopy (SEM) on hypocotyls

Five day old hypocotyls grown on media containing various concentrations of compound were frozen in nitrogen slush and loaded into a Philips XL30 SEM with a cyro stage installed. Samples were sputter coated with platinum and transferred into the microscope chamber for image collection.

2.5 Plasmids and oligonucleotides

2.5.1 Oligonucleotides

The oligos used within this study were as follows (written 5' to 3'):

TFO1: TCTCTCTCTCTCTCTC (5' modification: biotin)

TFO1C: CCGACTCTCTCTCTCTCTCT

TFO1W: TCGGAGAGAGAGAGAGAGAG

2.5.2 Substrate plasmids

The following plasmids were used as substrates in the topoisomerase assays carried out during the course of this work:

*pBR322** (Boros et al, 1984): A high-copy number plasmid containing a single point mutation to increase copy number.

pNO1 (Maxwell et al, 2006): A modified version of pBR322* containing a triplex-forming insert. It was prepared by ligation of oligos TFO1W and TFO1C into the AvaI site of the plasmid.

2.5.3 Small-scale preparation of plasmid DNA

Plasmids preparations for cloning and transformation were prepared using a QIAprep Spin Miniprep kit (QIAGEN).

2.5.4 Large-scale preparation of plasmid DNA

Large-scale preparation of pNO1 for use in screening was carried out as in the established protocol (Jordan et al, 1999) with a few modifications. *E. coli* JM109 was transformed with the pNO1 plasmid. A 4 mL inoculum from a 10 mL overnight culture was added to 400 mL of PDM containing ampicillin and the cells grown at 37 °C, 300 rpm for 18 hours in a 2 L baffled flask.

The cells were then pelleted by spinning at 6000 x g (Evolution RC centrifuge, S-3000 rotor, Sorvall) for 10 mins at 4 °C. The supernatant was discarded and the pellet kept on ice whilst being resuspended in 32 mL

chilled GTE (500 mM glucose, 250 mM Tris·HCL pH7.5, 100 mM EDTA). A solution of 8 mL of GTE containing 20 mg/mL lysozyme was added and the cells incubated on ice for a 5 mins. A solution of 0.2 M NaOH and 2% SDS was freshly prepared and 80 mL added to the cell suspension. The suspension was carefully agitated by inversion and the cells allowed to lyse for a further 5 minutes on ice. The solution was neutralised by the addition of 45 mL of high salt solution (3 M KAc, 5% (v/v) formic acid) and carefully inverted several times. This was followed by a final incubation on ice for 5 minutes. Waste precipitate was pelleted by centrifuging at 10,000 x g for 10 mins at 4 °C (Evolution RC centrifuge, S-3000 rotor, Sorvall). The supernatant was transferred to a fresh tube and spun again to ensure complete removal of debris.

The nucleic acids were then precipitated with propanol as described in section 2.5.6 and resuspended in 65 mL T10E1. For each mL of sample 1 g of caesium chloride was added and dissolved. The preparation was then transferred into 2x 35 mL ultracrimp tubes (Sorvall). Tubes were filled to the shoulder then 210 µL of 10 mg/mL ethidium bromide was added followed by the remainder of the preparation. The tubes were meticulously balanced, sealed and inverted several times. Care was taken to minimise exposure to light from this point. The gradient was formed by centrifugation at 350,000 x g for 16 hrs at 18 °C (WX ultra series centrifuge, TV-860 rotor, Sorvall), with a low deceleration rate.

After centrifugation, the tubes were secured with a clamp and pierced towards their top with a syringe needle. A wide bore syringe was used to carefully draw off the single visible band. The ethidium bromide was then removed by multiple extractions with aqueous butanol and the DNA precipitated as described in section 2.5.6. The concentration of the DNA was measured as in section 2.5.8 and its topological purity quantified by agarose gel electrophoresis (see section 2.7.1). The CsCl gradient steps were repeated until supercoiled pNO1 of sufficient purity was obtained.

2.5.5 Preparation of relaxed pNO1

Relaxed pNO1 was prepared by incubating the supercoiled form with chicken erythrocyte topoisomerase I (~40-50 µg plasmid with 200 units topoisomerase I in 1x Chicken erythrocyte topoisomerase I relaxation buffer) for 1 hr at 37°C. The DNA was extracted with two phenol: chloroform:isoamyl alcohol (section 2.5.6) extractions and purified by ethanol precipitation.

2.5.6 Phenol: chloroform:isoamyl alcohol extraction

Where thorough removal of bound protein or intercalators from DNA was needed, extractions were performed with a mixture of 24:24:1 phenol: chloroform:isoamyl alcohol. An equal volume of phenol mixture to sample was added and the two phases mixed either by vortexing or vigorous pipetting. The samples were then spun at 15,700 x g for 5 minutes. The organic phase was then removed and an equal volume of chloroform added before the sample was once again vortexed and spun at 15,700 x g for 5 minutes. The aqueous phase was then removed and retained.

2.5.7 Precipitation of DNA

Precipitation of DNA was carried out as detailed by *Zeugin and Hartley* (Zeugin & Hartley, 1985). The solution containing DNA was mixed with 10% volume 3 M KAc and either two volumes propan-2-ol or three volumes ethanol. The mixture was transferred to glass Corex tubes and incubated at room temperature for 15 mins before centrifugation at 16, 000 x g for 45 minutes at 21°C to pellet the DNA (Evolution RC centrifuge, SS-34 rotor, Sorvall). The supernatant was drained and replaced with 80% ethanol. The solution was spun for a further 10 minute centrifugation at 16,000 x g, room temperature DNA (Evolution RC centrifuge, SS-34 rotor, Sorvall). The supernatant was discarded and the tubes spun briefly to draw residual liquid to the bottom which was then removed by pipetting. The DNA was carefully resuspended in the desired volume of T10E1 buffer. For smaller scale precipitations the above procedure was carried out using Eppendorf tubes

and centrifugation at 6000 x g for 10 min (5415D centrifuge, F45-24-11 rotor, Eppendorf).

2.5.8 Determination of DNA concentrations

DNA concentration was determined either with a BioPhotometer (Eppendorf) or a Lambda 18 UV/Vis spectrometer (Perkin Elmer) with paired quartz cuvettes. The former was primarily used for cloning work whilst the latter was used to determine the concentrations of substrate plasmids. Samples were diluted 1 μL with 49 μL Milli-Q water and the absorbance at 260 nm was recorded. The concentration of DNA was determined by the Beer-Lambert Law (Equation 2.1).

$$A = \varepsilon l c$$

Equation 2.1 The Beer-Lambert Law. A = absorbance; ε = extinction coefficient (dsDNA = 0.020 (μg/mL)$^{-1}$ cm^{-1}); l = path length (cm); c = concentration (μg/mL).

2.5.9 Polymerase Chain Reaction (PCR)

The polymerase chain reaction (PCR) was used for the cloning of DNA, with either Pfu (from *Pyrococcus furiosus*) or Taq (from *Thermus aquaticus*) DNA polymerases utilised (Pfu Ultra from Agilent Technologies, GoTaq from Promega). Reactions with GoTaq were typically carried out in 20 μL reaction volumes containing 10 μL GoTaq Master Mix (Promega), 50-500 ng DNA template and 100 pmol of oligonucleotide primers. All PCR reactions were carried out in a PTC-200 Thermo Cycler (MJ Research).

Three types of PCR reaction were carried out: constant temperature (Table 2.4), touchdown (Korbie & Mattick, 2008) (Table 2.5) or colony. Colony PCR was identical to constant temperature PCR but instead of a DNA template a single colony of interest was picked and swirled in the reaction mix. The reaction was then heated for 5 min. at 94°C during the initial denaturing step rather than 3 min. Touchdown PCR was primarily used to obtain products which constant temperature PCR failed to produce. Initial rounds of primer annealing start above melting temperature of primers and decreases 1°C after each cycle. This helps eliminate non-specific annealing. Final rounds of primer annealing are carried out at a constant temperature.

Temperature	Time	No. cycles	Purpose
94°C	3 min.	1	Initial denaturing
94°C	45 sec	30	Denaturation
50-70°C (~5°C below Tm of primers)	45 sec		Primer annealing
72°C	1 min. per kb of product.		DNA synthesis
72°C	10 min.	1	Completes any partial products.
10°C	Forever	1	

Table 2.4 Constant temperature PCR.

of 55°C to amplify product. At this point specific product should be numerous enough to out-compete any non-specific interactions.

2.5.10 Restriction digests and ligations

Restriction digests were carried out with a wide range of restriction endonucleases from New England Biolabs. In general, the desired amount of substrate DNA was incubated with 1-200 units endonuclease and the appropriate reaction buffer (New England Biolabs) in a reaction volume of 50 μL at 37°C for 1-2 hrs. Samples were then treated with 2x STEB and the product of the digestion gel purified (Section 2.5.11).

Ligations were carried out in 10 μL reaction volumes with 400 units T4 DNA ligase (New England Biolabs), 1 x ligation buffer (New England Biolabs), and 50-100 ng linear DNA (vector to insert ration 1:3). The reaction was allowed to proceed for at least 30 minutes at room temperature.

2.5.11 Isolation of PCR products from agarose gels

Linear products from PCR and restriction digests were purified by electrophoresis on a 1% (w/w) agarose gel. The required bands were excised and purified using a QIAquick Gel Extraction kit (QIAGEN) as per the supplied protocol.

Temperature	Time	No. cycles	Purpose
94°C	3 min.	1	Initial denaturing
94°C	45 sec	10	Denaturation
Initially 60-80°C (~2°C above Tm of primers) -1°C per cycle	45 sec		Primer annealing
72°C	1 min. per kb of product.		DNA synthesis
94°C	45 sec		Denaturation
Initially 60-80°C (~2°C above Tm of primers) -1°C per cycle	45 sec		Primer annealing
72°C	1 min. per kb of product.		DNA synthesis
94°C	45 sec	15	Denaturation
55°C	45 sec		Primer annealing
72°C	1 min. per kb of product.		DNA synthesis
72°C	10 min.	1	Completes any partial products.
10°C	Forever	1	

Table 2.5 Touchdown PCR program.

2.5.12 DNA Sequencing

DNA was sequenced using a BigDye v3.1 kit (Applied Bioscience) in a 10 μL reaction volume. Reactions contained BigDye 3.1 mix, 1x reaction buffer, 50-100 ng DNA template and 20 μM sequencing primer. Reactions were carried out in a PTC-200 Thermo Cycler (MJ Research) with the program detailed below (Table 2.6). Once the reaction was completed the samples were sent to The Genome Analysis Centre (John Innes Centre) for

Temperature	Time	No. cycles	Purpose
95°C	1 min.	1	Initial denaturing
95°C	30 sec	30	Denaturation
45°C	15 sec		Primer annealing
60°C	4 min.		DNA synthesis
72°C	10 min.	1	Completes any partial products.
10°C	Forever	1	

Table 2.6 Program for BigDye 3.1 sequencing reactions.

processing. Sequencing data was returned in the form of .txt and .abi chromatogram trace files.

2.6 Protein preparation

2.6.1 Insect cell culture conditions

Spodoptera frugiperda Sf21 cells were grown in TC-100 media with L-glutamate (PAA), 10% (v/v) fetal calf serum (FCS), penicillin, streptomycin and neomycin at 27°C. Cells were cultured in 75 cm^2 culture flasks (PAA) until confluent then harvested by sloughing and subcultured into fresh flasks. After 30 passages the cells were discarded and fresh cultures were prepared from frozen stocks. The initial Sf21 cells were a kind gift from Dr Keith Saunders.

2.6.2 *Escherichia coli* GyrA

E. coli GyrA was expressed and purified as per published protocols (Maxwell & Howells, 1999). *Escherichia coli* JM109 (pLysS) was transformed with the expression plasmid pPH3 (Hallett et al, 1990). A 10 mL inoculum from a 100 mL overnight grown culture was added to 1 L LB containing chloramphenicol and ampicillin. The cells were allowed to grow at 37°C until they reached an OD_{600} of around 0.4, whereupon expression was induced by the addition of IPTG to the final concentration of 0.2 mM. The culture was

incubated for a further 4 hours at 37°C before being spun at 6000 x g for 10 min. (Evolution RC centrifuge, S-3000 rotor, Sorvall). The supernatant was discarded whilst the pellets were resuspended in 30 mL of Tris·HCL pH 7.5, 10% sucrose and EDTA-free protease inhibitors (Roche). The cells were then lysed by freeze-thawing.

Upon thawing DTT, EDTA and KCl were added to 2 mM, 1 mM and 50 mM respectively. The cells were then spun for 1 hr at 120, 000 x g (WX ultra series centrifuge, T-865 rotor, Sorvall) and the supernatant decanted. The supernatant was loaded onto a Hi-Load Q-Sepharose column (2.5 mL/min., Pharmacia 16/10) and developed with a shallow gradient (250 mL) 0-450 mM NaCl in TED (50 mM Tris·HCL (pH 7.5), 1mM EDTA, 2 mM DTT). Fractions containing GyrA were identified via SDS-PAGE (section 2.6.9) and pooled before dialyse overnight at 8°C into DNA gyrase dilution buffer. Protein concentration was determined by Bradford assay (section 2.6.8) before the enzyme was snap-frozen in liquid nitrogen and stored at -80°C.

2.6.3 *Escherichia coli* GyrB

E. coli GyrB was expressed and purified as per published protocols (Maxwell & Howells, 1999). *Escherichia coli* JM109 (pLysS) was transformed with the expression plasmid pAG111(Hallett et al, 1990). Cultures of 1 L were prepared and induced as with the expression of GyrA above.

After freeze-thaw lysis DTT, EDTA and KCl were added to 2 mM, 1 mM and 50 mM respectively. Cells were then spun for 1 hr at 34,000 rpm and the supernatant decanted. The lysate was then diluted 50:50 in TGED buffer (50mM Tris·HCL pH 7.5, 10% glycerol (w/v), 1mM EDTA, 2mM DTT) +200 mM NaCl. Diluted lysate was applied to a 350 mL Heparin-Sepharose column (2.5 mL/min., Pharmacia 16/10). GyrB was eluted by stepping off with TGED +400 mM NaCl. Fractions containing GyrB were identified by SDS-PAGE (section 2.6.9), pooled and dialysed into TGED overnight at 8°C. The protein was then loaded onto a Mono-Q column (0.75 mL/min., Pharmacia) and developed with a shallow gradient of 0-400mM NaCl in TED. Fractions containing GyrB were identified by SDS-PAGE, pooled and dialysed into gyrase elution buffer overnight at 8°C. Protein concentration was

determined by Bradford assay (section 2.6.8) before the enzyme was snap-frozen in liquid nitrogen and stored at -80°C.

2.6.4 *Methanosarcina mazei* topoisomerase VI

M. mazei topoisomerase VI was expressed and purified as per published protocols (Corbett et al, 2007). Codon Plus *E. coli* were transformed with a polycistronic duel expression vector *for M. mazei top6A* and *top6B* (Corbett et al, 2007). The proteins were overexpressed in autoinduction growth media containing kanamycin by incubating for 24 hrs at 37^{o}C (the expression vector was kindly gifted by Prof. James M. Berger and Dr Kevin. Corbett; University of California Berkley). The cells were harvested by centrifugation at 9900 x g, 4^{o}C for 10 min. (Evolution RC centrifuge, S-3000 rotor, Sorvall), resuspended in Buffer A (20 mM HEPES pH 7.5, 10% (v/v) glycerol, 800 mM NaCl, 20 mM imidazole, 2 mM β-mercaptoethanol, EDTA-free protease inhibitors) and lysed by freeze-thawing and French press.

The lysate was centrifuged at 48, 000 x g, for 1 hr at 4^{o}C (Evolution RC centrifuge, SS-34 rotor, Sorvall). The clarified lysate was then passed over a HisTrap™ FF Ni^{2+} affinity column (5 mL/min, GE Healthcare) and washed with Buffer B (20 mM HEPES pH 7.5, 10% (v/v) glycerol, 150 mM NaCl, 20 mM imidazole, 2mM β-mercaptoethanol, EDTA-free protease inhibitors). The protein was eluted with a 20-300 mM imidazole gradient (70 mls, 5 mL/min.) and the protein containing fractions passed through a HisTrap™ SP Sepharose HP column (3 mL/min, GE Healthcare) in Buffer B to remove proteolyzed B-subunits. The flow-through was collected and waste protein bound to the column was stepped off with 800 mM NaCl. The flow-through was loaded onto a HisTrap™ Q HP (3 mL/min, GE Healthcare) column in Buffer B the protein eluted with a 150-800 mM NaCl gradient over 70 mls. The fractions were pooled and the amount of protein present was determined by a Bradford assay (section 2.6.8).

The protein was then incubated overnight at 4°C with His-tagged Tobacco Etch Virus (TEV) protease using a ratio of 1:50 (wt/wt) TEV protease: *M. Mazei* topo VI. The protein was passed over a second Ni^{2+} affinity column to remove uncleaved protein, uncleaved tags, and His-tagged TEV protease. The flow-through was collected and waste protein

stepped off with 0.5 M imidazole. The flow-through was passed through a S300 gel filtration column (0.5 mL/min., GE Healthcare) in Buffer C (20 mM HEPES pH 7.5, 10% (v/v) glycerol, 150 mM NaCl, 500 mM imidazole, 2 mM β-mercaptoethanol, EDTA-free protease inhibitors). The fractions containing protein were identified with SDS-PAGE, pooled and concentrated with centrifugal concentrators (10-30 kDa molecular weight cut offs) by centrifugation at 3250 x g at 4°C (Sorvall Legend RT centrifuge, Heraeus rotor). Fractions were pooled, concentrated by ultrafiltration, and aliquots were frozen in liquid nitrogen and stored at -80°C. Protein concentration was determined by Bradford assay (section 2.6.8) before the enzyme was snap-frozen in liquid nitrogen and stored at -80°C.

2.6.5 *Plasmodium falciparum* hypothetical topoisomerase VI

Expression trials were carried out with the hypothetical *Plasmodium falciparum* topoisomerase VI genes *PF10_0412* (PfTopo6A1), *PFL0825c* (PfTopo6A2) and *MAL13P1.328* (PfTopo6B) identified by *Aracind et al* (Aravind et al, 2003). PfTopo6A1 and PfTopo6A2 were cloned into the pET28-a (Novagen) expression vector and trials conducted with *E. coli* strains BL21 (pLysS), Codon Plus, Rosetta and Rosetta 2.

Expression trials were carried out in a baculovirus-insect cell expression system (*Spodoptera frugiperda* Sf21 cells) as per the Bac-to-Bac™ Expression System Manuel (Invitrogen). PfTopo6A1, PfTopo6A2 and PfTopo6B were cloned into the pFastBac-Duel baculovirus expression vector then transformed into *E. coli* strain DH10Bac containing a bMON14272 baculovirus shuttle vector (bacmid) and a transposition helper plasmid (pMON7124). After transformation Tn7 transposition occurs, transferring the gene of interest into the bacmid. The transformation mix is then plated on LB agar plates containing kanamycin, tetracycline, gentamycin and 200 μg/mL X-gal (bromo-chloro-indolyl-galactopyranoside). The plates were incubated at 37°C for 48 hrs and recombinant colonies chosen by blue-white selection. Selected colonies were picked and transferred to 1 mL PDM media containing tetracycline and gentamicin.

The cells were allowed to grow overnight at 37°C then centrifuged 6000g for 10 min (5415D centrifuge, F45-24-11 rotor, Eppendorf). The supernatant was discarded and the cell pellet resuspended gently in 0.3 mL of 15 mM Tris·HCl pH 8.0, 10 mM EDTA, 100 μg/mL RNAse. A solution of 0.3 mL 0.2M NaOH, 1% SDS was then added and samples gently mixed. After 5 mins. at room temperature 0.3 mL of 3 M KAc (pH 5.5) was added and the samples transferred to ice for 10 mins. The samples were then centrifuged at 6000 x g for 10 min (5415D centrifuge, F45-24-11 rotor, Eppendorf). The supernatant was transferred to a fresh tube and 0.8 mL propan-2-ol was added. After a further 10 min. on ice the samples were centrifuged at 6000 x g for 45 min. at room temperature (5415D centrifuge, F45-24-11 rotor, Eppendorf). The supernatant was then discarded, the samples spun briefly once more and residual propan-2-ol removed by pipetting. The DNA was then carefully resuspended in 40 μL T10E1 buffer.

Approximately 1x 10^6 SF21 insect cells in Complete TC-100 media with L-glutamate (PAA) (+10% (v/v) FCS, penicillin, streptomycin and neomycin) were placed in 35 mm cell culture dishes and allowed to attach. After approximately 1 hr the media was drained and 2.5 mL Plating Medium (TC-100 media with L-glutamate + 1.5% (v/v) FCS) was added. Solutions of 100 μL 8% (v/v) Cellfectin II (Invitrogen) in TC-100 medium with L-glutamate and 100 μL 1% (v/v) bacmid in TC-100 medium with L-glutamate were prepared, mixed and left at room temperature for 25 min. The mixture was then applied dropwise to the cell cultures and left for 5 hrs. The medium was then removed and replaced with Complete TC-100 media and the cells left to grow at 27°C until they displayed signs of late-stage infection (i.e. detachment from the plate surface after ~ 3 days). P1 viral particles were harvested by removing and retaining the media. Viral particles were stored in the dark at 4°C.

To amplify the viral titre 2x 10^6 SF21 insect cells in Complete TC-100 with L-glutamate media were placed in 35 mm cell culture dishes. After approximately 1 hr 220 μL P1 virus was added and the cells allowed to grow at 27°C until they displayed signs of late-stage infection. P2 virus was harvested by removing and retaining the media. Expression trials were then conducted using P2 viral stocks.

2.6.6 Chicken erythrocyte topoisomerase I

Chicken erythrocyte topoisomerase I was kindly provided as a gift by Mrs. Alison J. Howells of Inspiralis Ltd, Norwich Research Park, Norwich.

2.6.7 Wheat germ topoisomerase I

Wheat germ topoisomerase I was purchased from Inspiralis Ltd.

2.6.8 Protein concentration determination

Protein concentrations were determined by Bradford assay (Bradford, 1976). Bradford reagent was prepared by the addition of 100 mg Coomassie Brilliant blue G to 50 mL of 95% (v/v) ethanol plus 100 mL of 85% (v/v) phosphoric acid and made up to one litre with Milli-Q water. To determine protein concentration, 5 μL of protein solution was diluted to 100 μL in a suitable dilution buffer and mixed with 900 μL Bradford reagent in a 1 cm path length cuvette. Samples were left to react for 5 min. at room temperature, before they were mixed by inversion and their absorbance at 595 nm was measured by a BioPhotometer (Eppendorf). The samples were compared to a blank solution consisting of 100 μL dilution buffer mixed with 900 μL Bradford reagent. The concentration of the samples was obtained by comparison of their absorbance to a calibration curve of BSA standards.

2.6.9 SDS-PAGE

Protein analysis was carried out by sodium dodecyl sulfate polyacrylamide gel electrophoresis (SDS-PAGE) using a Bio Rad Miniprotein-III setup (Bio Rad). Samples were boiled for 5 minutes in 1x SAB (125 mM Tris·HCL, 4% (w/v) SDS, 20% (w/v) glycerol, 10% (v/v) β-mercaptoethanol, 0.002% (w/v) bromophenol blue). Samples were run on 12.5% discontinuous polyacrylamide gels with a 4% stacking gel for 15 min. at 120 V the 1 hr at 200 V. Gels were stained with a Coomassie stain (15% (v/v) acetic acid, 10% (v/v) methanol and 0.1% (w/v) Coomassie stain). Gels were destained in Milli-Q water and photographed using a Syngene GeneGenius Bio-Imaging Gel Doc system (Synoptics).

2.7 DNA topoisomerase assays

2.7.1 Agarose gel electrophoresis assay

The DNA gyrase supercoiling reactions were conducted under the following conditions in a reaction volume of 30 µL: 500 ng of relaxed or negatively supercoiled pNO1, 1x reaction buffer (either DNA gyrase supercoiling or topoisomerase VI relaxation buffer) and up to 5% (v/v) DMSO. Reactions were incubated with 1 unit of DNA gyrase and the desired concentration of drug at 37°C for 30 min. then stopped with 30 µL volume chloroform:isoamyl alcohol (24:1) and 30 µL 2x STEB (+2% (w/v) sodium dodecyl sulphate for *M. mazei* topoisomerase VI reactions). The reactions were vortexed and centrifuged at 6000 x g for 10 min (5415D centrifuge, F45-24-11 rotor, Eppendorf). The upper phase was analyzed by electrophoresis on a 1% agarose gel in TAE buffer for 2-3 hrs at 80 V. The gel was then stained by soaking in 2 µg/mL ethidium bromide for 10 min. and visualized under UV light with a Syngene GeneGenius Bio-Imaging Gel Doc system (Synoptics). One unit of enzyme is defined as the amount of topoisomerase required to supercoil or relax 500 ng of substrate in 30 min. at 37°C under standard assay conditions.

2.7.2 Cleavage-complex stab stabilization assay

Assays to detect the stabilization of cleavage complexes were identical to the protocol for topoisomerase activity detection detailed above except as follows. Cleavage experiments with DNA gyrase were carried out in DNA gyrase relaxation buffer instead of DNA gyrase supercoiling buffer. Reactions were stopped with 3 µL 10% SDS and incubated with 3 µL 1 mg/mL proteinase K solution at 37°C for 1 hr. The reactions were then treated with chloroform:isoamyl alcohol (24:1) and 2x STEB before analysis by gel electrophoresis, as detailed above. For cleavage complex protection assays with suramin, the standard DNA relaxation supercoiling was modified to contain 4 mM CaCl rather than MgCl.

2.7.3 ATPase assay

To determine the effect on ATPase activity of various compounds the required amount of topoisomerase was prepared in clear, colorless 96-well Microtitre plates (Pro-bind™, Becton Dickinson) in a 100 μL reaction containing 1x reaction buffer lacking ATP (DNA gyrase supercoiling or topoisomerase VI relaxation), 800 μM phosphoenolpyruvate (PEP), 400 μM NADH, 1% (vol/vol) PK/LDH (pyruvate kinase-lactate dehydrogenase mixture in 50% (w/v) glycerol,100 mM KCL, 10 mM HEPES (pH 7.0) and compound as desired and 1 mM ATP (initially withheld). The mixture was allowed to sit for 5 min. then initiated by the addition of ATP. A control was always included in which the addition of ATP was replaced with Milli-Q water. The absorbance at 340 nm was then measured over the course of an hour by a Spectra Max Plus absorbance reader (Molecular Devices).

Data was processed by omitting the first 10-15 minutes of collection and normalizing the first retained time point (i.e. the 10 or 15 minute data point). This was done to exclude artifacts observed with this time frame and for ease of comparison of rates. The slope of the control lacking ATP was then subtracted from that of the other reactions to exclude the effect of contaminants.

2.7.4 Native gel-shift assay

Samples of topoisomerase and drug were prepared under the following conditions in a final volume of 10 μL: 1 nM 140 bp linear fragment of DNA derived from pBR322 (Pierrat & Maxwell, 2005) with 1x gel shift binding buffer. Samples were incubated for 30 mins at room temperature before being run on a 5% (29:1) Protogel acrylamide (National Diagnostics) gel in TBM buffer at 150 V for 45 min. The DNA was stained by soaking in 2 mg/mL ethidium bromide for 10 min. and visualized under UV light.

2.7.5 Microtitre plate-based assay

Note: due to the fluorometric nature of the assay it was vital to ensure all solutions were free of particles, which may result in light scattering and increased noise. To eliminate this possibility all solutions should be filtered before use.

Wells in a black 96-well Microtitre plate (Pierce) were washed with 3 x 200 µL of Wash Buffer. The wells were then loaded with 100 µL 500 nM TFO1 oligo (diluted from stock in Wash Buffer) and immobilization was allowed to proceed for 2 min. The oligo solution was removed and the wells washed with 3 x 200 µL volumes of Wash Buffer. Assays were performed in the wells in a 30 µL reaction volume containing: 1-2 units topoisomerase; 1 µg relaxed or negatively supercoiled pNO1 and 1x reaction buffer (DNA gyrase supercoiling buffer or topoisomerase VI relaxation buffer).

The reactions were incubated at 37°C for 30 min. and stopped with the addition of 100 µL TF buffer or 75 mM calcium acetate (pH 4.7). The plate was incubated at room temperature for 30 min. to allow triplex formation to occur. Supercoiled DNA became immobilized on the plate while relaxed DNA remained in solution.

Unbound relaxed and linear plasmid was removed by washing the wells thoroughly with 3 x 200 µL volumes of TF buffer. After the final wash the wells were drained and bound DNA stained with 200 µL 1 x SYBR Gold (Sigma) diluted in T10E1 buffer. The plate was incubated for a further 20 min. at room temperature. After incubation, the contents of the wells were mixed and their fluorescence readings at excitation wavelength 470 nm and emission wavelength 520 nm detected in a SpectraMax Gemini fluorometer (Molecular Devices).

2.8 Screening of a compound library for topoisomerase inhibitors

2.8.1 Library used

Both screens were conducted on the Genplus library from Microsource Ltd., a collection of 960 compounds in twelve 96-well Microtitre plates. The library consists of 80% U.S.A., European, and Japanese approved drugs, with the remaining 20% compounds being experimental entities selected for their unique biological character. Daughter plates were prepared with a compound concentration of approximately 250 µM.

2.8.2 Screening protocol

Twelve plates were screened in duplicate over three days manually using a multichannel pipette. Wells in a black 96-well Microtitre plate (Pierce) plate were washed with 3 x 200 µL of Wash Buffer. The wells were then loaded with 100 µL 500 nM TFO1 oligo (diluted from stock in Wash Buffer) and immobilization was allowed to proceed for 2 min. The oligo solution was removed and the wells washed with 3 x 200 µL volumes of Wash Buffer. A solution of 1 µg pNO1 (relaxed for DNA gyrase or negatively supercoiled for topoisomerase VI) in 27 µL reaction buffer (either DNA gyrase supercoiling buffer or topoisomerase VI relaxation buffer) was then dispensed into each well followed by 3 µL library compound in 100% DMSO giving a final concentration of approximately 25 µM compound. The reactions were then initiated with by the addition of two units of topoisomerase in 30 µL reaction buffer. Each plate contained 16 control reactions: eight positive for enzyme activity which contained 3 µL 100% DMSO instead of a library compound and eight negative for enzyme activity, which lacked both enzyme and library compounds.

The plates were then incubated at 37°C for 30 min. before the reactions were stopped by the addition of 100 µL 75 mM calcium acetate (pH 4.7) and incubated at room temperature for further 30 min. The wells were then washed with 3 x 200 µL 75 mM calcium acetate (pH 4.7). DNA retained in the wells was stained with 200 µL 1x SYBR Gold (Sigma) in T10E1 buffer and the plates were incubated for 20 min. at room temperature before quantification by fluorometry at excitation wavelength 470 nm and an emission wavelength of 520 nm, detected in a SpectraMax Gemini fluorometer (Molecular Devices).

2.8.3 Data processing, hit selection and hit validation

Once the data had been collected from the screen the fluorescence signals for the duplicates were averaged and converted into percentage inhibition using the positive and negative controls. The standard deviation of the controls was calculated and converted into percentage inhibition. From these values the 95% confidence interval for the screen was calculated,

which was used as an indicator of significance. Compounds giving percentage inhibitions above and around this value were selected for further studies. The Z' factor for the assay was calculated (Equation 2.2) to determine the quality of the data, with a good Z' value being defined as greater than 0.5 and a Z' value being defined as 1 (Zhang et al, 1999). Hits obtained from the screen were verified using the agarose gel electrophoresis assay detailed above. Fresh stocks of compounds were purchased (Sigma) for verification, rather than solutions taken from the library to ensure that the inhibition seen is not due to any cross-contamination or degradation which may have occurred during library storage.

$$Z' = 1 - \frac{3\sigma\ negative\ control + 3\sigma\ positive\ control}{|\bar{x}\ positive\ control - \bar{x}\ negative\ control}$$

Equation 2.2 Equation to calculate the Z' of an assay. Positive control refers to positive control for enzyme activity whilst negative control refers to a sample containing substrate but lacking enzyme.

Chapter 3

Exploration of Topoisomerase Assays

3.1 Introduction

Topoisomerase supercoiling or relaxation activity has been traditionally detected by agarose gel electrophoresis (Section 2.7.1.). This technique produces a remarkably information rich picture of the topological changes DNA undergoes when processed by topoisomerases. Unfortunately, it is slow (with combined assay and gel running times of 3-4 hours), qualitative (non-quantative) and requires a high degree of manual handling. The microtitre plate-based assay (Section 2.7.5.) on the other hand is quicker, has the possibility to be automated and produces quantitative results.

As such it was decided that the technical limitations of the agarose gel assay and their possible mitigation would be explored. The key factor in undesirably long running times involved in agarose gel electrophoresis is the generation of heat during the assay if high voltages are used, which can reduce the integrity of both the gel and the sample. Brody and Kern demonstrate (Brody & Kern, 2004) that the inclusion of Tris and sodium ions (in the form of Na_2EDTA) results in a positive feedback loop in which the conductivity of the media and the heat generated increases over time even though the voltage is kept constant. The solution they proposed was the elimination of EDTA (which was thought to be superfluous) from the running buffer and switching from Tris to a lower conductivity medium (Brody et al, 2004). They showed that running buffers designed under these principles could be run at higher voltages and for much shorter times without compromising resolution. Since all of these studies were carried out on linear DNA fragments it remained to be found whether these buffers could also be used for the separation of different topoisomers by electrophoresis. These studies were focused on a 5 mM lithium acetate

running buffer, since this was thought to be the best at resolving high-molecular weight DNA fragments (Brody et al, 2004).

The use of the triplex-formation principles from the Microtitre plate assay to purify supercoiled DNA away from other topoisomers was also investigated. The current method of choice to topologically purify plasmid DNA is the caesium chloride gradient (section 2.5.4), a process requiring lengthy centrifugation times and large quantities of ethidium bromide. The purification of supercoiled DNA by triplex-affinity column chromatography has already been attempted (Schluep & Cooney, 1998; Schluep & Cooney, 1999), but attained only modest yields. By changing the triplex forming buffer and, as suggested by Schluep and Cooney, using Continuous Affinity Recycle Extraction (CARE) it was hoped that yields would be improved to an acceptable level. Since triplex formation is greatly influenced by the buffer's pH (Singleton & Dervan, 1992), the valency of cation present (Hampel et al, 1991; Rougee et al, 1992) and the buffer's ionic strength (Rougee et al, 1992; Singleton & Dervan, 1993) this study focused on these three factors. Additionally the effects of using various different alkaline earth and transition metal ions as triplex stabilizers were also tested.

As an extension of this work, the performance of the most promising triplex forming buffers from the column work was tested in the assay relative to the standard TF buffer. The majority of the work below focuses on calcium and magnesium acetate based buffers due to promising results from the column work and preliminary tests.

3.2 Results

3.2.1 Lithium Acetate as a running buffer.

To investigate if 5 mM lithium acetate (LiOAc) would be a superior running buffer of agarose gel electrophoresis stocks of 20 ng/μL relaxed or supercoiled pNO1 were prepared in T10E1 buffer. This concentration was chosen since it was roughly equivalent to that used in a topoisomerase reaction. A 10x stock solution of 50 mM LiOAc (~pH 6.5) was also prepared for the making and running of agarose gels. Samples were prepared by mixing 30 μL DNA stock with either 30 μL 2x STEB (for TAE gels) or 30 μL LiOAc loading buffer (10 mM lithium acetate, 40% sucrose, 0.5 mg/mL bromophenol blue). The samples were then loaded on to 1% agarose gels prepared with either TAE or 5 mM LiOAc and run for the desired amount of time.

Under standard running conditions (80 V, 6.5 V/cm, 3 hrs.) it was observed that both relaxed and supercoiled plasmid run with a LiOAc running buffer progressed much slower through the gel than when it was run with the TAE buffer (Figure 3.1 A. and B.), moving ~3 cm rather than ~7 cm through the gel. Additionally, the degree of separation between topoisomers was reduced in the LiOAc running buffer compared to the TAE. This was puzzling since the separation of different sized fragments of linear DNA was not reported to be affected in a similar way (Brody et al, 2004). Since the only major difference between the two buffers, apart from the conductive ions, was the presence or absence of EDTA it was decided to see if adding back the EDTA to the LiOAc buffer would improve its ability to separate topoisomers. To avoid the inclusion of sodium ions EDTA free acid (pH 8.0 with LiOH) was used to prepare a 10x stock of Lithium Acetate EDTA (LAE) running buffer (5 mM lithium acetate, 2 mM EDTA). Inclusion of EDTA in the running buffer restored the resolution, allowing for easy separation of topoisomers under standard running conditions (Figure 3.1. C.)

Next the ability of LAE buffer to resolve topoisomers at higher voltages for shorter times was examined (Figure 3.2). Since TAE gels melted at the voltages used in these experiments comparison between buffers was impossible. To investigate the effects of these voltages on the resolution of linear DNA a 1 kb DNA ladder was run in addition to the relaxed and supercoiled pNO1. Although there was no difference in the resolution of linear fragments from each other as voltage was increased, resolution between topoisomers decreased. Relaxed topoisomers were seen to become more condensed and migrate faster through the gel as voltage was increased, whilst supercoiled topoisomers seemed to migrate more slowly. This meant that the maximum voltage samples could be run and still retain a decent degree of resolution was 160 V (13 V/cm), decreasing the running time by half (1.5 hrs.).

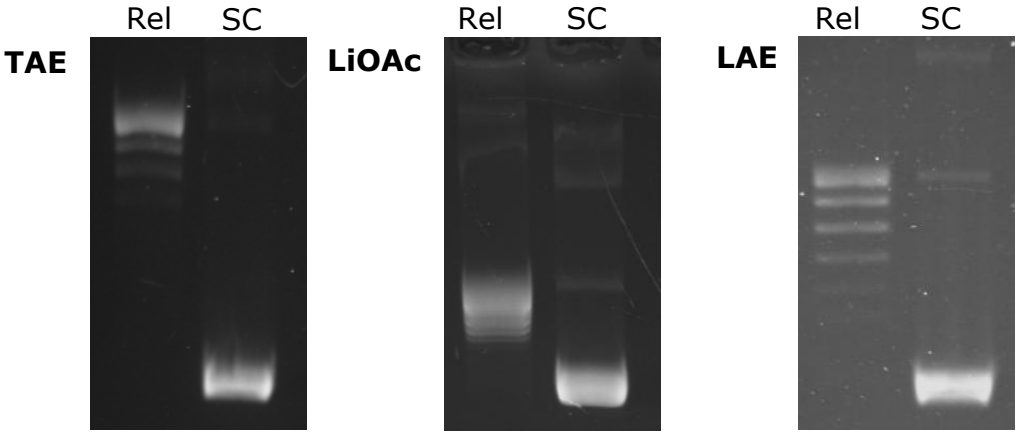

Figure 3.1 Running relaxed and SC pNO1 in lithium acetate buffer. Gels run for 3 hrs. at 80 V (6.5 V/cm) in 1% agarose gels either in TAE running buffer, 5 mM lithium acetate running buffer or 10 mM lithium acetate, 2 mM EDTA (free acid) running buffer (LAE).

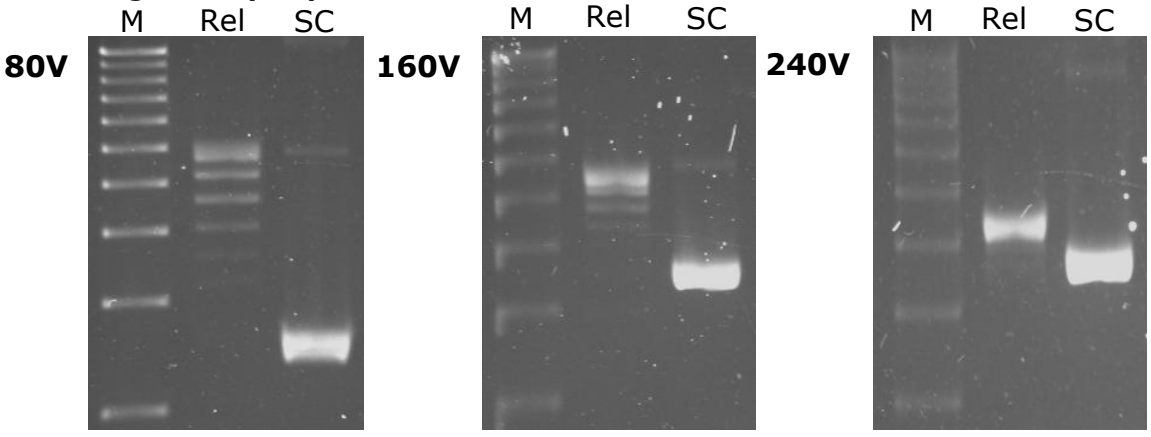

Figure 3.2 Running LAE gels at high voltages. 1 kb marker (M), relaxed pNO1 and SC pNO1 run on 1% agarose gels in LAE buffer at: 80 V (6.5 V/cm) for 3 hrs.; 160 V (13 V/cm) for 1.5 hrs. or 240 V (19.5 V/cm) for 45 min.

3.2.2 Resolution of a second band from supercoiled plasmid with LAE.

When working with the LAE running buffer, it was observed that supercoiled topoisomers when run at low voltages (20 V, 1.625 V/cm) for long periods of time (16 hrs.) seemed to partially resolve into two bands (Figure 3.3 A.). Better resolution of this second band, which is not normally observed under these conditions with TAE, was attempted by running SC pNO1 for 24 hrs. at 15 V (1.219 V/cm). These conditions clearly resolved a second band from the classic supercoiled topoisomer band (Figure 3.3 B.). This second band appeared fainter than the standard SC band, and ran slightly faster than the main band. This additional band could represent denatured plasmid or a more exotic topoisomer such as Form V DNA (two single-stranded DNA molecules coupled by supercoiling) (Stettler et al, 1979). Unfortunately, lack of time meant that the exact nature of the secondary band was unable to be determined.

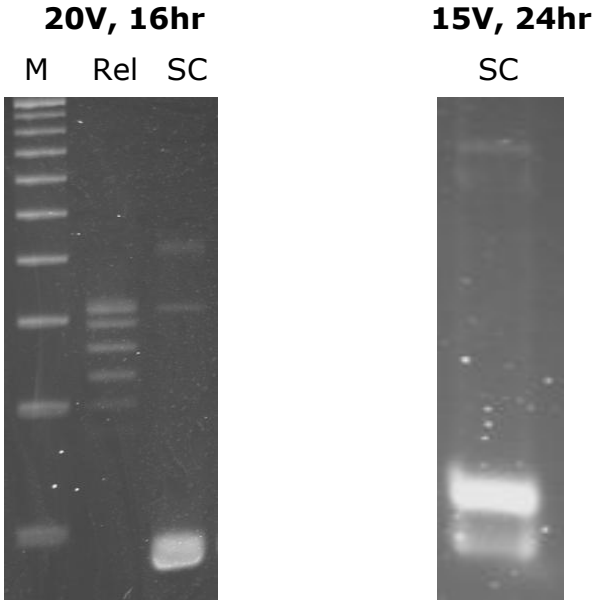

Figure 3.3 SC plasmid run for long periods on an LAE gel. 1 kb marker (M), relaxed pNO1 and SC pNO1 run on 1% agarose gels in LAE buffer at 20 V (1.625 V/cm) for 16 hrs.. SC pNO1 run on 1% agarose gels in LAE buffer at 15 V (1.219 V/cm) for 24 hrs.

3.2.3 Triplex affinity purification of supercoiled plasmid

To test for initial conditions for triplex affinity purification (Figure 3.4) 100 μL bed-volume spin columns were prepared by incubating 100 μL streptavidin coated 4% agarose beads (Sigma) with 100 nM TFO1 oligo in T10E1 buffer. After leaving the oligo to bind for 1 minute the columns were centrifuged at 2300 x g for 30 s (5415D centrifuge, F45-24-11 rotor, Eppendorf) to remove the fluid. The columns were then equilibrated with 1 mL of the appropriate triplex forming buffer (Table 3.2), spun them dry and added 2.5 μg of topologically impure pNO1 (containing a range of DNA species) in 100 μL triplex forming buffer. All experiments were carried out with twin spin columns, one using standard TF buffer and the other with the experimental triplex forming buffer, in order to gauge relative effectiveness. After 30 min the columns were spun again and retained the flow-through for analysis. The columns were washed with 100 μL triplex forming buffer and eluted four times with μL T10E100 buffer (10 mM Tris·HCl (pH 8.0), 100 mM EDTA) by centrifugation under the conditions listed above. Samples were mixed with 2x STEB and analysed by gel electrophoresis (Figure 3.5). Band intensity was quantified by Syngene and processed to get the buffers purification and binding potential relative to the standard buffer (Table 3.1).

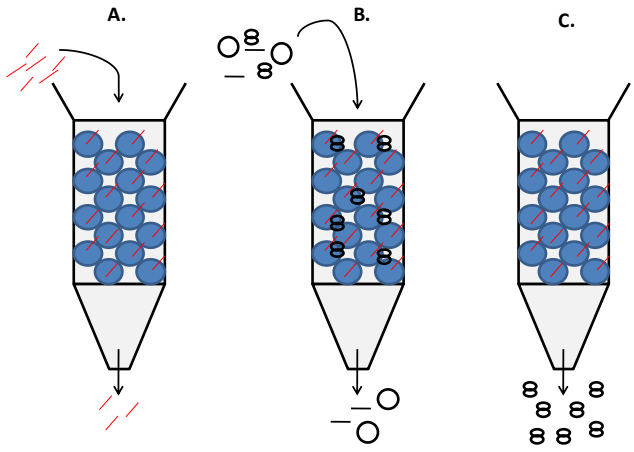

Figure 3.4 Triplex-affinity column chromatography of DNA. *A*. Streptavidin coated agarose beads incubated with biotin labeled TFO in a column. Excess oligo washed off. *B*. Mixture containing nicked, supercoiled and linear pNO1 plasmid added to column in a low pH, high salt buffer. Supercoiled plasmid forms triplexes with the TFO and is captured in the column, whilst linear and nicked forms are washed away. *C*. Supercoiled plasmid eluted in a high pH buffer.

Since pH is integral to the formation of DNA triplexes a range of buffers above and below the pH of the standard TF buffer were tested (Buffers 1-3). The expected result was that lowering the pH would result in greater triplex formation and therefore increased DNA binding. However, lowering the pH seemed to preferentially promote triplex formation by OC plasmid, resulting in decreased SC yield and purity. Addition of the polyvalent cation spermine (Buffers 4-5) had little effect on binding but reduced purity at 10 mM, whilst replacement of magnesium with spermine or spermidine (Buffers 6-7) reduced purity and, in the case of spermine, binding. Decreasing the concentration of $MgCl_2$ to 5 mM had no effect on purity, but drastically reduced binding (Buffer 8). However, the replacement of the traditional buffer with 75 mM MgOAc (pH 4.7, Buffer 9) increased binding without changing the purity. Strangely, when the concentration of MgOAc was increased to 150 mM (Buffer 10) a reduction in binding was observed compared to 75 mM. A variety of divalent metal acetates were tested in the place of MgOAc, including alkaline earth metals and transition metals, in the place of or supplementary to MgOAc (Buffers 11-14). The effects of utilizing zinc or silver acetate in the buffer were investigated since they had previously been shown to promote triplex formation in novel ways

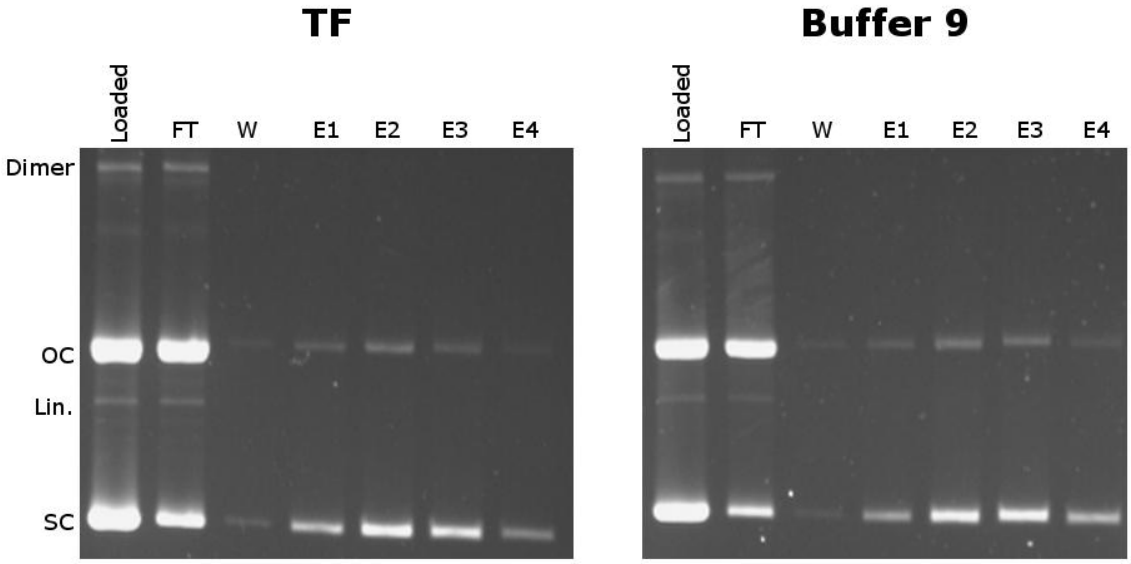

Figure 3.5 Triplex-affinity purification with TF or buffer 9. Composition of buffer 9 found in Table 3.2. The following samples were loaded on the gels: Sample before purification; Flow-Through; Wash with either TF or buffer 9; and four Elutions with T10E100.

		Initial material		Flow-through		Wash		Elution 1		Elution 2		Elution 3		Elution 4	
		TF	*Buffer 9*	*TF*	*Buffer 9*	*TF*	*Buffer 9*	*TF*	*Buffer 9*	*TF*	*Buffer 9*	*TF*	*Buffer 9*	*TF*	*Buffer 9*
Fraction of sample (%)	*Dimer*	3	2	4	3	0	0	0	0	0	0	0	0	0	0
	OC	44	45	60	67	38	56	16	20	17	20	12	17	9	11
	L	1	1	1	1	0	0	0	0	0	0	0	0	0	0
	SC	52	51	35	28	62	44	84	80	83	80	88	83	91	89

	TF	Buffer 9
Total Yield (%)	58	77
Final Purity (%)	85	83
Relative Yield (%)	100	133

Table 3.1 Example of band quantification and data processing for TF and buffer 9. Intensities of bands were quantified for samples from each step of the purification (Syngene). The percentage of the total sample intensity attributed to each DNA species was calculated (fraction of sample). The percentages of the recovered SC present in the elution samples, rather than in the flow-through or wash samples, were calculated to act as a guide for the yield of both buffers (total yield). The overall purity was calculated by combining the data from the four elutions (final purity). These values were then used calculate the efficiency of Buffer 9, in terms of SC purification and binding, relative to the values for the standard TF. As such, a relative purity or binding of 100% indicates identical efficiency to the TF buffer, with higher and lower scores indicating greater or less efficiency respectively.

(Bernues et al, 1989; Tanaka et al, 2002). The majority of these lowered both purity and binding, with the exception of CaOAc (Buffer 12), which produced results comparable to MgOAc. A summary of the buffers performances can be found below (Table 3.3).

Buffer	Composition
1	TF (pH 3.6)
2	TF (pH 4.25)
3	TF (pH 5.25)
4	TF (pH 4.7), 1 mM spermine
5	TF (pH 4.7), 10 mM spermine
6	50 mM NaOAc (pH 4.7), 10 mM spermine
7	50 mM NaOAc (pH 4.7), 10 mM spermidine
8	50 mM NaOAc (pH 4.7), 5 mM $MgCl_2$,
9	75 mM MgOAc (pH 4.7)
10	150 mM MgOAc (pH 4.7)
11	75 mM MgOAc (pH 4.7), 50 µM AgOAc
12	75 mM CaOAc (pH 4.7)
13	75 mM ZnOAc (pH 4.7)
14	75 mM BaOAc (pH 4.7)

Table 3.2 Compositions of triplex forming buffers tested. TF refers to the standard Triplex forming buffer (Table 2.1) with indicated modifications.

Buffer	Relative SC purity (%)	Relative SC Yield (%)
TF	100	100
1	80	85
2	92	111
3	99	110
4	111	104
5	81	116
6	63	74
7	63	116
8	100	62
9	97	133
10	101	110
11	87	77
12	92	129
13	89	38
14	98	68

Table 3.3 Efficiencies of different buffers in triplex-affinity purification of SC plasmid. The purity and yield of SC was determined by quantitative software (Syngene) and calculated relative to the performance of standard TF buffer (Table 2.1).

Having established that 75 mM MgOAc (Buffer 9) was the best of the buffers tested a scaled up purification was attempted by preparing a 1 mL bed volume gravity column and attempting to purify 1 mg of plasmid (~80% purity). DNA was prepared as per section 2.5.4. but halted before the caesium chloride gradient. The sample was then overdigested with RNAse and diluted the sample into 5 mL of 75 mM MgOAc (giving 1 mg at a concentration of 0.2 mg/mL). The sample was loaded 1 mL at a time and collected the flow-through and eluting with 1 mL T10E100 before adding the next millilitre. To remove the large quantities of EDTA present the fractions were ethanol precipitated before being quantified by Syngene (as described above) and determining their concentration by Uv/Vis spectrometry. By combining these two methods the yield for the purification of supercoiled plasmid was calculated to be 65% with 95% purity.

Since a large proportion of the DNA was still present in the initial flowthrough, Continuous Affinity Recycle Extraction (CARE) was investigated as a method to improve upon the yield. The above experiment was repeated and the initial flowthrough after sample loading was retained. After the bound DNA was eluted the column was re-equilibrated with Buffer 9. The previously retained flowthrough was then applied to the column. Bound DNA was then eluted, ethanol precipitated and analysed as above. The yield of this setup was calculated to be 68% (97% purity). Unfortunately due to time constraints this work could not be pursued any further.

3.2.4 Performance of buffers 9 and 12 in the microtitre plate-based assay

Since buffers 9 and 12 (Table 3.2) seemed to promote triplex formation more effectively than the classic TF buffer in the triplex-affinity columns experiments were carried out to see how they compared in the microtitre plate-based assay (Section 2.7.5.). Samples were prepared by mixing 30 μL of Milli-Q water containing 0.5 μg of either relaxed or supercoiled pNO1 with 100 μL of the appropriate triplex forming buffer. Samples were incubated in microtitre plate wells prepared with TFO1 for 30 min at 18°C and then washed with the appropriate triplex-forming buffer, stained and analysed as

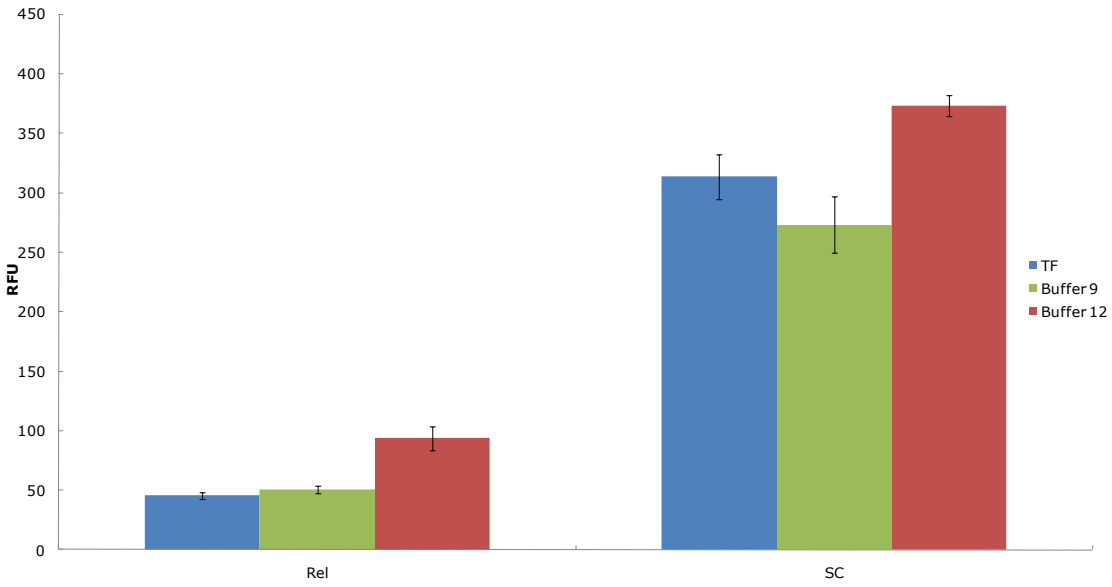

Figure 3.6 Buffers 9 and 12 as triplex forming buffers in the Microtitre plate assay. 30 µL Milli-Q water containing 0.5 µg of relaxed or supercoiled pNO1 was mixed with either TF buffer (Table 2.1), Buffer 9 (75 mM MgOAc, pH 4.7) or buffer 12 (75 mM CaOAc, pH4.7). Reactions were carried out in triplicate. Error bars represent the standard deviations of the three repeats.

detailed in Section 2.7.5 (Figure 3.6). Each buffer was tested in triplicate their relative signal variation and Z' factor could be determined (Section 2.8.3.). From these data the Z' factor was calculated to be 0.92 for TF buffer, 0.88 for Buffer 9 and 0.92 for Buffer 12.

3.3 Discussion

3.3.1 Lithium Acetate EDTA as an electrophoresis running buffer

Although lithium acetate running buffers have been previously used to resolve linear fragments of DNA based on their size in gel electrophoresis, separation of closed circular topoisomers had not been attempted. The experiments above have shown that lithium acetate can act as a running buffer for the resolution of relaxed and supercoiled plasmid but only when supplemented with EDTA. In the absence of EDTA both relaxed and supercoiled plasmids migrate much slower, with reduced resolution between topoisomers. Since it is unlikely that the EDTA is interacting directly with the plasmid one explanation for this observation would be that trace amounts of contaminating divalent metal ions are binding to the DNA. Since

the binding of such small amounts would not result in a change in overall charge it is possible that the reduced migration is due to conformational changes in the plasmid. Two explanations for this phenomenon would be the binding of divalent ions subtly altering the rigidity of the DNA or the ions are binding in clusters at the intersections where two double strands cross (where there would be a high density of negative charge) and disrupting conformation by repulsion.

Although lithium acetate EDTA (LAE) seemed a good buffer for running gels under standard conditions, often producing crisper bands and generating less heat than TAE, increasing the voltage in order to reduce running times proved untenable. Whereas the migration of linear DNA increases proportional to the increase in voltage, high voltages reduced the resolution of closed-circular DNA topoisomers. At 240 V, three times the standard voltage, an increase in the mobility of relaxed and open-circle plasmid was observed, as well as clustering of the relaxed topoisomers. Supercoiled plasmid, on the other hand, decreased in mobility. This effect had been observed previously with TAE at much lower voltages than the ones tested here (Johnson & Grossman, 1977), although the exact reason for this phenomenon remains mysterious. From these findings it can be concluded that the fastest an agarose gel can be run and still achieve decent resolution of topoisomers is 160 V for 1.5 hrs.

Additionally it was observed that by using LAE as the running buffer and running the gel for long time periods (16-24 hrs.) at low voltage (20-15 V) the band corresponding to the supercoiled topoisomers could be resolved as two discrete bands. This resolution could be the result of either the binding of lithium ions to the DNA resulting in a change in charge or conformation for some supercoiled topoisomers but not others, or could be a result of the lower conductivity of the buffer allowing more charge to pass directly through the sample rather than short-circuiting through the buffer. As to what these two bands represent, they might signify topoisomers with different degrees of supercoiling beginning to be resolved or the resolution of some other kind of topoisomer from the supercoiled band, such as denatured or Form V DNA (two single-stranded DNA molecules coupled by

supercoiling) (Stettler et al, 1979). Unfortunately there was insufficient time to follow this up any further.

3.3.2 Triplex-affinity purification of supercoiled plasmids

For triplex affinity purification of supercoiled plasmids two buffers have been identified (Buffers 9 and 12) which produced superior yields to the standard TF without decreasing purity. These buffers were comprised of 75 mM magnesium or calcium acetate (pH 4.7). The increase in binding due to the elimination of sodium is likely to be due to the fact that monovalent ions act antagonistically to the more efficient triplex stabilizing divalent ions (Singleton & Dervan, 1993). The other alkaline earth metal tested, Beryllium (Buffer 14), and zinc (Buffer 13) performed poorly as triplex stabilizers under the conditions tested. This may be due either to their physical properties or their coordination. Decreasing the pH increased the binding of OC plasmid (Buffer 1) which resulted in a decrease in purity. Increasing the pH to 5.25 (Buffer 3) seemed to marginally improve the purity without changing the yield. These observations suggest that the triplex formation of open circular DNA is much more sensitive to pH than supercoiled plasmid. Using a sodium acetate buffer containing either spermine (Buffer 6) or spermidine (Buffer 7), which were predicted to promote triplex formation (Singleton & Dervan, 1993), resulted in a lower purity and, the case of spermine, a lower yield which is possibly due to competition with sodium ions. Addition of silver acetate (Buffer 11) reduced both purity and yield, implying it disrupted triplex formation. This is likely a competition effect between the silver and magnesium ions.

The purification of 1 mg of SC plasmid using Buffer 9 produced a high degree of purification and a modest yield of 64%. This is comparable to previously published data (Schluep & Cooney, 1999), which focused on improving the matrix rather than the buffer. It is possible that by using the matrix devised by Schluep and Cooney and Buffer 9 even higher yields could be reached. The use of Continuous Affinity Recycle Extraction (CARE) only marginally improved the yield, although due to the labour intensive nature of the procedure the flow-through was only recycled once (more

cycles, and probably high yields, could be achieved if the process was automated). However, it was surprising that the increase in yield was so low (~3%), which implies the level of binding for the second cycle was much lower than the first. It is unlikely that the binding capacity of the column shifted since it was thoroughly washed and re-equilibrated between cycles. It may be the case that only certain supercoiled topoisomers are binding efficiently to the column, as it has been previously observed that triplex formation is proportional to the level of supercoiling of the DNA (Maxwell et al, 2006). In fact, our results with the lithium acetate EDTA agarose gels demonstrate that the supercoiled topoisomers are not homogenous since it is possible to separate the band into two species.

Testing Buffers 9 and 12 as triplex-forming buffers in the Microtitre plate assay revealed that Buffer 12 performs marginally better than the classic TF buffer. Since it had a simpler composition to the classic TF buffer it was used in all further experiments in this study.

Chapter 4

Escherichia coli DNA Gyrase Screen

4.1 Introduction

DNA topoisomerases are essential enzymes which have been found in all known cells to date (Bates & Maxwell, 2005). They are responsible for controlling the topological state of DNA within the cell, and the catalysis of a wide range of reactions: knotting/unknotting, catenation/decatenation and supercoiling/relaxation of DNA (Schoeffler & Berger, 2008). The crucial nature of their role has led them being successfully exploited as targets for a range of antimicrobial and anti-cancer drugs as well as potential targets for herbicidal, anti-viral and anti-protozoal agents. The bacterial topoisomerase DNA gyrase, for example, is the target for the quinolone class of drug (Gellert et al, 1977; Sugino et al, 1977) which includes some of the most successful antimicrobials currently in clinical use (Saravolatz & Leggett, 2003; Thadepalli et al, 1988; Wispelwey & Schafer, 2010). Unfortunately the development of therapeutic drugs which target topoisomerases have been limited by the low-throughput and labour-intensive nature of traditional assays for their activity.

To address this issue a novel assay (Maxwell et al, 2006) has been developed based on DNA triplex formation and exploiting the preferential formation of DNA triplexes in supercoiled over relaxed DNA (Hanvey et al, 1988; Sakamoto et al, 1996). During the assay a biotinylated, single-stranded triplex-forming oligo is annealed to the surface of a streptavidin coated microtitre plate well, to which the reaction mix containing the enzyme and substrate plasmid is added. After the reaction is completed a low pH, high salt buffer is added to promote triplex formation. As a result supercoiled plasmid is bound to the plate, whilst relaxed plasmid can be washed away. Addition of a fluorescent dye allows quantification of the retained DNA and consequently the activity of the enzyme.

Although this technique has been trialed on a small scale successfully (Anderle et al, 2008) it had yet to be assessed in a high-throughput format. As such, the main focus of this project was validating the assay as a high-throughput screen and exploring any hits uncovered. Initially a pilot screen of 960 compounds against the well characterised *Escherichia coli* DNA gyrase would be conducted. The library chosen for screening was the Genplus library from Microsource (http://www.msdiscovery.com/spectrum.html; last accessed 06/06/11) 80% of which is comprised of U.S.A., European and Japanese drug standard body approved drugs with the remaining 20% being natural products with novel structures. It was hoped that by screening compounds already known to be biologically active that our hit rate would be increased and reduce the time required for clinical trials of any hits which were viable novel antibiotics (Chong & Sullivan, 2007).

4.2 Results

4.2.1 Initial screening

After some preliminary attempts, the standard Microtitre plate-based assay was modified to make it more amenable to a high-throughput format. To improve consistency the reaction volume was increased from 30 μL to 60 μL, which made sample handling easier. All buffers and solutions used in the screen were filtered to prevent scattering by contaminating particles during the staining step. Finally, the triplex forming and staining steps were carried out at 18°C to minimise variation due to ambient temperature changes. The library was screened at a relatively low concentration and after a few trials decided on 25 μM. The screen was conducted in duplicate over four days (see Section 2.8.2. for details of the protocol used). An arbitrary hit threshold of 25% inhibition was set, and any compound exceeding this limit were investigated (Figure 4.1, Figure 4.2). Twenty one compounds were identified as inhibitors by the screen, whilst two compounds seemed to give a increase in DNA gyrase activity: quinacrine and merbromin (35 and 37% activation respectively).

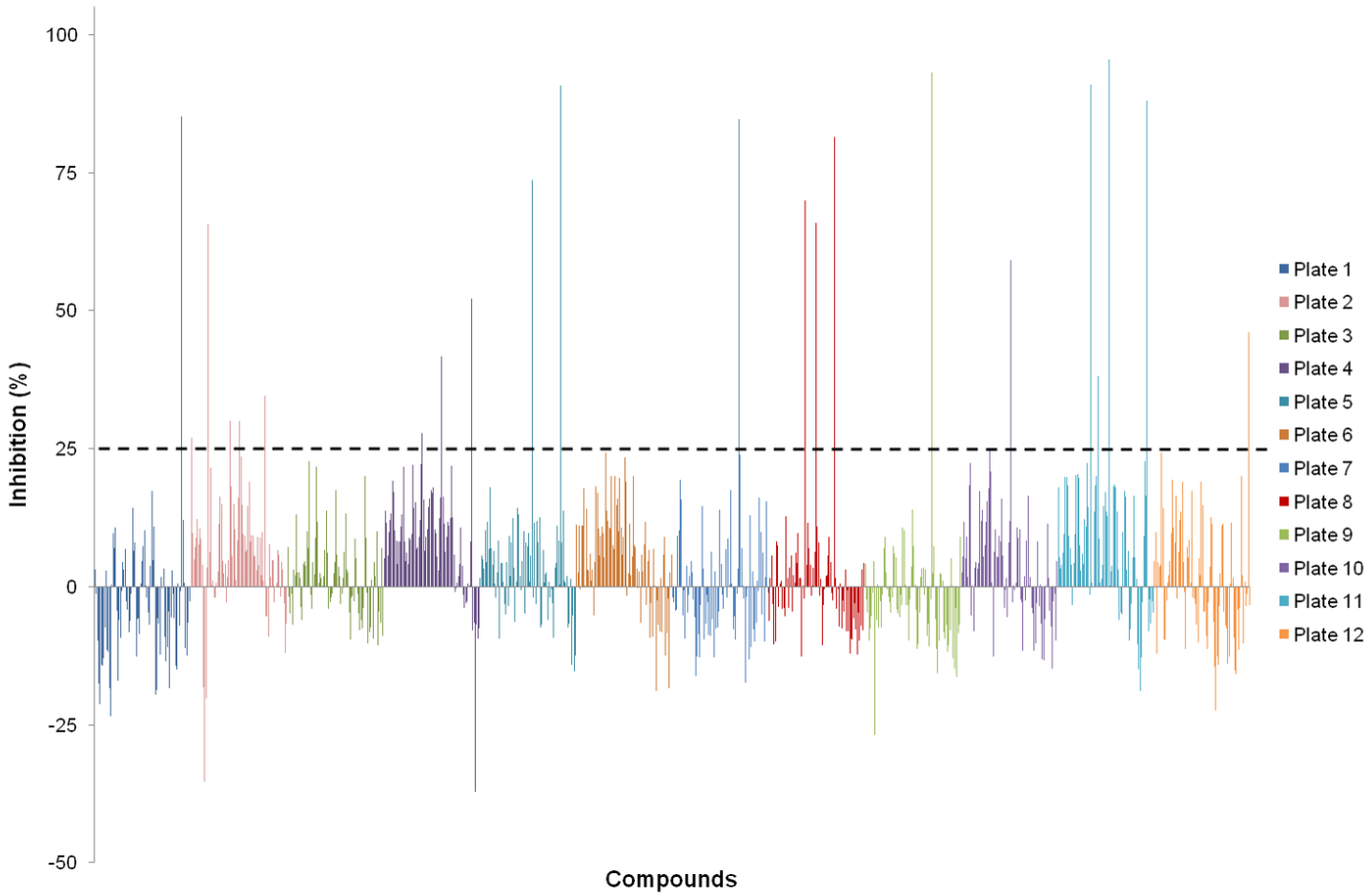

Figure 4.1 Results of *E. coli* gyrase screen*. A.* **Percentage inhibition for a duplicated screen of the Genplus library against *E. coli* DNA gyrase. Each bar represents the average value for a single compound screened in duplicate. The dotted line indicates the arbitrary hit threshold of 25% inhibition. See the Appendix for the data for individual plates.**

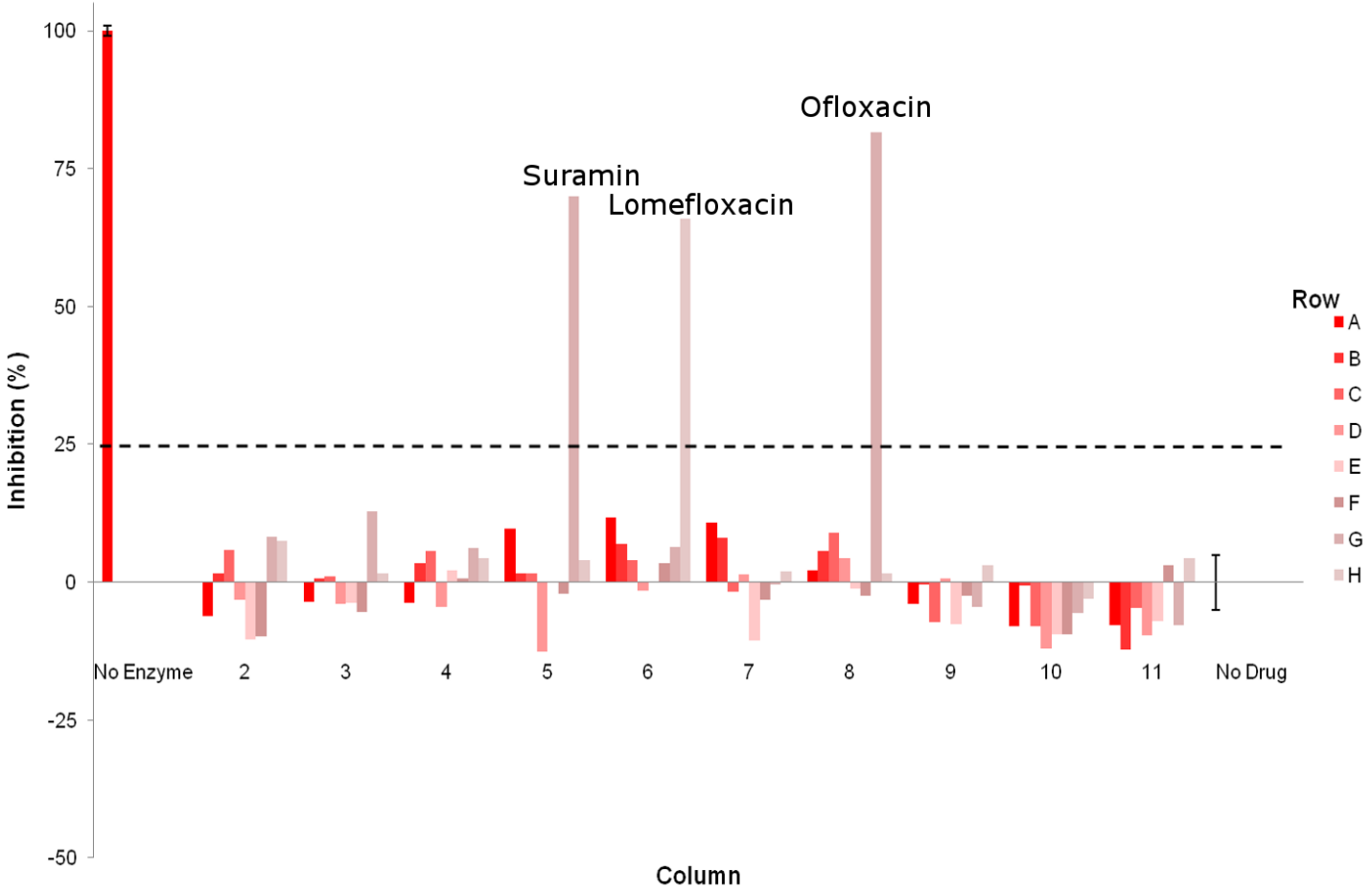

Figure 4.2 Percentage inhibition for Genplus plate 8 against *E. coli* DNA gyrase with hits labelled. Percentage inhibition was calculated from the 'no enzyme' and 'no drug' controls. Error bars for the no enzyme and no drug controls were calculated from the standard deviation of sixteen repeats.

4.2.2 Intrinsic fluorescence of the library

To identify compounds with intrinsic fluorescence, which could interfere with the assay if they persisted in the wells, fluorescence readings (Ex: 470 nm, Em: 520 nm) were taken during the screen prior to incubation of the plates at 37°C (Figure 4.3). Four compounds were identified which fluoresced under the conditions of the screen: quinacrine, calcein, merbromin and riboflavin.

4.2.3 Elimination of false positives

The majority of the 21 compounds picked up in the screen (Table 4.1) were already characterised DNA gyrase inhibitors, including a large number of the highly successful fluoroquinolone class. This was not particularly surprising since DNA gyrase is a well-exploited antimicrobial target and the library screened was largely made up of commercial drugs. In fact, the screen's ability to detect these already known inhibitors was heartening. Since they were already characterised, they were excluded from further study.

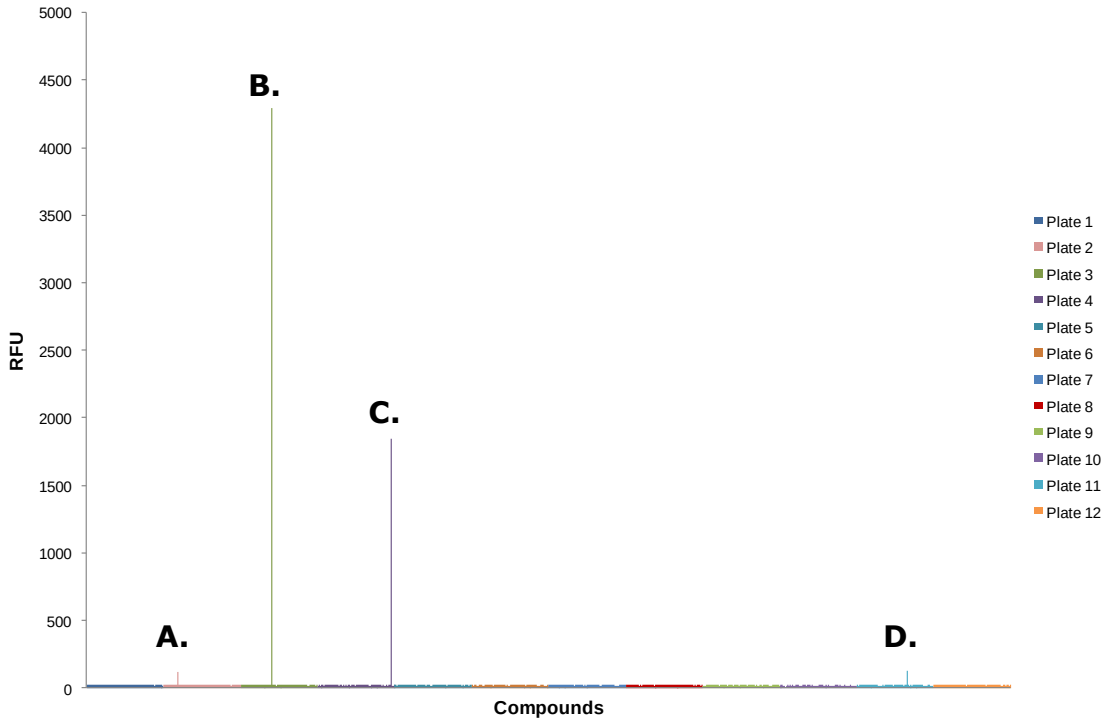

Figure 4.3 Intrinsic fluorescence of Genplus library. Fluorescence readings taken in the presence of DNA gyrase and pNO1. Each bar represents a single compound. *A*. Quinacrine *B*. Calcein *C*. Merbromin *D*. Riboflavin.

False positives	*Inhibition (%)*	Known inhibitors	*Inhibition (%)*	Novel inhibitors	*Inhibition (%)*
Harmalol	85	Gatifloxacin	96	Mitoxanthrone	93
Biotin	52	Moxifloxacin	91	Suramin	70
Quinalizarin	42	Novobiocin	91		
Acrisorcin	38	Levofloxacin	88		
Quercetin	35	Perfloxacine Mesylate	85		
Digitoxin	30	Lomefloxacin	82		
Roxarsone	30	Norfloxacin	74		
Niacin	28	Ofloxacin	66		
p-chlorophenylalanine	27	Acriflavinium	66		
		Ciprofloxacin	59		
		Surafloxacin	46		

Table 4.1 Summary of compounds selected by the *E. coli* gyrase screen. Percentage inhibition of compound in screen given.

The effects of the remaining hits on DNA gyrase activity at 100 μM were tested using the agarose gel assay (Figure 4.4) to determine if they were genuine inhibitors or whether they had been detected due to interference with other aspects of the microtitre plate-based assay (e.g. triplex formation). To exclude the effects of any contaminants or degradation products present in the library, fresh stocks of each hit were purchased from the appropriate supplier (Sigma, Microsource). Acrisorcin, one of the hits to be tested, was actually a mixture of 9-aminoacridine and hexylresorcinol. As such the two compounds were tested separately. Out of the hits tested 9-aminoacridine, a component of acrisorcin, seemed to actually stimulate gyrase activity in the gel assay whilst mitoxanthrone and suramin displayed inhibition (see Section 4.2.6 below). The remaining nine

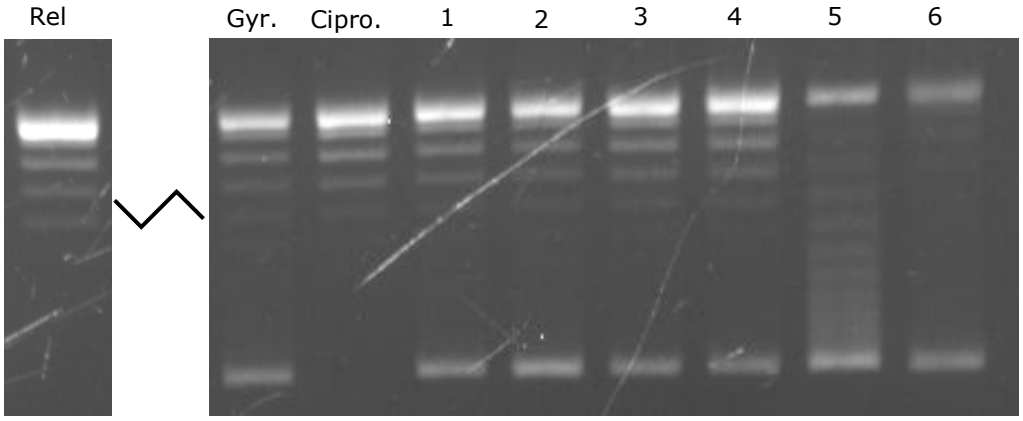

Figure 4.4 Example of validation assay for putative *E. coli* gyrase screen hits. Similar experiments were carried out for all potentially novel hits. Relaxed DNA incubated with 0.5 units of DNA gyrase to produce partial supercoiling. Samples incubated with or without 100 μM compound. Ciprofloxacin was used as a positive control for inhibition. *1*. Harmalol. *2*. p-chlorophenylalanine. *3*. Roxarsone. *4*. Niacin. *5*. 9-aminoacridine. *6*. Hexylresorcinol.

compounds tested did not seem to affect DNA gyrase activity in the gel-based assay.

This made me curious as to why these compounds had been picked out by the screen to begin with. It was especially interesting that harmalol, which gave a high percentage inhibition in the screen, seemed entirely inactive in the gel assay. To test whether the compounds had interfered with either the triplex-formation or staining steps of the microtitre-plate based assay, the compounds were incubated with supercoiled plasmid in the absence of gyrase under standard assay conditions (Figure 4.5). A decrease in signal compared to the control indicated the compound was either disrupting triplex formation or interfering with the staining. Of the compounds tested, it appeared that both 9-aminoacridine and hexylresorcinol reduced the signal. This explained why Acrisorcin (a mixture of the two) was picked up by the screen even though 9-aminoacridine activates DNA gyrase. The remaining compounds had no effect.

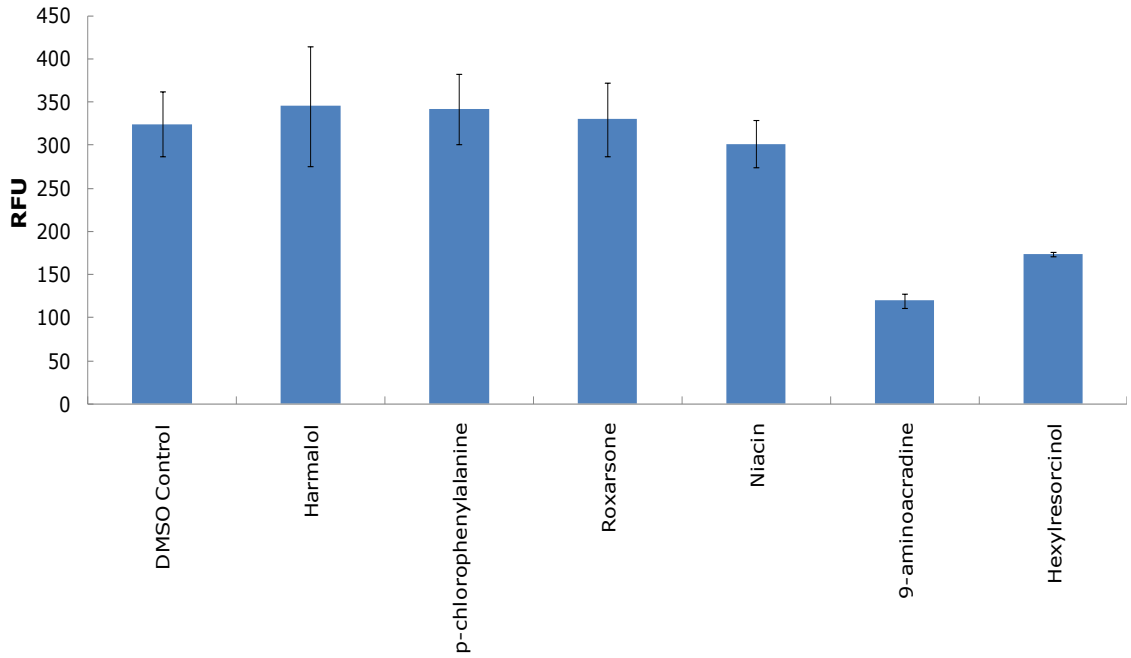

Figure 4.5 Example of testing the ability of false positives to interfere with the assay. Similar experiments were carried out for all false positives. Supercoiled pNO1 in 1x gyrase assay buffer incubated with 100 μM of the indicated compound. The total concentration of DMSO present in all samples was 5%. Error bars represent the standard deviation of three repeats.

Since harmalol had given such a strong response in the screen but neither displayed inhibition in the gel assay nor appeared to be interfering with the microtitre plate-based assay it was possible that the sample in the library had become contaminated in some way. To test this the freshly bought stock to the library sample were compared in both the gel assay and in the microtitre plate-based assay (Figure 4.6). It was found that neither inhibited DNA gyrase in the gel assay, but the sample from the library strongly reduced the signal of supercoiled plasmid in the microtitre plate-based assay. It was likely therefore that the library sample had either become contaminated or degraded during storage, and the strong inhibition

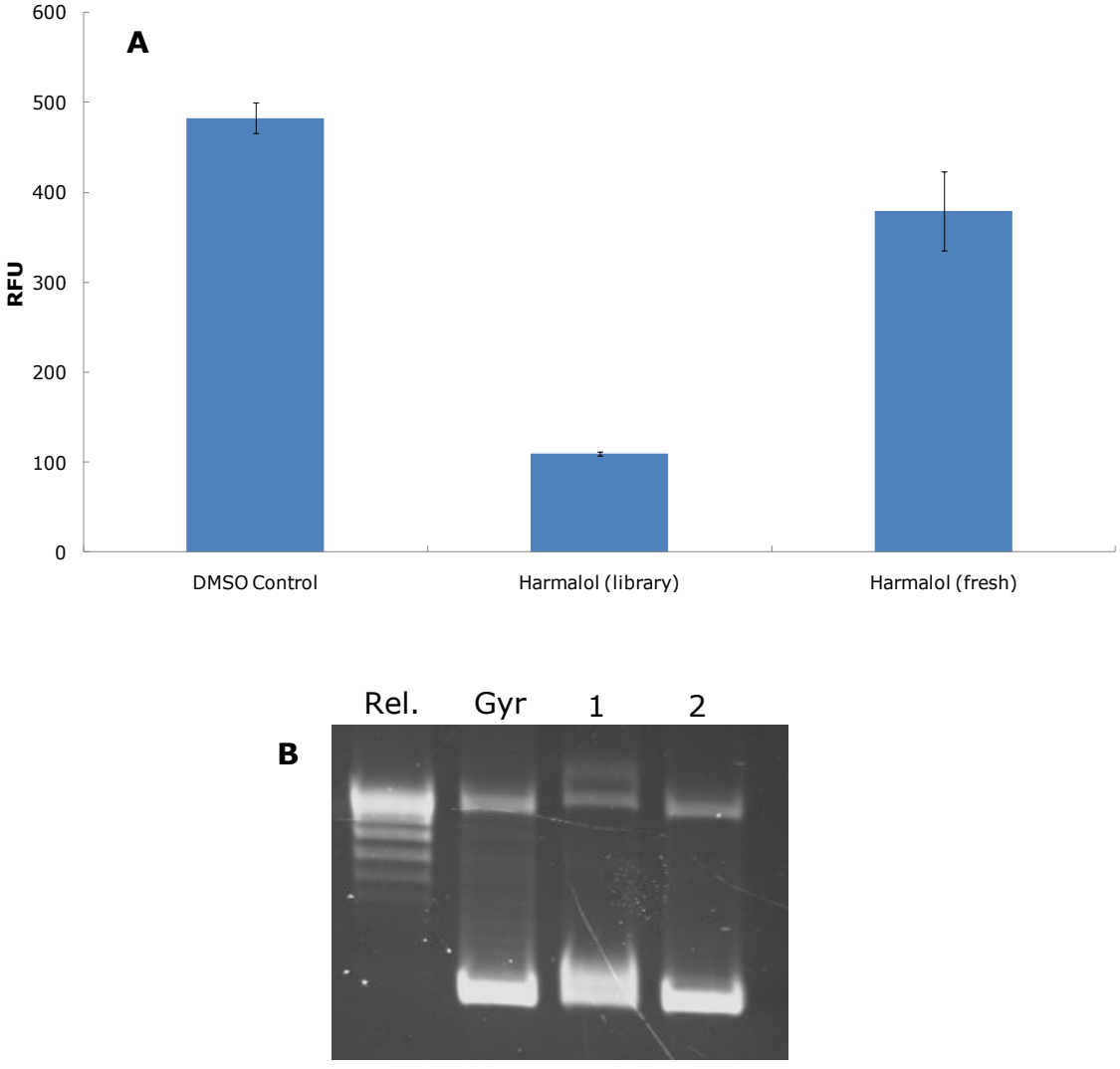

Figure 4.6 Comparing harmalol library stock to fresh preparation. *A*. Testing for interference with the microtitre plate-based assay. 0.75 μg supercoiled pNO1 incubated with 100 μM harmalol from the library or freshly prepared. *B*. Comparing effects on DNA gyrase activity in the gel assay. 0.5 μg relaxed pNO1 incubated with 0.75 units DNA gyrase in the presence or absence of compound. 1. Harmalol from library stock. 2. Harmalol from fresh preparation.

seen in the screen was entirely due to this contaminant interfering with the assay. Some smearing of the supercoiled band was observed with the library stock in the gel assay, suggesting the contaminant is an intercalator and was not fully removed by the extraction process.

4.2.4 Statistical evaluation of screen

The mean fluorescent signal for the 192 negative (relaxed plasmid, no enzyme) and 192 positive (relaxed plasmid with DNA gyrase and no drug) controls was calculated to be 80 and 370 RFU respectively, with standard deviations of 6 and 29 RFU (Table 4.2). The signal-to-background ratio was calculated to be 5 whilst the signal-to-noise ratio was 10. From the control data the average Z' value for the screen was calculated to be 0.64 (See Equation 2.2). This value indicated that there was a good degree of separation between the positive and negative controls, implying that data quality for the screen was good. The distribution of the Z' value for each plate around the mean (Figure 4.7) was close, with no single plate giving a value below 0.5. This assured me that this average value was a good representation of the screens overall quality. Thirteen compounds detected by the screen were validated as hits, giving a hit rate of 1.35%. Of these two were novel inhibitors of DNA gyrase, giving a novel hit rate of 0.21%. Checking the list of compounds present in the library revealed that four known DNA gyrase inhibitors were missed by the screen: nalidixic acid, cinoxacin, oxolinic acid and enoxacin.

		Average (RFU)		S.D. (RFU)		S.D. (%I)		Z'
		No enzyme	*No drug*	*No enzyme*	*No drug*	*No enzyme*	*No drug*	
Plate	*1*	52	161	2	11	2	10	0.65
	2	107	464	9	39	3	11	0.59
	3	64	262	3	22	2	11	0.62
	4	61	257	4	17	2	9	0.68
	5	61	218	5	19	3	12	0.56
	6	90	454	7	50	2	14	0.53
	7	70	310	5	20	2	8	0.68
	8	94	467	4	18	1	5	0.82
	9	99	535	4	46	1	11	0.65
	10	96	458	7	39	2	11	0.61
	11	84	466	6	36	2	9	0.67
	12	83	394	10	31	3	10	0.60
Average		80	370	6	29	2	10	0.64

Table 4.2 Table of control data and Z' values per plate for the *E. coli* gyrase screen. Averages and standard deviations are derived from 16 repeats. Standard deviations were also converted to percentage inhibition.

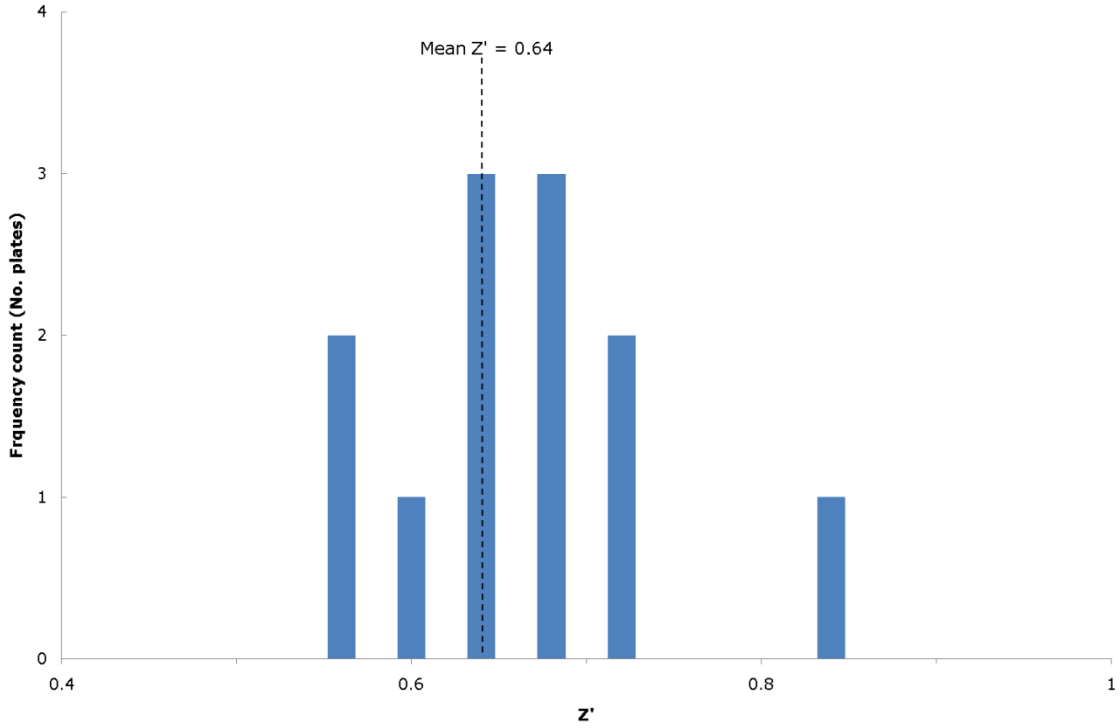

Figure 4.7 Histogram of Z' values for the *E. coli* gyrase screen, with the average Z' value for the twelve plates indicated by the dotted line.

4.2.5 Quinacrine and 9-aminoacridine as activators of DNA gyrase

As shown above (Figure 4.4), 9-aminoacridine appears to act as an activator of DNA gyrase. Two compounds from the screen appeared to be also activating the enzyme: quinacrine and merbromin. It had also been observed that these two compounds fluoresced at the wavelengths used in the assay (Figure 4.3). It was therefore interesting to see if these compounds were genuine activators or if the apparent increase in activity was due to them persisting in the wells after the final wash steps. To investigate this 100 μM of each of the compounds was incubated under standard assay conditions either with no plasmid present, relaxed pNO1 or supercoiled pNO1 (Figure 4.8). Merbromin gave me a high signal even when no plasmid was present, suggesting it persisted in the wells after the wash steps. This made sense since merbromin is a protein dye which reacts with thiol groups (Wilken et al, 2010). The increase in signal and apparent activation was therefore likely due to the compound covalently binding to the streptavidin coats of the wells. Merbromin also appeared to inhibit DNA gyrase in the gel assay, but due to its general reactivity with proteins this

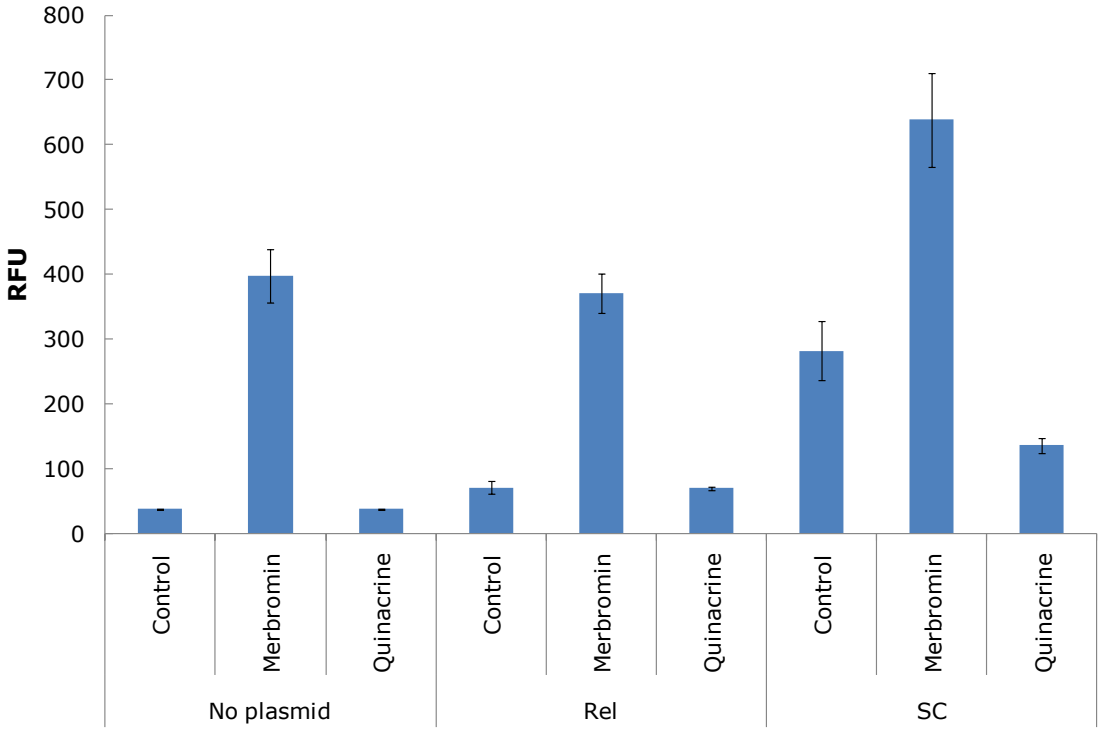

Figure 4.8 Testing the effects of merbromin and quinacrine on the microtitre plate-based assay. 100 μM of each compound incubated under standard assay conditions either in the absence of plasmid, with relaxed pNO1 or supercoiled pNO1. Error bars are the standard deviation of three repeats.

inhibition was discounted as being non-specific. Quinacrine, on the other hand, did not seem to persist within the well and in fact reduced signal when incubated with supercoiled plasmid. This suggested that the activation observed was genuine rather than due to the intrinsic fluorescence of the compound.

To investigate further the activation of DNA gyrase by quinacrine, a titration of gyrase in the presence of either 10 or 20 μM quinacrine was performed (Figure 4.9). Activation of DNA gyrase was observed with both concentrations, resulting in a doubling of the supercoiling activity of the enzyme. However, this increase in activity was identical for both the concentrations tested. This suggests that which was observed here is the limit of quinacrine's ability to promote supercoiling by DNA gyrase.

In order to address the cause of this activation, relaxed and supercoiled pNO1 were run on on a 1% agarose gel in the presence or absence of 2 μM quinacrine in the gel and running buffer (Figure 4.10). Supercoiled plasmid was unaffected by the presence of the drug, whilst

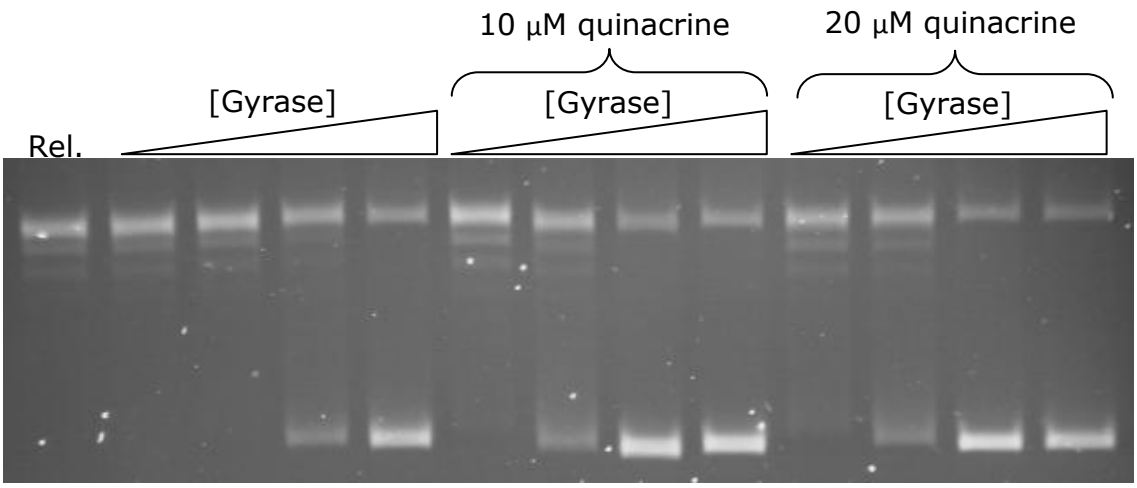

Figure 4.9 DNA gyrase activation in the presence of quinacrine. DNA gyrase titrated from 0.25 units to two units under standard assay conditions. Reactions contained either 0, 10 or 20 μM quinacrine. Samples lacking quinacrine had an equivalent amount of DMSO added.

relaxed plasmid ran as a single band slightly ahead of the supercoiled DNA. This suggested that activation of DNA gyrase by quinacrine may be a result of the drug intercalating with relaxed DNA and causing it to adopt a form which was a better substrate for the enzyme (e.g. positively supercoiled plasmid).

4.2.6 Mitoxanthrone and suramin as novel DNA gyrase inhibitors

Out of the thirteen hits identified by the screen two were novel gyrase inhibitors: mitoxanthrone and suramin. Both these compounds have been previously shown to have activity against eukaryotic topoisomerase II (topo II) (Bojanowski et al, 1992; Smith et al, 1990), but they had not been previously tested against DNA gyrase. As such, the IC_{50}s of these compounds against *E. coli* DNA gyrase were determined to be 12 μM for mitoxanthrone and 80 μM for suramin in the gel assay (Figure 4.11 A and B).

Mitoxanthrone is from the anthraquinone class of drugs and is currently used as an antineoplastic agent (Schrappe, 2010). It is thought to inhibit topo II by stabilisation of the DNA cleavage intermediate, leading to generation of double-stranded breaks in DNA (Smith et al, 1990). To determine if this mode of action is the same for its inhibition of gyrase, an agarose gel assay was conducted under conditions which reveal formation

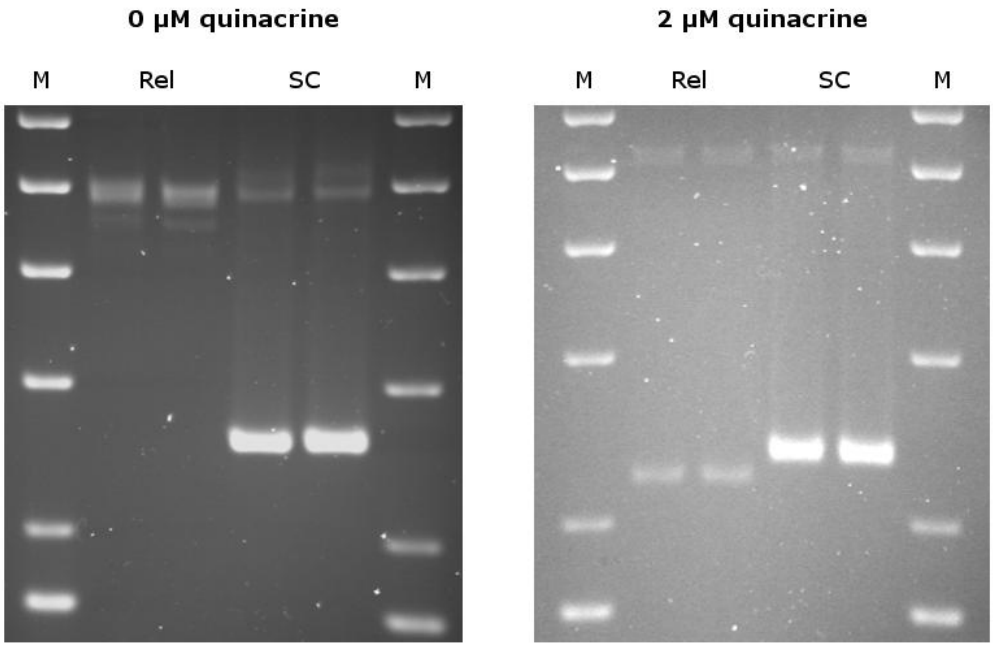

Figure 4.10 Effect of 2 µM quinacrine on the migration of relaxed and supercoiled pNO1. 1% agarose gels in TAE with or without 2 µM quinacrine in the gel and running buffer run for 3 hr at 80 V. Samples for the gel containing quinacrine were prepared in the presence of 2 µM quinacrine. A 1kb DNA ladder (M) was also included. The samples were prepared in duplicate.

of the cleavage intermediate (Figure 4.11 C; Section 2.7.2). It was observed that mitoxanthrone induced DNA cleavage strongly at 10 µM in the presence of 10 units of DNA gyrase, comparable to the known cleavage intermediate stabiliser ciprofloxacin, showing that mitoxanthrone stabilises the cleavage complex of gyrase as well as topoisomerase II. This is likely due to the drug intercalating at the DNA break generated in the cleavage complex in both enzymes. It also appears that at 100 µM the drug's ability to stabilize the cleavage complex is reduced. This is probably because mitoxanthrone is an intercalator and at this concentration it is distorting the DNA in such a way which prevents the enzyme binding.

Suramin is an antiprotozoal drug that has also entered clinical trials for the treatment of several forms of cancer (Stein, 1993). Although it has been shown to protect against cleavage of DNA by topo II induced by cleavage-intermediate stabilising agents (Bojanowski et al, 1992), its exact mode of inhibition was yet to be determined (Swift et al, 2008). As such the ability of suramin to protect DNA from gyrase-induced cleavage was tested (Figure 4.11 D; Section 2.7.2). To eliminate the possibility of drug—drug

interactions Ca^{2+} was used to induce cleavage by DNA gyrase (Reece & Maxwell, 1989). Suramin was able to completely protect DNA from cleavage by gyrase in the presence of 4 mM calcium chloride at 80 μM, indicating that its mode of action is similar to that found with topo II and is independent of drug—drug interactions.

To determine if the drug was protecting from cleavage by preventing binding of the protein to DNA, rather than preventing cleavage directly, a native gel shift assay of the binding of DNA gyrase to a 147 bp fragment of DNA in the presence or absence of 100 μM suramin was carried out (Figure 4.12; Section 2.7.4). In the absence of suramin the conversion of free DNA to a slower migrating form was observed as enzyme was titrated in, whereas the presence of 100 μM suramin abolishes this shift. This suggests that the drug is preventing the binding of the enzyme to DNA rather than

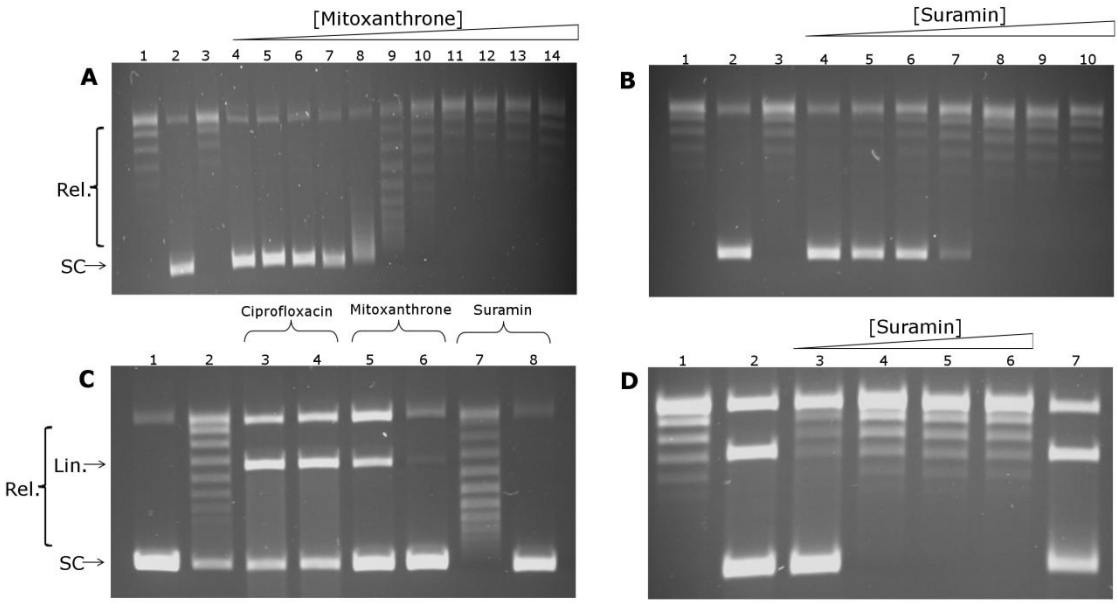

Figure 4.11 In vitro characterisation of mitoxanthrone and suramin. *A*. Determining the IC_{50} of mitoxanthrone. 1. Relaxed pNO1. 2. With 1 unit of DNA gyrase. 3. With 100 μM ciprofloxacin. 4-14. With 2 to 22 μM mitoxanthrone in 2 μM increments. *B*. Determining the IC_{50} of suramin. 1. Relaxed pNO1. 2. With 1 unit of DNA gyrase. 3. With 100 μM ciprofloxacin. 4-10. With 10 to 400 μM suramin in doubling increments. C. Cleavage complex stabilization assay with mitoxanthrone and suramin. 1. Supercoiled pNO1. 2. With DNA gyrase under relaxation conditions. 3-4. With 10 and 100 μM ciprofloxacin. 5-6. With 10 and 100 μM mitoxanthrone. 7-8. With 10 and 100 μM suramin. D. Cleavage protection by suramin. Reactions carried out in the presence of 4 mM CaCl to promote DNA gyrase mediated cleavage. 1. Relaxed pNO1. 2. With DNA gyrase. 3-6. 80-640 μM suramin in doubling increments. 7. With 0.8 μM novobiocin. Novobiocin is a strong (nM) ATPase inhibitor of DNA gyrase, and does not protect against cleavage.

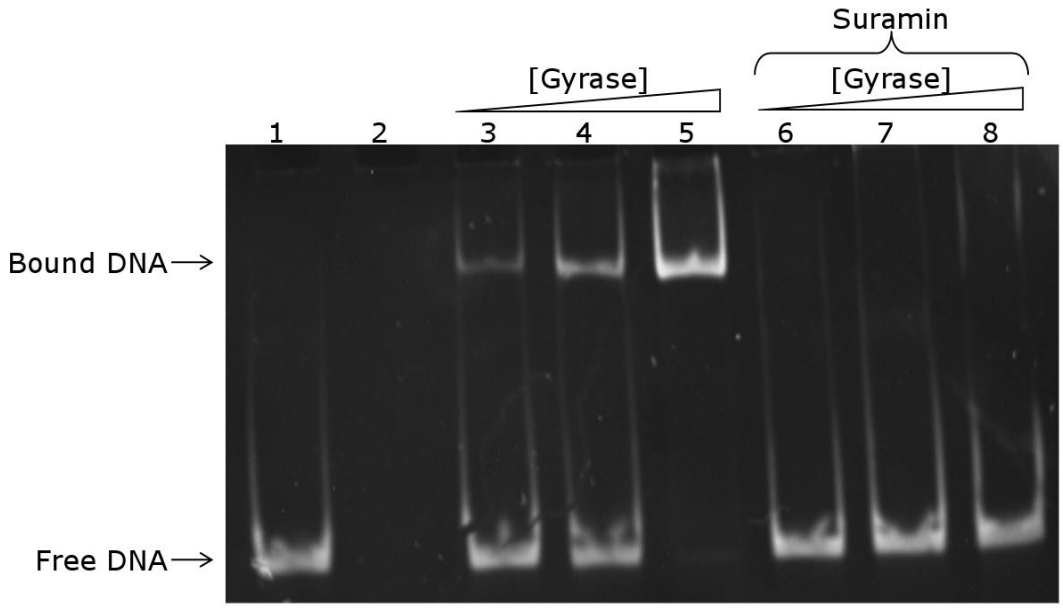

Figure 4.12 Gel shift analysis of the binding DNA gyrase to DNA in the presence of suramin. 1. 25 nM 147 bp DNA fragment. 2. 200 nM DNA gyrase (no 147 bp). 3-5. 50, 100 and 200 nM DNA gyrase with 25 nM 147 bp. 6-8. 50, 100 and 200 nM DNA gyrase with 25 nM 147 bp and 100 μM suramin.

preventing cleavage directly, similar to the antibiotic simocyclinone D8 (Flatman et al, 2005).

4.2.7 Effect on growth of Gram-negative and Gram-positive bacteria.

Having characterised the mechanisms of both mitoxanthrone and suramin their antimicrobial activities were explored. For these studies the effect of the drugs on the growth of both Gram-negative bacteria (in the form of the wild-type *E. coli* strain MG1655 (Blattner et al, 1997)) and Gram-positive bacteria (in the form of wild-type *M. smegmatis* strain mc^2155) was investigated. Additionally the growth of the membrane permeable *E. coli* strain NR698 in the presence of the drugs was investigated (Ruiz et al, 2005). *E. coli* NR698 carries an in frame deletion for the *imp* gene (*imp4213*), the product of which is responsible for lipopolysaccharide assembly in the outer membrane (Ruiz et al, 2006). This mutation causes the outer membrane of the bacteria to become leaky, making it more sensitive to antimicrobials. It was hoped that using this mutant would help me discount entry into the cell as a cause of resistance if the bacteria turned out to be unaffected by the drugs.

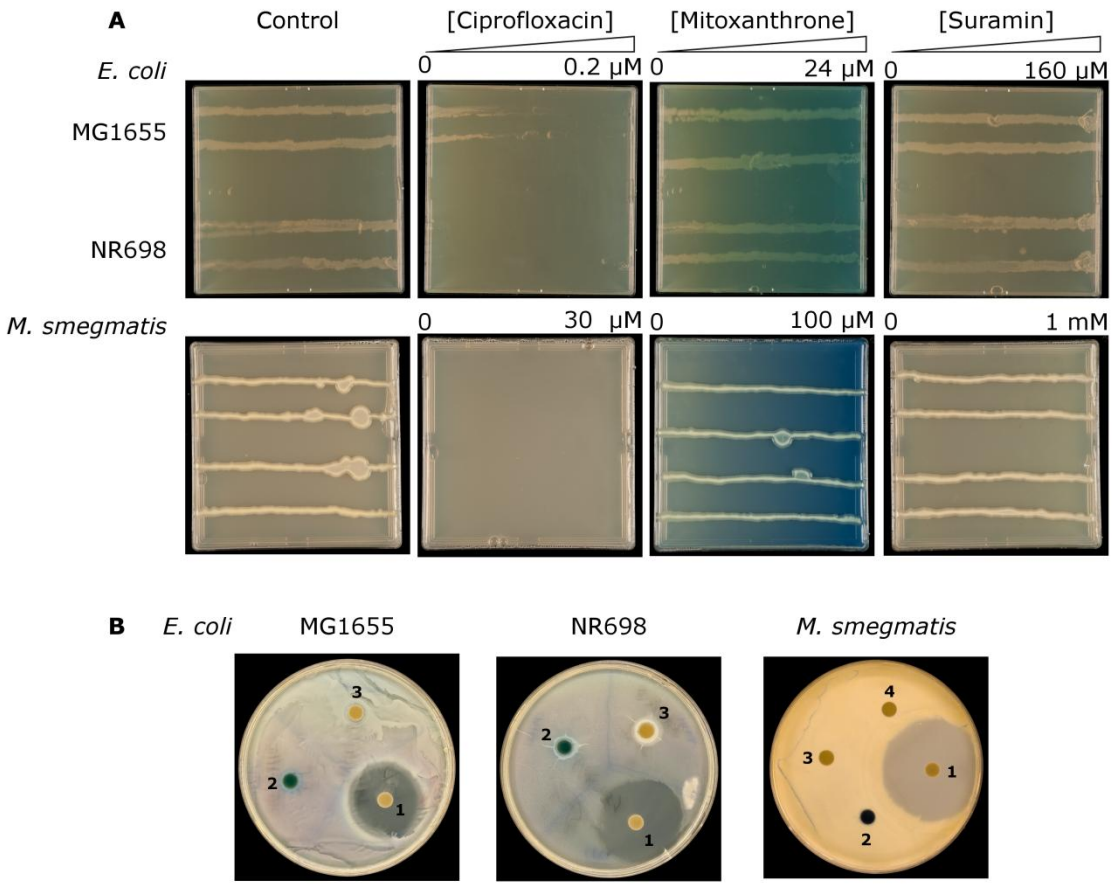

Figure 4.13 The effects of mitoxanthrone and suramin on bacterial growth on solid media. *A*. Slope assays for *E. coli* MG1655, NR698 and *M. smegmatis* mc^{2}155. Control plates have only had DMSO added to them. All other plates have a gradient of increasing compound from left to right. The *E. coli* strains were streaked in duplicate, whereas the *M. smegmatis* plates contained four repeats. Ciprofloxacin gradient: 0-0.2 µM for *E. coli*, 0-30 µM for *M. smegmatis*. Mitoxanthrone gradient: 0-24 µM for *E. coli*, 0-100 µM for *M. smegmatis*. Suramin gradient: 0-160 µM for *E. coli*, 0-1 mM for *M. smegmatis*. *B*. Halo assays for *E. coli* MG1655, NR698 and *M. smegmatis* mc^{2}155. All disks soaked with 2 mM compound. 1. Ciprofloxacin. 2. Mitoxanthrone. 3. Suramin. 4. 100% DMSO.

Initially the effect of the drugs on bacteria grown on solid agar was studied. Experiments were conducted using slope assays (Section 2.3.5), in which a single colony is streaked across an agar plate containing a gradient of compound (Figure 4.13 A). Since no antimicrobial activity was observed for the compounds at the concentrations tested, halo assays were used (Section 2.3.4) in which paper disks soaked in 2 mM compound are placed on a bacterial lawn (Figure 4.13 B). Antimicrobial activity is measured by the zone of clearing generated around the disk. Unfortunately no effect was observed with either compound.

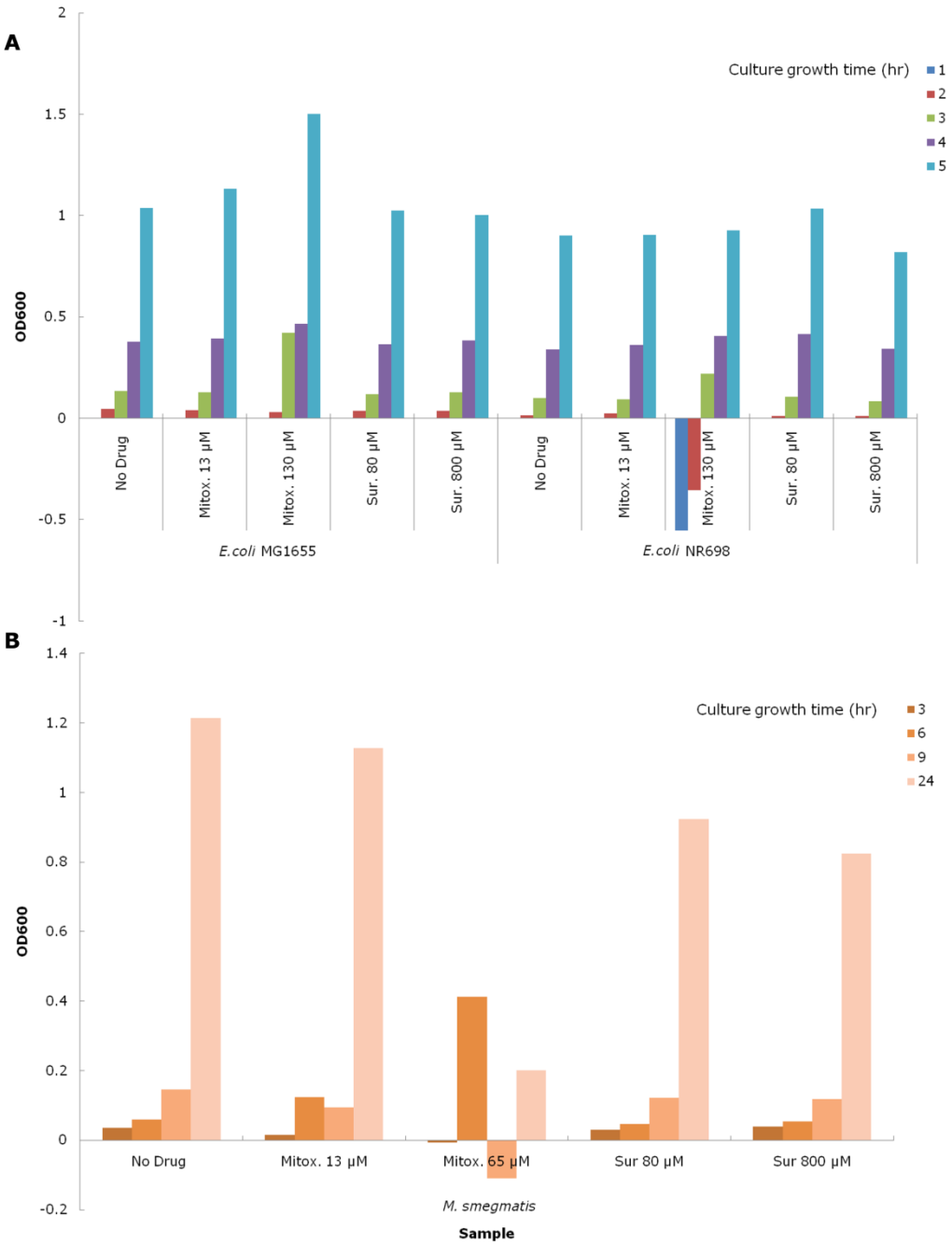

Figure 4.14 Bacterial growth in liquid media. *A. E. coli* MG1655 or NR698 after 1, 2, 3, 4 or 5 hr growth the presence of the indicated concentration of compound. *B. M. smegmatis* mc^{2}155 after 3, 6, 9 or 24 hr growth the presence of the indicated concentration of compound.

One concerning question was whether this lack of antibacterial activity was genuine or whether the compounds were having difficulty diffusing through the agar. To address this problem, growth curve assays in liquid media were carried out (Section 2.3.6) in the presence or absence of the compounds (Figure 4.14).

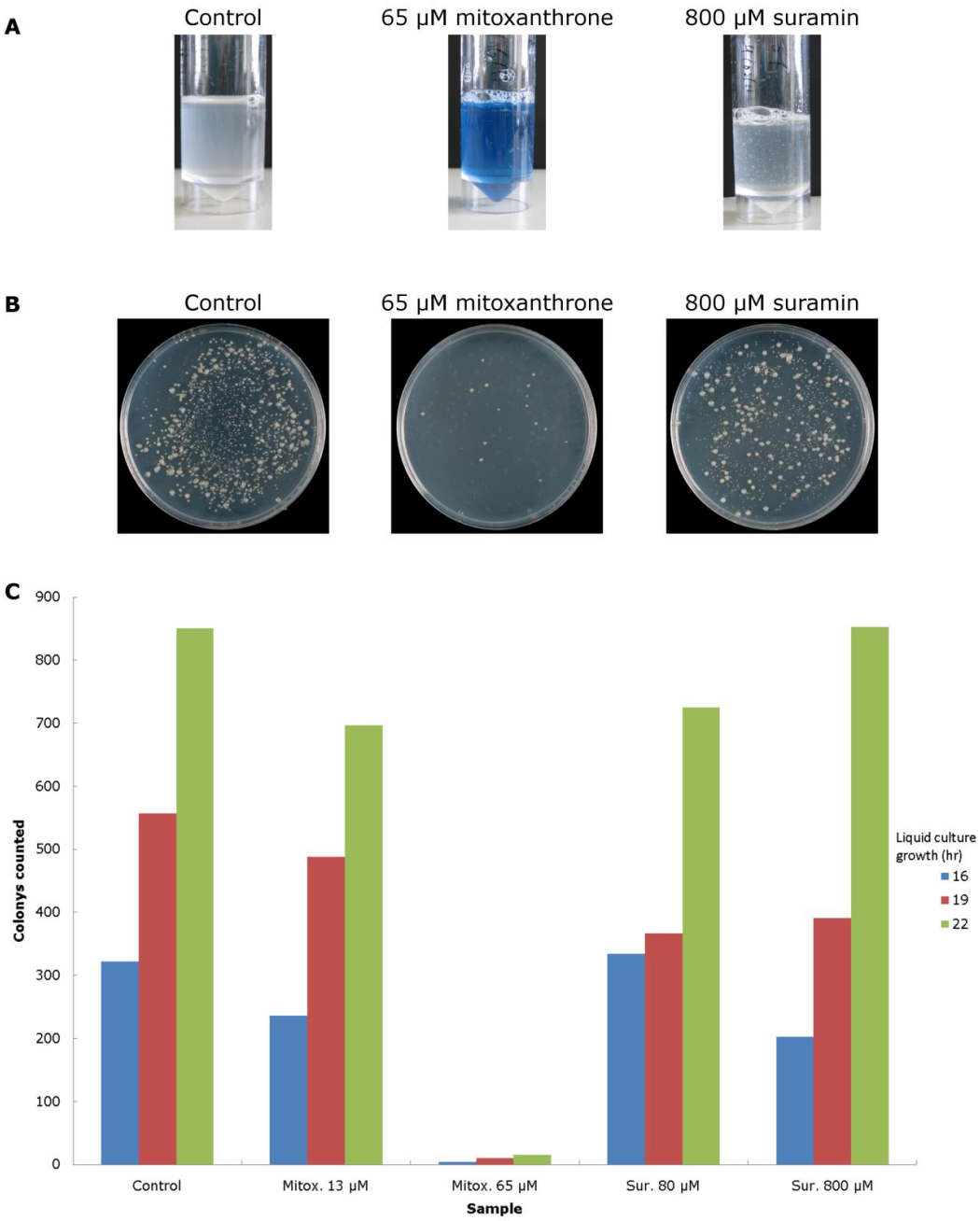

Figure 4.15 Colony counting of *M. smegmatis* mc^{2}155 in the presence of mitoxanthrone or suramin. *A*. Liquid cultures after 22 hr growth in the presence of 65 µM mitoxanthrone or 800 µM suramin. Similar cultures were prepared for 13 µM mitoxanthrone and 80 µM suramin. *B*. Aliquot of liquid cultures after 22 hr growth, plated onto Middlebrooks 7H11 agar free of test compounds and grown for a further 48 hr. Similar plates were prepared after 16 and 19 hr liquid culture growth. *C*. Colony counts for all compound concentrations and time points.

Neither mitoxanthrone nor suramin had any effect on the growth of *E. coli* MG1655 or NR698, both in terms in the final OD reached and in the doubling times of the bacteria. However, 65 µM mitoxanthrone reduced the growth of *M. smegmatis*. The presence of mitoxanthrone often disrupted

OD600 readings, possibly due to it having poor solubility in the media or due to its bright pigmentation.

To get a more accurate idea of the effect of mitoxanthrone on *M. smegmatis* growth colony counting assays were carried out (Section 2.3.7) on both mitoxanthrone and suramin (Figure 4.15). In these experiments *M. smegmatis* was grown in liquid media with or without test compound. An aliquot was taken after various time points (16, 19 and 22 hr), diluted 1 in 10,000 and plated onto Middlebrooks 7H11 agar plates which did not contain the test compounds. After 48 hr growth the colonies on each plate were counted manually. Bacteria grown in the presence of suramin grew similarly to the control at all time points. *M. smegmatis* grown in the presence of 65 μM mitoxanthrone produced fewer colonies than the control, indicating that the drug was inhibiting their growth at this concentration. The bacteria grown in 13 μM mitoxanthrone produced fewer colonies at each time point compared to the control, but since the differences were marginal it's difficult to say if this is due to genuine antimicrobial activity or to variation in the assay.

This raised the question why mitoxanthrone was inhibiting *M. smegmatis* growth in the liquid media and not on solid agar. To try and clarify if it was due to the drug diffusing poorly through the solid media, a single *M. smegmatis* colony was streaked onto a Middlebrooks 7H11 agar plate containing 100 μM mitoxanthrone (Figure 4.16). In this setup the drug would be evenly dispersed across the plate, rather than having to diffuse as

Figure 4.16 *M. smegmatis* streaked on Middlebrooks 7H11 agar containing 100 μM mitoxanthrone. Plates incubated at 37°C for 48 hr.

in the slope assays. Mitoxanthrone still did not affect bacterial growth, suggesting that the lack of inhibition on the plates wasn't due to diffusion. Alternatively, it could be due to the difference in bacterial growth states between the liquid and solid media setups.

4.3 Discussion

4.3.1 Performance of the screen

The work above has shown that the microtitre plate-based assay can be used in a high-throughput format to identify known and novel inhibitors of DNA gyrase, with an average Z' factor of 0.64. No single plate had a Z' factor below 0.5, indicating that there was good separation of positive and negative controls on all plates. There was no obvious pattern to the readings for the compounds on any of the plates. However it was observed that for some plates the majority of compounds showed either mild inhibition or activation. This was likely due to day-to-day or run-to-run variations of the screening process. With a hit threshold of 25% inhibition, 21 compounds were selected for further investigation. Thirteen of these were confirmed as hits. Four known DNA gyrase inhibitors were missed by the screen. They were likely missed due to variations within the assay or degradation of the compounds during storage.

Out of the 13 hits discovered by the screen only two were novel gyrase inhibitors, both of which were already known topoisomerase II inhibitors. This was likely a result of the library selection, since both DNA gyrase and human topoisomerase II are well exploited drug targets with similar modes of action. This causes a number of problems when using a library of existing drugs to screen for novel and therapeutically relevant inhibitors of these enzymes. Firstly, any DNA gyrase inhibitors you find may also be cytotoxic chemotherapy drugs which target human topoisomerase II. Such compounds are toxic to humans and produce numerous unpleasant side effects. Although it may be possible to re-engineer these compounds to mitigate the side effects, doing so would negate one of the points of selecting a library in this way, since their physiochemical properties would have to be re-characterised. Secondly, when looking for human

topoisomerase II inhibitors for cancer therapy you will find hits which have activity against DNA gyrase. If these drugs shared common binding sites to currently used antibiotics you would run the risk of inadvertently breeding antibiotic resistant bacteria. Thirdly, many of your hits will already be known to affect the target you were screening against. As such, a tailored library of known drugs excluding already known inhibitors would be essential for a larger-scale screen.

Nine of the compounds selected by the screen turned out to be false positives. Out of these only one, harmalol, was shown to interfere with the assay. The library stocks for this compound must have become degraded or contaminated in some way, since fresh stocks didn't show any interference. The remaining false positives were probably selected because the hit threshold was set too low (See Chapter 6 for further discussion).

4.3.2 9-aminoacridine and quinacrine as DNA gyrase activators

Two activators of DNA gyrase were identified through the screen: 9-aminoacridine and quinacrine. Both of these compounds are intercalators, and have been shown that quinacrine is capable of causing relaxed plasmid to run as a single band with a faster mobility than negatively supercoiled plasmid. One explanation for the identity of this band is that it is positively supercoiled plasmid. This could explain the enhancement in DNA gyrase activity brought about by the drug, since positively supercoiled plasmid is a superior substrate for DNA gyrase compared to relaxed DNA (Bates et al, 1996). Although the migration of DNA in the presence of 9-aminoacridine was not tested it is likely that it operates by a similar mode of action.

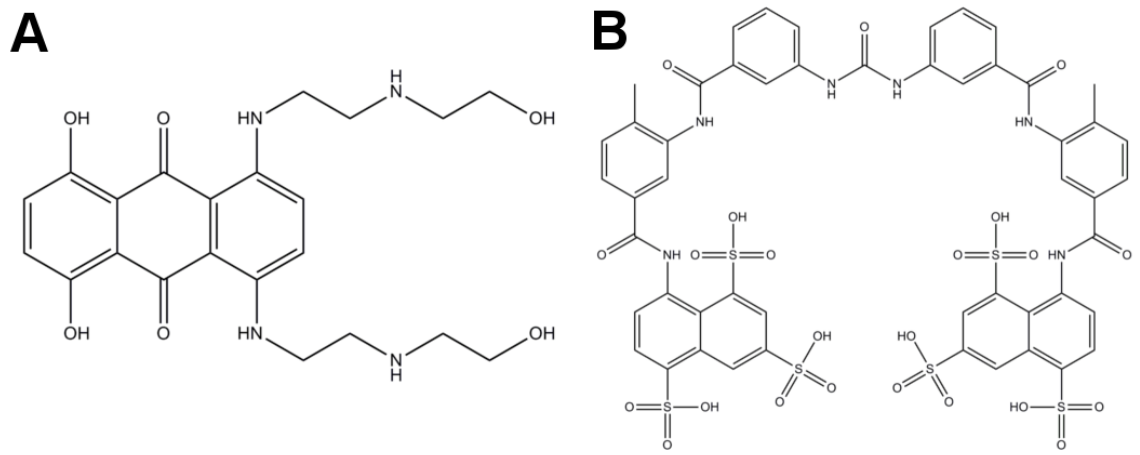

Figure 4.17 Structures of novel DNA gyrase inhibitors from screen. *A*. Mitoxanthrone. *B*. Suramin.

4.3.3 Mitoxanthrone and suramin as novel DNA gyrase inhibitors

Two of the hits from the screen were novel DNA gyrase inhibitors: mitoxanthrone and suramin (Figure 4.17). However, neither of these compounds are novel topoisomerase inhibitors both having been previously shown to inhibit topoisomerase II. (Bojanowski et al, 1992; Smith et al, 1990). The IC_{50}s were determined to be 12 μM and 80 μM, respectively, in the agarose gel assay.

Mitoxanthrone has been shown to inhibit topoisomerase II by stabilising the cleavage complex (Smith et al, 1990). As shown above this mode of action holds true for its inhibition of DNA gyrase. This makes it similar to ciprofloxacin in terms of its inhibitory potential and mechanism.

Suramin, on the other hand, had been shown to protect against drug mediated DNA cleavage by topoisomerase II (Bojanowski et al, 1992). However, it was not clear from this if this protective activity was due to direct inhibition of cleavage, due to the blocking of DNA binding or a drug—drug interaction. With DNA gyrase was shown that suramin can protect from calcium mediate cleavage of DNA. This eliminated the possibility of drug—drug interactions being involved in the process. It has also been shown by native gel shift experiments that suramin prevents the binding of the DNA gyrase to DNA. These facts imply that suramin chiefly inhibits DNA gyrase, and protects against gyrase-mediated cleavage, by preventing binding of

the enzyme to DNA. An interesting possibility is that the sulfonic acid groups on suramin could allow it to mimic the 5'-phosphate group of a nicked DNA backbone and compete for binding with DNA directly at the active site.

4.3.4 Mitoxanthrone as an antimicrobial compound

Although suramin displayed no antimicrobial activity with any of the bacterial strains tested, it has been shown that mitoxanthrone is capable of inhibiting the growth of *M. smegmatis* in liquid cultures at 65 μM. However, no inhibition of growth was seen with either wild-type *E. coli* MG1655 or the membrane permeable strain NR698. This was true for bacteria grown on both liquid and solid media, suggesting that either the drugs still cannot gain entry to the bacteria, despite the mutation present in NR698, or that *E. coli* is naturally resistant to them (e.g. via an efflux pump or degradation pathway).

The reason why mitoxanthrone can inhibit bacterial growth only in liquid cultures may be because the bacteria exist in a very different growth state whilst they are growing on solid media. It has been shown that bacteria growing in biofilms can be more resistant to antimicrobial agents than free-floating planktonic cells (Mah & O'Toole, 2001). Reasons why this might be are numerous including: the colony preventing diffusion of drug; slower growth rate of the bacteria on the solid media and the induction of biofilm-specific stress responses and phenotypes.

Although mitoxanthrone may also inhibit growth of pathogenically relevant *Mycobacterium*, such as *Mycobacterium tuberculosis,* its prospects as a commercial antibiotic are fairly limited. It is currently administered via injection as a treatment for some forms of cancer and multiple sclerosis (Hartung et al, 2002; Schrappe, 2010). This mode of delivery is undesirable for antibiotics since it requires administration by trained medical personnel and sterile needles. It would also reduce patient compliance due to the discomfort caused by the injections, with the result being higher rates of people abandoning the treatment before the course was completed. This would in turn lead to faster development of resistance. These factors are of particular importance for the developing world where tuberculosis is a major

epidemic. Several potentially lethal side effects have been identified for mitoxanthrone, including increased chance of leukaemia and heart failure (Le Page et al, 2011), further decreasing its appeal. It is conceivable, however, that the structure of mitoxanthrone could be used as a scaffold for synthesis of compounds with more favourable characteristics and lower cytotoxcitiy.

Chapter 5

Methanosarcina mazei topoisomerase VI screen

5.1 Introduction

In the previous chapter it has been shown that the microtitre plate-based assay could be used to screen for new inhibitors of the well characterised *E. coli* gyrase. Having carried out this proof-of-principle screen, it was decided to progress to a less well studied enzyme: topoisomerase VI (topo VI). Topo VI is member of the type IIB class of topoisomerases and has been discovered in archaea and plants (Bergerat et al, 1997; Corbett & Berger, 2003). However few inhibitors have been described in the literature for this enzyme, including the HSP90 inhibitor radicicol (Gadelle et al, 2006). The IC_{50} of this compound with the *Sulfolobus shibatae* topo VI has been shown to be 250 μM, making it a poor inhibitor. This lack of inhibitors and the relatively small amount of study conducted with the enzyme made topo VI an interesting candidate for the screen: any novel inhibitors found would have the potential to give us greater insight into how the enzyme functions.

In plants topo VI has been shown to be essential for endoreduplication (the process by which plants create multiple copies of their genome without fission) and cell expansion (Corbett & Berger, 2003; Yin et al, 2002), meaning that inhibitors targeting the enzyme have potential as dwarfing agents or herbicides. Unfortunately, the *Arabidopsis* topo VI has yet to be expressed in a soluble form. Topo VI from the archaea *Methanosarcina mazei* is easy to express and has been crystallised by one of our collaborators (Corbett et al, 2007). In addition, the majority of the biochemical studies on topo VI have been conducted with the *S. shibatae* enzyme meaning that *M. mazei* topo VI has not been extensively characterised. It was therefore decided to screen against the *M. mazei* version of the enzyme in the hopes that any inhibitors discovered would

help probe the mechanism of the enzyme. Any hits could be tested against the *Arabidopsis* enzyme *in vivo* with an assay using a hypocotyl extension assay.

Additionally, genes for topo VI have been identified in the genome of the malaria parasite *Plasmodium falciparum* (Aravind et al, 2003). These include two genes with homology for the topo VI A subunit (*PF10_0412,* abbreviated to PfTopo6A1; *PFL0825c,* abbreviated to PfTopo6A2) whilst one gene had homology for the topo VI B subunit (*MAL13P1.328*, abbreviated to PfTopo6B). The presence of a topo VI makes sense in terms of the biology of the parasite since it undergoes a process called schizogony as part of its life cycle, which bears similarities to endoreduplication in plants. During the process of schizogony the parasite replicates its genome several times without cell division before budding daughter cells (Gantt et al, 1998; Sturm & Heussler, 2007). This convinced us that it would be worthwhile attempting to express and purify these hypothetical proteins to test for topo VI activity. The hits from the *M. mazei* topo VI screen could then be tested against the *P. falciparum* enzyme. If successfully validated, this enzyme may be a novel target for anti-malarial drugs.

5.2 Results

5.2.1 Characterisation of *M. mazei* topo VI

Since *M. mazei* topo VI was relatively unstudied this study began with biochemical characterisation of the enzyme. Initially enzyme was titrated in the presence of the published assay buffer (Corbett et al, 2007) in both the agarose gel based and microtitre plate-based assays (Figure 5.1). Reactions were incubated at 37°C for 30 min. In the gel-based assay almost complete relaxation of 0.5 μg supercoiled pNO1 was observed with between 23 and

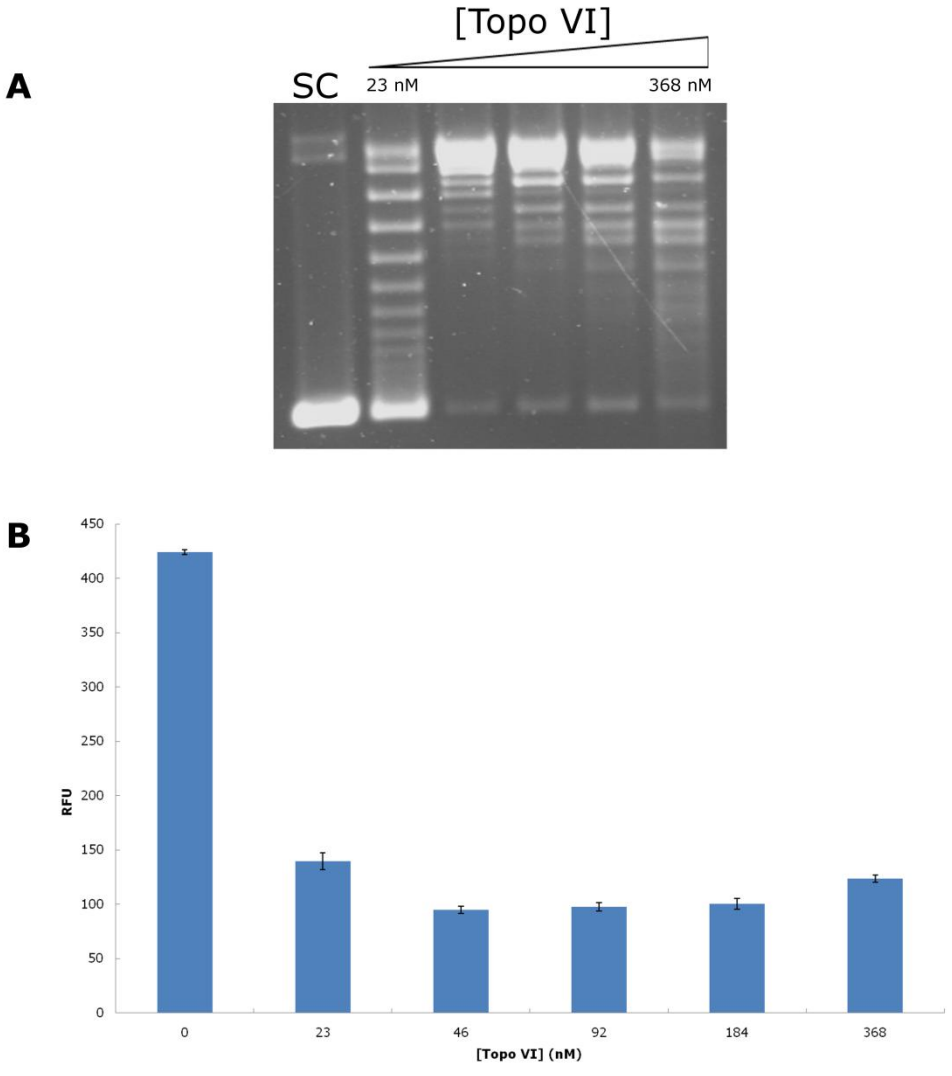

Figure 5.1 Activity of *M. mazei* topo VI. *A*. Titration *M. mazei* topoisomerase in the agarose gel-based assay: 23, 46, 92, 184 or 368 nM enzyme. *B*. Titration *M. mazei* topoisomerase in the microtitre plate-based assay.

46 nM topo VI. However, strangely, not all the supercoiled plasmid appeared to be relaxed by the enzyme. Increasing the concentration of enzyme did not result in relaxation of the lingering SC DNA, and lead to the formation of a series of defined bands. The banding pattern produced at high concentrations was distinct from the patterning seen for partial relaxation at 23 nM. Faster migrating species emerged as the concentration of enzyme increased. In the plate assay the majority of the fluorescence signal attributable to supercoiled DNA was lost with the addition of 24 nM topo VI. Increasing the concentration to 46 nM caused a further, but minor, decrease in signal. Raising the concentration above 46 nM had hardly any effect with the exception of 368 nM topo VI, which exhibited a very slight increase in signal.

To further investigate the formation of the unusual banding pattern formed by topo VI at high concentrations a titration of the enzyme in the presence of relaxed DNA was performed (Figure 5.2 A). It was observed that topo VI was capable of forming the strange banding pattern with relaxed as well as supercoiled DNA, implying that it was a not due to auto-

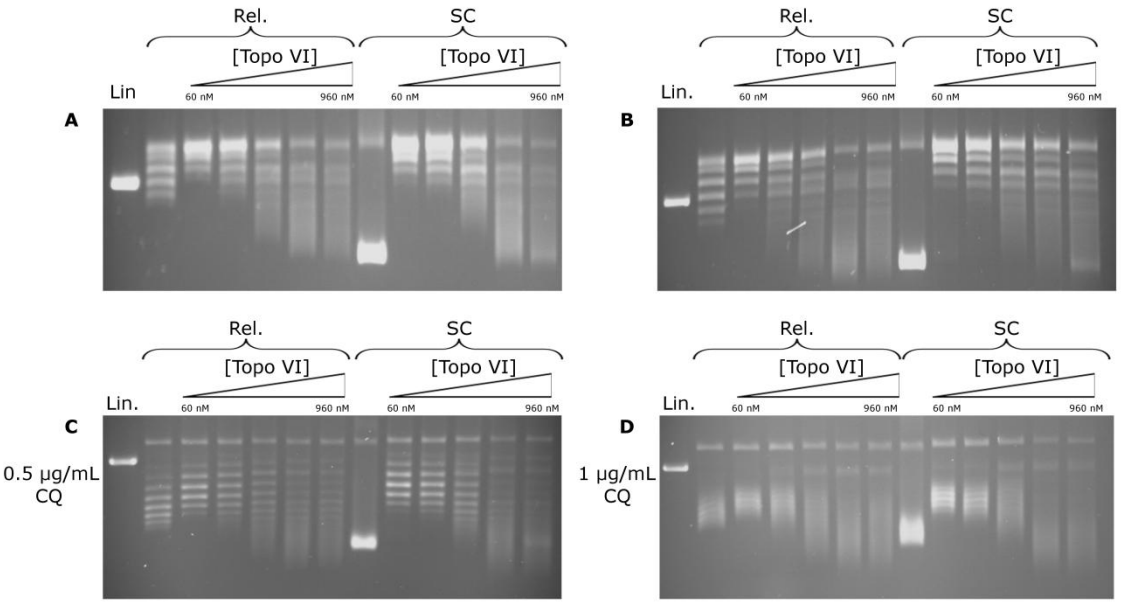

Figure 5.2 Titration of *M. mazei* topo VI with relaxed or SC pNO1. *A*. 60, 120, 240, 480 or 960 nM topo VI with relaxed or SC pNO1. *B*. Reactions stopped with 1% SDS and incubated with 0.1 mg/ml proteinase K for a further 1 hr at 37°C. *C*. Samples from *A* run on a gel containing 0.5 µg/mL chloroquine. *D*. Samples from *A* run on a gel containing 1 µg/mL chloroquine.

inhibition of the enzyme at the higher concentrations. Since it was possible the patterning could be due to enzyme remaining stuck to the DNA whilst it was on the gel the experiment was repeated with a more stringent protein removal protocol (Figure 5.2 B). After the standard topo VI reaction the samples were stopped with 1% SDS and digested with 0.1 mg/mL proteinase K for 1 hr at 37°C. The remaining protein was then removed via phenol/chloroform extraction. The unknown bands remained unaffected compared to the standard extraction protocol, implying that the banding pattern was not due to protein remaining bound to the DNA. To try and discern the topological state of the unexplained bands the samples were re-run on gels containing either 0.5 or 1 μg/mL chloroquine (Figure 5.2 C and D). Chloroquine is a weak DNA intercalator whose binding causes the writhe of DNA to become more positively supercoiled. As such, relaxed DNA treated with chloroquine begins to migrate faster whilst negatively supercoiled DNA begins to shift up the gel. Samples treated with up to 120 nM topo VI displayed behaviour typical of relaxed DNA. However samples with 240 nM or more topo VI were less affected by the chloroquine. This suggested that the band emerging at these concentrations may be something other than supercoiled or relaxed DNA.

In order to further explore the identity of these bands it was decided to see if they could be relaxed by wheat germ topoisomerase I (topo I) (Figure 5.3). Since the topo VI reaction is Mg^{2+} dependent whilst the topo I reactions is not, it was possible to selectively stop the topo VI with EDTA after it had completed its reaction. Topo I could then be added and its affect on the unusual bands observed. In the absence of topo VI or EDTA, topo I was capable of fully relaxing supercoiled DNA. The inclusion of EDTA at the beginning of the reaction decreased its activity slightly. Topo VI, on the other hand, was completely stopped by the presence of EDTA from the start of the reaction. In the absence of ATP topo VI was not capable of forming the unusual bands, suggesting they were not general degradation due to a contaminant. However, a linear band was observed which is likely attributable to a contaminant in this batch of enzyme. Some relaxation activity was seen with topo VI in the presence of ATP and absence of $MgCl_2$ and EDTA, which was probably due to trace amounts of Mg^{2+} from other

sources. These controls made us confident that topo VI could be selectively stopped with EDTA but leave topo I active, and the appearance of the strange bands was both ATP- and Mg^{2+}-dependent. The samples incubated with EDTA, topo I and topo VI from the beginning showed the standard relaxation pattern for topo I. However samples in which topo VI was allowed to react for 30 min before the addition of EDTA and topo I showed the strange banding pattern. This showed that topo I was unable to process the DNA topoisomers generated by topo VI, which implies they are something other than relaxed or supercoiled DNA.

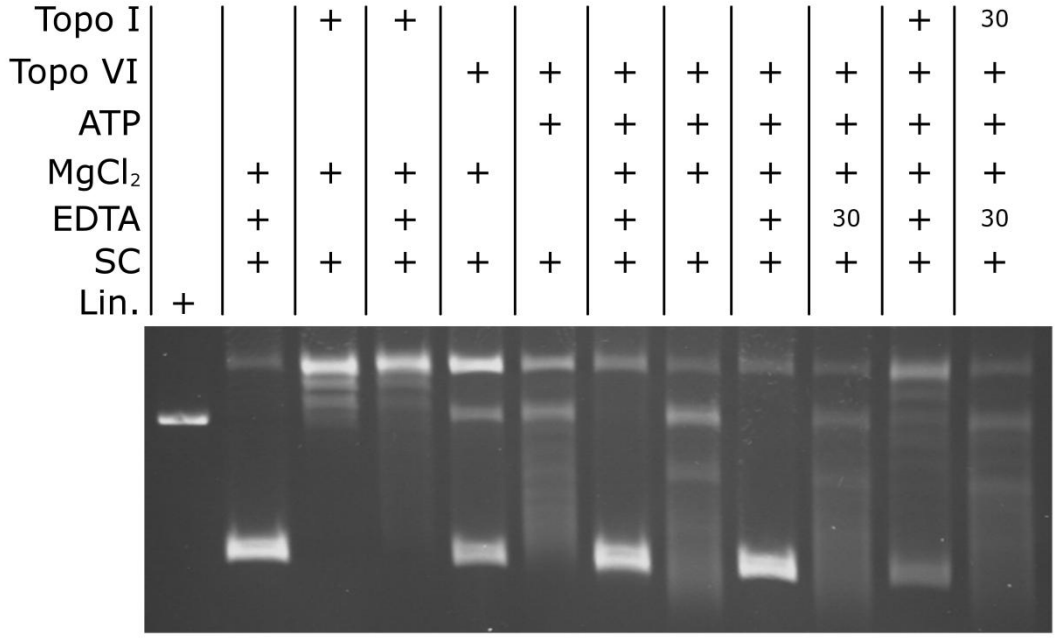

Figure 5.3 Processing of unusual products of topo VI by wheat germ topoisomerase I. All reactions were carried out in 1x topo VI assay buffer lacking ATP or $MgCl_2$. Various components were added to the assays either at the beginning of the experiment (+) or after 30 min (30). These components included: wheat germ topo I (4 U), *M. mazei* topo VI (940 nM), ATP (1 mM), $MgCl_2$ (10 mM), EDTA (17 mM), SC pNO1 (0.5 μg) or linear pNO1 (0.5 μg). Reactions lacking topo VI were incubated for 1.5 hours at 37°C whilst reactions with topo VI were incubated for 2 hours at 37°C. This was done to keep topo I incubation times identical in all reactions.

It was of interest whether these bands were the end product of the topo VI reaction or whether they were purely a concentration-dependent effect. As such time course reactions with topo VI were carried out at 5, 10, 20 or 80 nM (Figure 5.4). The unusual banding was observed after 15 min with 20 or 80 nM, with the reaction having reached completion after 30 min. In contrast, the strange bands were never observed with 5 or 10 nM topo VI even after 160 minutes. The reactions containing 20 nM topo VI appeared to reach completion after 10 minutes, considerably faster than the samples with 80 nM.

One possibility was that the enzyme was somehow introducing knots into the plasmids. Generating single-strand nicks in supercoiled or relaxed topoisomers results in conversion to open circular DNA (due to release of tension from the molecule). Knotted DNA, on the other hand, would be unaffected by the presence of single-strand nicks since its structure arises from the crossing over of double-stranded DNA (Bates & Maxwell, 2005). DNA processed by topo VI at high concentrations was treated with the nicking endonuclease Nb.BstI (Figure 5.5). pNO1 was predicted to have a

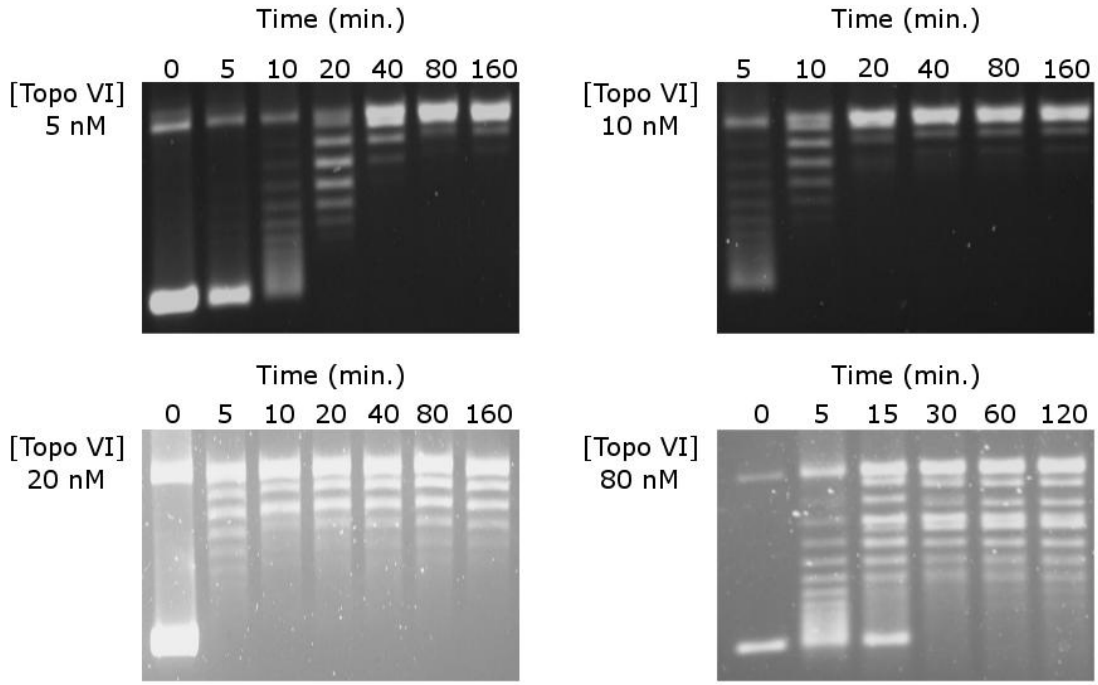

Figure 5.4 Time course reactions for *M. mazei* topo VI. Reactions with 5, 10, 20 or 80 nM topo VI were stopped at the indicated time points.

single nicking sequence for Nb.BstI, meaning supercoiled or relaxed pNO1 treated with this enzyme should be entirely converted to open circular DNA with a single nick present. It was observed that this was the case with supercoiled pNO1 in the presence or absence of topo VI with no ATP. Some linear DNA formation was observed when topo VI was included in the reaction (with or without ATP), but this was likely due to a contaminant being present with the enzyme. However, addition of Nb.BstI after the reaction with topo VI has been allowed to complete did not result in the conversion of the unusual bands to the open circular form. This implied that these bands were not relaxed or supercoiled topoisomers, and suggested that they might be either knotted or linear DNA of different sizes.

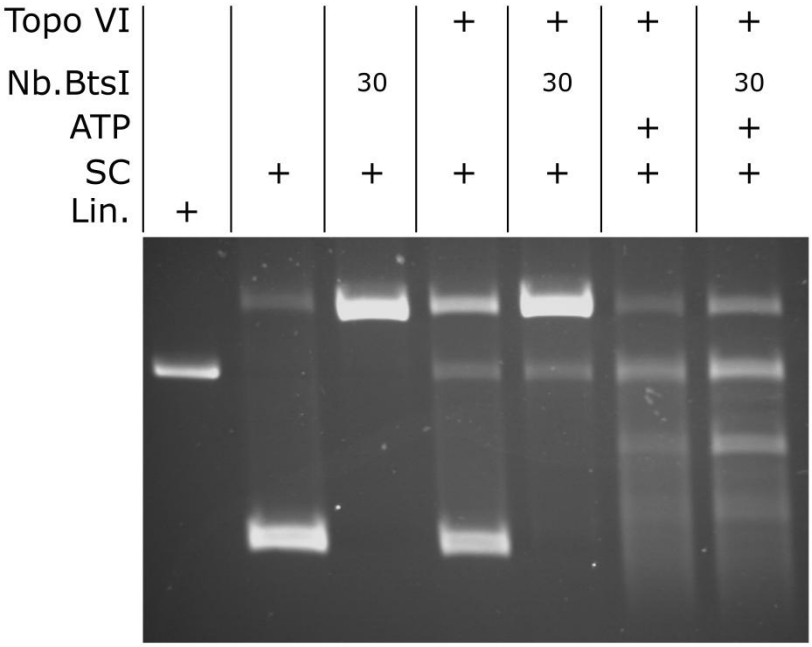

Figure 5.5 Processing of unusual topo VI products by nicking endonuclease Nb.BtsI. All reactions carried out in 1x topo VI assay buffer lacking ATP. Various components were added to the assays either at the beginning of the experiment (+) or after 30 min (30). These components included: *M. mazei* topo VI (940 nM), Nb.BtsI (10 U), ATP (1 mM), SC pNO1 (0.5 μg) or linear pNO1 (0.5 μg). Reactions were incubated for a total of 2 hr at 37°C.

To determine the topology of these bands our collaborators August Johansson and Dr Neil Thompson (University of Leeds) conducted atomic force microscopy on samples of supercoiled, wheat germ topo I relaxed, *M. mazei* topo VI (50 nM) relaxed and *M. mazei* topo VI (960 nM) relaxed pNO1 (Figure 5.6). These reactions were prepared in the same way as in the reactions above and their characteristics verified by agarose gel electrophoresis. After the reactions had been completed the samples were treated with 1% SDS and digested with proteinase K for 1 hr at 55°C. They were then subjected to phenol-chloroform extraction and ethanol precipitated. The samples were sent as dried pellets to our collaborators for

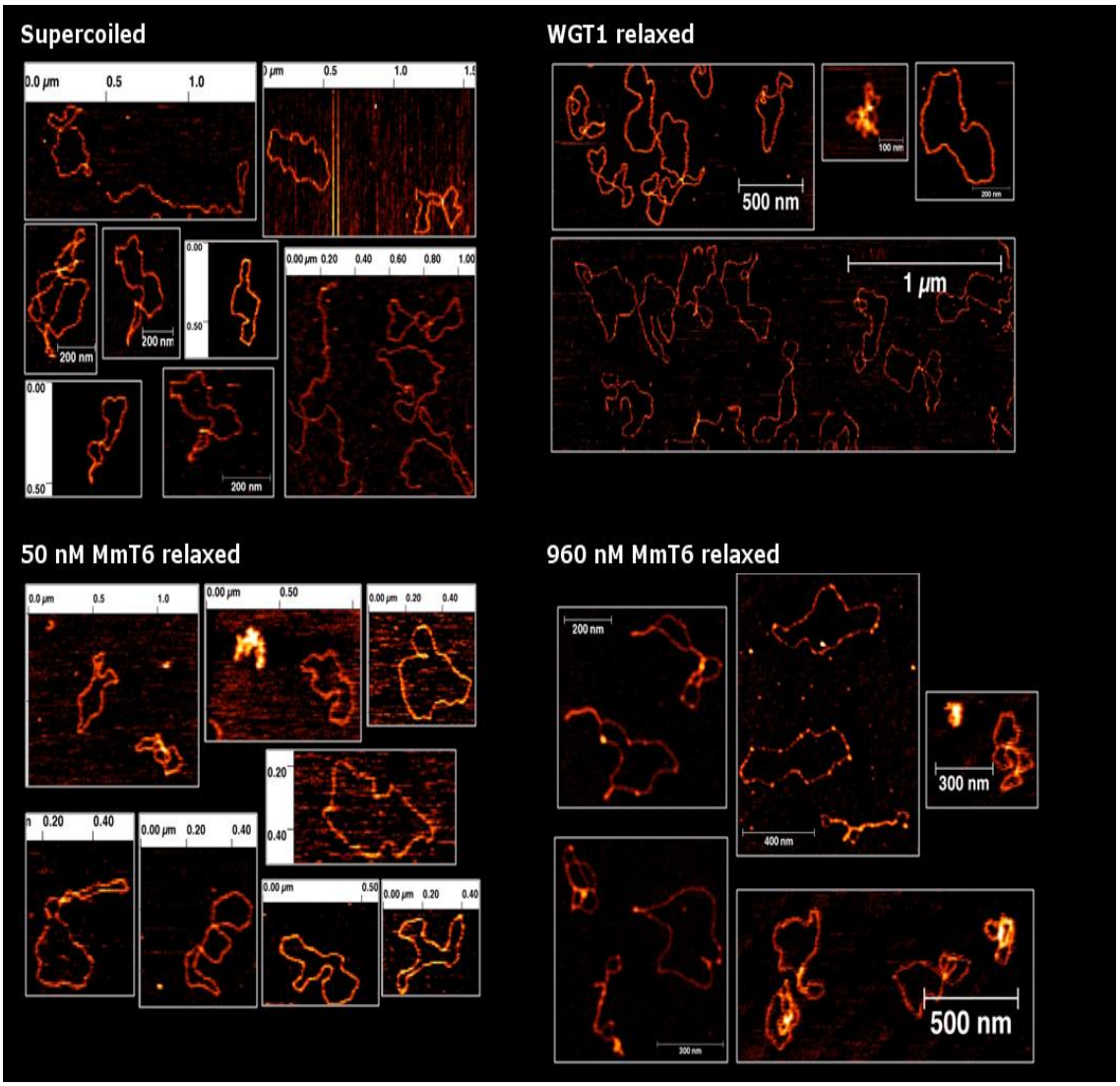

Figure 5.6 AFM images of *M. mazei* topo VI reaction products. Samples of substrate supercoiled pNO1 and the resulting products after relaxation by either 4 U wheat germ topo I, 50 nM *M. mazei* topo VI or 960 nM *M. mazei* topo VI. Images kindly provided by August Johansson and Dr Neil Thompson.

analysis. All samples were prepared on mica using Mg^{2+} as the binding cation, so all the molecules should be in their 2D surface relaxed form (i.e. binding method to the surface should not introduce further strain energy into circular DNA).

The supercoiled control did not display the expected frequency of cross-overs, being only between one to three, whilst some molecules appeared to be open-circles. This may have been due to writhe being converted to twist by surface interactions or the sample becoming damaged in transportation. The samples treated with wheat germ topo I or 50 nM *M. mazei* topo VI appear more relaxed than the supercoiled samples although some cross-overs remain, which was expected for relaxed DNA. The sample treated with 960 nM *M. mazei* topo VI appeared more like the supercoiled DNA, but possessed structures not seen in the other samples including plectonemes and DNA condensation. Additionally, many molecules appear to be decorated with protein molecules that have not been removed during sample preparation. This was surprising due to the thoroughness of the protein extraction. It has been observed in this study that the enzyme binds to DNA in the absence of ATP (see native gel shift experiments below) and that the formation of the strange banding pattern the gel is ATP-dependent. Therefore the decoration observed in the AFM and the strange banding seen the gel assays may indicate topo VI-DNA cleavage complexes.

5.2.2 Inhibition of *M. mazei* topo VI by radicicol

The only published inhibitor of topo VI is the HSP90 inhibitor radicicol, which has been shown to target the ATPase activity of the enzyme (Corbett & Berger, 2006). Since the majority of studies on topo VI have been on the enzyme from *S. shibatae* it remained to be tested radicicol also inhibited the *M. mazei* enzyme in a similar way. The compound was titrated from 0 to 400 μM into reactions containing 0.5 units *M. mazei topo* VI for analysis in the agarose gel assay (Figure 5.7). The reported IC_{50} for radicicol with *S. shibatae* topo VI is 250 μM. *The M. mazei* enzyme appeared less sensitive to the inhibitor, with an IC_{50} of around 400 μM.

Having established that *M. mazei* topo VI was sensitive to radicicol experiments were conducted to confirm the drug targeted the ATPase activity of the enzyme. Preliminary ATPase assays (see Section 2.7.3) were performed with the *E. coli* GyrB subunit which was known to work well in the assay. Titrating in novobiocin, a well characterised ATPase inhibitor for DNA gyrase, resulted in a reduction in the enzyme's rate of ATP hydrolysis at nanomolar concentrations (Figure 5.8). Radicicol, on the other hand, only showed modest inhibition at 500 μM. At concentrations below 500 μM radicicol appeared to stimulate the ATPase activity of GyrB in a dose-responsive manner. This could either be a genuine activation of the

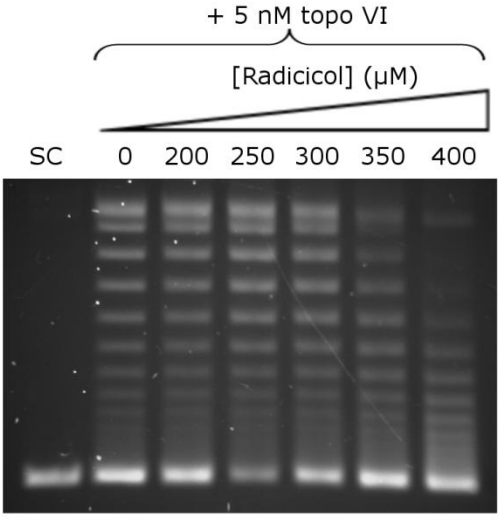

Figure 5.7 Titration of radicicol with *M. mazei* topo VI in the agarose gel assay.

enzyme, or the drug interfering with linked assay in some manner. Reactions with GyrB and 500 μM radicicol but lacking ATP did not display any change in absorbance compared to similar reactions lacking radicicol. This showed that the compound did not affect absorbance just by being present.

Next the effect of radicicol on the ATPase activity of *M. mazei* topo VI was investigated. To establish the best concentration of enzyme to use in future studies a titration of topo VI from 80 to 580 nM was performed

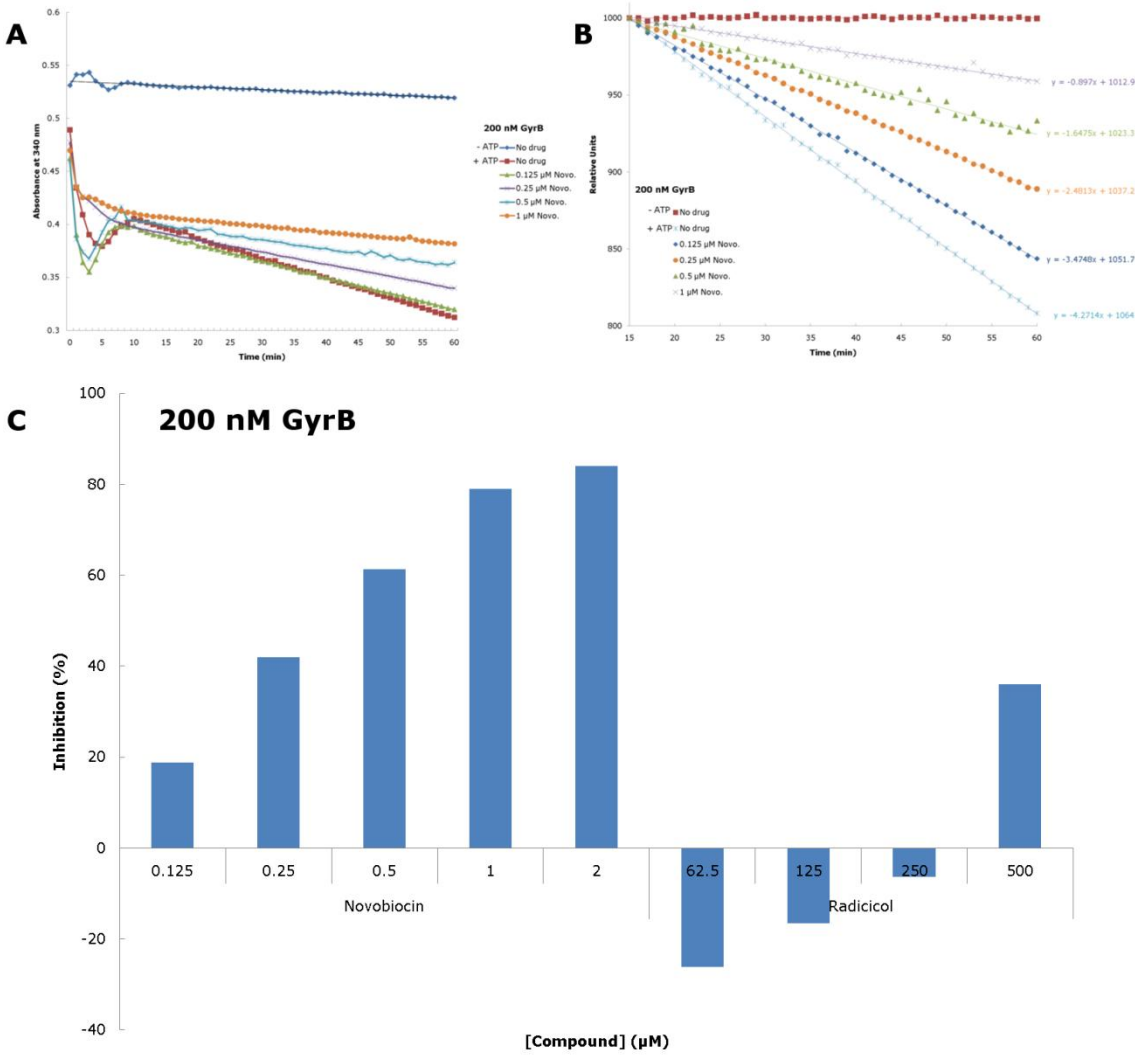

Figure 5.8 Titrations of novobiocin and radicicol with *E. coli* GyrB in the ATPase assay. *A*. Sample raw data. Novobiocin titrated from 0 to 1 μM. *B*. Sample processed data. The first 15 min were excluded due to artefacts and the remaining data were normalised to the 15 minute data point. The slope of the control lacking ATP was subtracted from all data sets to eliminate any background changes in absorbance. The rates of ATP hydrolysis could be calculated from the gradient of the slopes. *C*. Summary of percentage inhibition for novobiocin and radicicol at the indicated concentrations. The percentage inhibition was calculated relative to the rate of ATP hydrolysis in the absence of compound.

(Figure 5.9 A). Although the enzyme displayed ATPase activity at all concentrations tested the 580 nM concentration produced the clearest results. As such, both novobiocin and radicicol were titrated into reactions containing 580 nM topo VI (Figure 5.9 B). Novobiocin had no effect on ATPase activity at 2 μM, whereas this concentration of drug had almost entirely stopped the ATPase activity of *E. coli* GyrB. However, radicicol inhibited the ATPase activity of the enzyme in a dose-responsive manner. From these data the IC_{50} of radicicol in this assay was estimated to be approximately 350 μM. This value was similar to that which had been observed in the agarose gel assay. From this it can be concluded that *M. mazei* topo VI is sensitive to radicicol (although less so that *S. shibatae* topo VI) and that radicicol inhibits the ATPase activity of the enzyme.

5.2.3 Screening against *M. mazei* topo VI

Since the previous protocol had worked well for the DNA gyrase screen it was duplicated exactly for the *M. mazei* topo VI screen (Section 4.2.1). The screen was conducted in duplicate over four days (Figure 5.10 and Figure 5.11; see Section 2.8.2. for details of the protocol used). The arbitrary hit threshold of 25% inhibition from the previous screen was kept since the number of false positives generated was manageable. The nine compounds which exceeded this threshold were selected for further study.

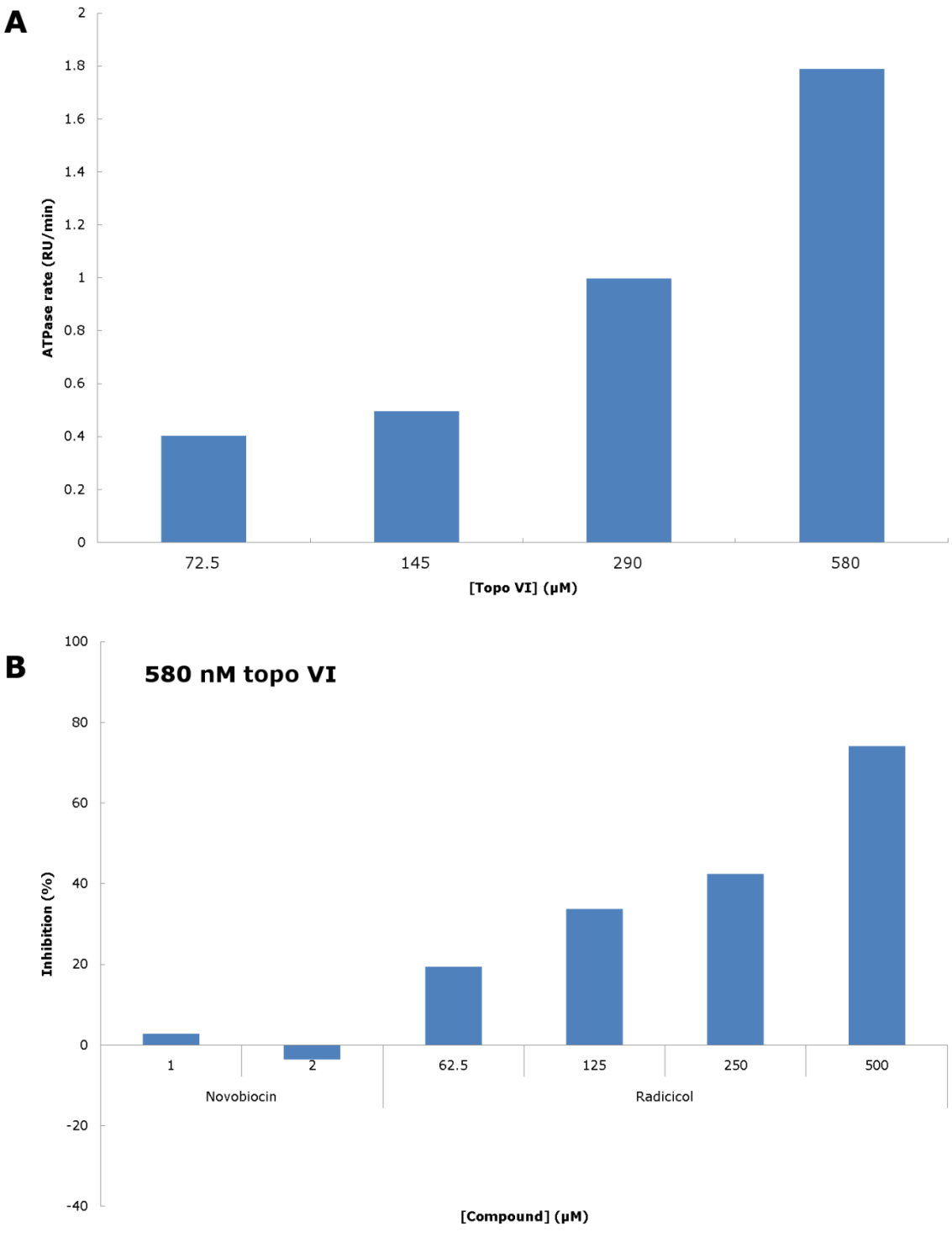

Figure 5.9 Titrations of novobiocin and radicicol with *M. mazei* topo VI in the ATPase assay. *A*. Rates of ATP hydrolysis for *M. mazei* topo VI at 72.5, 145, 290 or 580 nM. *B*. Summary of percentage inhibition for novobiocin and radicicol at the indicated concentrations with 580 nM *M. mazei* topo VI.

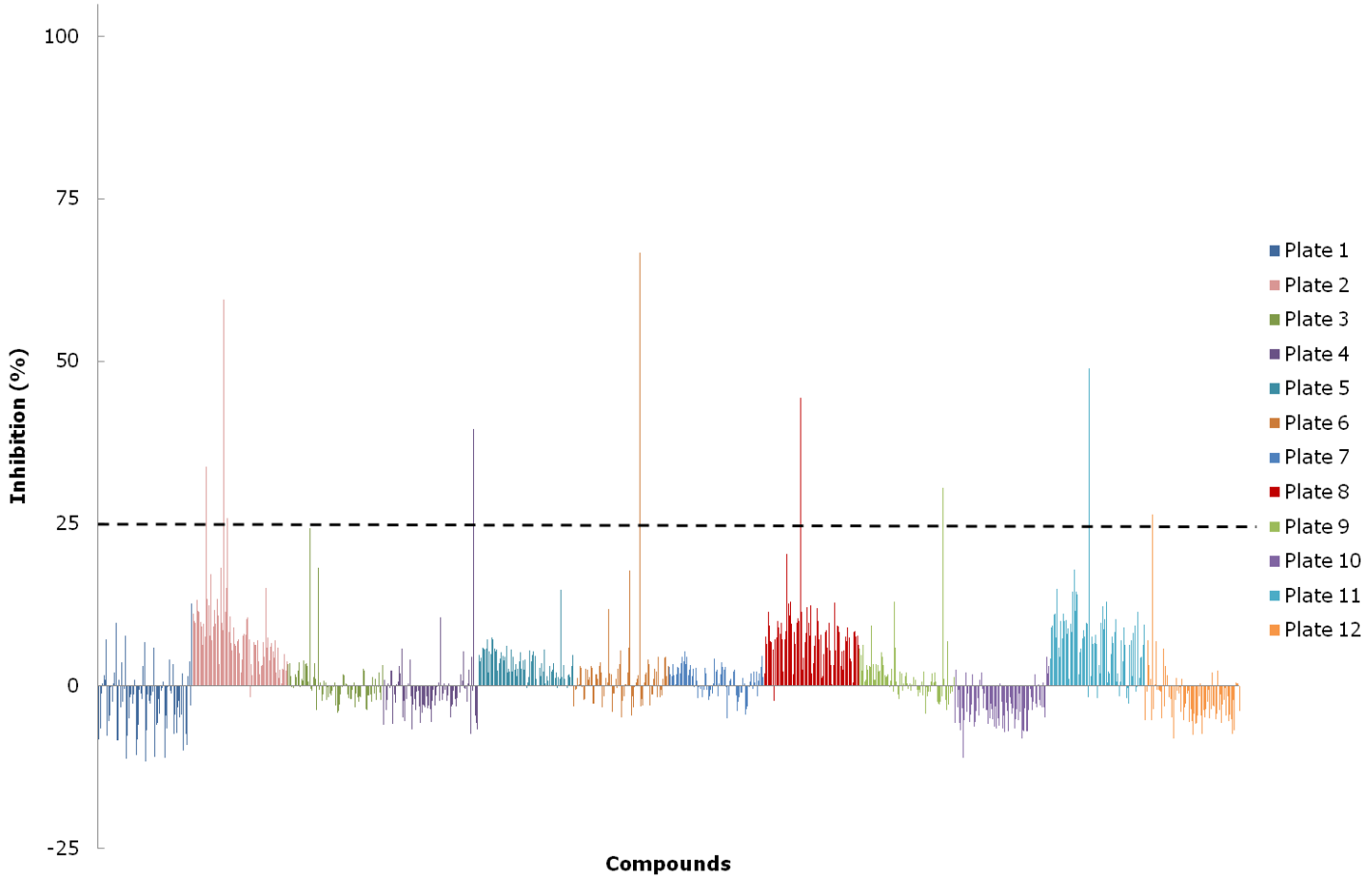

Figure 5.10 Results of *M. mazei* topo VI screen. *A.* Percentage inhibition for a duplicated screen of the Genplus library against *M. mazei* topo VI. Each bar represents the average value for a single compound screened in duplicate. The dotted line indicates the arbitrary hit threshold of 25% inhibition. See the Appendix for the data for individual plates.

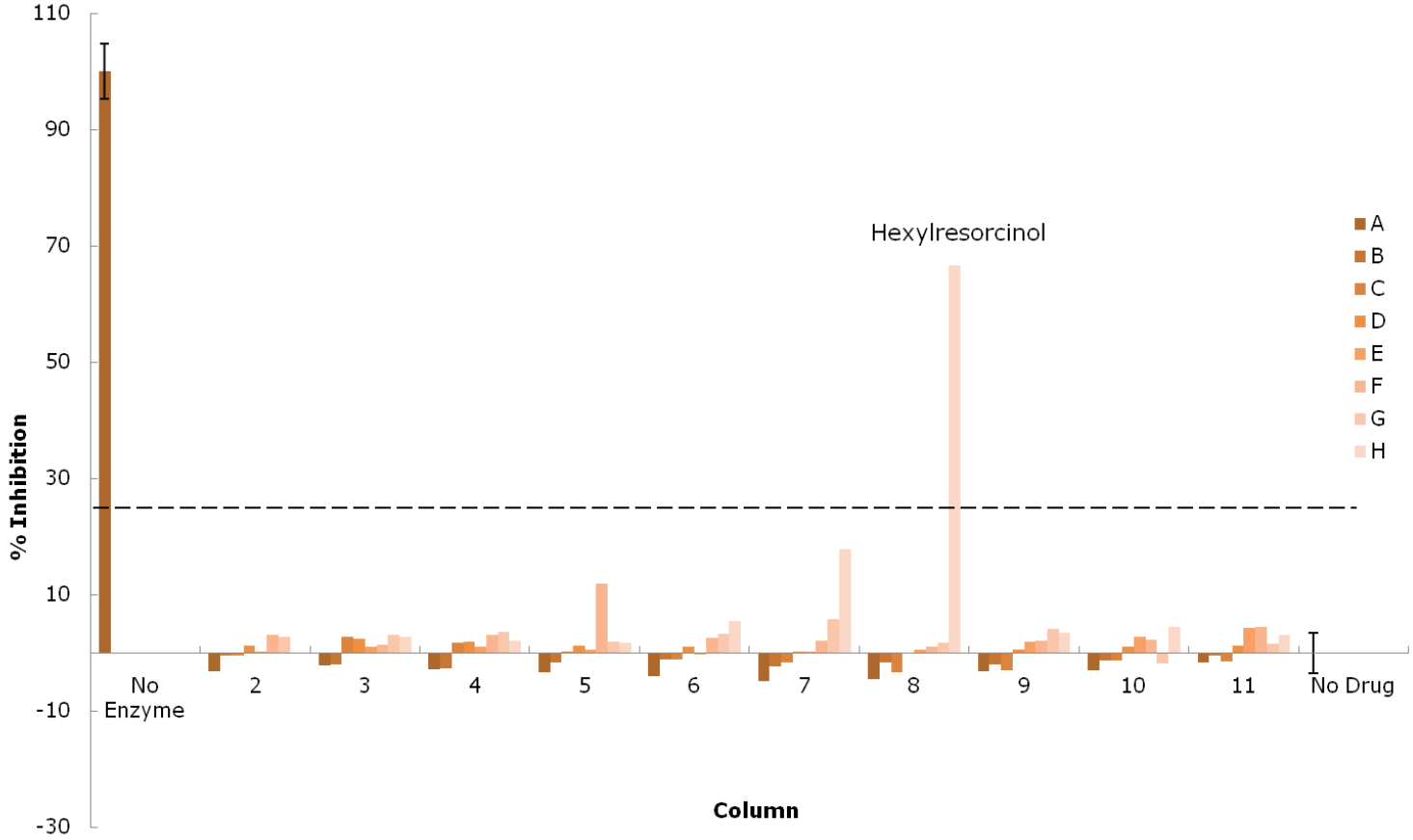

Figure 5.11 Percentage inhibition for Genplus plate 6 against *M. mazei* topo VI with hits labelled. Percentage inhibition was calculated from the 'no enzyme' and 'no drug' controls. Error bars for the no enzyme and no drug controls were calculated from the standard deviation of sixteen repeats.

5.2.4 Elimination of false positives

Out of the potential hits selected by the screen (Table 5.1) only m-amsacrine had been previously reported as an inhibitor of topo VI (Bergerat et al, 1994), and only against the *S. shibatae* enzyme. All nine hits were tested in the agarose gel-based assay (Figure 5.12). All the compounds tested, except for pristimerin, inhibited *M. mazei* topo VI in the gel assay. However, two of the compounds turned out to be non-specific inhibitors: cetylpyridinium and merbromin. Cetylpyridinium is a cationic detergent which has been used to precipitate both DNA and proteins (Geck & Nasz, 1983; Grote & Fromme, 1984), whilst merbromin is a fluorescent protein stain which reacts with thiol groups (Wilken et al, 2010). This contrasted to the DNA gyrase screen, where merbromin masqueraded as an activator by binding to the streptavidin coat of the plate and fluorescing. This arose from the fact that topo VI is a relaxing enzyme, meaning enzyme activity is donated by a decrease in fluorescence signal. Therefore a fluorescent drug, like merbromin, persisting in the wells would appear to be an inhibitor rather than an activator. The remaining six compounds were declared hits.

Two of the six compounds identified as hits were already known to be type IIA topoisomerase inhibitors: amsacrine and suramin. Since the latter had already been identified in the *E. coli* gyrase screen. Amsacrine is an antineoplastic drug which has been shown to target human topo II (Finlay et al, 1999; Horstmann et al, 2005). Hexylresorcinol and 9-aminoacridine are the two active ingredients of acrisorcin (Akrinol), a topic antifungal (Nierman, 1961). In addition, hexylresorcinol has been used as an oral antiseptic (Kraal et al, 1979) and is an active ingredient in Strepsil Extra

False positives	*Inhibition (%)*	**Novel inhibitors**	*Inhibition (%)*
Cetylpyridinium	59	Hexylresorcinol	67
Merbromin	40	Acrisorcin	49
Pristimerin*	26	Suramin	44
		Quinacrine	34
		Amsacrine	30
		Purpurin*	26

Table 5.1 Summary of compounds selected by the *M. mazei* topo VI screen. Percentage inhibition of compound in screen given.

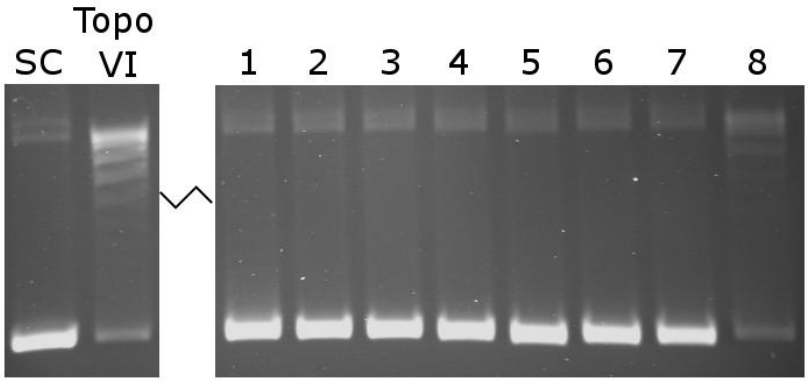

Figure 5.12 Validation for putative *M. mazei* topo VI screen hits. Supercoiled DNA was incubated with 0.5 units of *M. mazei* topo VI to produce partial relaxation. Samples incubated with or without 100 μM compound. *1*. Hexylresorcinol. *2*. Cetylpyridinium. *3*. Suramin. *4*. Merbromin. *5*. Quinacrine. *6*. Amsacrine. *7*. Purpurin. *8*. Pristimerin.

throat lozenges. Purpurin (1,2,4-trihydroxyanthraquinone) is a red dye and a member of the anthraquinone family, which includes mitoxanthrone (one of the hits from the *E. coli* gyrase screen). Quinacrine is an anti-malarial drug (Chauhan & Srivastava, 2001) whose target is not yet known, but has been shown to be a human topoisomerase II inhibitor (Preet et al, 2011)

In the previous chapter it was shown that both quinacrine and 9-aminoacridine were intercalators that interfered with the *E. coli* DNA gyrase screen. Intercalators decrease the twist of DNA when they bind, which is relieved as positive writhe. Relaxing enzymes, such as topo I and topo VI, can remove these positive supercoils. When the intercalator is extracted from the DNA the positive writhe it induces is also removed and the DNA ends up being negatively supercoiled rather than relaxed. This process is used in the production of negatively supercoiled DNA of specific superhelical densities (Courey, 1999). As such, intercalators may appear as inhibitors of topoisomerase relaxation activity when in fact they have no effect on the activity of the enzymes.

Since quinacrine was of potential medical interest it was desirable to investigate if it was a genuine topo VI inhibitor as well as an intercalator. Reactions with both wheat germ topo I and *M. mazei* topo VI with various concentrations of quinacrine were carried out. These reactions were then run on gels with or without 1 μg/mL chloroquine to determine the relative supercoiling states of the DNA (Figure 5.13). Supercoiled DNA incubated

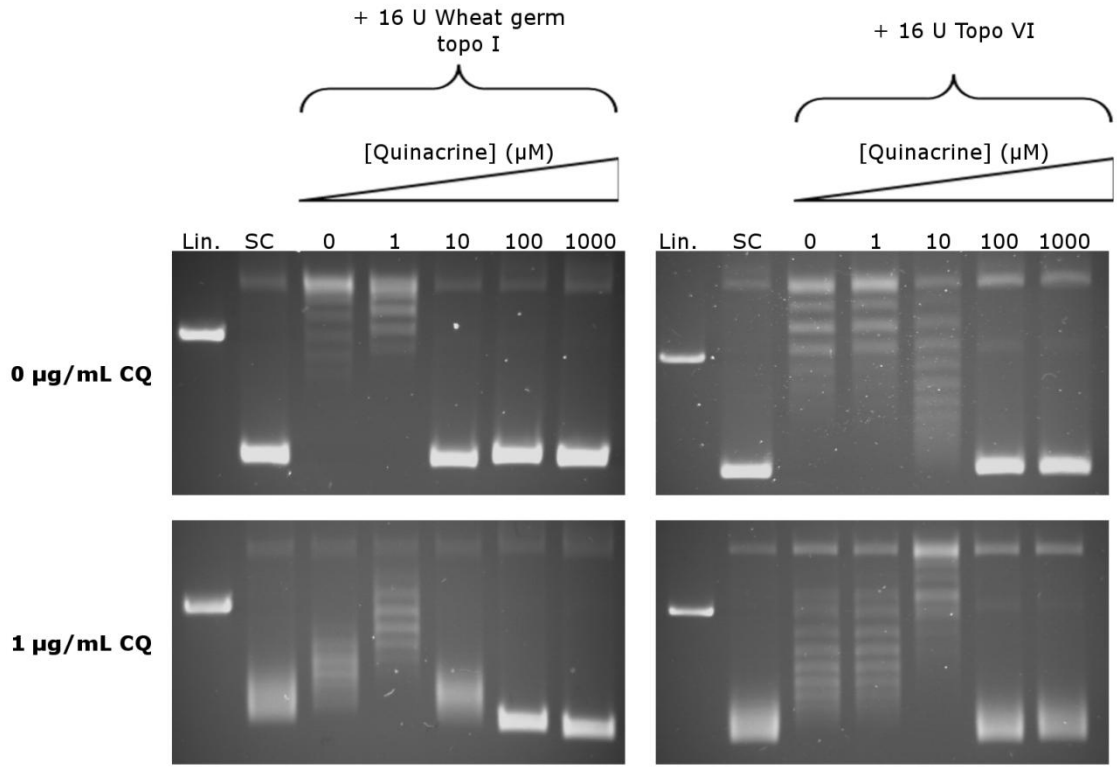

Figure 5.13 Titrations of quinacrine with wheat germ topo I or *M. mazei* topo VI. Samples run on agarose gels with or without 1 μg/mL chloroquine present in the gel and running buffer.

with wheat germ topo I and 10 μM displayed apparent inhibition of enzyme activity. However, running these samples on the chloroquine gel revealed that reactions containing 100 or 1000 μM quinacrine were more tightly supercoiled than DNA which had not been treated with enzyme. This indicates that with topo I the intercalation of quinacrine is causing the enzyme to introduce negative supercoils into the DNA. In contrast, similar reactions treated with *M. mazei* topo VI did not display any difference in mobility to the control DNA. This suggested that quinacrine is a genuine inhibitor of *M. mazei* topo VI. Similar experiments were carried out with 9-aminoacridine which produced identical results, suggesting that it too is a genuine inhibitor.

5.2.5 Statistical evaluation of screen

The mean fluorescent signals for the 192 negative (supercoiled plasmid, no enzyme) and 192 positive (relaxed plasmid with topo VI and no drug) controls were calculated to be 667 and 160 RFU respectively, with standard deviations of 33 and 18 RFU (Table 5.2). The signal-to-background ratio was calculated to be 4 whilst the signal-to-noise ratio was 15. From the control data the average Z' value for the screen was calculated to be 0.69 (See Equation 2.2). This value indicates that there was a good degree of separation between the positive and negative controls, implying that data quality for the screen was good. The distribution of the Z' value for each plate around the mean (Figure 5.1) was broader than with the *E. coli* DNA gyrase screen, with plates 8 and 12 giving a Z' below 0.5 but above 0.4. This meant that the separation of the positive and negative controls was generally good, but slightly worse for these two plates. Six compounds detected by the screen were validated as hits, giving a hit rate of 0.63%.

		Average (RFU)		S.D. (RFU)		S.D. (%I)		Z'
		No enzyme	*No drug*	*No enzyme*	*No drug*	*No enzyme*	*No drug*	
Plate	*1*	594	177	46	20	11	5	0.52
	2	665	134	39	16	7	3	0.69
	3	617	156	36	20	8	4	0.63
	4	566	159	25	14	6	3	0.71
	5	748	147	29	12	5	2	0.79
	6	739	168	27	20	5	3	0.75
	7	739	179	31	27	5	5	0.69
	8	859	255	30	22	5	4	0.74
	9	853	236	83	32	13	5	0.44
	10	683	218	35	18	8	4	0.66
	11	599	188	12	31	3	8	0.69
	12	612	204	48	25	12	6	0.46
Average		667	160	33	18	7	4	0.69

Table 5.2 Table of control data and Z' values per plate for the *M. mazei* topo VI screen. Averages and standard deviations are derived from 16 repeats. Standard deviations were also converted to percentage inhibition.

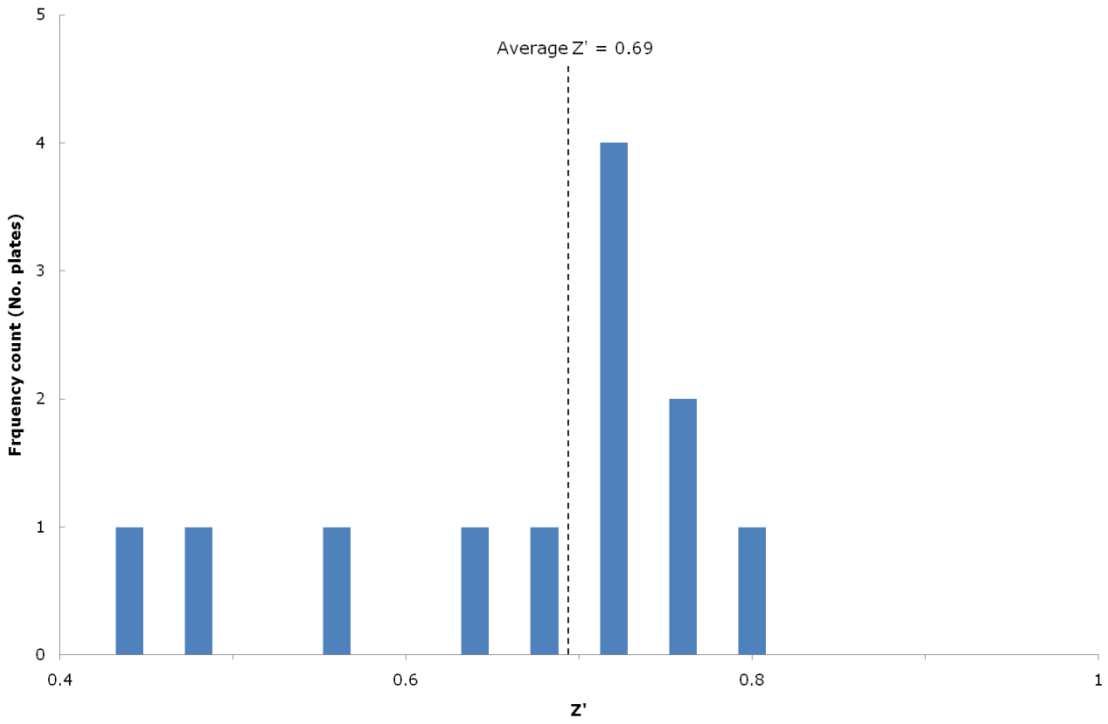

Figure 5.14 Histogram of Z' values for the *M. mazei* topo VI screen, with the average Z' value for the twelve plates indicated by the dotted line.

5.2.6 Characterisation of novel topo VI inhibitors *in vitro*

Having identified six novel inhibitors of *M. mazei* topo VI this study progressed to explore their mechanism of action in the agarose gel assay. The IC_{50}s of the compounds were determine by titrating the various compounds into reactions containing 1 unit topo VI (Figure 5.15, Table 5.3). The most potent hit was 9-aminoacridine, with an IC_{50} of 6 μM, whilst the least potent inhibitor was hexylresorcinol, with an IC_{50} of 40 μM. The IC_{50} of suramin was estimated to be 30 μM with *M. mazei* topo VI whereas it'd previously been shown it had an IC_{50} of 80 μM with *E. coli* DNA gyrase.

To test if any of the hits inhibited *M. mazei* topo VI by preventing the binding of the enzyme to DNA native gel shift assays were carried out with *M. mazei* topo VI in the presence of the screen hits (Figure 5.16). The topo VI-DNA complex did not seem to enter very far into the gel, which was probably due to the fact that the buffer used was designed for use with DNA gyrase.

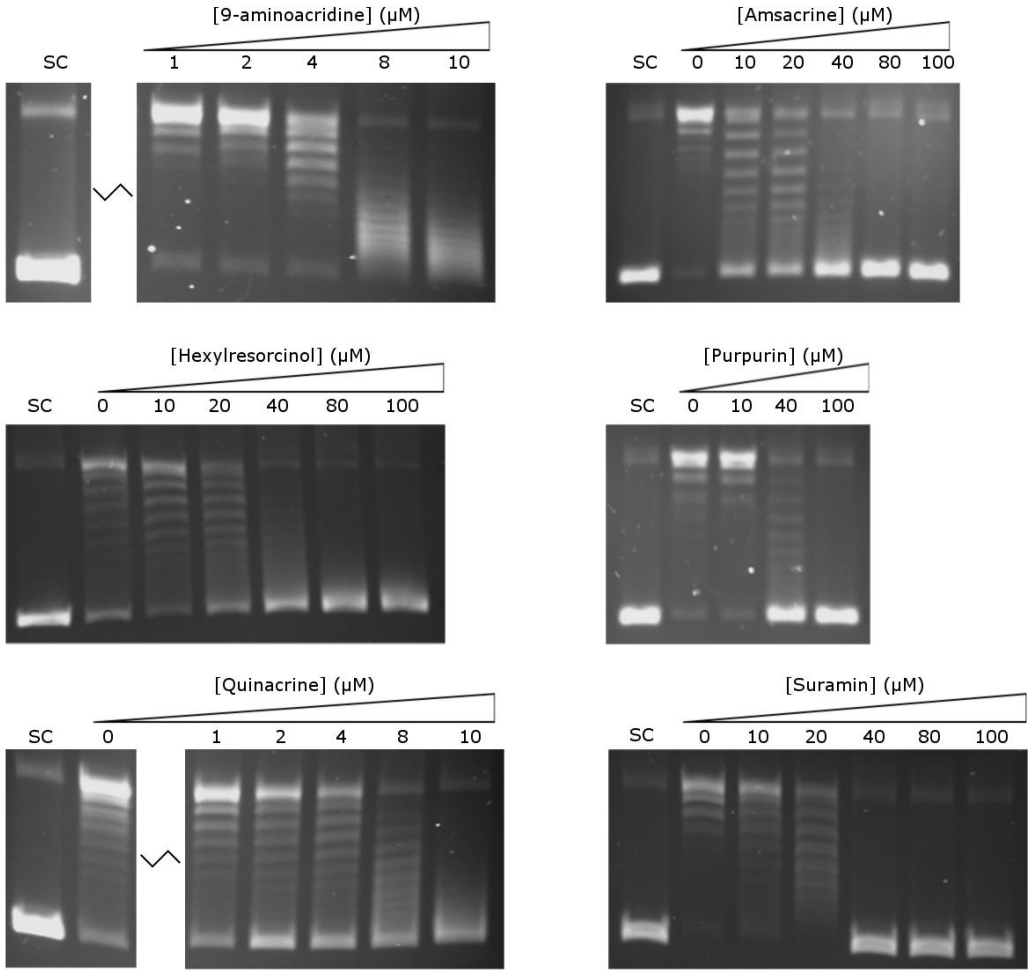

Figure 5.15 Determination of IC_{50}s for *M. mazei* topo VI hits. Reactions carried out with 1 U topo VI.

Compound	IC_{50} (μM)
9-aminoacridine	6
Quinacrine	8
Purpurin	25
Amsacrine	30
Suramin	30
Hexylresorcinol	40

Table 5.3 Approximate IC_{50}s for *M. mazei* topo VI hits. Determined by visual inspection of agarose gel assay results.

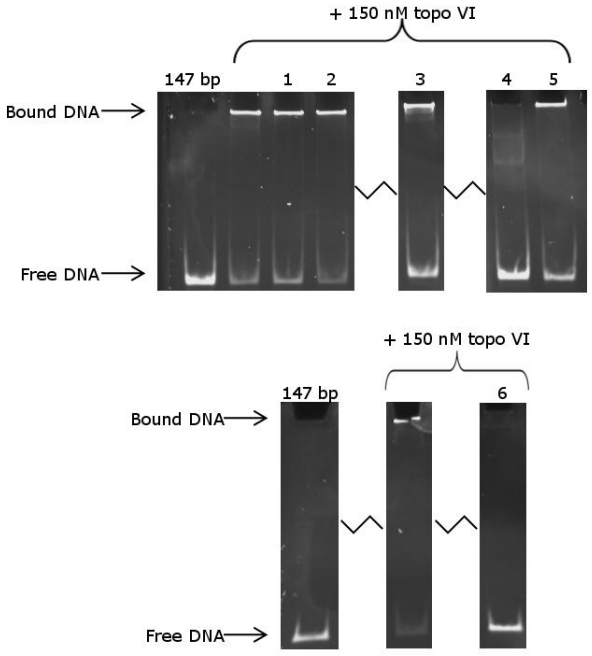

Figure 5.16 Native gel shift assays for the binding of *M. mazei* topo VI to a 147 bp DNA fragment in the presence of screen hits. 105 nM 147 bp and 150 nM topo VI used (1 pmol: 5 pmol). *1*. 120 μM 9-aminoacridine. *2*. 600 μM Amsacrine. *3*. 800 μM hexylresorcinol. *4*. 500 μM purpurin. *5*. 160 μM quinacrine. *6*. 600 μM suramin.

However since it was possible to differentiate between bound and unbound DNA this was not considered a problem. Out of the six compounds both suramin and purpurin appeared to prevent the binding of topo VI to DNA. Since this study had previously determined that suramin had a similar mechanism of action with *E. coli* DNA gyrase it was likely this result was genuine, and suramin was excluded from further mechanistic tests. For the sample containing purpurin two faint bands part way into the gel were observed. This could indicate that the drug is actually causing the subunits of the enzyme to dissociate rather than preventing the binding of DNA directly. As such, these bands could signify DNA bound to topo VIA subunit monomers or dimers.

Next the hits were tested in the ATPase assay to see if they had any effect on the enzyme's rate of ATP hydrolysis (Figure 5.17). Controls were included in which the enzyme and hit were incubated in the absence of ATP to account for any non-specific effects of the drug. These controls were used as baselines for the remaining reactions. Out of the compounds tested purpurin and quinacrine displayed inhibition. However, a precipitant was

seen to form in the wells containing purpurin and no topo VI. This suggested that it was reacting with something in the ATPase assay mix, and as such its inhibition of ATPase activity is probably an artefact. Quinacrine, on the other hand, appeared to genuinely inhibit ATPase activity of the enzyme with an IC_{50} of ~400 μM. Hexylresorcinol appeared to increase the ATPase activity of the enzyme, an effect which was reproducible in several repeats.

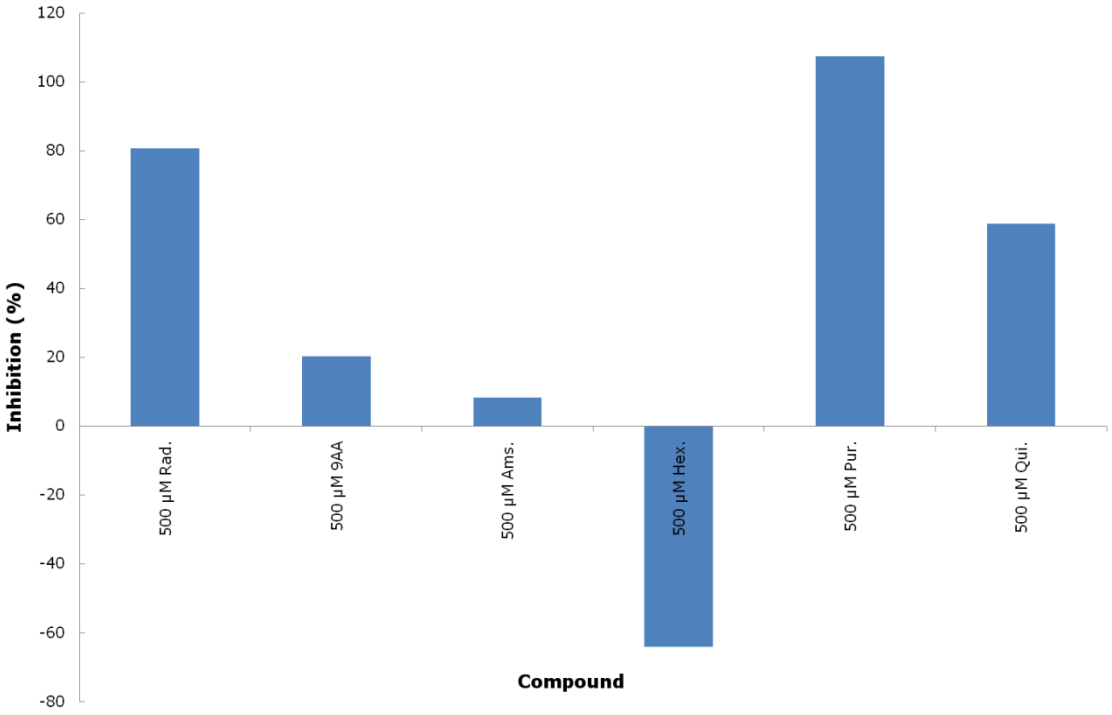

Figure 5.17 Inhibition of the ATPase activity of *M. mazei* topo VI by screen hits. The percentage inhibition was calculated relative to the rate of ATP hydrolysis of a control lacking drug. Radicicol was used as a positive control for inhibition. All compounds were tested at 500 μM with 580 nM topo VI. From left to right: radicicol, 9-aminoacridine, amsacrine, hexylresorcinol and purpurin.

Since the ATPase activity is a linked assay with pyruvate kinase it was desirable to investigate if hexylresorcinol and quinacrine were affecting the pyruvate kinase rather than topo VI. To assay pyruvate kinase activity reactions similar to the topo VI ATPase assays were prepared, but lacking topo VI. The absorbance at 340 nm was measured in the plate reader for 30 minutes then initiated the reaction with 10 μL of various concentrations of ADP (Figure 5.20 A). The absorbance was measured for a further 30 minutes. Pyruvate kinase activity was indicated by a sharp drop in absorbance upon ADP addition. A blank control was included into which 10 μL of water was added instead of ADP. Data was processed similarly to the ATPase assays (zeroing of the slope to the background and conversion of absorbance into relative units). Additionally the change in absorbance for the blank control (which represented the change due to dilution) was subtracted from all samples and the data was normalised to the time point immediately prior to ADP addition. This was done to make the decrease in signal due to pyruvate kinase ability easier to compare. Since 800 μM ADP produced a very clear decrease this concentration was used to test the effects of 500 μM hexylresorcinol or quinacrine on pyruvate kinase activity (Figure 5.18 B). The inclusion of quinacrine in the reaction resulted in a less pronounced decrease in signal, indicating that the compound was inhibiting the pyruvate kinase activity. This suggested that the apparent inhibition of topo VI ATPase activity was actually due to its inhibition of pyruvate kinase. Hexylresorcinol, on the other hand, had no effect on pyruvate kinase activity.

To exclude the possibility of hexylresorcinol hydrolysing ATP on its own control reactions were carried out which contained the standard reaction mix, ATP, and 500 μM hexylresorcinol but with no enzyme (Figure 5.19). Since these controls revealed that the drug was not able to hydrolyse ATP by itself it appears that hexylresorcinol is a genuine activator of *M. mazei* topo VI ATPase activity. It may be that hexylresorcinol somehow uncouples the ATPase activity of the enzyme from its ability to perform strand passage, increasing the rate of hydrolysis whilst reducing the overall activity of the enzyme.

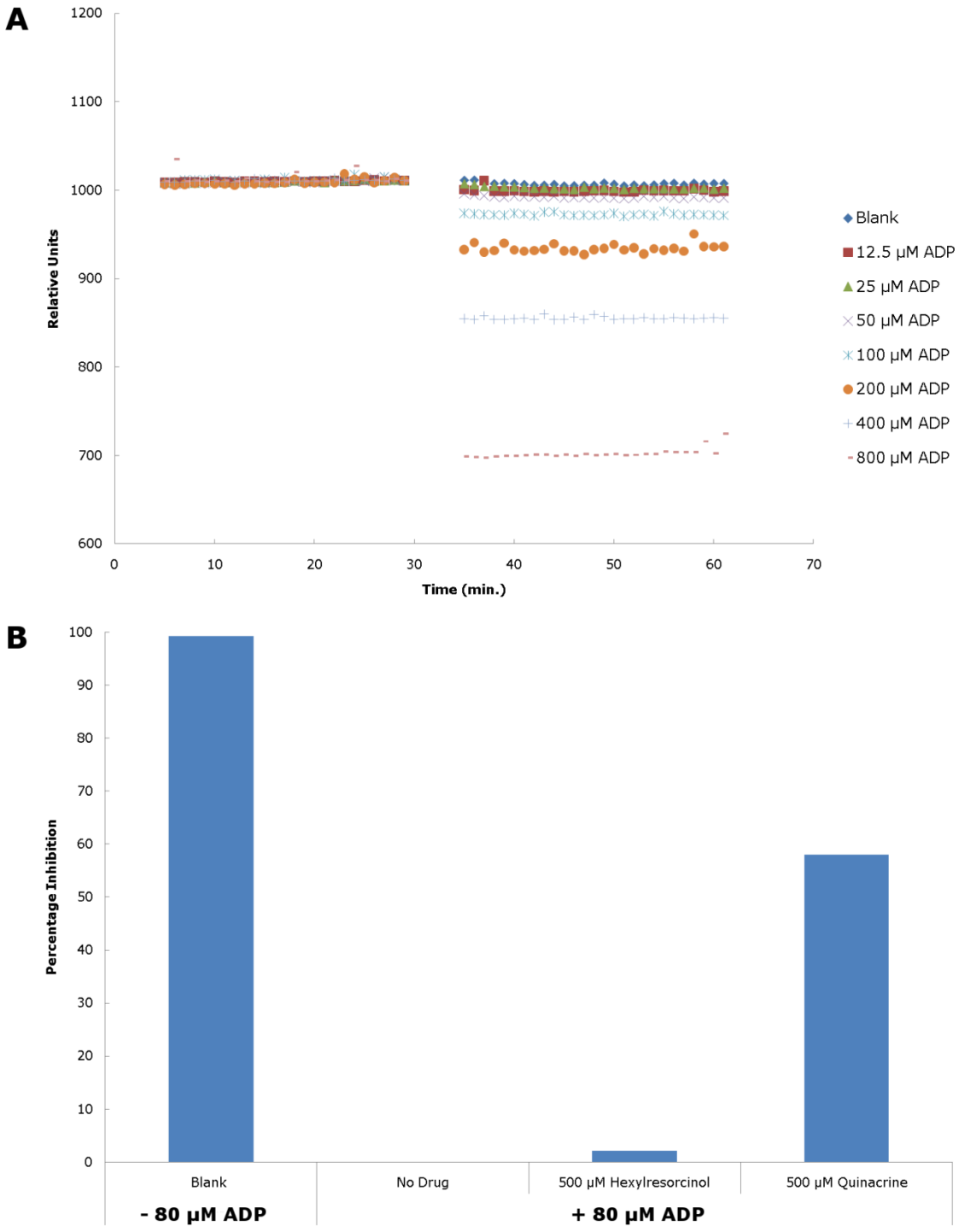

Figure 5.18 Pyruvate kinase assays with hexylresorcinol and quinacrine. *A*. Titration of ADP from 12.5 µM to 800 µM with pyruvate kinase. *B*. Percentage inhibition values for 500 µM hexylresorcinol or quinacrine in the presence of 800 µM ADP and pyruvate kinase.

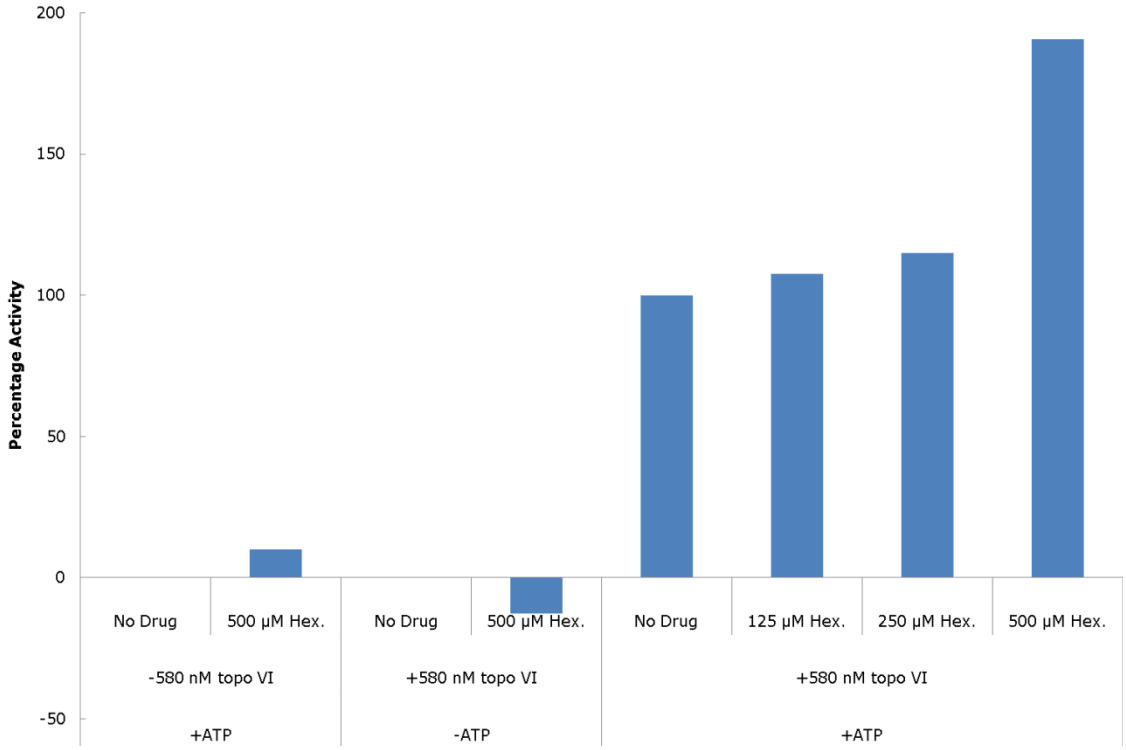

Figure 5.19 Activation of *M. mazei* topo VI ATPase activity by hexylresorcinol. Percentage activity is relative to the sample containing 580 nM topo VI, ATP and no drug.

Finally the ability of the hits to stabilize the cleavage complex of *M. mazei* topo VI was tested. Since stabilization of the cleavage complex had not yet been described with this enzyme, it was necessary to carry out some preliminary tests. Since both the non-hydrolysable ATP analogue ADPNP and $CaCl_2$ had been previously shown to stabilize the cleavage complexes of *S. shibatae* topo VI (Buhler et al, 2001) their effect on the *M. mazei* enzyme in the cleavage assay was tested (Section 2.7.2.; Figure 5.20). Some background cleavage was seen in the absences of ATP at 240 nM topo VI. This was likely due to the presence of some contaminant in the enzyme preparation. Replacing ATP with ADPNP resulted in the formation of a small amount of linear DNA at all concentrations tested and an increase in the amount of nicked DNA. A similar result was seen when $MgCl_2$ was replaced by $CaCl_2$ in the reaction buffer. However some relaxation activity was observed at 240 and 480 nM topo VI in the presence of $CaCl_2$. This was likely due to trace amounts of magnesium being present in the enzyme preparation. These results contrast with the findings for the *S. shibatae* enzyme, which displayed a higher level of cleavage with both ADPNP and

$CaCl_2$ than *M. mazei* topo VI. To try and improve the formation of linear DNA the reaction was stopped with an increased amount of SDS (2%), 170 μM NaOH (pH 11 final), 600 μM guanidinium hydrochloride or 800 μM urea. None of these conditions increased ADPNP-induced cleavage of DNA by *M. mazei* topo VI.

As such the ability of the screen hits to stabilize the cleavage complex was tested by using the standard conditions for the cleavage assay (Figure 5.21). An enzyme concentration of 50 nM was chosen since background cleavage would be negligible at this level. Reactions containing enzyme were incubated with 0, 1, 10, 100 or 1000 μM compound to test for cleavage-complex stabilization. To test if the compounds had any intrinsic DNA cleavage activity control reactions were included containing pNO1 and the highest concentration of each drug tested with no enzyme. To establish the level of background cleavage a control was included containing topo VI in the standard reaction buffer but lacking ATP. As a positive control for cleavage a reaction was included containing topo VI and 1 mM ADPNP. No increase was observed in DNA cleavage above the background with any of the compounds, which suggests that none of the compounds tested stabilize the cleavage complex. However, the level of cleavage observed in the

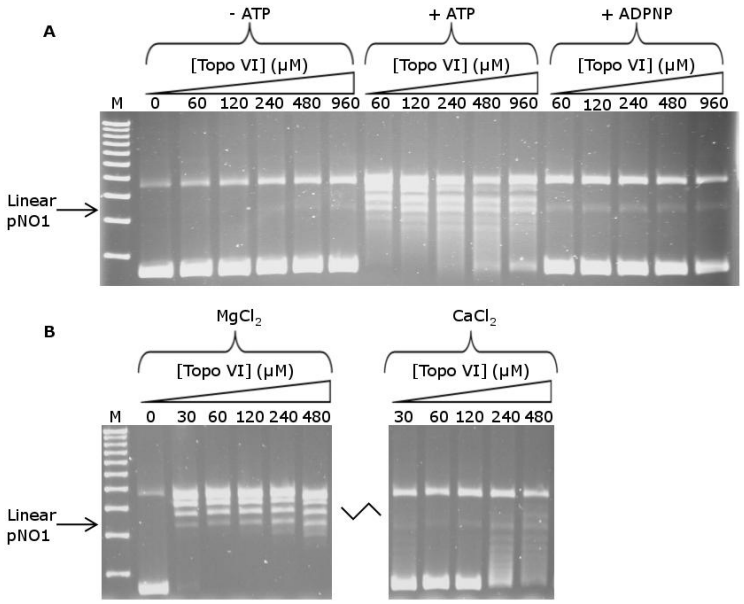

Figure 5.20 Testing cleavage conditions with *M. mazei* topo VI. *A*. Titrations of topo VI in standard relaxation buffer with or without 1 mM ATP or ADPNP. *B*. Titrations of topo VI in standard relaxation buffer with or without 10 mM $MgCl_2$ or $CaCl_2$.

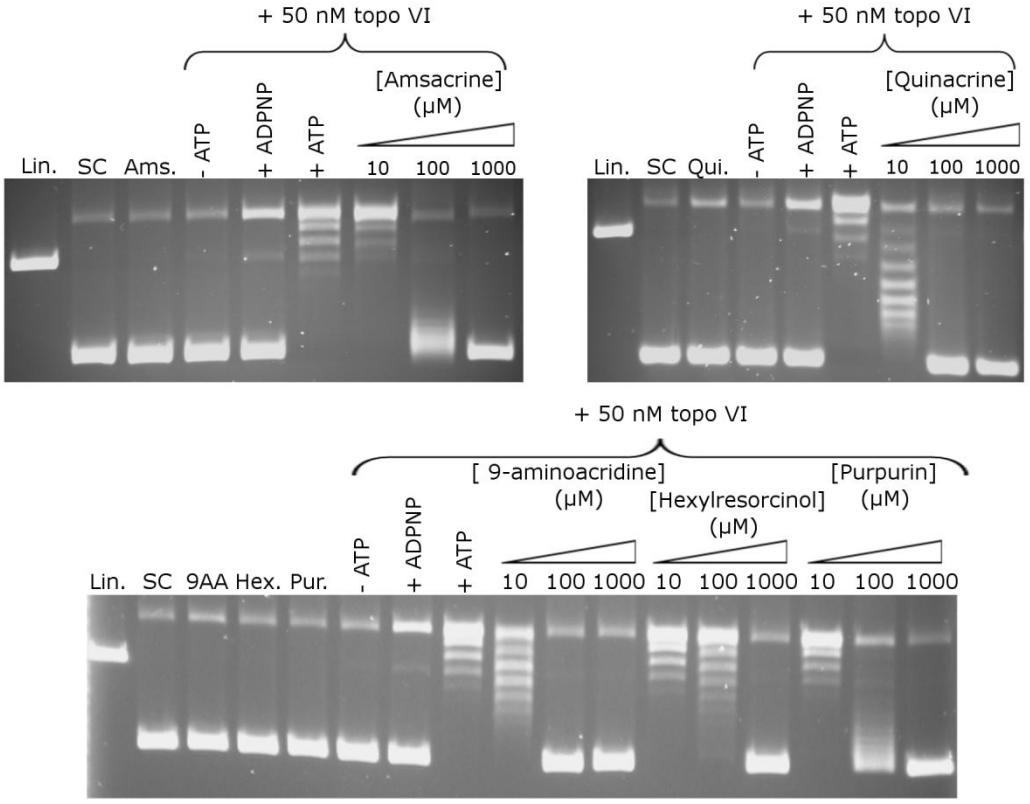

Figure 5.21 Cleavage complex stabilization assays with *M. mazei* topo VI hits. Reactions carried out in topo VI relaxation buffer with or without 1 mM ATP or ADPNP. Controls with: 1000 μM amsacrine, quinacrine, 9-aminoacridine, hexylresorcinol or purpurin; SC pNO1 and no enzyme included to check for intrinsic cleavage activity of drugs.

positive control containing ADPNP was very low when compared to similar experiments with *E. coli* DNA gyrase (Figure 4.11). This low level of cleavage in the positive control and the presence of some background cleavage in the absence of ATP made it difficult to definitively conclude much from these experiments. These results were reproducible and were observed with two independent batches of enzyme. Since the AFM data had shown that topo VI remained bound to the DNA despite proteinase K digestion, this may indicate that the enzyme-DNA complex is both resistant to proteinase digestion and very stable.

5.2.7 Cross-reactivity of *M. mazei* topo VI and *E. coli* DNA gyrase hits

Since some compounds, such as suramin, were hits in both the *E. coli* DNA gyrase and *M. mazei* topo VI screens it was decided to cross-test the hits from the two screens. By doing this it was hoped that some compounds

which had been a false negative in one screen but a hit in the other, and to get an idea of the selectivity of the inhibitors. This study has already shown that suramin was a common inhibitor of both *E. coli* gyrase and *M. mazei* topo VI, and whilst quinacrine and 9-aminoacridine inhibited topo VI activity they acted as stimulators of DNA gyrase. The remaining two topo VI hits, hexylresorcinol and purpurin, did not display any ability to inhibit 0.5 U of DNA gyrase in the agarose gel assay at 100 μM.

Testing the DNA gyrase screen hit mitoxanthrone against *M. mazei* topo VI in the gel assay revealed that it was also a potent inhibitor of topo VI with an IC_{50} of 1.5 μM, meaning it was a false negative in the topo VI

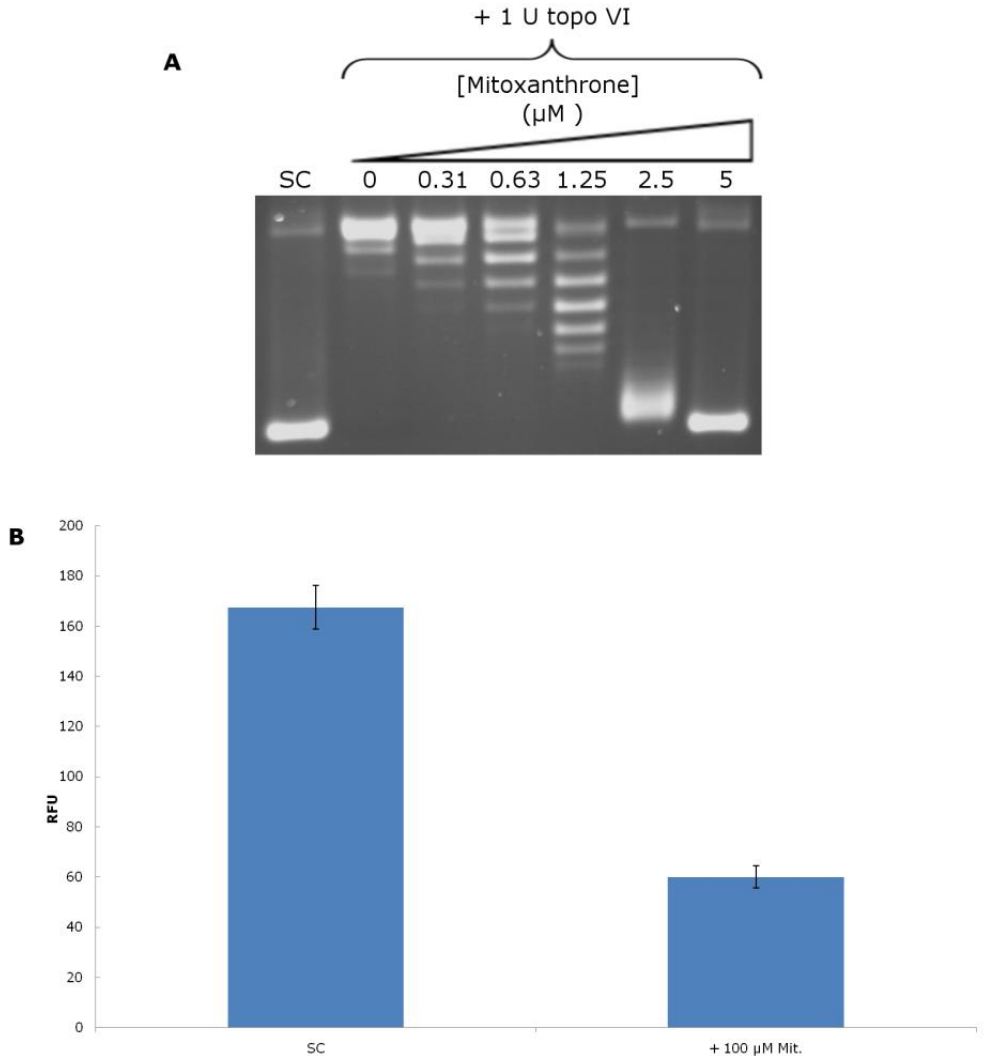

Figure 5.22 Mitoxanthrone as an inhibitor of *M. mazei* topo VI. *A*. Titration of mitoxanthrone in the gel assay with 1 unit topo VI. *B*. Testing the effect of mitoxanthrone on the binding of supercoiled pNO1 in the microtitre plate assay. Supercoiled plasmid was incubated in the absence or presence of 100 μM mitoxanthrone. The error bars are the standard deviation of three repeats.

screen (Figure 5.22). Previously this study has shown that its IC_{50} against *E. coli* gyrase was 12 μM, meaning mitoxanthrone was approximately four times more potent against topo VI. This raised the question of why it had not been picked up as a hit in the topo VI screen. Since mitoxanthrone was known to be an intercalator it was suspected it was able to interfere with DNA triplex formation. To test this hypothesis 100 μM mitoxanthrone was incubated with supercoiled pNO1 under standard microtitre plate-assay conditions. The presence of the drug caused a substantial decrease in signal, suggesting it was preventing the formation of DNA triplexes. Since topo VI relaxation activity is indicated by a decrease in signal in the assay the drop in signal due to the interference of mitoxanthrone could mask the drugs inhibitory potential. This would explain why mitoxanthrone was missed in the topo VI screen. As such, it was included as a hit in all further experiments.

5.2.8 Inhibition of *S. shibatae* topo VI by the *M. mazei* topo VI hits.

Since it had proved difficult to achieve clear results for cleavage complex stabilization of *M. mazei* topo VI by the screen hits it was decided to test them against the *Sulfolobus shibatae* enzyme. Cleavage complex stabilization with *S. shibatae* topo VI by ADPNP and $CaCl_2$ has been demonstrated previously.. The *S. shibatae* topo VI for these experiments was kindly provided by Danielle Gadelle (University of Paris XI, Orsay).

Initial experiments focused on testing for inhibition of *S. shibatae* topo VI by the screen hits at 10 or 100 μM compound (Figure 5.23 A). Neither hexylresorcinol nor suramin showed any inhibitory activity against the enzyme at 100 μM. Amsacrine showed partial inhibition at 100 μM, suggesting its IC_{50} was around this concentration. 9-aminoacridine, purpurin and quinacrine all displayed strong inhibition at 100 μM but no inhibition at 10 μM, suggesting their IC_{50}s lay between these concentrations. Mitoxanthrone, on the other hand, showed complete inhibition at 10 μM.

The compounds which were inhibitors of *S. shibatae* topo VI were then tested in the cleavage assay at concentrations which were predicted to give complete inhibition (Figure 5.23 B). ADPNP was used as a positive

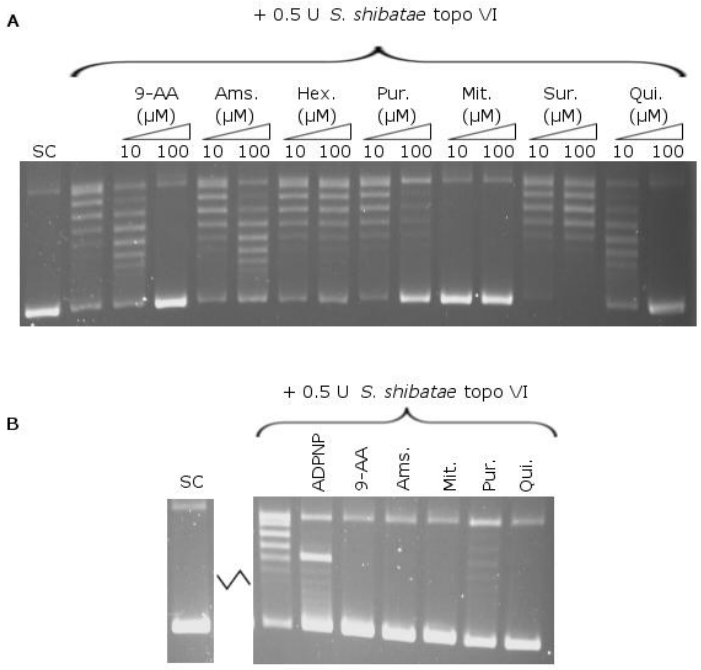

Figure 5.23 Testing *M. mazei* topo VI hits against *S. shibatae* topo VI. *A*. 9-aminoacridine, amsacrine, hexylresorcinol, purpurin, mitoxanthrone, suramin and quinacrine tested for inhibition of *S. shibatae* topo VI relaxation activity. *B*. Testing for cleavage complex stabilization by *S. shibatae* topo VI inhibitors. A positive control for cleavage complex formation was included which contained 1 mM ADPNP instead of ATP. The compounds were tested at the following concentrations: 50 μM 9-aminoacridine, 500 μM amsacrine, 20 μM mitoxanthrone, 200 μM purpurin and 200 μM quinacrine.

control for cleavage complex stabilization and showed a good level of cleavage. However no induction of cleavage by any of the screen hits was observed.

To test if any of the inhibitors operated by preventing the cleavage of DNA by *S. shibatae* topo VI, cleavage assays were carried out in the presence of ADPNP with or without the compounds (Figure 5.24). A reduction in intensity of the linear band would indicate the drug was able to prevent ADPNP-induced cleavage of the DNA by topo VI. All five compounds displayed a marked ability to reduce the amount of cleavage, suggesting either they were preventing the binding of ADPNP or stopping the enzyme cleaving DNA. This was expected for purpurin, which was shown in earlier experiments to prevent the binding of *M. mazei* topo VI to DNA but was surprising for the other compounds, none of which had shown any ability to affect DNA binding. It may be that these compounds are capable of preventing cleavage of DNA by topo VI directly.

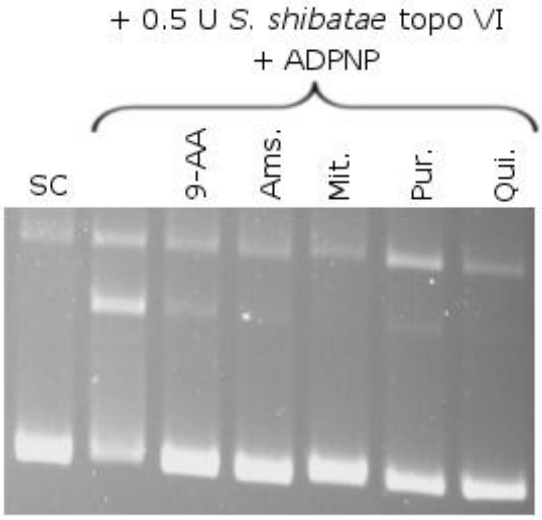

Figure 5.24 Cleavage protection assay for screen hits with *S. shibatae* topo VI. 0.5 units of *S. shibatae* topo VI was incubated with 1 mM ADPNP in the absence or presence of: 50 μM 9-aminoacridine, 500 μM m-amsacrine, 20 μM mitoxanthrone, 200 μM purpurin or 200 μM quinacrine.

5.2.9 Testing against *Arabidopsis* topo VI *in vivo*

Despite years of trying *Arabidopsis* topo VI has not been expressed in a soluble form by our lab nor has its soluble expression been reported in the literature. However, knock-out mutants for topo VI in *Arabidopsis* have been shown to have a very clear "dwarf" phenotype. This arises from the fact topo VI is involved in the process of endoreduplication in plants, which is in turn linked to cell expansion. As such plants lacking topo VI are generally smaller than wild-type plants and have reduced cell size and ploidy (chromosome count). It is therefore possible to assay for compounds that inhibit *Arabidopsis* topo VI in vivo by looking for the induction of these characteristics.

As such, the ability of the hits from the *M. mazei* topo VI screen to inhibit the growth of *Arabidopsis columbia* seedlings in a hypocotyl extension assay was tested (Section 2.4.3). *Arabidopsis* seeds were sowed onto square Petri dishes containing MS agar with or without 100 μM hit compound and grew the plants vertically in the dark for 5 days. During this time the plant hypocotyls extend along the surface of the agar. It was then possible to measure the length of each seedling using a light microscope and calculate an average length for plants grown in the presence of each

compound. Out of the six hits tested (mitoxanthrone was not included in these experiments since it had not been shown it was a topo VI inhibitor at this point) only hexylresorcinol displayed any effect on plant growth, completely preventing seed germination at 100 μM.

To explore this further the ability of hexylresorcinol to inhibit plant growth was tested at a range of concentrations. For each concentration the average plant length and the percentage of seeds which had germinated was calculated (Table 5.4, Figure 5.25). It was observed that the number of seeds germinated remained constant up to 50 μM hexylresorcinol, whilst the average length of the seedlings dropped rapidly. At 80 μM germination was reduced, whilst no seeds germinated at 100 μM.

		Seedlings tested	Germinations		Lengths (mm)	
			Number	*Percentage (%)*	*Average*	*S.D.*
[Hexylresorcinol] (μM)	*0*	95	83	87	9.6	3.3
	20	64	57	89	8.4	2.8
	30	63	57	90	3.0	2.3
	40	96	83	86	1.4	1.1
	50	64	59	92	1.0	0.0
	80	32	1	3	1.0	0.0
	100	32	0	0	0.0	0.0

Table 5.4 Table of compiled data from *Arabidopsis* hypocotyl assays with hexylresorcinol. All seedlings were grown for 5 days in the dark. A seedling was classified as having germinated if the petioles or roots had emerged from the seed casing after this time.

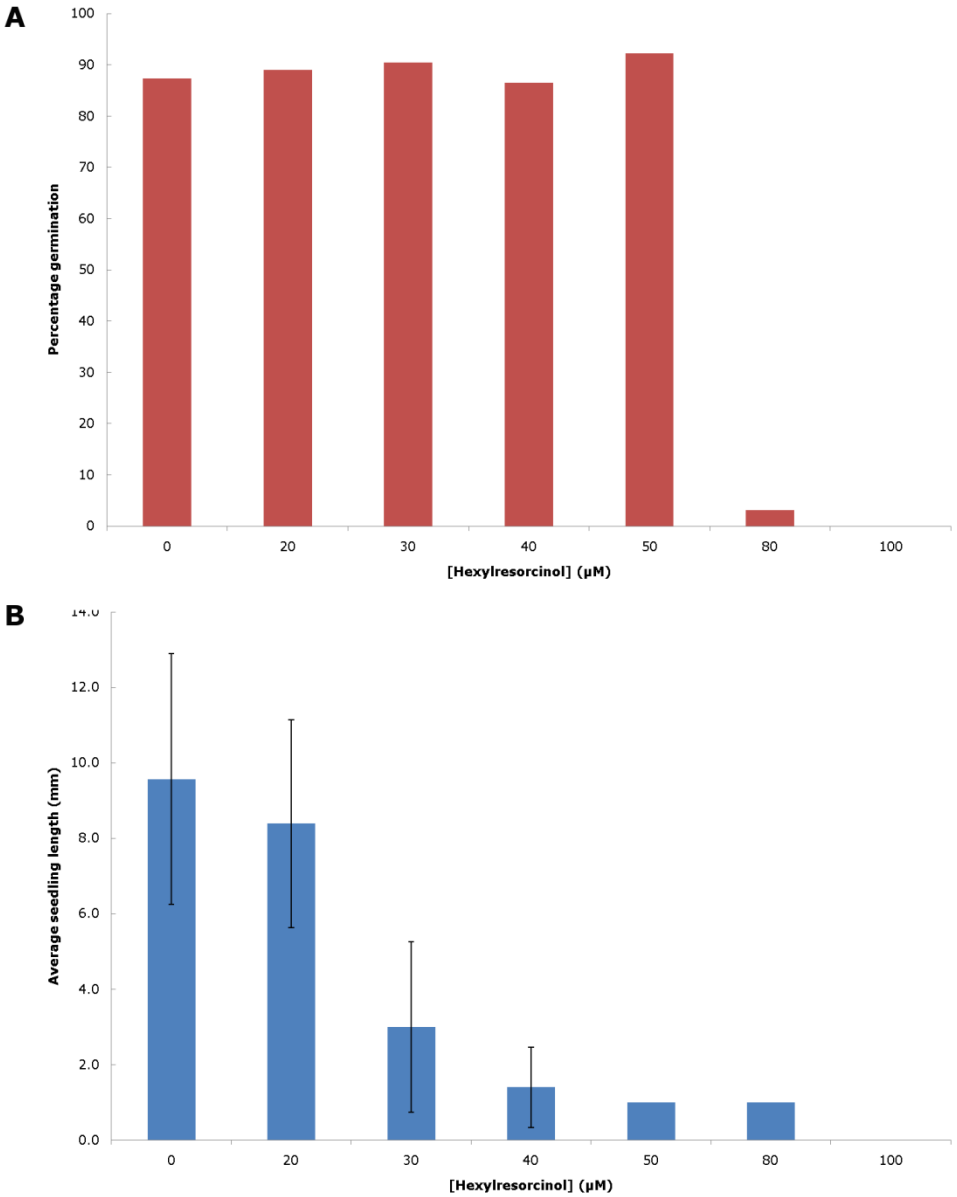

Figure 5.25 Inhibition of *Arabidopsis* hypocotyl extension by hexylresorcinol. All plants were grown for 5 days in the dark. *A*. Percentage germination of seedlings grown on 20, 30, 40 50, 80 or 100 µM hexylresorcinol. *B*. Average length of seedlings grown on 20, 30, 40 50, 80 or 100 µM hexylresorcinol. Error bars represent the standard deviation of the samples.

Although seedlings germinated at 50 µM the plants were too small to discern any differences in morphology. As such further studies were focused on plants grown on 40 µM hexylresorcinol. A closer examination of the *Arabidopsis* seedlings grown in the presence of this concentration of drug reveal a range of responses to the compound (Figure 5.26). Although the average hypocotyl length was considerably reduced a few plants appeared to be unaffected by the drug, reaching similar hypocotyl lengths as plants grown in the absence of compound. Out of the shorter plants some

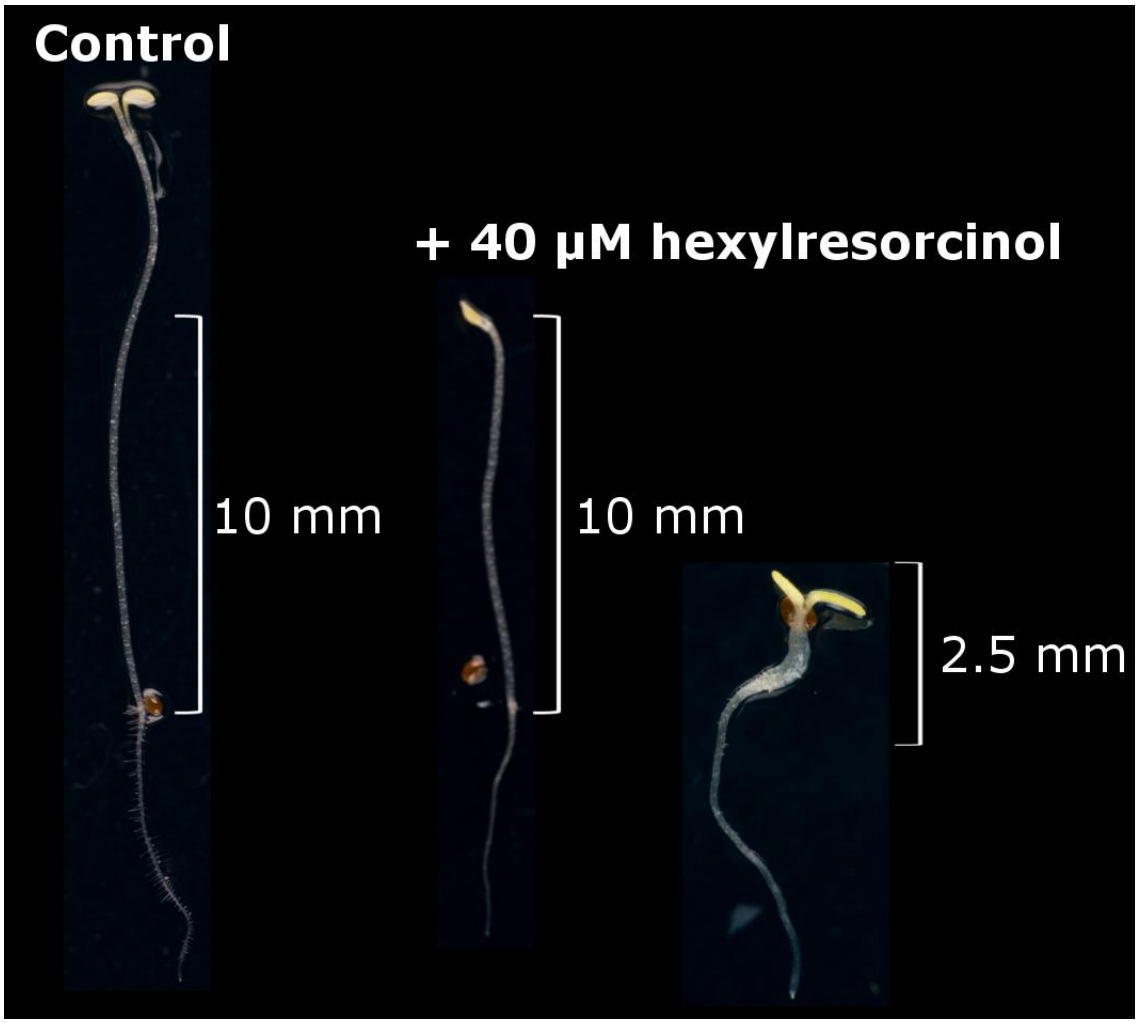

Figure 5.26 Sample *Arabidopsis* seedlings from hypocotyl assay grown on 40 µM hexylresorcinol. The plants were grown for 5 days in the dark in the absence or presence of 40 µM hexylresorcinol. Some plants grown on hexylresorcinol grew shorter than the control but displayed normal morphology (centre), whilst others exhibited "dwarf" morphology (right). The photo of "dwarf" plant taken with smaller scale to the other two plants.

appeared to have normal morphology (apart from their reduced size) whilst others were very short with fatter hypocotyls, the latter of which matched the description of topo VI knock-out mutants. These plants were therefore designated as having "dwarf" morphology.

Plants grown on 40 µM hexylresorcinol were allowed to mature into a rosette (Figure 5.27). Plants were grown on MS salts agar with or without 40 µM hexylresorcinol in a 22°C growth cabinet under a 16 hr day for 3 weeks. Although the majority of the seeds germinated, only seven of the 32 plants were able to develop into a rosette. All seven of these plants appeared pale, yellowish and slightly transparent compared to control plants grown without drug. Some of the plants (plants 1 and 6) displayed

normal morphology and were close to the control in size. One plant (plant 3) displayed normal morphology, but was greatly reduced in size suggesting its growth was slowed. The remaining plants (plants 2, 4, 5 and 7), which had displayed the "dwarf" morphology whilst they were hypocotyls, were very small with shortened leaf stems. Some of these plants (such as plants 5 and 7) had a trace of red pigmentation.

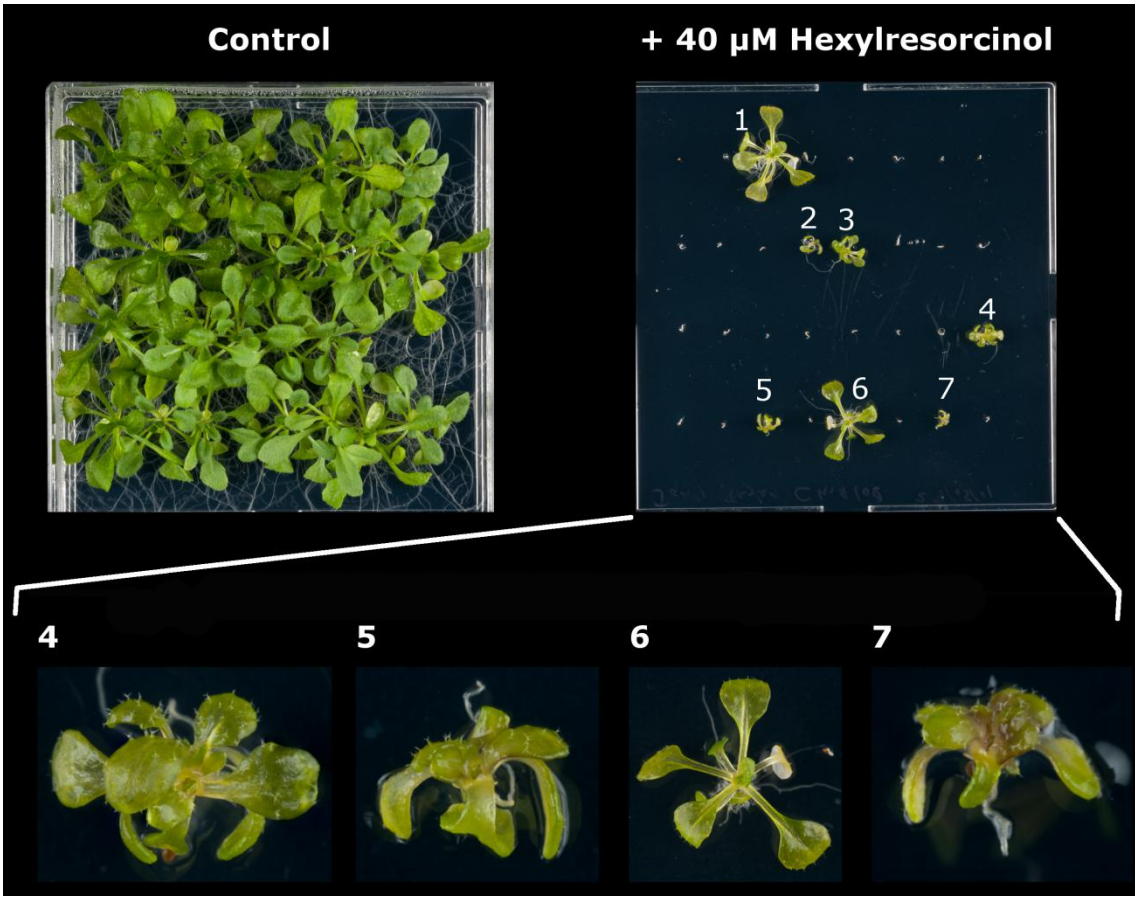

Figure 5.27 Light-grown *Arabidopsis* grown on 40 µM hexylresorcinol. The plants were grown horizontally for 3 weeks under a 16 hr day. A control plate which did not contain the compound was also included. Photos at a higher magnification were taken of plants displaying different morphologies. Plants 2, 5 and 7 displayed the "dwarf" morphology, whilst plants 1 and 6 were similar to the control in appearance. Plants 3 and 4 appeared intermediate in morphology. All hexylresorcinol-grown plants appeared somewhat transparent compared to the control plants.

To see if the effects of hexylresorcinol were reversible, plants which had been grown on 40 μM hexylresorcinol for three weeks were taken and transplanted them to a fresh MS salts agar plate with no drug. The plants were then grown for a further two weeks (Figure 5.28). Plants which had

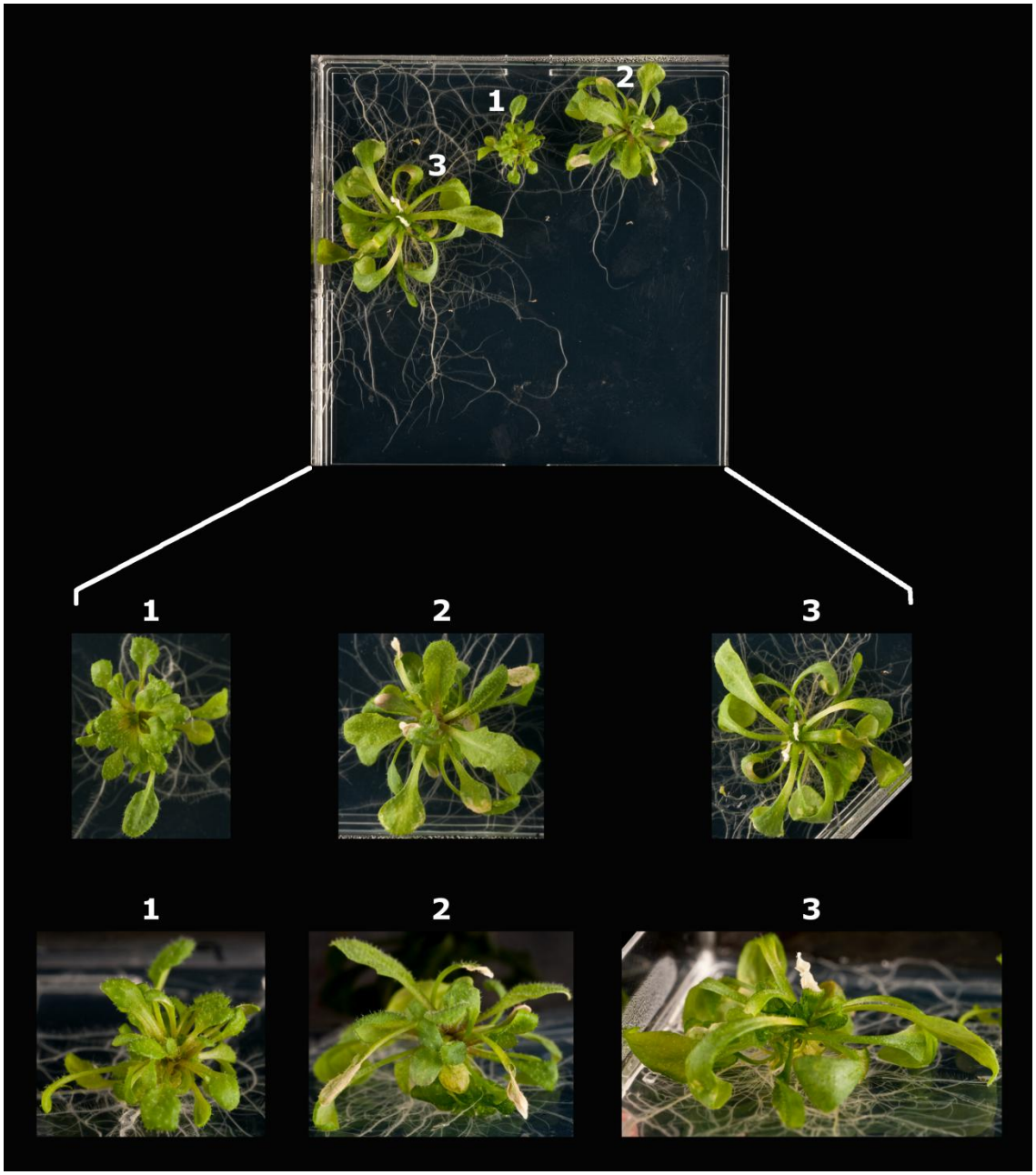

Figure 5.28 Recovery of hexylresorcinol fed *Arabidopsis* plants. The plants were grown for 3 weeks on 40 μM hexylresorcinol under a 16 hr day. They were then transferred to a fresh agar plate lacking hexylresorcinol and grown for a further 2 weeks in order to recover. Higher magnification photos of the three plants which recovered provided (from above and the side). Plant 1 exhibited "dwarf" morphology prior to recovery. Plant 2 displayed normal morphology, reduced size and slight transparency prior to recovery. Plant 3 displayed normal morphology, normal size and slight transparency prior to recovery.

failed to develop into rosettes on the hexylresorcinol containing agar were still unable to mature, suggesting that these plants had died. All the plants which were able to form rosettes lost the paleness and transparency observed whilst they were growing on hexylresorcinol containing media. Plants which had exhibited normal morphology and either normal size (plant 3) or reduced size (plant 2) displayed notable recovery with both plants growing to roughly the same size. This suggests that hexylresorcinol had been slowing the growth of plant 2 rather than altering its morphology. Patches of necrotic tissue was also observed on some of their leaves, which in extreme cases caused entire leaves to become white and shrivelled. This is likely due to the plants sequestering the drug in those leaves in order to purge the compound from its system. The plant which had displayed the "dwarf" morphology whilst grown on the media containing hexylresorcinol remained considerably smaller than the other plants (roughly half the size) although it possessed a similar number of leaves which suggested it was at the same stage of development to them. It also did not appear to have any necrotic tissue like the other two plants. This may indicate that the "dwarf" plant was susceptible to the hexylresorcinol since it was unable to effectively sequester the compound at this concentration.

To see if the reduction of size in the "dwarf" plants was due to a reduction in cell size, rather than a reduction in the number of cells, Cyro-Scanning Electron Microscopy (SEM) was conducted on *Arabidopsis* hypocotyls grown for 5 days in the dark (section 2.4.5). It was observed that the hypocotyls of control seedlings grown without hexylresorcinol were comprised of cells ~300 μm in length (Figure 5.29A). Seedlings which possessed normal morphology when grown on 40 μM hexylresorcinol had cell lengths very similar to the control (Figure 5.29B). In contrast, seedlings which displayed the "dwarf" morphology had drastically reduced cell sizes of ~50 μm (Figure 5.29 C). These results suggested that the "dwarf" plants reduced size was due to a reduction in cell size rather than number, an observation consistent with the hypothesis hexylresorcinol targets topo VI in the plants.

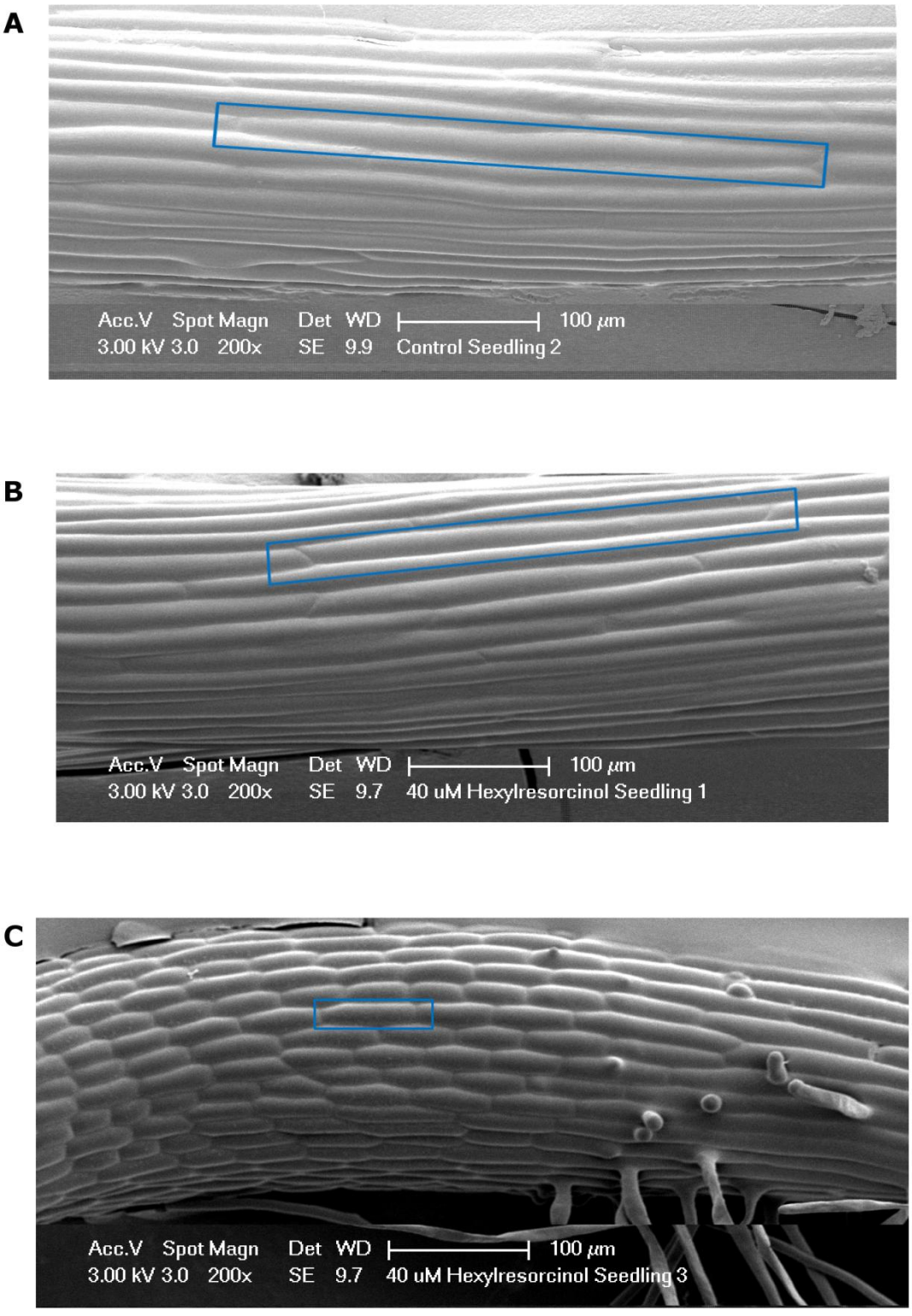

Figure 5.29 SEM images of *Arabidopsis* seedling hypocotyls grown on hexylresorcinol. Single cell highlighted in blue for each image. *A*. Control seedling which was not grown with the compound. *B*. Seedling grown on 40 µM hexylresorcinol that did not display the "dwarf" morphology. *C*. Seedling grown on 40 µM hexylresorcinol that did display the "dwarf" morphology.

To examine if there was any difference in ploidy between seedlings grown on hexylresorcinol and those which were not flow cytometry was conducted on 3 week-old plants grown at 22°C under a 16 hr day on MS salts media with or without 30, 40 or 50 μM hexylresorcinol (Section 2.4.4, Figure 5.30). For 40 μM seedlings displaying the "dwarf" morphology were tested separately to those which did not. Ploidy counts were taken for two plants of each concentration or morphology. The counts attributable to each ploidy peak were converted into a percentage of the overall counts obtained in order to ease comparison between samples. Finally, the values for the two duplicates were averaged. Very similar peak distributions were

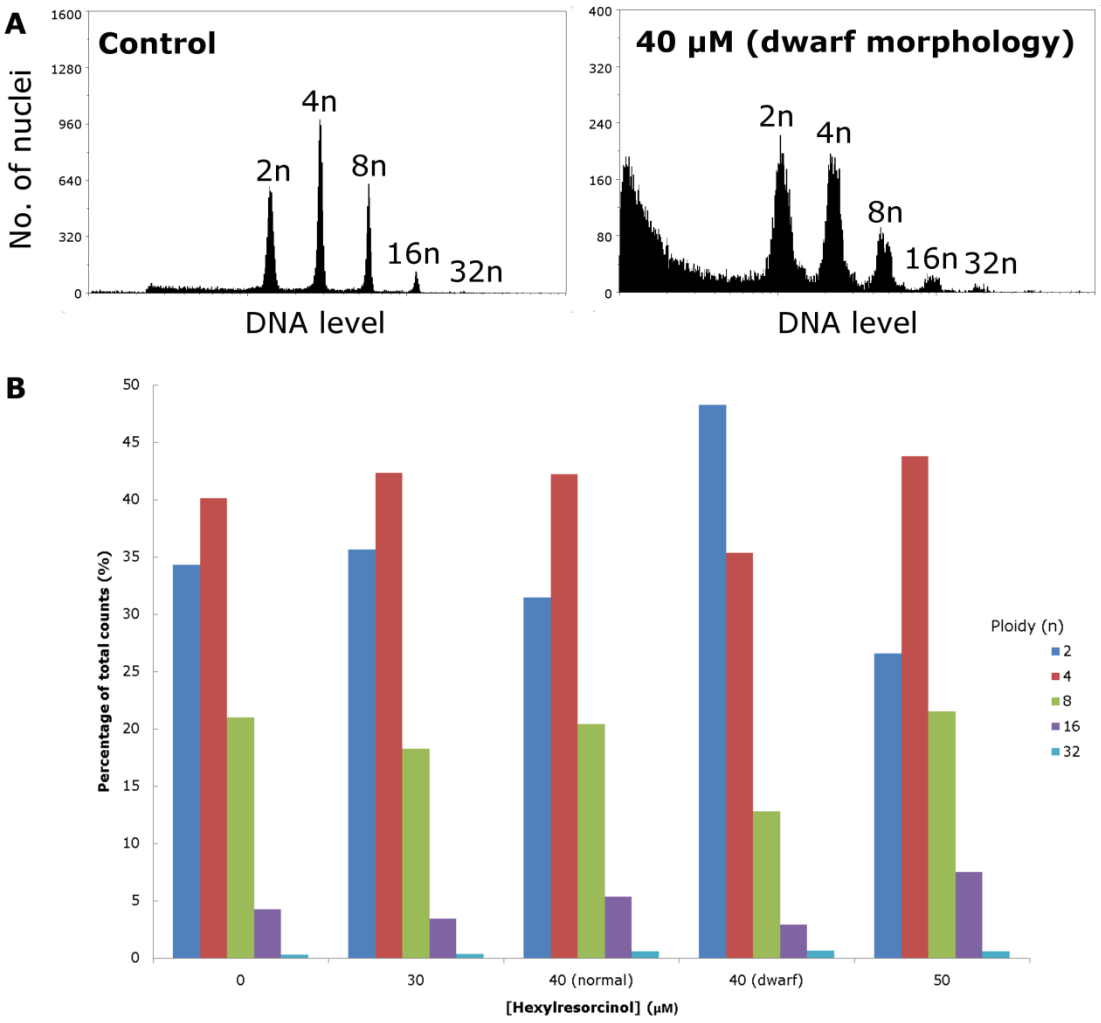

Figure 5.30 Flow cytometry of *Arabidopsis* plants grown on hexylresorcinol. The plants were grown horizontally for 3 weeks under a 16 hr day. Readings were taken in duplicate. Plants grown on 40 μM hexylresorcinol displaying the "dwarf" morphology were tested separately from those displaying normal morphology at that concentration.

observed for plants grown on 0, 30 and 50 μM hexylresorcinol, as well as plants grown on 40 μM which did not display the "dwarf" morphology. However, those grown at 40 μM which did display the "dwarf" morphology showed a skewed distribution with a decrease in the number of counts attributable to the 4n and 8n peaks, and a increase in counts attributable to the 2n peak. This reduction in ploidy for these plants suggests that they also have a reduction in their levels of endoreduplication. This provides further circumstantial evidence that hexylresorcinol is targeting topo VI in the *Arabidopsis* plant.

5.2.10 Expression trials with *P. falciparum* topo VI

Previous studies have identified that the malaria causing protozoa *Plasmodium falciparum* possesses genes homologous to both topo VI subunits in its genome (Aravind et al, 2003). Two homologues of the A subunit were identified whilst only one was found for the B subunit: PfT6A1 (*PF10_0412*), PfT6A2 (*PFL0825c*) and PfT6B (*MAL13P1.328*). *P. falciparum* undergoes a process called schizogony as part of its life cycle, which has similarities to endoreduplication in plants. As such it made sense that *P. falciparum* would have a topo VI. A cursory examination using BLAST and online genomics databases (Table 5.5) revealed that two other protozoa which underwent schizogony also possessed homologues to the B subunit whereas *Toxoplasma gondii*, which does not undergo schizogony, did not. In addition quinacrine, one of the hits from the *M. mazei* topo VI screen, is an anti-malarial drug with an as of yet unknown mode of action.

Protozoa	Schizogeny?	Gene	Function	Identity (%)	Score	Database
Theileria annulata	Yes	Tap372a08.q1kb	Unknown	60	591	http://old.genedb.org/genedb/annulata/
Babesia bigemina	Yes	big424a09.q1k	Unknown	61	511	http://www.sanger.ac.uk/resources/downloads/protozoa/babesia-bigemina.html
Toxoplasma gondii	No	-	-	-	-	http://toxodb.org/toxo/

Table 5.5 BLAST search results for the putative *P. falciparum* topo VI B subunit in various protozoa. Homologues were found in the two parasites which underwent schizogony. The databases were last visited on 09/08/11.

As such expression of the hypothetical *P. falciparum* topo VI subunits was attempted with the view to test the hits from the *M. mazei* screen against it. All three genes were commercially synthesised in a form codon optimized for *E. coli* expression (Geneart) and cloned into the pEt-28a (+) expression vector (Figure 5.31). pEt-28a (+) was chosen because it codes for an N-terminal His-tag which would ease purification. After a conversation with our collaborators Prof. Patrick Forterre and Daniele Gadelle (University of Paris XI, Orsey), who had independently drawn the same conclusions as ourselves, we decided that we should focus our efforts on expressing the A subunits. As such expression of PfT6A1 and A2 in various *E. coli* strains (BL21, Rosetta, Rosetta 2 and Codon Plus) was attempted with induction at an OD_{600} of 0.6. Since no expression was observed, a method for the expression of plasmodium proteins in *E. coli* from the literature was attempted where induction is carried out at an OD_{600} of 2 (Flick et al, 2004). Using this method strong expression was achieved, but the protein appeared to be entirely insoluble (Figure 5.32). Growing the

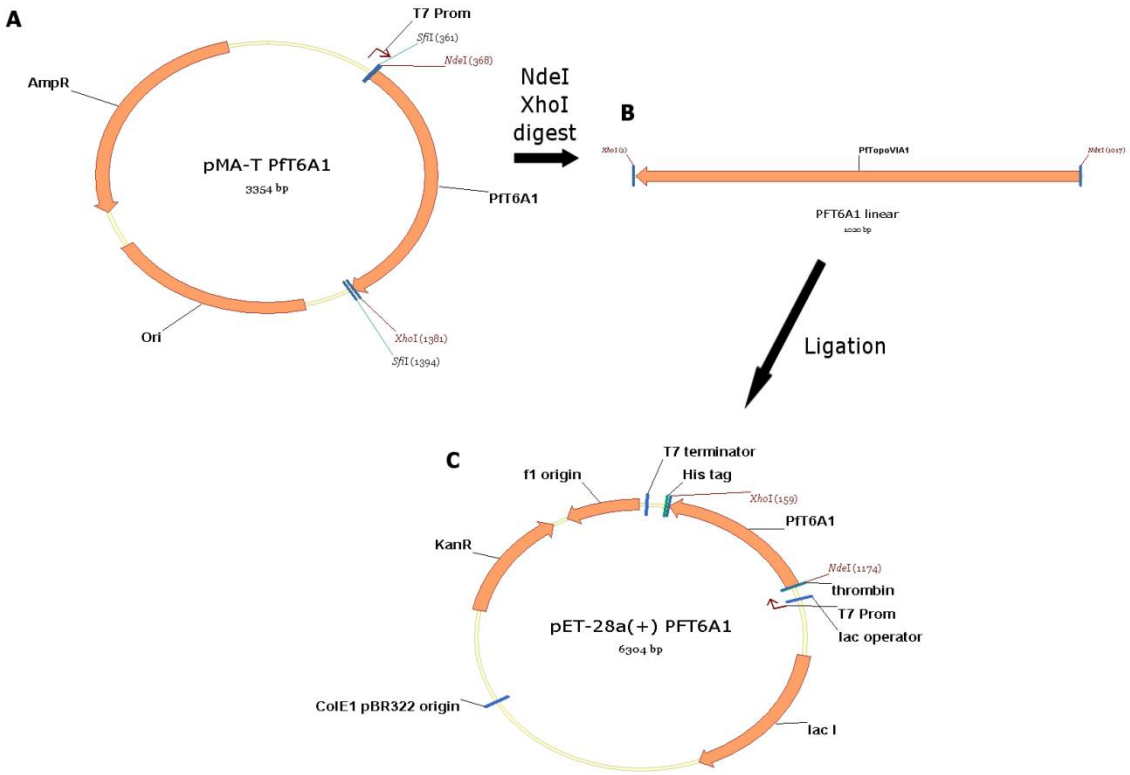

Figure 5.31 Cloning strategy for expression of *P. falciparum* topo VI A1 in *E. coli*. An identical strategy was followed for PfT6A2. *A*. PfT6A1 in pMA-T vector, as provided by Geneart. *B*. PfT6A1 excised by double digest with NdeI and XhoI. *C*. PfT6A1 ligated into pET-28a(+).

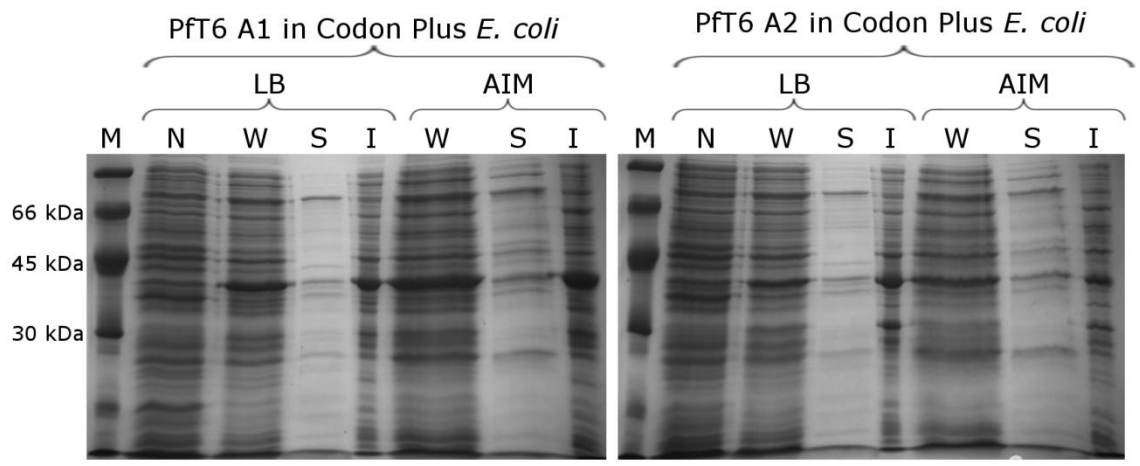

Figure 5.32 Expression of *P. falciparum* topo VI A1 and A2 in *E. coli*. Expression in the Codon Plus *E. coli* strain either carried out in LB media (induced at an OD_{600} of 2) or in Auto Induction Media (overnight). Marker (M), Non-induced (N), Whole-cell (W), Soluble (S) or Insoluble (I) samples run on acrylamide gels. Both PfT6A1 and A2 have a molecular weight of 40 kDA.

bacteria in Auto Induction Media (AIM) produced identical results. Although there appeared to be a faint band present at the correct molecular weight for the soluble extract this was confirmed by MALDI mass spectrometry (Dr Mike Naldrett and Dr Gerhard Saalbach, JIC Proteomics Facility, Norwich) to not be the correct protein.

Since achieved soluble expression had not been achieved with the *E. coli* system expression of PfT6A1, A2 and B in a *baculovirus*-insect cell system was attempted (Section 2.6.5). Meanwhile, our collaborators in Paris would continue attempting expression in *E. coli*. PCR was used to add restriction sites (EcoRI and SphI for PfT6A1/2, or BamHI and SpeI for PfT6B) to the ends of the genes which were compatible with one of the two cloning nests in the pFastBac-Duel baculovirus expression vector (Figure 5.34 A). The initial cloning strategy adopted also contained a step in which the initial PCR fragment was blunt ligated into the Zero Blunt TOPO expression vector (Invitrogen) to allow for proliferation of the fragment and to ease later cloning. However, since the vector contained cutting sites for the restriction enzymes a confusing combination of fragments was produced. As such the strategy was re-designed to omit the Zero Blunt TOPO vector step, with the initial PCR fragment being directly ligated into pFastBac-Duel (Figure 5.33). The presence of the correct fragment in the

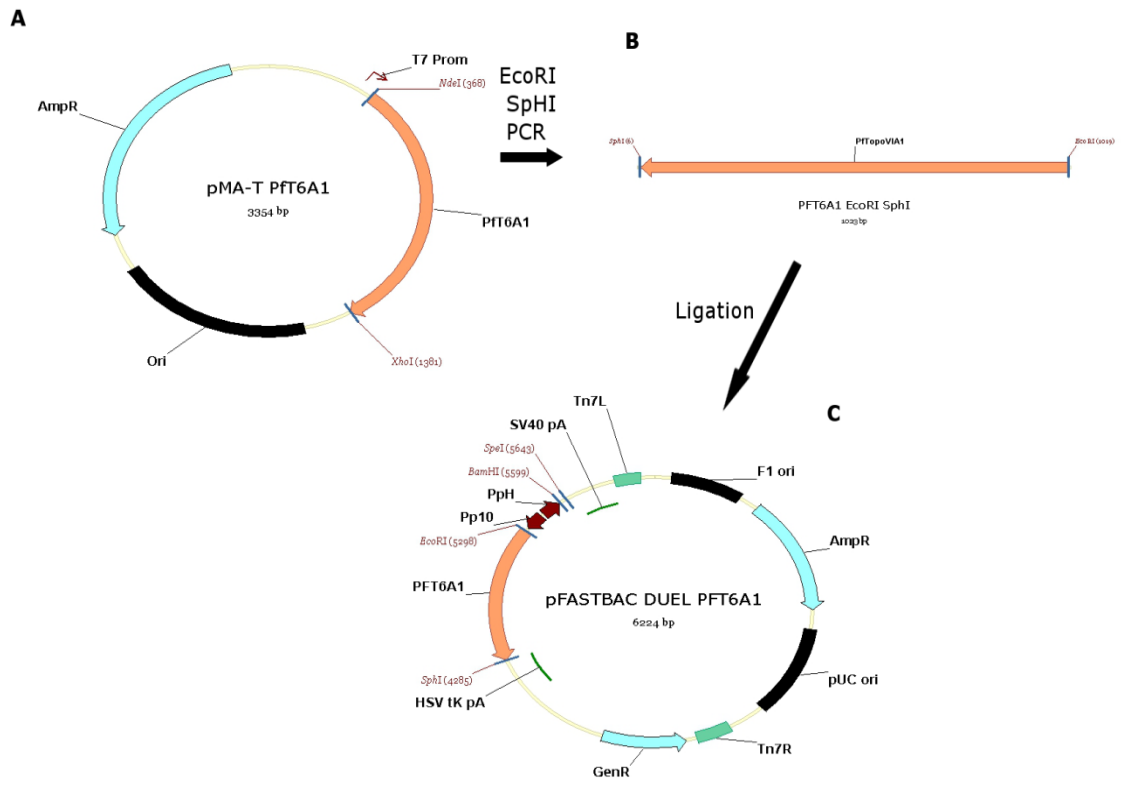

Figure 5.33 Cloning strategy for baculovirus expression of *P. falciparum* topo VI A1. Similar strategies were carried out for PfT6A2 and PfT6B, with EcoRI and SphI being replaced by BamHI and SpeI for PfT6B. *A*. The synthesised genes were provided by Geneart in the pMA-T vector. *B*. Appropriate restriction sites were added to the genes via PCR and linear fragments gel purified. *C*. The genes were ligated into a modified version of the bacmid transfer vector pFASTBAC-Duel containing a EcoRI restriction site in the P10 cloning nest. PfT6A1 and PfT6A2 were put under the control of the P10 promoter (Pp10) whereas Pft6B was ligated into the site controlled by the polyhedral promoter (Pph).

vector was confirmed by double digesting with the relevant restriction enzymes (Figure 5.34 B).

The plasmids were then transformed into *E. coli* strain DH10Bac containing a bMON14272 baculovirus shuttle vector (bacmid) and a transposition helper plasmid (pMON7124). After transformation Tn7 transposition occurs, transferring the gene of interest into the bacmid. Since the bacmid contained pUC/M13 forward and reverse primers either side of the transposition site the presence of the genes in the bacmid by PCR was confirmed with different combinations of pUC/M13 and gene-specific primers (Figure 5.35). These reactions resulted with fragments of the expected sizes, with the exception of the combination of the PfT6B reverse primer and the pUC/M13 forward primer. Sequencing (The Genome Analysis Centre, Norwich) of the genes in the pMFastBac-Duel vector revealed that a

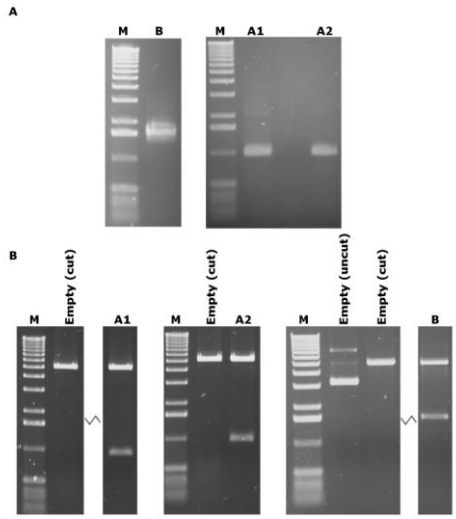

Figure 5.34 Cloning of *P. falciparum* genes for baculovirus expression. *A*. PCR products from pMA-T vectors containing the genes of interest. The primers were designed to add EcoRI and SphI cut sites to the 5' and 3' ends respectively of PfT6A1 and A2. The primers for PfT6B were designed to add BamHI and SpeI sites to the genes 5' and 3' ends. *B*. Double restriction digest of pMFastBac-Duel vectors containing the genes of interest with the appropriate restriction enzymes.

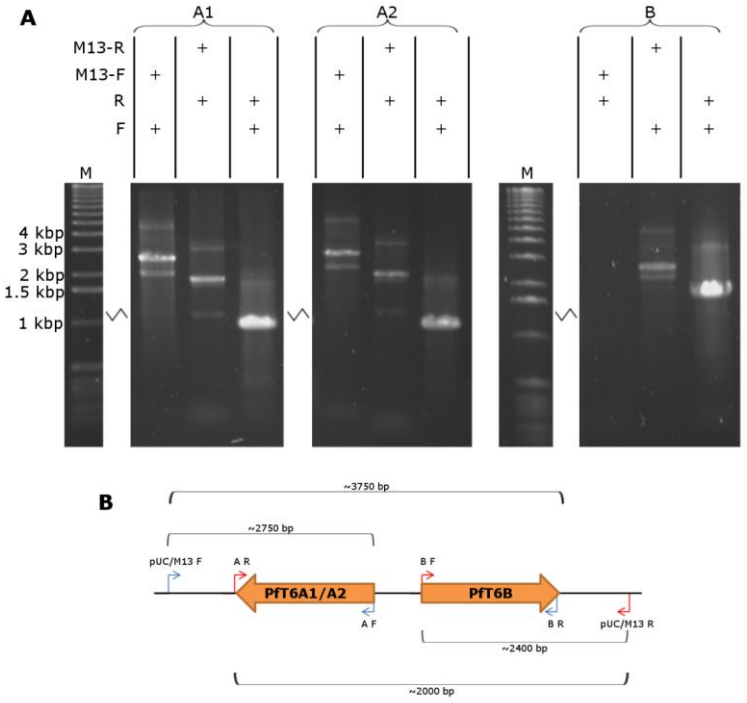

Figure 5.35 PCR analysis of bacmids containing *P. falciparum* topo VI genes. *A*. PCR reactions with bacmids and various primers. A 1 kb ladder (M) was included in all gels. The PCR reactions were carried out a constant annealing temperature of 55°C with a combination of either pUC/M13 forward (M13-F) or pUC/M13 reverse (M13-R) primer with the relevant forward (F) or reverse (R) primer for the gene to be analysed. *B*. Cartoon of the genes in the bacmid with the expected sizes for products with various primer pairs. Both PfT6A1 and A2 are approximately 1 kb in length, whilst PfT6B is ~1.7 kb.

point deletion had resulted in an 86 amino acid truncation on the C-terminus of PfT6B, which explained why the PCR using the PfT6B reverse primer failed. Strangely, the reaction using the PfT6B forward and reverse primers produced a fragment of approximately the correct size.

Regardless, expression trials proceeded with all three genes and used the bacmids to transfect surface grown SF21 insect cells. After 72 hr the P1 virus which had been released into the media was collected and used it to infect fresh cells with a multiplicity of infection (MOI) of approximately 0.5. The viral titre was estimated as per the guidelines from Invitrogen. After another 72 hr the virus released in the media was again harvested to obtain the P2 viral stocks. These stocks were then used in expression trials. The initial expression trials were carried out at a MOI of approximately 3, again estimated from the Invitrogen guidelines (Figure 5.36). The cells were harvested after 48, 72 or 96 hrs and analysed by acrylamide gel electrophoresis. No expression was observed with any of the genes at any of the time points tested. This process was repeated with a second preparation of bacmids, but expression was still not observed. Since time was running short, the remaining trials were focused primarily on the most likely candidate of the two A subunits: PfT6A1. One of the troubleshooting suggestions from Invitrogen was that if the viral titre of the P1 virus used to generate the P2 virus was too high deleterious mutations could accumulate

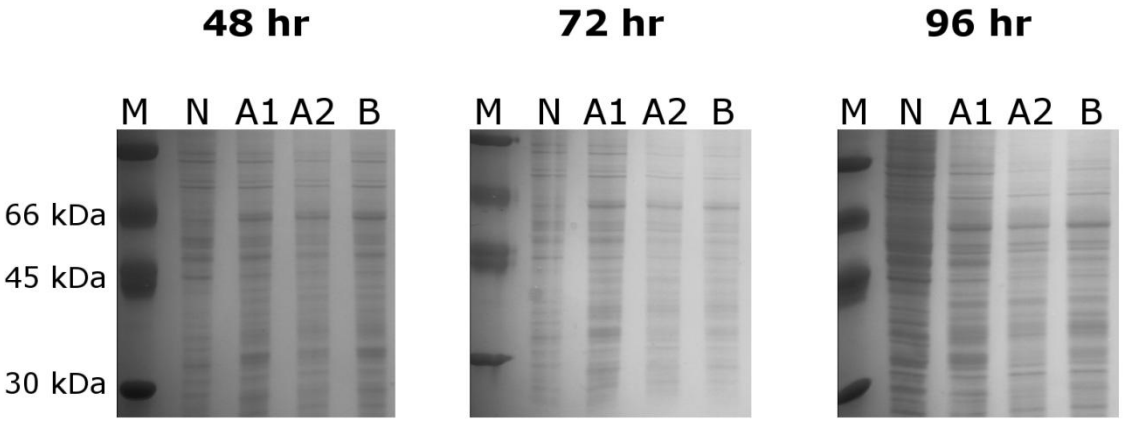

Figure 5.36 Initial time course baculovirus expression of *P. falciparum* topo VI genes. Non-infected (N) and cells infected with transgenic P2 virus containing the PfT6A1 (A1), PfT6A2 (A2) or PfT6B (B) genes harvested after the indicated time point. The multiplicity of infection was approximately 3, as calculated from Invitrogen estimates.

and prevent expression. As such P2 viral stocks were prepared from P1 virus diluted 1:10, 1:100 or 1:1000 and used them to infect fresh cells (Figure 5.37). Since it was not possible to estimate the viral titre 1x 10^6 cells were infected with 200 μL of virus. The cells were then harvested after 34, 72 or 96 hr. In addition some cells were infected using thePfT6B P2 virus from a previous expression for comparison. No expression of PfT6A1 was observed, but surprisingly expression of a band the right size for PfT6B was seen. Unfortunately the PfT6B produced was likely in a truncated form, (as previously indicated by sequencing and PCR analysis) and there was no time to pursue this work further.

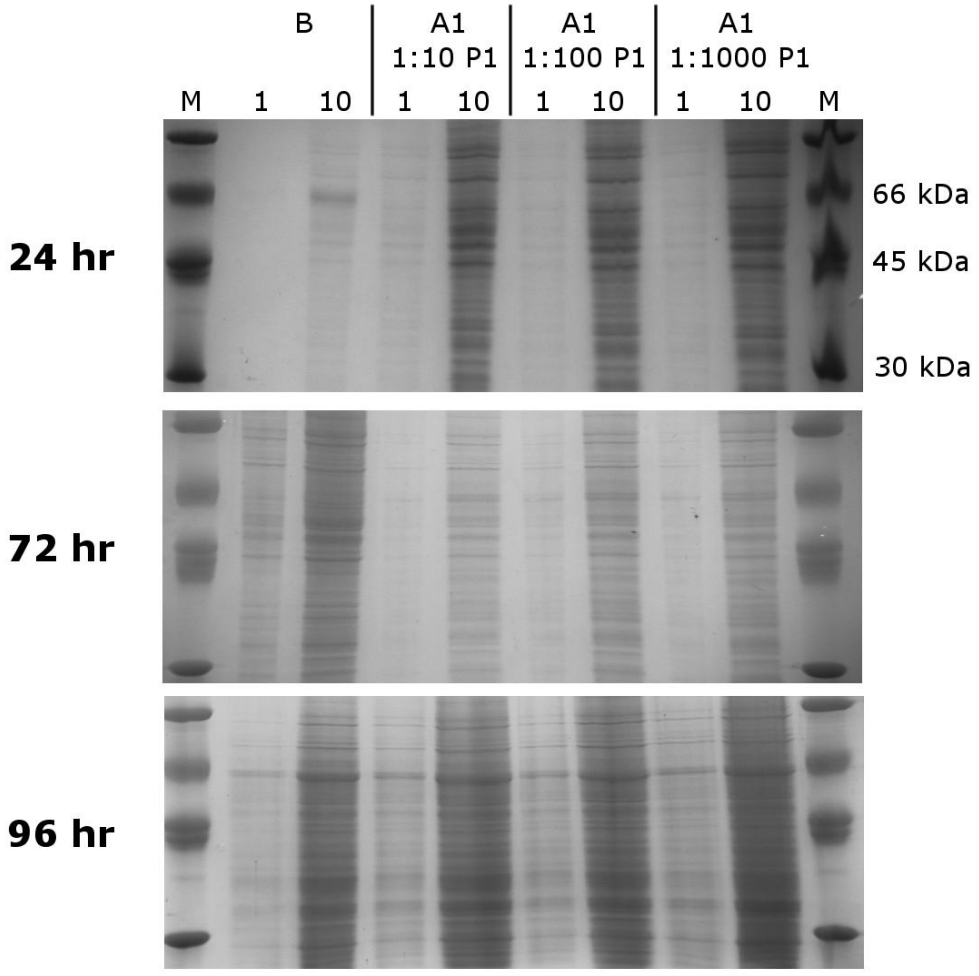

Figure 5.37 Expression of PfT6A1 and PfT6B in the baculovirus system. Either 1 or 10 μL of each sample was loaded onto the gel. The PfT6A1 P2 virus used was generated with either a 1:10, 1:100 or 1:1000 dilution of the P1 viral stock. The cells were harvested at the time point indicated.

5.2.11 Activities of anti-malarial compounds against *M. mazei* topo VI

Since quinacrine was one of the hits from the *M. mazei* topo VI screen, and is an anti-malarial (Chauhan & Srivastava, 2001) of unknown mechanism it was decided to test other related anti-malarial compounds against the enzymes which were available in our lab. Reactions containing 0.5 units *M. mazei* topo VI with 100 μM chloroquine, mefloquine, primaquine, quinacrine or quinolone were prepared. Out of these compounds only quinacrine produced inhibition, although there may have been a very low level of inhibition from chloroquine. As such we were interested in investigating compounds related to quinacrine. Dr Mark Thompson (University of Sheffield) has previously generated a range of thiazole compounds derived from quinacrine (Thompson et al, 2011) which showed varying potency against the malaria parasite (Figure 5.39). Dr Thompson provided a selection of these compounds as well as a collection of β-carboline compounds designed for anti-malarial activity (paper under review at the time of writing; structures not disclosed). Unfortunately none of the compounds tested had any effect on the activity of 1 unit of *M. mazei* topo VI (Figure 5.40).

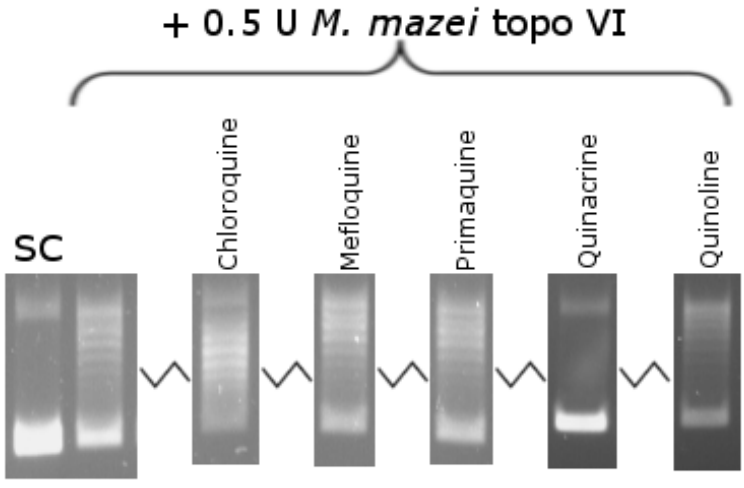

Figure 5.38 *M. mazei* topo VI with various anti-malarial compounds. All compounds tested at 100 μM.

β-Carboline compounds

1. MT-IC16
2. MT-IC41
3. MT-IC43
4. MT-IC46
5. MT-IC47
6. MT-IC48
7. MT-IC49
8. MT-IC52

Thiazole compounds

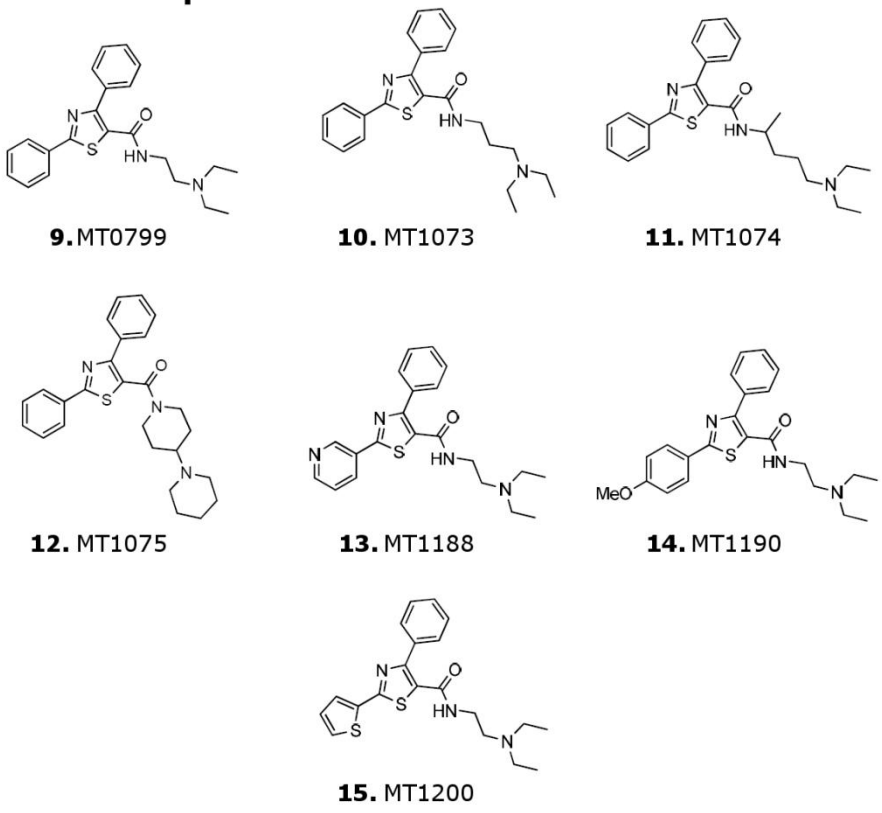

Figure 5.39 Structures of experimental anti-malarial compounds. All compounds were purified to >95% by HPLC, except 13. whose purity was unable to be determined due to an unusual interaction with the column. The structures in this image were kindly provided by Dr Mark Thompson.

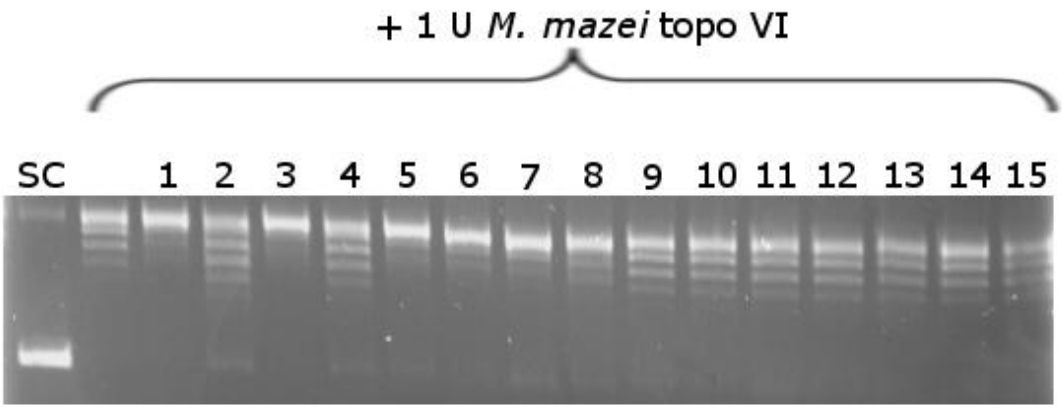

Figure 5.40 Testing putative anti-malarial compounds against *M. mazei* topo VI. Various β-carboline and thiazole derivatives were tested for their ability to inhibit topo VI at 100 μM. The numbering of compounds is as in Figure 5.39.

5.3 Discussion

5.3.1 *M. mazei* topo VI ATPase activity and DNA cleavage

In this work the biochemical properties of *M. mazei* topo VI have been explored, as well as confirming some expected ones based on the work previously carried out on *S. shibatae* topo VI. Several basic facts about the enzyme have be validated, including the necessity of ATP and Mg^{2+} for the relaxation activity of the enzyme. It has also been demonstratedthat *M. mazei* topo VI could be inhibited by radicicol, but with a two-fold greater IC_{50} than that reported for *S. shibatae* topo VI. With an IC_{50} value of around 400 μM, radicicol is a very poor inhibitor of *M. mazei* topo VI. Furthermore radicicol has been demonstrated to inhibit the ATPase activity of the enzyme with an IC_{50} close to that in the gel assay, indicating this was its likely mode of action. In contrast the DNA gyrase ATPase inhibitor novobiocin had no effect on the activity of the enzyme, similar to that which has been observed with the *S. shibatae* enzyme.

Stabilization of the cleavage complex by *M. mazei* topo VI with ADPNP or Ca^{2+} proved difficult. A very slight increase in linear DNA over the background could be observed which was likely attributable to contaminants in the enzyme preparation, but this was less than that which DNA gyrase or *S. shibatae* topo VI produced under similar conditions. It is possible that *M.*

mazei topo VI does not bind ADPNP very well, which would account for the low level of cleavage in that control. Trying different ATP analogues may yield better results. However, a lack of compatibility with ADPNP does not explain the low amount of cleavage seen with Ca^{2+}.

The AFM images revealed that *M. mazei* topo VI appeared to remain on the DNA even after SDS-proteinase K digest and phenol-chloroform extraction. This may indicate that *M. mazei* topo VI is resistant to proteinase K digestion, and that the interactions holding the enzyme-DNA cleavage complex are strong enough to remain associated despite exposure to SDS and phenol. This would make sense in light of the fact that, unlike type IIA topoisomerases, the A subunit of topo VI lacks a C-terminal exit gate. It has been suggested that the primary function of this C-terminal gate is to hold the complex together during DNA-gate opening in order to prevent disassociation and the formation of double-strand breaks (Bates et al, 2011; Stuchinskaya et al, 2009). The lack of this additional interface in topo VI may be compensated for by an increase in the strength of subunit association. This is supported by the fact that both topo VI enzymes to date can only be produced in a soluble, active form when the two subunits are co-expressed. Furthermore the subunits remain bound together on a His-trap column even when exposed to elution buffers containing 2 M NaCl, 10% PEG or nothing but water. This implies that the interactions within the topo VI complex are very strong. It was possible to observe ADPNP-induced cleavage of DNA by *S. shibatae* topo VI, but the thermophilic nature of the enzyme makes drawing comparisons difficult. It could be that only the *M. mazei* orthologue of the enzyme is resistant to proteinase K digestion. It may be possible to reveal the cleavage complex of *M. mazei* topo VI by using a more aggressive proteinase.

5.3.2 Unusual topoisomers produced by *M. mazei* topo VI

Perhaps the most unusual observation made about the biochemistry of *M. mazei* topo VI was the formation of unexplained bands at high concentrations of the enzyme. This banding pattern was distinct from that of partial activity, with certain bands becoming more prominent than others,

suggesting that the enzyme was not self-inhibiting at these high concentrations. Furthermore, the formation of this pattern was observed with both relaxed and supercoiled DNA which eliminates the potential of auto-inhibition. By carrying out time-course reactions it was observed that the strange banding never appeared below a certain concentration of enzyme despite extended reaction times. This suggested that the DNA topoisomers these bands represent are not the standard end product for the topo VI reaction, and may require some distortion of the DNA brought about by the presence of multiple enzymes on a single DNA molecule to be produced. They were not abolished by carrying out an SDS/proteinase K digest which appeared to show that they were not due to enzyme remaining bound to the DNA whilst it was being run on the gel.

Although some cleavage activity attributable to contamination was observed in the absence of ATP the formation of this banding pattern was largely ATP-dependent, indicating it was an activity of the enzyme rather than a contaminant. The bands shifted slightly when run on an agarose gel containing chloroquine, which suggested that they were still closed-circular and not linear DNA fragments. In addition the bands could not be converted back to the standard relaxed form by wheat germ topo I and were not converted to a single open circle band by the nicking endonuclease Nb.BstI. These data show that these bands cannot be explained as negatively or positively supercoiled DNA. It is possible that they might represent the formation of DNA knots, which would not be resolvable by either topo I or Nb.BstI. How the enzyme would introduce knots under these conditions is unclear, although it may be that a large number of enzyme molecules present on a single plasmid may cause the DNA to distort in such a way to permit knotting.

However the AFM images of DNA treated with high concentrations of *M. mazei* topo VI do not appear to support this hypothesis, since no knotted structures were definitively observed. Rather, the DNA appeared condensed and with a plectonemic appearance. Some molecules appeared highly decorated with enzyme molecules, suggesting that the protein was resistant to proteinase digestion. This was interesting, since the bands did not appear when enzyme was incubated with DNA in the absence of ATP and native gel

shift assays have shown that the enzyme does bind DNA in the absence of ATP. Since their formation is ATP dependent, they could represent cleavage complexes of the topo VI with DNA trapped by the SDS treatment. This makes sense in light of our failure to stabilize the *M. mazei* topo VI cleavage complex with ADPNP or the inhibitors from the screen.

5.3.3 Performance of the screen

The quality of data for the screen against *M. mazei* topo VI remained high, with an average Z' value of 0.69. This figure was close to that which was previous calculated for the DNA gyrase screen. However, looking at the Z' factor for individual plates revealed there was a broader distribution for the *M. mazei* screen with two reaction plates having Z' less than 0.5 (plates 9 and 12, with Z' = 0.44 and 0.46 respectively). This indicates that the data for these two plates were of marginally poorer quality than the rest of the screen, although still of an acceptable standard. There were no obvious patterns to the data; however it was observed again that most compounds showed some inhibition or activation activity. On some plates (such as 2, 4, 8 and 11) the majority of the compounds showed a low level of inhibition whilst other plates (such as 10 and 12) showed a low level of activation. The remaining plates did not have a bias either way. These variations were likely the result of day-to-day or run-to-run variations of the screening process. Nine compounds gave percentage inhibitions values above the 25% threshold, with six being confirmed as hits. Of these only m-amsacrine had been previously reported as an inhibitor of *S. shibatae* topo VI (Bergerat et al, 1994), giving a novel hit rate of 0.52%.

5.3.4 Novel inhibitors of *M. mazei* topo VI

Out of the nine compounds selected by the screen six were validated as hits in the gel assay. None of these compounds had been previously shown to inhibit *M. mazei* topo VI and only m-amsacrine had been shown to inhibit *S. shibatae* topo VI (Bergerat et al, 1994).The hits from the screen came predominately from two classes of compound: the acridines and anthraquinones (Figure 5.41). Members of both these classes have been described as topoisomerase inhibitors (including amsacrine and mitoxanthrone).

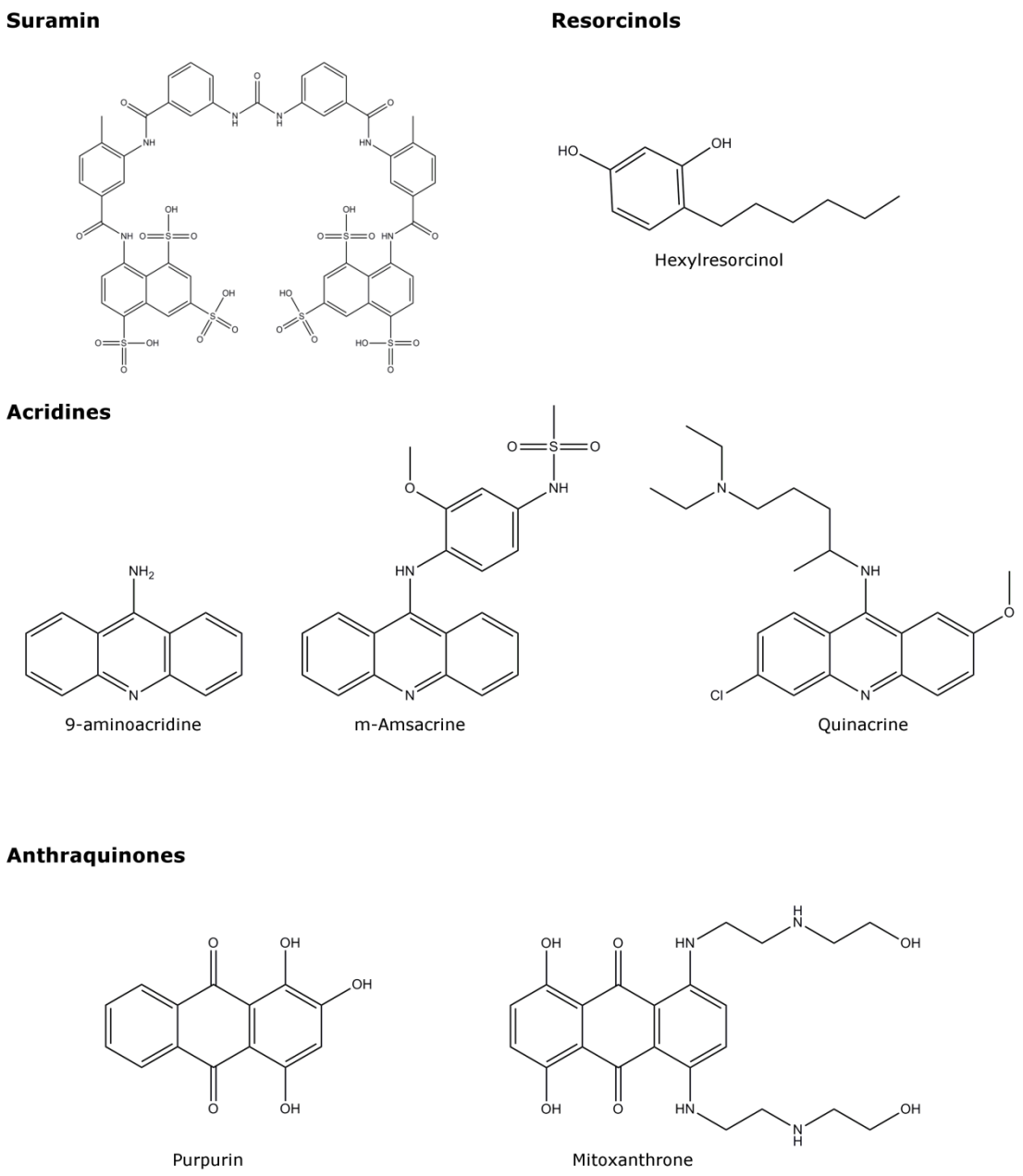

Figure 5.41 Structures of *M. mazei* topo VI screen hits.

Two of the hits, quinacrine and 9-aminoacridine, were also intercalators. DNA relaxation in the presence of intercalators causes negative supercoils to be introduced rather than removed. To prove that these compounds were genuine inhibitors, relaxation reactions were carried out with either *M. mazei* topo VI or wheat germ topo I (a type I topoisomerase with a different mechanism), and various concentrations of the two drugs. The relaxation activity of both enzymes appeared to be reduced by the drugs. However, when the samples were run on agarose

gels containing the weak intercalator chloroquine it was revealed that the samples containing topo I and either quinacrine or 9-aminoacridine had become more tightly supercoiled than the substrate DNA. In contrast the samples which contained *M. mazei* topo VI and either drug did not display this tightening, which indicated that the enzyme was genuinely being inhibited. A clearer experiment would have been to repeat the experiment but with relaxed DNA as a substrate. With this setup wheat germ topo I would start supercoiling the DNA when a certain concentration of drug was reached (around 100 μM from our data) whereas *M. mazei* topo VI would not.

Having verified that the all six hits were genuine experiments were carried out to determine their IC_{50}s. The two most potent inhibitors were 9-aminoacridine and quinacrine with IC_{50} values around 10 μM. The weakest was hexylresorcinol with an IC_{50} of 40 μM, which still was a respectable value. Interestingly, quinacrine was an anti-malarial of unknown mechanism, as discussed below, and that hexylresorcinol was an oral antiseptic. Although there are currently no known pathogenic archaea one study has found the number methanogenic archaea, similar to *M. mazei*, in the mouths of people suffering from chronic periodontitis is increased (Lepp et al, 2004). Since hexylresorcinol is used to treat this type of infection, it would be interesting to see its effect on the growth of methanogenic archaea *in vitro* and *in vivo*.

5.3.5 Cross-reactivity of *M. mazei* topo VI and *E. coli* gyrase screen hits

The compound suramin was a hit in both the *E. coli* gyrase and the *M. mazei* topo VI screen. Its IC_{50} was determined to be approximately two-fold more potent with *M. mazei* topo VI. However, it is difficult to interpret whether this difference in potency is due to the difference in activity of the two enzymes as well the different definition of what concentration of enzyme constitutes one unit of activity.

Interestingly none of the other hits from the *M. mazei* topo VI screen inhibited *E. coli* gyrase at the concentrations tested, which suggests a level of specificity of these compounds for topo VI. This may arise from them

binding to novel binding sites on the topo VI enzyme which are either not present or very weak in the gyrase enzyme. This would only be confirmable by structural techniques such as X-ray crystallography which were beyond the scope of this project. Since the *M. mazei* topo VI enzyme has already been crystallised (Corbett et al, 2007), it would be relatively simple (with the appropriate investment of time) for this to be followed up.

On the other hand mitoxanthrone, the second of the novel *E. coli* DNA gyrase hits, was also an inhibitor of *M. mazei* topo VI. This identified it as a "false negative" for the screen, and was due to the compound's ability to interfere with DNA triplex formation by intercalation. Mitoxanthrone was substantially more potent against *M. mazei* topo VI than DNA gyrase with an IC_{50} approximately ten-fold lower. This means that mitoxanthrone is able to inhibit topo II (Smith et al, 1990), DNA gyrase and topo VI making it a prolific inhibitor of topoisomerases. It is likely that it intercalates at the DNA break generated in the G-segment during the reaction, since this step is common to the reactions of all three enzymes. However, it is also a strong intercalator and there was no time to check if its apparent inhibition against topo VI was an artefact of this property (such as was carried out with quinacrine and 9-aminoacridine). The validity of mitoxanthrone as a topo VI inhibitor would need to be confirmed in this regard before any major conclusions should be drawn from these results.

5.3.6 Mechanism of action for screen hits

The hits were run through a range of assays to determine their modes of action. Suramin was show to prevent the binding of topo VI to DNA making its mode of action identical for both topo VI and DNA gyrase as well as likely the same for topo II (Bojanowski et al, 1992).

Purpurin also displayed the ability to prevent the binding of DNA to topo VI, but instead of a straight abolition of binding the formation of two bands was observed with molecular weights intermediate those corresponding to bound and unbound. It may be that these bands correspond to DNA bound to A subunit monomers or dimers, which would mean that purpurin inhibits the enzyme by disrupting protein—protein interactions rather than preventing DNA binding directly. In this scenario it

would make sense if the binding site for the compound was located at the interface between the A and B subunits. The question arises how specific purpurin is as an inhibitor, since it may just interfere with protein—protein interactions generally. However, its inability to inhibit *E. coli* DNA gyrase does show that it possesses some level of specificity for *M. mazei* topo VI. This specificity may be linked to the incredibly high strength of the interaction between the A and B subunits of *M. mazei* topo VI. Since it has been observed that the subunits are very difficult to separate during column chromatography it would be interesting to see if the inclusion of a low concentration of purpurin in the elution buffer would allow for separation of the two subunits.

Testing the remaining hits for their ability to inhibit topo VI ATPase activity revealed that quinacrine appeared to inhibit the ATPase activity of the enzyme. However, the IC_{50} for this inhibition was approximately 400 μM which was around forty-fold greater than its IC_{50} in the gel assay. In addition it was shown that this apparent inhibition is likely due to quinacrine interfering with the linked assay by inhibiting the activity of pyruvate kinase. These data lead to conclude that quinacrine does not target the enzymes ATPase activity as part of its mode of action.

Interestingly, hexylresorcinol appeared to activate the ATPase activity of topo VI when present at a concentration of 500 μM (roughly ten-fold its IC_{50} in the gel assay). Since the drug had no effect on the activity of pyruvate kinase in the absence of topo VI and possessed no intrinsic ability to hydrolyse ATP this activation of topo VI ATPase activity is likely genuine. It may be that the drug operates by uncoupling ATP hydrolysis from the conformation changes it usually induces. Whether this phenomenon is relevant to the mechanism of hexylresorcinol still remains unclear, since the concentration at which it manifests strongly is much higher than its IC_{50} in the gel assay.

Unfortunately since *M. mazei* topo VI seemed unusually resistant to stabilization of the cleavage conditions the ability of the remaining hits to stabilize the cleavage complex was difficult to determine as discussed above. However, the *S. shibatae* topo VI proved to be a viable substitute

achieving a good level of cleavage with the ADPNP control, although neither hexylresorcinol nor suramin were able to inhibit the enzyme. Although none of the hits tested appeared to stabilize the cleavage complex they all seemed to reduce the stabilization of the cleavage complex by ADPNP. It may be that these compounds operate by directly preventing the cleavage of DNA by topo VI. However there was neither the time nor the enzyme to explore this further, and these results would greatly benefit from further study. Furthermore, it would be superior to repeat the experiment using Ca^{+2} as the cleavage complex stabilizing agent. This would eliminate the possibility that the drugs were preventing the binding of ADPNP rather than preventing cleavage.

5.3.7 Hexylresorcinol as an inhibitor of *Arabidopsis* endoreduplication

Out of the hits from the screen only hexylresorcinol had an effect on the growth of *Arabidopsis thaliana*. Treating plants with 40 μM hexylresorcinol resulted in an overall decrease in plant size and caused plants to become pale and transparent. At this concentration there appeared to be a range of responses to the drug with some plants largely unaffected, some with slowed growth and others exhibiting a reduction in overall size and root hair size and frequency (the "dwarf" morphology) (Figure 5.42). The characteristics of the "dwarf" morphology are similar to those observed in topo VI knock-out mutants (Hartung et al, 2002; Sugimoto-Shirasu et al, 2002). Additionally all plants took on a yellowish colour, which was noted in some of the topo VI mutants (Hartung et al, 2002). However, it does appear that the trichromes size of these remains largely unaffected, whereas they were reduced in the topo VI mutants.

The difference between slow growing plants was more apparent when treated plants were transferred to fresh agar lacking hexylresorcinol. After three weeks the plants which had either not been affected or had their growth slowed had mostly recovered, growing to full size and regaining their pigmentation. Interestingly, a few leaves on these plants turned a vivid white and withered. In contrast plants which had exhibited the dwarf morphology remained smaller and did not have any withered leaves,

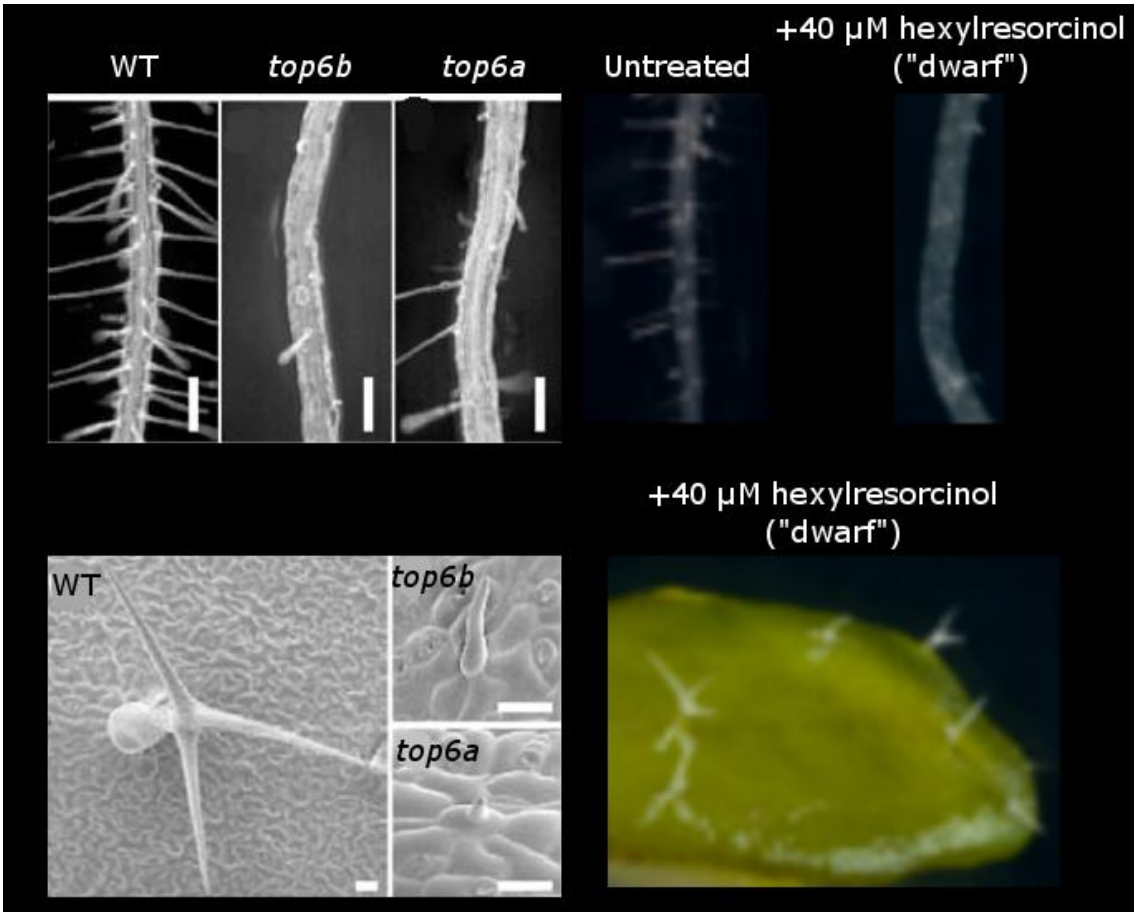

Figure 5.42 Comparing hexylresorcinol "dwarf" morphology to topo VI knock-out mutants. Electronmicrographs of *Arbadopsis* roots (top left) and trichromes (bottom left) in wild-type and topo VI knock-outs from (Sugimoto-Shirasu et al, 2002) compared to photographs of plants treated with 40 µM hexylresorcinol displaying the "dwarf" morphology. The roots of an untreated Arbadopsis hypocotyl is shown for comparison.

although they did grow considerably and retain their pigmentation. These observations suggest that the withering of leaves is an immune response to the drug, most likely the sequestering of the herbicide into certain leaves. A similar response has been reported for weeds resistant to the common herbicide glyphosate (Shaner et al, 2011). Plants which are able to sequester the drug successfully are able to grow normally or have their growth slowed as a stress response, whereas those who can't exhibit the "dwarf" morphology.

To discern whether the "dwarf" morphology was due to *in vivo* inhibition of endoreduplication both cyro-SEM and flow cytometry were carried out on hexylresorcinol grown seedlings. Since endoreduplication results in both increased ploidy and cell size the expected result for its

inhibition is a reduction in both of these characteristics. Plants which had grown normally or slowly both exhibited a cell size of around 300 μm whereas plants exhibiting the "dwarf" phenotype were reduced at around 50 μm. Furthermore the ploidy of the "dwarf" plants was found to alter with a large increase in the 2n peak and a reduction in the 4n and 8n peaks. These observations suggest that endoreduplication is indeed decreased in these plants. This is different to what was observed with topo VI knock out plants where endoreduplication was stopped above 8n. In contrast the "dwarf" plants do display a slight reduction in the 16n peak although it is difficult to tell if this change is. This difference may have arisen since the original studies carried out flow cytometry on the leaves of the plants, whereas the whole plant was used in these experiments. Since ploidy varies between tissue types this may explain the discrepancy.

As to whether this decrease in endoreduplication is due to the inhibition of *Arabidopsis* topo VI *in vivo* it is difficult to say for certain since there is always the possibility that hexylresorcinol just happens to target another key enzyme involved in the process. The drug does provoke other morphologies (such as reduction in pigmentation) which are not solely explainable as the effect of reduced endoreduplication. It is therefore likely that it has multiple targets within the plant. Additionally, although the "dwarf" morphology shares some of the features with the topo VI knock-out mutants (overall size reduction, yellowish colour, altered ploidy, and reduced root hair size and frequency) there are some key differences. Thrichrome size appears to be unaffected, whereas it was reduced in the mutants, and endoreduplication above 8n was observed with the "dwarf" plants which was abolished in the knock-out mutants. These differences could imply that hexylresorcinol is targeted to specific tissues within the plant.

However, the only way to prove for definite that topo VI is the target within the plant would be to express the enzyme from the plant and demonstrate that hexylresorcinol inhibited it *in vitro*. Resistant mutants could then be designed and introduced back into the plant. If these mutant plants were resistant to the dwarfing effect of hexylresorcinol then one could say for definite that topo VI was its target *in planta*. However, the fact

that the drug inhibits *M. mazei* topo VI *in vitro* and *Arabidopsis* endoreduplication *in planta* lends circumstantial evidence to that conclusion.

5.3.8 Expression of *P. falciparum* topo VI

Having read about hypothetical topo VI in the malaria parasite *Plasmodium falciparum* in the literature expression of the two potential A subunits (PfT6A1 and PfT6A2) and the B subunit (PfT6B) was attempted. Unfortunately none of the proteins were expressed in a non-truncated, soluble form in either the *E. coli* or *baculovirus* expression systems.

The expression of PfT6A1 and A2 in the *E. coli* system was a success, although neither protein was soluble. Expression was best when induction was carried out at high a OD_{600} (~2) or when carried out in auto-induction media (which also allows for high densities prior to expression). An exploration of expression conditions (such as temperature or expression strain) may lead to the production of soluble protein. However a large-scale analysis of *P. falciparum* proteins expressed in a soluble form in *E. coli* has revealed that the pI of the desired protein contributes heavily to the chances of successful soluble expression (Mehlin et al, 2006). Solubility was found to decrease with increasing pI, with the effect being most pronounced with pI >8. The pIs of PfT6A1 and A2 are 8.8 and 9.3 respectively (as calculated by the ExPASy Compute pI/MW tool), putting them well above this value. It may be more fruitful to search for homologues of these genes in other *Plasmodia spp*. which have more favourable characteristics and attempt expression of these genes instead of those from *P. falciparum.*

Expression of the B subunit was successful in the *baculovirus* system, but sequencing and PCR analysis revealed that this was likely a 86 amino acid truncation of the proteins C-terminus. This was due to a single base pair deletion resulting in a frame-shift. The mutation occurs in a stretch of 14 A-T repeats with the final pair being deleted (1410 bp). This results in the formation of a stop codon 6 codons downstream. It is likely that the high number of repeats in this region caused an error with the polymerase. In the *M. mazei* enzyme these residues form the C-terminal domain of the B subunit, which are thought to control substrate specificity and localisation of the enzyme (Corbett et al, 2007). It was noted that this C-terminal domain

was only found in archaea which also possessed a DNA gyrase, implying that it was necessary for regulating the activity of the two enzymes in respect to one another. It would therefore make sense for *P. falciparum* topo VI to also posses this domain, since it too has a DNA gyrase. Deletion of this domain from the *M. mazei* enzyme results in a five-fold decrease in activity. It is therefore possible that the truncated version of PfT6B would retain some activity if purified. However it would be superior to reattempt the cloning and alter the codons in that region to reduce the number of A-T repeats without changing the amino acid sequence (AAA to AAG, for example). This would reduce the chance of a polymerase error, and may be worth considering for other such regions in the sequence (although this appears to be the longest).

The failure to express either A subunit in the *baculovirus* system was likely either due to the necessity for dual expression (see below) or purely a matter of optimization. Since the expression procedure is very lengthy there was only time to trial a few conditions, so a more detailed exploration may be fruitful. Our laboratory was not equipped to accurately determine the multiplicity of infection (MOI) for the viral stocks, so it was necessary to estimate them. The control of the MOI is commonly held to be crucial for successful expression. As such further studies should invest in the appropriate equipment and training to allow for this.

The topo VIs currently successfully expressed in a soluble form (i.e. *S. shibatae* and *M. mazei*) have only been done so by co-expressing the two subunits. This may in fact be the key to their expression and is possibly due to the strong interaction between the two subunits. It would be interesting to test dual expression of the subunits in both *E. coli* and *baculovirus*, since suitable vectors are available for both systems.

Finally, it was noted that the gene for PfT6A2 has since been duplicated in the *Plasmodium* database: PFL0825c-a and PFL0825c-b. PFL0825c-b is the same as the original sequence (which was used in this study) whilst PFL0825c-a contains a 20 amino acid deletion towards the C-terminal end. Which of these two, if any, is the correct gene remains to be seen.

5.3.9 *P. falciparum* topo VI as a drug target

Although we were unable to express the *P. falciparum* topo VI our results with the *M. mazei* enzyme can allow us to speculate somewhat about its possible interactions with the compounds found in the screen. Several of the compounds from the screen have been shown to have efficiency against *P. falciparum*: suramin and quinacrine. Since suramin has such a prolific range of enzymes it can inhibit (including: topo II, DNA gyrase, topo VI, kinases (Hosoi et al, 2004; Lopez-Lopez et al, 1994), malarial surface receptors (Fleck et al, 2003) and P2 receptors (Abbracchio et al, 2006)) it is difficult to say anything of its target *in vivo*. Although it may target topo VI in *P. falciparum*, it almost certainly has multiple targets.

Quinacrine is a well-established anti-malarial drug (Chauhan & Srivastava, 2001) but its mode of action remains elusive. It is a member of the acridine class of compounds which includes two other hits: 9-aminoacridine and amsacrine. Derivatives of amsacrine have been shown to have potency against *Plasmodium falciparum* (Figgitt et al, 1992). Quinacrine has been shown to target the erythrocyte stage of the *Plasmodium* life cycle, during which the parasite undergoes schizogony (a process similar to endoreduplication). This makes it very tempting to imagine that topo VI as its target. Interestingly none of the other anti-malarial compounds tested had any effect on the activity of *M. mazei* topo VI. This was particularly interesting in the cases where the compound was an almost direct analogue of quinacrine but with a different scaffold such as chloroquine, MT-IC52 or MT1074 (Figure 5.43). All of these compounds have been shown to have anti-malarial activity despite having no activity against topo VI, strongly suggesting they have some other target. This demonstrates the necessity of the acridine scaffold for the inhibition of topo VI by quinacrine, which may be useful for further design of inhibitors against the enzyme.

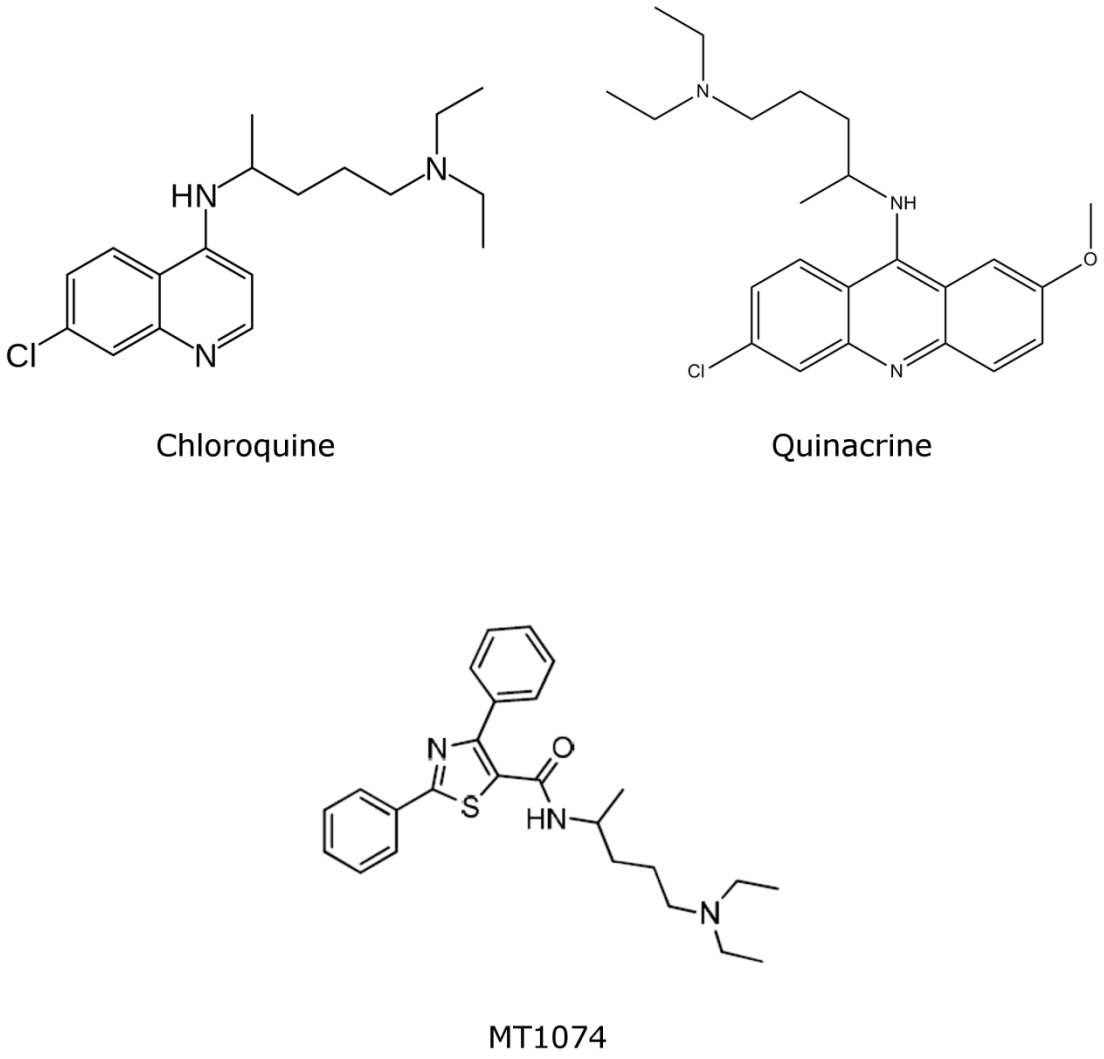

Figure 5.43 Comparison of various anti-malarial compounds with different scaffolds.

It would be interesting to test some of the other hits from the screen against the parasite *in vitro*. However, making any strong conclusions about the *Plasmodium* enzyme is impossible without having it expressed in a soluble form. This would be a step forward to validating topo VI as a target in *Plasmodium* and possibly the development of a whole new range of anti-malarial compounds.

Chapter 6

General Discussion

6.1 Introduction

DNA topoisomerases are important targets for antimicrobial drugs. With the emergence of strains of various pathogens resistant to many clinical antibiotics there is a dire need to discover compounds which inhibit topoisomerases in novel ways. However, high-throughput screening for these compounds has been limited by the traditional assays for topoisomerase activity. The initial aims of this project were to validate the use of a novel, microtitre plate-based assay for topoisomerase inhibitors (Maxwell et al, 2006) in a high-throughput format and use it for the discovery of novel DNA gyrase and topoisomerase VI inhibitors. In chapters 4 and 5 it was shown that it is possible to screen for novel inhibitors of *E. coli* DNA gyrase and *M. mazei* topo VI with the microtitre plate-based assay. Several novel inhibitors were found for each enzyme and their modes of action characterised. In chapter 5 the inhibitors of *M. mazei* topo VI were tested against the *Arabidopsis thaliana* orthologue of the enzyme *in planta*, and one compound was discovered which produced a similar morphology to previously documented topo VI knock-out mutants (Hartung et al, 2002; Sugimoto-Shirasu et al, 2002).

In addition it was observed that *M. mazei* topo VI produced an unusual banding pattern at high concentrations. AFM experiments have revealed that this is likely due to protein remaining bound to the DNA even after the proteinase digestion and phenol extraction. This and other observations may provide an interesting insight into the mechanism of this enzyme.

Finally, the cloning and expression of the hypothetical topo VI from *P. falciparum* was attempted in order to investigate it as a drug target.

Unfortunately were unable to obtain soluble protein, so the question remains open.

6.2 Characteristics of *M. mazei* topo VI

This work has confirmed many of the already published biochemical characteristics of *M. mazei* topo VI (Corbett et al, 2007). It was also shown that although radicicol is less potent against the *M. mazei* enzyme than the *S. shibatae* orthologue, its mode of action remains the same for both topo VI enzymes (inhibition of ATPase activity).

In addition it was observed that the *M. mazei* enzyme appears to bind very tightly to DNA in an ATP-dependent manner, possibly resulting in the formation of unusual topoisomers. This has not been observed for the *S. shibatae* topo VI, but the thermophilic nature of the enzyme makes it difficult to compare the two. The subunits of the enzyme appear tightly associated, proving impossible to separate with high salt or ethylene glycol buffers in column chromatography. Furthermore the enzyme appeared highly resistant to agents which stabilized the cleavage complex such as ADPNP. Imaging of *M. mazei* topo VI-processed DNA molecules by AFM revealed that enzyme molecules seemed to remain associate with the DNA despite SDS-proteinase K digestion and phenol-chloroform extraction. It is possible this indicates that the topo VI-DNA cleavage complex is incredibly robust, remaining associated despite these harsh conditions, and that topo VI is intrinsically resistant to proteinase K digestion. This makes sense in light of the supposed role for the C-terminal gate in type IIA topoisomerases in holding the enzyme-DNA complex associated during DNA gate opening (Bates et al, 2011) and its absence in topo VI. Further AFM experiments and characterisation of the enzyme's susceptibility to proteinase digestion are necessary to confirm this hypothesis.

6.3 The suitability of the microtitre plate-based assay for screening

One of the main aims of this project was the adaption of the microtitre plate-based assay for topoisomerase activity to a high-throughput format and to evaluate its viability by screening a relatively small library of compounds. In chapters 3 and 4 two successful screens of a 960 compound library against *E. coli* DNA gyrase and *M. mazei* topo VI were described. The assay was able to identify both known and novel inhibitors during these screens (Table 6.1). The overall hit rate for the *E. coli* DNA gyrase screen was significantly higher than for the *M. mazei* topo VI screen (~1.5% compared to ~0.6%). Conversely, the novel hit rate was higher for the *M. mazei* screen (~0.5% compared to ~0.2%). These differences are likely due to the fact that DNA gyrase is a well established antimicrobial target and the library was primarily composed of clinical drugs.

Because DNA gyrase has such a large number of well known and clinically used inhibitors it was possible to scan the list of compounds in the library for known inhibitors which were missed by the screen. Four such compounds were found: nalidixic acid, cinoxacin, oxolinic acid and enoxacin. Nalidixic acid, cinoxacin and oxolinic acid are among the oldest members of the quinolone class of drugs, with comparably high IC_{50}s to the fluoroquinolones which may go some way in explaining why they were missed. Enoxacin, however, is a more recently developed fluoroquinolone which should have activity comparable to the other fluoroquinolones identified by the screen. It may be the case that these compounds have become degraded during storage, but it is more likely they were missed due to well-to-well or plate-to-plate variations within the assay. Although there were relatively few such compounds, it was concerning that the assay did not pick out all known inhibitors. This may have been due to compounds

Screen against:	Z'	False positives	Known false negatives	Hits	Novel hits	Novel hit rate (%)
Gyrase	0.64	9	4	13	2	0.21
Topo VI	0.69	3	1	6	5	0.52

Table 6.1 Statistical summary of the two screens.

becoming degraded or contaminated during storage, a possibility which should be ruled out before firm conclusions on the assay's ability to pick out known inhibitors can be drawn. Since there are few known inhibitors described for topoisomerase VI a similar analysis of the *M. mazei* topo VI hit is less informative. Apart from m-amsacrine none of the other previously described inhibitors (Bergerat et al, 1994; Gadelle et al, 2005) were present in the library. Crosschecking the hits from the DNA gyrase and topo VI screens revealed that mitoxanthrone, a hit in the DNA gyrase screen, was also an inhibitor of *M. mazei* topo VI which had been missed in the topo VI screen. It was likely mitoxanthrone had been overlooked during the screen because of its ability to disrupt triplex formation, which results in a decrease of fluorescence signal. Since relaxation activity in the assay is also denoted by a decrease in signal the inhibition of topo VI by mitoxanthrone would be masked in the assay.

The number of false positives was acceptable for these screens but may become prohibitive for larger-scale operations. This can be addressed by increasing the hit threshold, or adopting different criteria for hit selection (such as taking a certain proportion of the most potent hits).

The Z' factor for both screens lay within the range associated with excellent separation of positive and negative signals, although there was variation of this from plate-to-plate. It has been shown that the Z' is only a good indicator of an assay's power to separate positive and negative results if the standard deviation of samples does not vary too much with signal (i.e. higher signal resulting in higher variation) (Sui & Wu, 2007). To test if this was the case for the microtitre plate-based assay the average signals for the positive and negative controls from the two screens were plotted against their standard deviation (calculated from 192 reactions) (Figure 6.1). Fortunately the results showed that there was only a small increase in standard deviation as signal increased, meaning the Z' values were likely good representations of the separation power of the assay (Sui & Wu, 2007). Interestingly the relationship between signal and standard deviation does not appear to be linear, with the standard deviation plateauing at high signal levels.

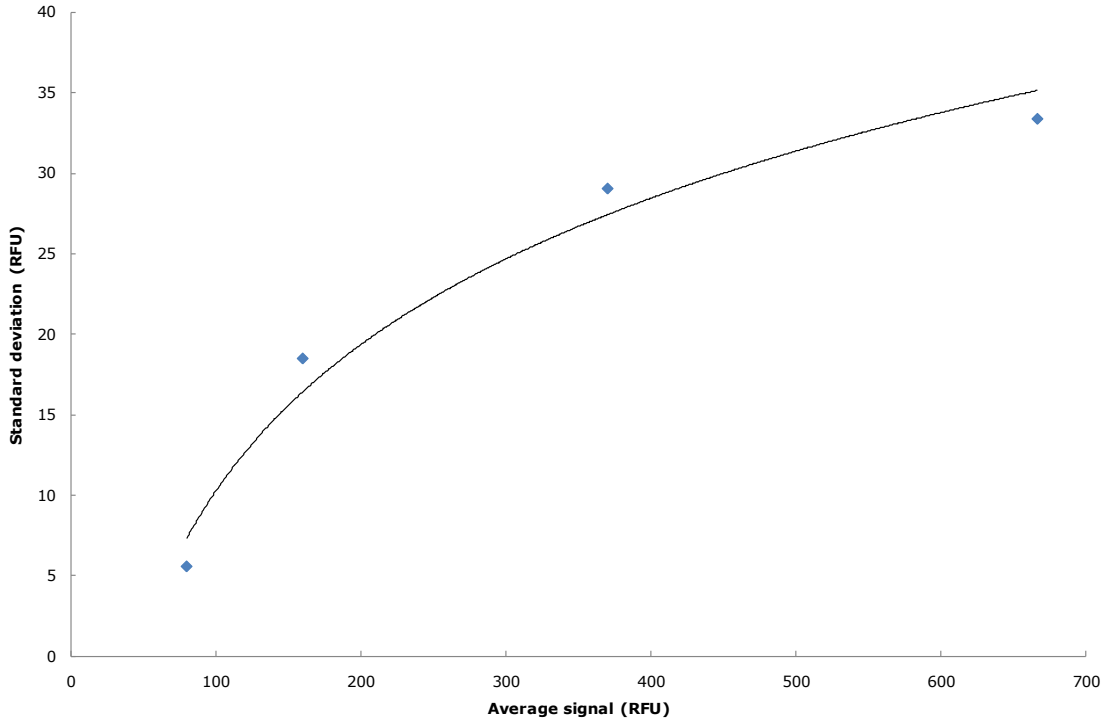

Figure 6.1 Variation of standard deviation with increasing fluorescence signal. The data was compiled from the controls of both screens, with each point calculated from the values for 192 repeats.

6.4 Perspectives on screen hits

A number of hits were discovered for each of the two enzymes. Since DNA gyrase is a type IIA topoisomerase and topo VI is a type IIB topoisomerase, cross-testing the hits may provide some insight into the differences in mechanism between these two families.

In chapter 5 the cross-testing of DNA gyrase hits against *M. mazei* and *S. shibatae* topo VI was described (Table 6.2). Interestingly only two compounds appear to be inhibitors of both *E. coli* DNA gyrase and *M. mazei* topo VI: mitoxanthrone and suramin. Both of these compounds have also been reported as inhibitors of eukaryotic topoisomerase II (topo II) (Bojanowski et al, 1992; Smith et al, 1990), a type IIA topoisomerase. It has been previously described that topo VI appears to be more susceptible to topo II inhibitors than it is to specific inhibitors of DNA gyrase (Bergerat et al, 1994). This is true for the majority of topo VI hits described in this work with m-amsacrine, quinacrine and 9-aminoacridine all being implicated in topo II inhibition (Finlay et al, 1989; Nelson et al, 1984). What is

Compound	*Inhibits?*			
	***E. coli* DNA gyrase**	***M. mazei* topo VI**	***S. shibatae* topo VI**	**Eukaryotic topo II**
Mitoxanthrone	✓	✓	✓	✓
Suramin	✓	✓	✗	✓
m-Amsacrine	✗	✓	✓	✓
Hexylresorcinol	✗	✓	✗	?
Quinacrine	✗	✓	✓	✓
9-Aminoacridine	✗	✓	✓	✓
Purpurin	✗	✓	✓	?

Table 6.2 Summary of type II topoisomerase inhibition by screen hits. A tick indicated inhibition at least 100 μM by the compound for *E. coli* DNA gyrase, *M. mazei* topo VI or *S. shibatae* topo VI. A tick for eukaryotic topo II indicates existing literature describing its inhibition by a compound. A question mark indicates no such literature was found.

interesting about mitoxanthrone and suramin is that they appear to inhibit DNA gyrase, topo II and topo VI (although suramin did not inhibit *S. shibatae* topo VI, but this may have been because the drug was not stable at the temperature the assay was conducted at). This prolific inhibition probably means they target fundamental aspects of type II topoisomerase reaction.

In the case of suramin this appears to relate to the binding of the enzymes to DNA, possibly by acting as a DNA mimic. For mitoxanthrone this is likely intercalation at the double-strand break in the G-segment DNA, since it is able to stabilize the cleavage complex of both DNA gyrase (Section 4.2.6) and eukaryotic topo II (Smith et al, 1990). It was therefore surprising that DNA cleavage was not detectable with either *M. mazei* or *S. shibatae* topo VI. In the case of *M. mazei* topo VI this may be explained by the difficulty in revealing the cleavage complex with the enzyme, but this does not hold true for the *S. shibatae* enzyme for which cleavage with ADPNP was observed. It may be that mitoxanthrone's apparent inhibition of topo VI arises from its general ability to intercalate with DNA. To rule out the second possibility tests like those described for quinacrine and 9-

aminoacridine in section 5.2.4 should be conducted before firm conclusions are drawn.

For the majority of the *M. mazei* topo VI inhibitors, except for suramin and purpurin which both appeared to prevent G-segment binding, it was not possible to conclusively determine mechanisms of action. They did not appear to inhibit the ATPase activity of the enzyme, prevent G-segment binding or stabilize the cleavage complex with *M. mazei* topo VI. Out of those which inhibited *S. shibatae* topo VI none appeared to stabilize the cleavage complex. However mitoxanthrone, quinacrine and 9-aminoacridine all appeared to prevent ADPNP-induced cleavage of DNA by the enzyme. This was interesting since both quinacrine and 9-aminoacridine have been reported to prevent the cleavage of DNA by eukaryotic topo II (Thielmann et al, 1991). It could be that the mechanism of action for these compounds against topo VI is their ability to prevent the formation of the cleavage complex. However, this would need to be confirmed by further experiments as suggested in Section 5.3.6.

Very few of the hits are of immediate pharmaceutical or commercial interest. The cytotoxicity of mitoxanthrone and suramin make them poor candidates for antimicrobials, although derivatives of the compounds may have more favourable characteristics. The compounds containing the anthraquinone scaffold of mitoxanthrone have already been shown to inhibit DNA gyrase meaning this is not a novel class of inhibitors for the enzyme, although by no means a highly exploited one (Burckhardt et al, 1998). In contrast the inhibition of topo VI by the anthraquinones, such as mitoxanthrone and purpurin, has not been previously reported.

The antimalarial potential of the topo VI inhibitors proved impossible to determine since it was not possible to express soluble *P. falciparum* topo VI. Further expression trials with the enzyme, possibly with the two subunits expressed in a single vector or with different *Plasmodium* orthologues, may lead to success. Testing of the compounds against *Plasmodium* parasites in cell cultures, and study of any morphologies induced may provide circumstantial evidence for the presence of a topo VI in *Plasmodium* and its role as a drug target. However a large number of the

hits from the *M. mazei* topo VI screen have belonged to classes of drugs known to have antimalarial activity. These include the aminoacridines (such as m-amsacrine, quinacrine and 9-aminoacridine) (Chavalitshewinkoon et al, 1993) and the anthraquinones (Sittie et al, 1999; Winter et al, 1995). It therefore remains possible that these compounds are targeted against *Plasmodium* topo VI *in vivo*.

One *M. mazei* topo VI screen hit displayed herbicidal properties against *Arabidopsis thaliana*: hexylresorcinol. For hexylresorcinol to be developed into an agriculturally useful herbicide its mode of action has to be precisely determined in order to design resistance genes for crops. This can be approached from either of two directions. The first possibility is to select for plants displaying resistance to hexylresorcinol and sequence across the *topo6* genes. The mutant versions of *Arbadopsis* topo VI can then be expressed and their resistance to hexylresorcinol confirmed in vitro. The opposite approach is to generate crystal structures of the drug bound to topo VI (preferably the *Arbadopsis* orthologue) and use these to design mutants resistant to the drug. These mutations can then be introduced into plants and their resistance to the drug assessed *in planta*. Both of these routes would lead to confirmation of topo VI as the drug's target *in planta* and allow for the design of resistant crops. The cost, environmental impact and spectrum of plants killed by hexylresorcinol would also need to be assessed before it could be brought to market.

6.5 Concluding remarks

In conclusion we feel that this project has fulfilled its initial aims of validating a screening process for novel topoisomerase inhibitors. Although none of the compounds which arose from the screening process appear to be of immediate pharmaceutical importance they have raised interesting questions about the relationships between the inhibitors of type IIA and type IIB topoisomerases, as well as probing the mechanism of topo VI. Larger-scale screens using this assay with more diverse libraries will hopefully lead to the discovery of compounds which lead to novel antimicrobials (in fact, one such screen is currently underway).

More generally we feel that this project highlights the difficulties of antimicrobial screening: although hits against DNA gyrase were found they are useless as antimicrobials due to their other unfavourable characteristics. On a more positive note, the work here on topoisomerase VI demonstrates the value of basic research. Initially topoisomerase VI appeared to be an "archaeal curiosity" only of academic interest. However, its potential presence in pathogenic protozoa means it may suddenly become very medically relevant. We very much hope this turns out to be so, and that topo VI becomes another weapon in our arsenal in the "war against pestilence".

Appendix

7.1 High-Throughput Microtitre Plate-Based Assay for DNA Topoisomerases

Functional Genomics: Methods and Protocols (Kaufmann, M. & Klinger, C., eds.), In press. Humana Press, New York.

James A. Taylor, Nicolas P. Burton and Anthony Maxwell

Abstract

We have developed a rapid, high-throughput assay for measuring the catalytic activity (DNA supercoiling or relaxation) of DNA topoisomerases. The assay utilizes intermolecular triplex formation between an immobilized Triplex-Forming Oligo (TFO) and a triplex-forming region inserted into the plasmid substrate (pNO1), and capitalizes on the observation that supercoiled DNA forms triplexes more readily than relaxed DNA. Thus supercoiled DNA is preferentially retained by the TFO under triplex-forming conditions, whilst relaxed DNA can be washed away. Due to its high speed of sample analysis and reduced sample handling over conventional gel-based techniques, this assay can be used to screen chemical libraries for novel inhibitors of topoisomerases.

Keywords: Topoisomerase, DNA gyrase, triplex formation, supercoiling, relaxation, high-throughput screening

1. Introduction

DNA topoisomerases are essential enzymes that control the topological state of DNA in all living cells (Bates and Maxwell 2005). The crucial nature of their role, plus the fact that they must cleave DNA as part of their mechanism, has made them effective targets for antimicrobial and anti-cancer drugs as well as potential targets for herbicides, anti-virals and anti-protozoal agents. All topoisomerases can relax supercoiled DNA, whilst only DNA gyrase is capable of introducing negative supercoils (Nollmann, Crisona et al. 2007). Topoisomerases can also catenate/decatenate DNA and introduce/remove knots from DNA, to greater or lesser degrees (Schoeffler and Berger 2008).

The traditional assay for topoisomerase activity is based on the principle that different DNA topoisomers have different mobilities on an agarose gel. This assay is information-rich, but is also slow and requires intensive handling. As such it is not suitable for the high-throughput format necessary for large scale screening for novel inhibitors. To address the limitations of this assay, a microtitre plate-based assay was developed (Maxwell, Burton et al. 2006) (*see* **Note 1**), which capitalizes on the fact that supercoiled plasmids form DNA triplexes more readily than relaxed plasmids (Hanvey, Shimizu et al. 1988; Sakamoto, Akasaka et al. 1996). Reactions are carried out in streptavidin-coated microtitre wells, which have had a single-stranded biotinylated oligo immobilized on their surfaces. This oligo can form triplexes with a target plasmid by the addition of a low pH triplex formation buffer, which also stops the topoisomerase reaction. Supercoiled DNA will be retained in the wells after washing, whereas

relaxed, open circle and linear DNA will be removed. The amount of DNA retained can be quantified with a fluorescent dye, and directly correlates with the level of enzyme activity (**Fig. 1A**).

2. Materials

The highest purity of materials and ultrapure water with a resistivity of ~18 MΩ.cm should be used throughout. Unless otherwise stated, materials were purchased from Sigma. The Wash, Triplex Formation (TF) and T10E1 buffers should be filtered with a 0.2 μM cellulose nitrate membrane before use (*see* **Note 2**).

7.1.1 2.1 Buffers and Solutions

1. DNA Gyrase Dilution buffer: 50 mM Tris·HCl (pH 7.5), 100 mM KCl, 2 mM DTT, 1 mM EDTA, 10% (w/v) glycerol. Store at -20°C.
2. DNA Gyrase Supercoiling buffer: 35 mM Tris·HCl (pH 7.5), 24 mM KCl, 4 mM $MgCl_2$, 2 mM DTT, 1.8 mM spermidine, 1 mM ATP, 6.5% (w/v) glycerol, 0.1 mg/mL bovine serum albumin. The buffer is stored as a 5× concentrate at -20°C.
3. PDM media: 7.9 g tryptone, 4.4. g yeast extract, 0.5 g NH_4Cl and 0.24 g $MgSO_4$ in 880 mL of water. After autoclaving add 20 mL 50% w/v glucose and 100 mL 10x Phosphate buffer (*see* **Note 3**).
4. Phosphate Buffer (10x): 128 g $Na_2HPO_4.7H_2O$, 30 g KH_2PO_4 in 1 L of water. Autoclave and store at room temperature.

5. STEB (x2): 40% sucrose, 100 mM Tris·HCl (pH 8.0), 100 mM EDTA, 0.5 mg/mL bromophenol blue.
6. T10E1 buffer: 10 mM Tris·HCl (pH 8.0), 1 mM EDTA. Store at room temperature.
7. TAE: 40 mM Tris·Acetate (pH 8.0), 1 mM EDTA.
8. Topoisomerase I Dilution buffer: 10 mM Tris·HCl (pH 7.5), 1 mM DTT, 1 mM EDTA, 50 % (v/v) glycerol, 100 μg/mL bovine serum albumin.
9. Topoisomerase I Relaxation buffer: 20 mM Tris·HCl (pH 8), 200 mM NaCl, 0.25 mM EDTA, 5% glycerol. The buffer is stored as a 10× concentrate at -20°C.
10. Topoisomerase VI Dilution buffer: 20 mM HEPES pH 7.5, 10% (v/v) glycerol. Store at -20°C.
11. Topoisomerase VI Relaxation buffer: 20 mM bis-tris propane pH 6.5, 100 mM potassium glutamate, 10 mM MgCl2, 1 mM DTT, and 1 mM ATP. The buffer is stored as a 5× concentrate at -20°C.
12. Triplex Column buffer: 75 mM calcium acetate (pH 4.7). Store at room temperature.
13. Triplex Column Elution buffer: 10 mM Tris·HCl (pH 8.0), 100 mM EGTA. Store at room temperature.
14. Triplex Formation (TF) buffer: 75 mM magnesium acetate (pH 4.7). Store at room temperature (*see* **Note 4**).
15. Wash Buffer: 20 mM Tris·HCl (pH 7.6), 137 mM NaCl, 0.01% (w/v) bovine serum albumin (acetylated), 0.05% (v/v) Tween-20. Store at 4°C.

2.2. DNA

1. Plasmid pNO1 is a modified version of the high-copy number plasmid pBR322* (Boros, Pósfai et al. 1984) containing a triplex-forming insert (Maxwell, Burton et al. 2006). It was prepared by ligation of oligos TFO1W and TFO1C (Table 1) into the AvaI site of the plasmid. Supercoiled pNO1 is prepared by transforming it into competent *Escherichia coli* cells (e.g. Top10, Invitrogen), growing cells overnight in PDM media (Danquaha 2007) (*see* **Note 3**) containing 100 μg/ml ampicillin (*see* **Note 5**) at 37^{o}C, 200 rpm. The DNA can then be purified using a Qiagen giga-prep kit (or similar) or by a cesium chloride density gradient.
2. Relaxed pNO1 is prepared by incubating the supercoiled form with chicken erythrocyte topoisomerase I (~40-50 μg plasmid with 200 units topoisomerase I in 1x Topoisomerase I Relaxation buffer) for 1 h at 37°C. The DNA is extracted with two phenol/chloroform extractions and purified by ethanol precipitation.
3. TFO1 oligo (Table 1) with a 5' biotin tag (e.g. Sigma-Genosys or Bioneer) is resuspended to 10 μM in T10E1 buffer and stored at -20°C.

2.3 Enzymes

1. *E. coli* DNA gyrase subunits GyrA and GyrB are expressed in *E. coli* and purified according to established protocols (Maxwell and Howells 1999). The subunits are stored separately in DNA Gyrase Dilution Buffer at -80^{o}C (*see* **Note 6**). The complete enzyme is reconstituted by mixing equimolar amounts of GyrA and GyrB and stored on ice prior to use.
2. Chicken erythrocyte topoisomerase I used was a gift from Alison Howells of Inspiralis Ltd, and was produced using the published protocol (Tricoli and Kowalski 1983).

2.4 Equipment and DNA Staining

1. Black, streptavidin-coated, high binding capacity, 96-well plates (Pierce) are used for the screen. Plates should be stored, covered, at 4°C.
2. DNA is stained with SYBR Gold (Invitrogen), which is stored as a 10,000x concentrate at 20°C. The dye is diluted 10,000 fold with T10E1 buffer to reach the working concentration. This should be prepared fresh each use.
3. Fluorescence measurements are made using a SPECTRAmax Gemini fluorimeter and Softmas Pro Software. Alternative fluorimeters and software can be used.

3. Methods

3.1. DNA Gyrase Microtitre Plate-Based Supercoiling Assay

1. Wash microtitre plate wells with 3x 200 µL of Wash Buffer (*see* **Note 7**).
2. Load 100 µL 500 nM biotinylated TFO1 oligo (diluted from stock in Wash Buffer) into wells and allow immobilization to proceed for 2 min.
3. Remove oligo solution and wash carefully with 3x 200 µL volumes of Wash buffer (*see* **Note 7**).
4. The DNA gyrase supercoiling reaction is performed in the wells in a 30 µL reaction volume containing: 1-6 µL reconstituted DNA gyrase (1-2 units (*see* **Note 8**); the total volume of DNA gyrase is made up to 6 µL with DNA Gyrase Dilution buffer), 1 µL of 1 µg/µL relaxed pNO1, 6 µL 5x DNA Gyrase Reaction buffer and H_2O to 30 µL (*see* **Note 9**). Incubate the reaction at 37°C for 30 min (this can be carried out in the plate reader if temperature control is available).
5. The reaction is stopped with the addition of 100 µL TF buffer, which lowers the pH, and the plate is incubated at room temperature for 30 min to allow triplex formation

to occur. Supercoiled DNA becomes immobilized on the plate while relaxed DNA remains in solution.

6. Remove unbound relaxed and linear plasmid by washing the wells thoroughly with 3 x 200 µL volumes of TF buffer.
7. Remove all the liquid from the wells and stain DNA with 200 µL 1 x SYBR Gold (diluted in T10 buffer). The plate is incubated for a further 20 min at room temperature. After incubation, mix the contents of the wells and then read the fluorescence in a fluorimeter.

3.2. Screening a Compound Library for DNA Gyrase Inhibitors

1. Wash the plates and immobilize the TFO1 as described in section 3.1, steps 1 to 3 (*see* **Note 10**).
2. Add 23.5 µL of a DNA Mix (*see* **Note 11**) containing 4.7 µL of 5x DNA Gyrase Reaction buffer, 2 µL of 1 µg/µL relaxed pNO1 and H_2O to each well by multichannel pipette.
3. Add 3 µL of compound to each well (the assay is tolerant of up to 10% DMSO in the reaction). Include a positive control well to which only DMSO is added.
4. Add 35.5 µL of Control Mix containing 2 µL DMSO, 12 µL DNA Gyrase Dilution Buffer, 7.1 µL 5 x DNA Gyrase Supercoiling Buffer and 14.4 µL H_2O to the negative control wells.
5. Add 33.5 µL Enzyme Mix containing 1.8 units (where 1 unit is defined as the amount of enzyme required to supercoil 1 µg of relaxed pBR322) of DNA Gyrase in 12 µL DNA Gyrase Dilution buffer, 6.7 µL 5x DNA Gyrase Supercoiling Buffer and 14.8 µL H_2O to the sample and the positive control wells.
6. Quickly mix (e.g. using the plate reader if it has such a facility), and incubate at 37°C for 30 min.

7. Follow steps 5 to 7 of section 3.1 to form DNA triplexes and visualize retained plasmid.

3.3. Data Processing and Hit Validation of Hits using Agarose Gel Assay

Once data has been collected from the screen (*Figure 1B*) the fluorescence signals for the duplicates should be averaged and converted into percentage inhibition using the positive and negative controls (*see* **Note 10**). The standard deviation of the controls should also be calculated and converted into percentage inhibition. By adding the percentage standard deviations of the controls together and multiplying them by three you can obtain the 95% confidence interval for the screen, which acts as an indicator of significance (the majority of hits which give a percentage inhibition over this number are likely to be genuine, and not within variance of the background). It is also possible to calculate the Z factor for the assay (Zhang, Chung et al. 1999) to determine the quality of the data (in our hands Z = ~0.75 for *E. coli* DNA gyrase). Hits obtained from the screen should be verified using an independent secondary assay, for example agarose gel electrophoresis. It is advisable to use fresh stocks of compounds for verification, rather than solutions taken from the library to ensure that the inhibition seen is not due to any cross-contamination or degradation which may have occurred during library storage.

1. The supercoiling reaction is conducted in 1.5 mL microcentrifuge tubes containing the following: 500 ng of relaxed pNO1, 6 µL 5x DNA Gyrase Supercoiling Buffer, 0.5 U of reconstituted DNA gyrase in 6 µL

Dilution Buffer, up to 1.5 µL of compound in 100% DMSO at the desired concentration and H_2O to 30 µL.

2. Incubate at 37°C for 30 min.
3. Stop the reaction with an equal volume chloroform:isoamyl alcohol (24:1), and an equal volume of 2x STEB, vortex vigorously to form an emulsion. Centrifuge at 16,000g for 10 min.
4. Load 15 µL of the top phase onto a 1% TAE agarose gel. Run the gel at 80 V for 2-3 hrs or until the gel has run for at least 7 cm, or 15-30 V overnight. The further that the gel is run, the better the topoisomers will be resolved.
5. Stain gel with 2 mg/mL ethidium bromide 10 min and visualize under UV.

3.4. Measuring Relaxation Activity with the Microtitre Plate-Based Assay

The plate assay can also be used to measure the activity of enzymes which relax DNA, and consequently used to screen to novel inhibitors for them. Below is a sample protocol for using the assay to measure *Methanosarcina mazei* topoisomerase VI, but it is easily adapted for other enzymes (such as human topoisomerase I and II, and bacterial topoisomerase IV). Likewise the screen protocol described for gyrase above can be modified to screen against such enzymes.

1. Wash the plates and immobilize the TFO1 as described in section 3.1., steps 1 to 3.
2. The topoisomerase VI relaxation reaction is performed in the wells in a 30 µL reaction volume containing: 1-6 µL reconstituted topoisomerase VI (1-2 units

(*see* **Note 8**); the total volume of topoisomerase VI is made up to 6 µL with Topoisomerase VI Dilution buffer), 1 µL of 1 µg/ µL supercoiled pNO1, 6 µL 5x Topoisomerase VI Reaction buffer and H_2O to 30 µL (*see* **Note 9**). Incubate the reaction at 37 °C for 30 min (this can be carried out in the plate reader if temperature control is available).

3. Follow steps 5 to 7 of section 3.1 to form DNA triplexes and visualise retained plasmid. Enzyme activity is denoted by a drop in signal as supercoiled substrate is converted to relaxed product and lost from the wells during subsequent wash steps.

3.5. Purification of Supercoiled Plasmid via Triplex Affinity Columns and Other Applications for the High-Throughput Assay

As well as its utility in high-throughput screening, the assay and the principles behind it have potential to be exploited in a range of other settings. Previously it has been used for the rapid determination of inhibitor IC_{50}s (Anderle, Stieger et al. 2008), which is useful for the characterisation of hits determined during screening. It is also possible to use the assay for measuring the activity (and inhibition) of any enzyme which alters the linking number of the plasmid substrate (such as restriction enzymes). In addition, the protocol above could be altered to screen for compounds which either promote or inhibit the formation of DNA triplexes, simply by omitting the enzyme. The compounds should be included in the TF buffer wash steps (section 3.1, step 6), as well as in the TF buffer for the triplex formation step. Finally the capture of supercoiled DNA plasmids by triplex-forming oligos has been utilized to create an affinity column for the specific purification of supercoiled plasmid (Schluep and Cooney 1999).

1. Add 1 mL of 4% agarose streptavidin coated beads to an empty gravity flow column (*see* **Note 12**).
2. Wash three times with 1 mL T10 Buffer.
3. Stop the flow and add 1 mL of 100 μM TFO1 in T10 buffer. Incubate at room temperature for 1 min.
4. Wash three times with 1 mL T10 Buffer.
5. Equilibrate the column by washing three times with 1 ml Triplex Column buffer.
6. Add 1 mg of DNA in 1 ml Triplex Column buffer. Retain the flow through for subsequent steps.
7. Elute bound DNA with 2 mls Triplex Column Elution buffer.
8. Re-equilibrate the column by washing three times with 1 ml Triplex Column buffer.
9. Re-circulate the flow through from step 6.
10. Repeat steps 6 to 9 until all plasmid is recovered.
11. Combine eluents and concentrate through ethanol precipitation.

4. Notes

1. The triplex assay described is protected by patent application WO06/051303. Commercial performance of the assay requires a license, available from Plant Bioscience Ltd. (Norwich, UK; http://www.pbltechnology.com/). The assay is available as a kit from Inspiralis Ltd. (Norwich, UK; http://www.inspiralis.com/) who also supply pNO1 and a range of topoisomerase enzymes including several bacterial DNA gyrases and topoisomerase IVs, and human topoisomerases I and II.

2. The presence of suspended particles will result in light scattering, which will reduce the quality of data and may introduce variation. It is also recommended that the microtitre plates are protected with a cover where possible to prevent airborne particles entering the wells.
3. Alternatively Luria-Bertani (LB) or Terrific Broth (TB) can be used, although lower yields and increased amounts of nicked plasmid may be observed.
4. The assay was originally developed using a TF buffer of 50 mM sodium acetate pH 5.0, 50 mM sodium chloride, 50 mM magnesium chloride. However, 75 mM magnesium acetate (pH 4.7) was found to give slightly improved results. Certain DNA binding compounds can promote or inhibit the formation of triplexes, resulting in them appearing either as false negatives or positives in the assay. Although the inclusion of proper controls and hit validation should minimize the impact of these compounds on the screen results, we have found that substituting magnesium with another divalent metal (e.g. calcium) can reduce the effect of intercalators upon triplex formation. However, no one metal ion has emerged as a panacea for the problem.
5. Alternatively, carbenicillin can be used, which is broken down more slowly than ampicillin, resulting in more sustained selective pressure which may increase plasmid yields.
6. Repeated freeze thaw cycles will reduce enzyme activity, so it is recommended that the subunits are aliquoted before freezing. The GyrB subunit can precipitate if stored at concentrations higher than 1 mg/mL.
7. It is essential to wash the wells thoroughly before and after TFO1 addition as unbound TFO1 can interfere with triplex formation. Buffer should be thoroughly

removed after the final wash to prevent it interfering with subsequent steps. Residual buffer can be removed by pipetting or aspiration.

8. It is highly advisable to calculate the concentration of DNA gyrase equivalent to one unit with the triplex assay prior to screening. One unit of supercoiling activity is defined as the amount of enzyme required to just fully supercoil 0.5 μg of relaxed pNO1 at 37°C in 30 min. The extent of supercoiling is determined by the inclusion of a control containing 1 μg supercoiled pNO1 without enzyme. Conversely, a unit of relaxation activity is defined as the amount of enzyme required to just relax 0.5 μg of supercoiled pNO1 at 37°C in 30 min. Units of enzyme activity are quantified by performing the reaction over a range of enzyme concentrations. For example, to quantify units of DNA gyrase supercoiling activity using the triplex assay, supercoiling would be assayed with DNA gyrase between 2 and 20 nM in triplicate, and the amount of enzyme corresponding to one unit can then be extrapolated from a linear regression of these data.
9. The assay can be carried out with less DNA (e.g. 0.75 μg) and correspondingly less enzyme. The enzyme should be added to the reaction mix last. It is possible to make a Master Mix of water, Gyrase Supercoiling buffer and relaxed pNO1, which is then aliquoted into the microtitre plate wells. The enzyme is then added to bring the volume to 30 μl and start the reaction.
10. A larger reaction volume (60 μl) is suggested here for performing the screen since although it uses more materials, it can give more consistent results. When designing the screen, the first and last column of each plate should be reserved for negative controls (substrate plasmid in identical buffer conditions to sample wells but lacking compounds and enzyme) and positive controls (substrate

plasmid in identical buffer conditions to sample wells including enzyme but without compounds). It is advisable to perform the screen in duplicate to ensure confidence in the results.

11. It is advisable to make both DNA and Enzyme Mixes as single stocks for the entire screen; these can be frozen at -20°C in appropriately-sized aliquots if necessary. However, the reconstituted DNA gyrase should only be added to the Enzyme Mix immediately before use, since repeated freeze/thaw cycles and storage at low concentrations can result in loss of activity. The amount of each mix required should be calculated on the number of wells required, plus ten percent to allow for reservoir dead volume.
12. Using the protocol provided, 1 mL of streptavidin coated agarose beads with the TFO1 oligo immobilized on them can capture ~0.2 mg of supercoiled plasmid. By re-circulating the flow-through after elution of the bound plasmid, more plasmid can be captured. We have found that five such rounds of elution/re-circulation result in a yield of ~60% with high purity. Higher yields may be obtainable with a matrix with a larger pore size (since it is theorised that plasmids are too large to gain access to the binding sites within the pores of 4% agarose), larger column volumes or with automated pumping.

References

Anderle, C., M. Stieger, M. Burrell, S. Reinelt, A. Maxwell, M. Page and L. Heide (2008). "Biological activities of novel gyrase inhibitors of the aminocoumarin class." Antimicrob. Agents Chemother. **52**(6): 1982-1990.

Bates, A. D. and A. Maxwell (2005). DNA Topology. Oxford, Oxford University Press.

Boros, I., G. Pósfai and P. Venetianer (1984). "High-copy-number derivatives of the plasmid cloning vector pBR322." Gene **30**: 257-260.

Danquaha, M. K. (2007). "Growth medium selection and its economic impact on plasmid DNA production." J. Biosci. Bioeng. **104**(6): 490-497.

Hanvey, J. C., M. Shimizu and R. D. Wells (1988). "Intramolecular DNA triplexes in supercoiled plasmids." Proc. Natl. Acad. Sci. USA **85**: 6292-6296.

Maxwell, A., N. P. Burton and N. O'Hagan (2006). "High-throughput assays for DNA gyrase and other topoisomerases." Nucleic Acids Res **34**(15): e104.

Maxwell, A. and A. J. Howells (1999). Overexpression and purification of bacterial DNA gyrase. DNA Topoisomerase Protocols I. DNA Topology and Enzymes. M.-A. Bjornsti and N. Osheroff. Totowa, New Jersey, Humana Press**:** 135-144.

Nollmann, M., N. J. Crisona and P. B. Arimondo (2007). "Thirty years of Escherichia coli DNA gyrase: from in vivo function to single-molecule mechanism." Biochimie **89**(4): 490-499.

Sakamoto, N., K. Akasaka, T. Yamamoto and H. Shimada (1996). "A triplex DNA structure of the polypyrimidine:polypurine stretch in the 5′ flanking region of the sea urchin arylsulfatase gene." Zoolog. Sci. **13**: 105-109.

Schluep, T. and C. L. Cooney (1999). "Immobilization of oligonucleotides on a large pore support for plasmid purification by triplex affinity interaction." Bioseparation **7**(6): 317-326.

Schoeffler, A. J. and J. M. Berger (2008). "DNA topoisomerases: harnessing and constraining energy to govern chromosome topology." Q. Rev. Biophys. **41**(1): 41-101.

Tricoli, J. V. and D. Kowalski (1983). "Topoisomerase I from chicken erythrocytes: purification, characterization, and detection by a deoxyribonucleic acid binding assay." Biochemistry **22**(8): 2025-2031.

Zhang, J. H., T. D. Chung and K. R. Oldenburg (1999). "A simple statistical parameter for use in evaluation and validation of high throughput screening assays." J Biomol Screen **4**(2): 67-73.

Figures and Tables

Name	Sequence (5'-3')	5' Modification
TFO1	TCTCTCTCTCTCTCTC	Biotin
TFO1W	TCGGAGAGAGAGAGAGAGAG	
TFO1C	CCGATCTCTCTCTCTCTCTC	

Table 1: Oligonucleotides used in the high-throughput assay

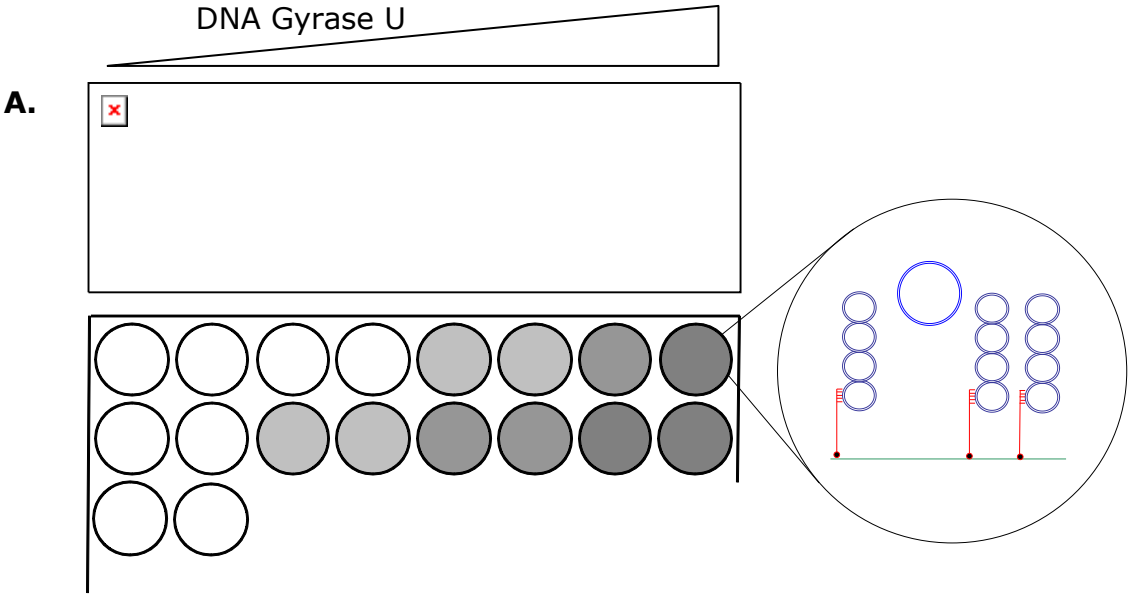

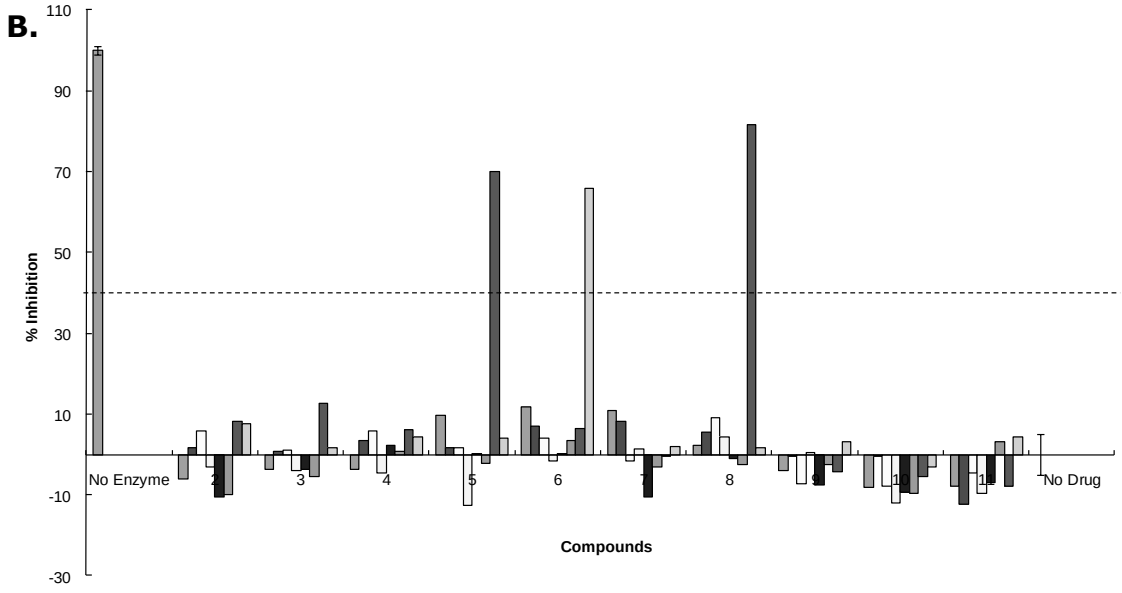

Fig. 1: **A**. Sample agarose gel assay for increasing units of DNA gyrase with a cartoon representation of its equivalence in the high-throughput assay. Conversion of relaxed to supercoiled DNA increases the amount of DNA retained in the well due to triplex formation and subsequently the intensity of the fluorescent signal after SBYR Gold staining. **B**. Sample data for a DNA gyrase inhibitor screen, performed in duplicate in a 96-well plate. Each bar represents the percentage inhibition of a single compound, calculated from the negative and positive controls for enzyme activity (of which there were sixteen repeats each). The dotted line denotes the hit threshold, as calculated from the standard deviation of the controls. Most of the compounds fall well below this threshold whilst three are clearly above it.

7.2 Screening data

Below are the plate-by-plate results of the *E. coli* DNA gyrase and *M. mazei* topo VI screens. Negative control (Neg. control) refers to wells with relaxed DNA and no enzyme whilst Positive control (Pos. control) refers to wells with DNA and enzyme but no test compound. The values for the controls represent the average of 16 repeats, with the error bars calculated from their standard deviation. The results for the samples are arranged by plate row and column, and represent the average of two repeats. Compounds of interest have been annotated. The dotted line indicates the hit threshold.

7.2.1 *E. coli* DNA gyrase screen

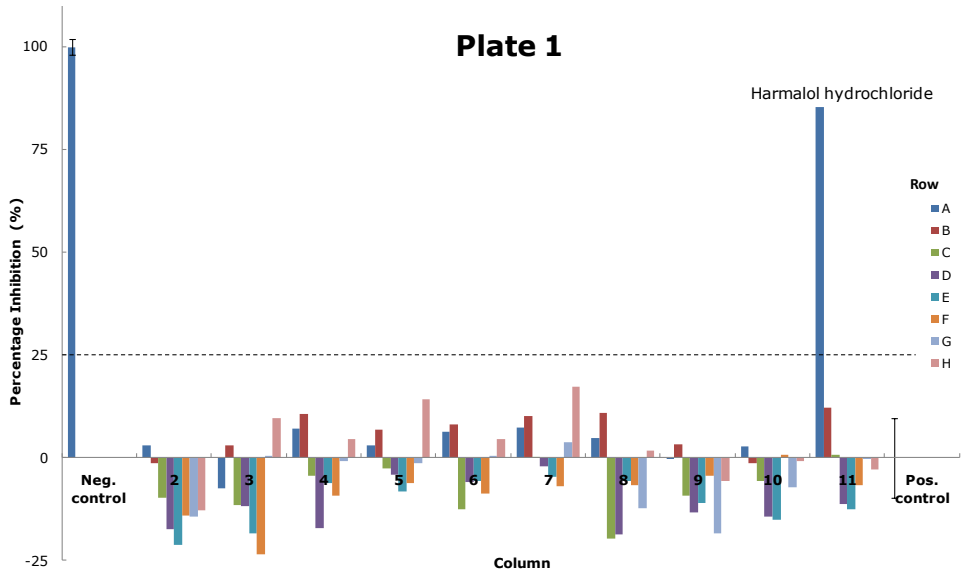

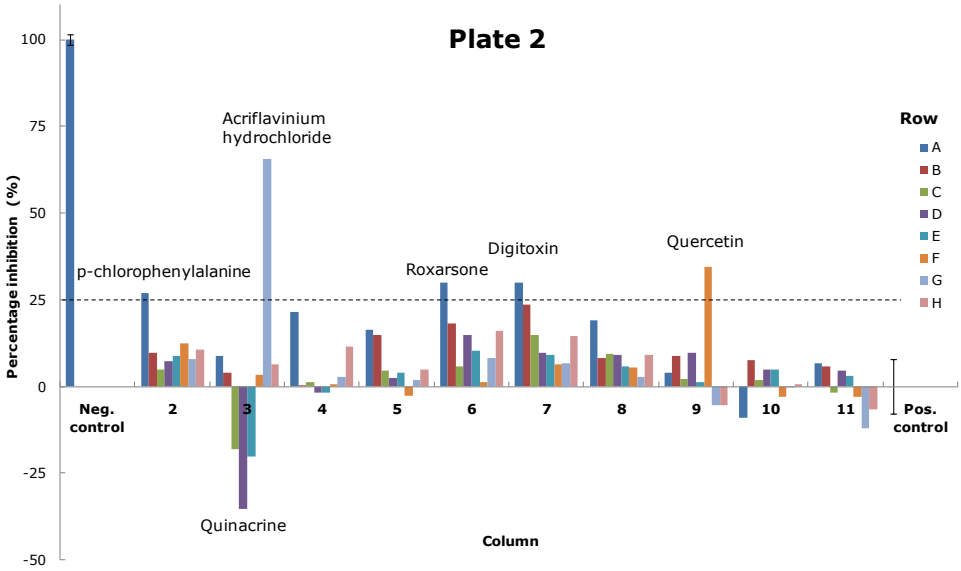
Plate 2
Percentage inhibition (%)
100
75
50
25
0
-25
-50
Acriflavinium hydrochloride
p-chlorophenylalanine
Roxarsone
Digitoxin
Quercetin
Quinacrine
Neg. control
2
3
4
5
6
7
8
9
10
11
Pos. control
Column
Row
A
B
C
D
E
F
G
H

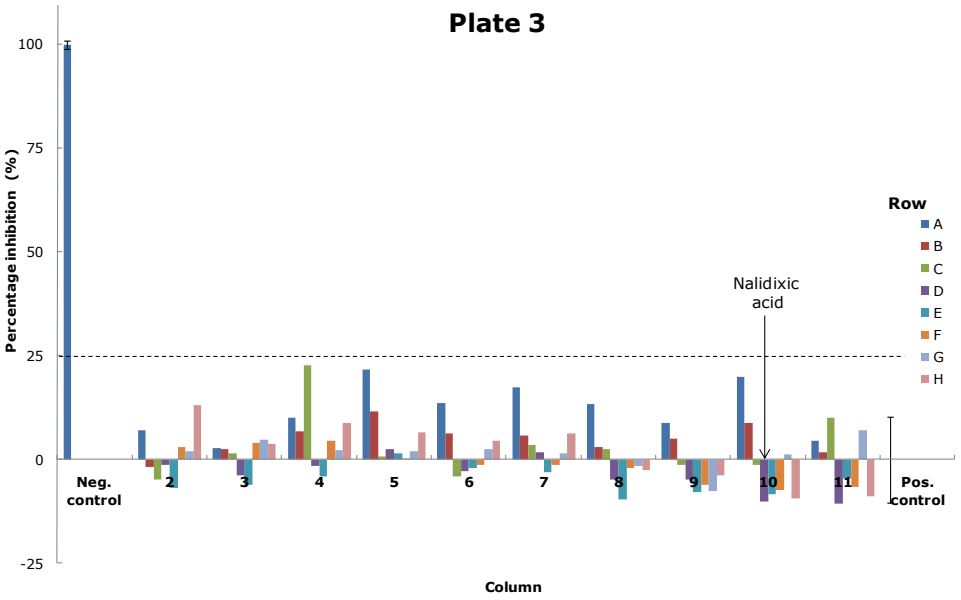
Plate 3
Percentage inhibition (%)
100
75
50
25
0
-25
Nalidixic acid
Neg. control
2
3
4
5
6
7
8
9
10
11
Pos. control
Column
Row
A
B
C
D
E
F
G
H

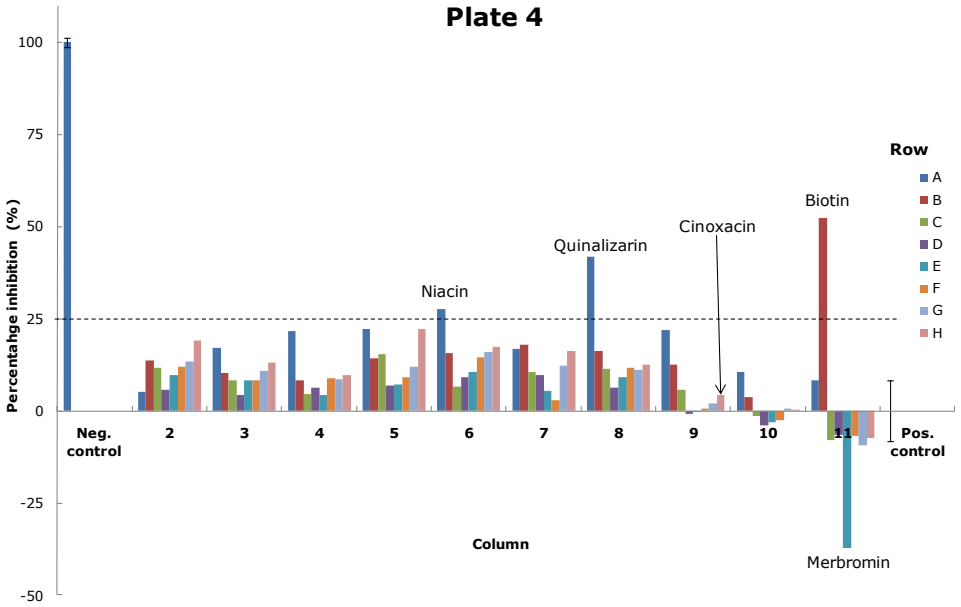
Plate 4
Percentahge inhibition (%)
100
75
50
25
0
-25
-50
Niacin
Quinalizarin
Cinoxacin
Biotin
Merbromin
Neg. control
2
3
4
5
6
7
8
9
10
11
Pos. control
Column
Row
A
B
C
D
E
F
G
H

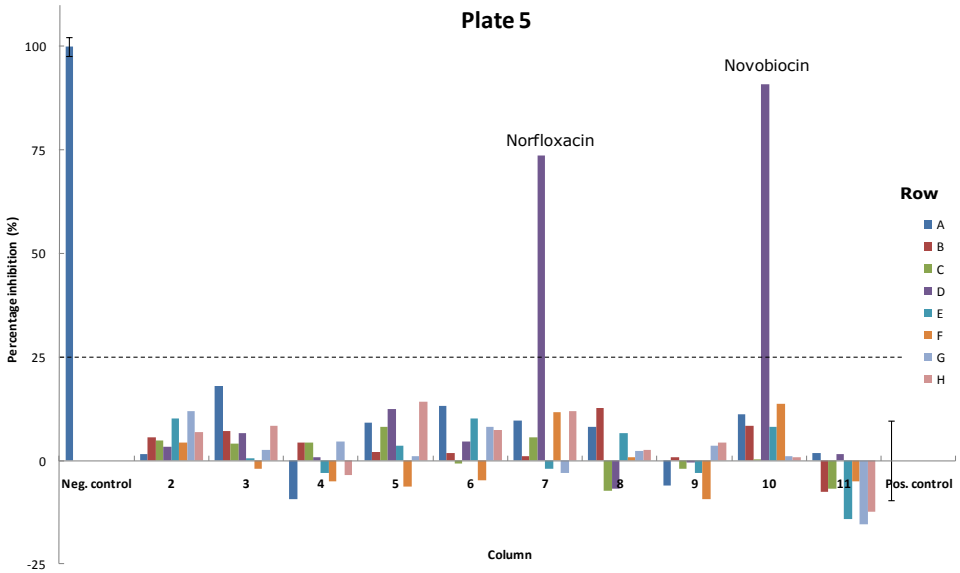
Plate 5
Novobiocin
Norfloxacin
Row
A
B
C
D
E
F
G
H
Percentage inhibition (%)
100
75
50
25
0
-25
Neg. control
2
3
4
5
6
7
8
9
10
11
Pos. control
Column

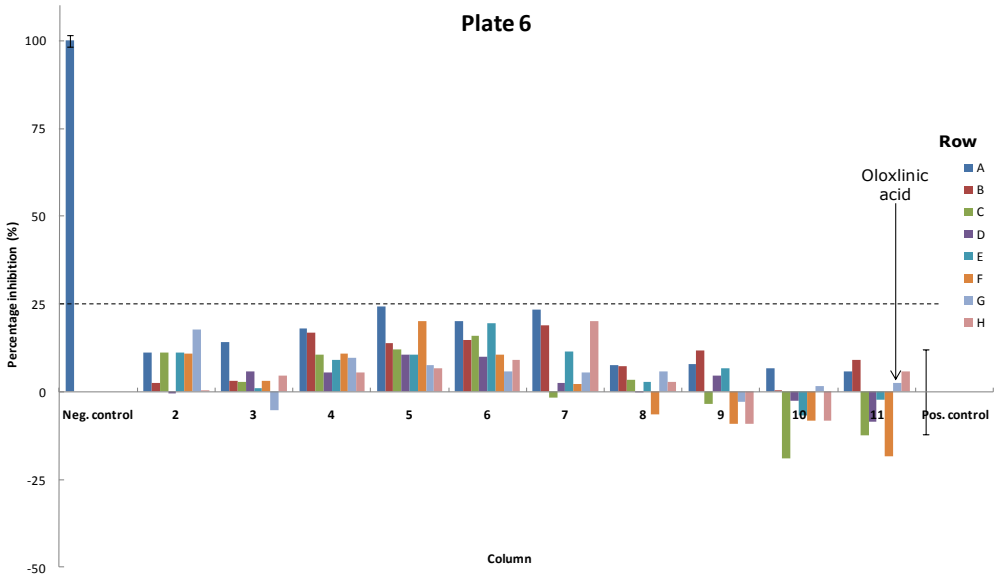
Plate 6
Oloxlinic acid
Row
A
B
C
D
E
F
G
H
Percentage inhibition (%)
100
75
50
25
0
-25
-50
Neg. control
2
3
4
5
6
7
8
9
10
11
Pos. control
Column

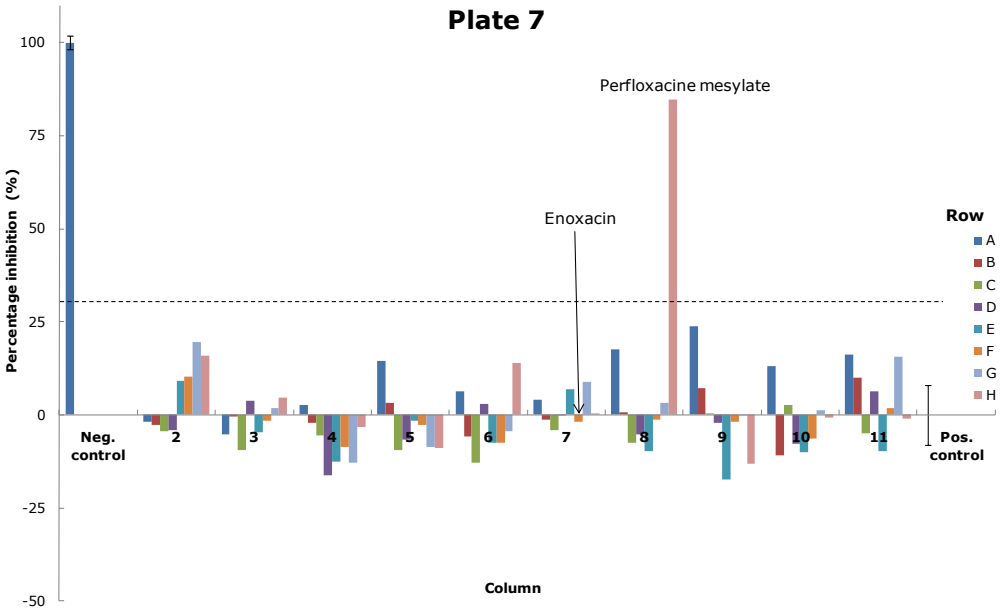
Plate 7
Perfloxacine mesylate
Enoxacin
Row
A
B
C
D
E
F
G
H
Percentage inhibition (%)
100
75
50
25
0
-25
-50
Neg. control
2
3
4
5
6
7
8
9
10
11
Pos. control
Column

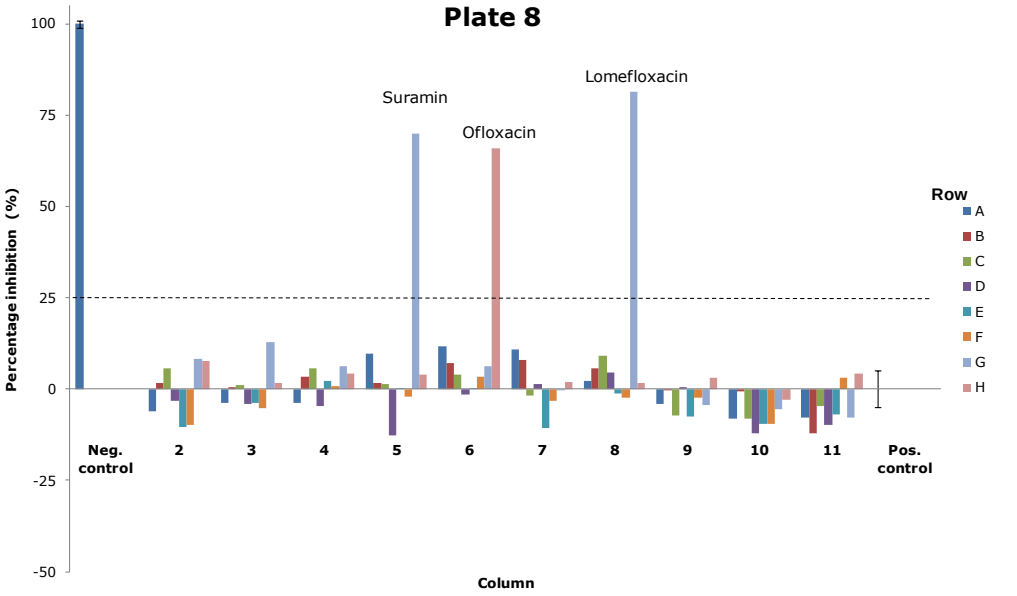
Plate 8
Suramin
Ofloxacin
Lomefloxacin
Percentage inhibition (%)
Row
A
B
C
D
E
F
G
H
Neg. control
Pos. control
Column

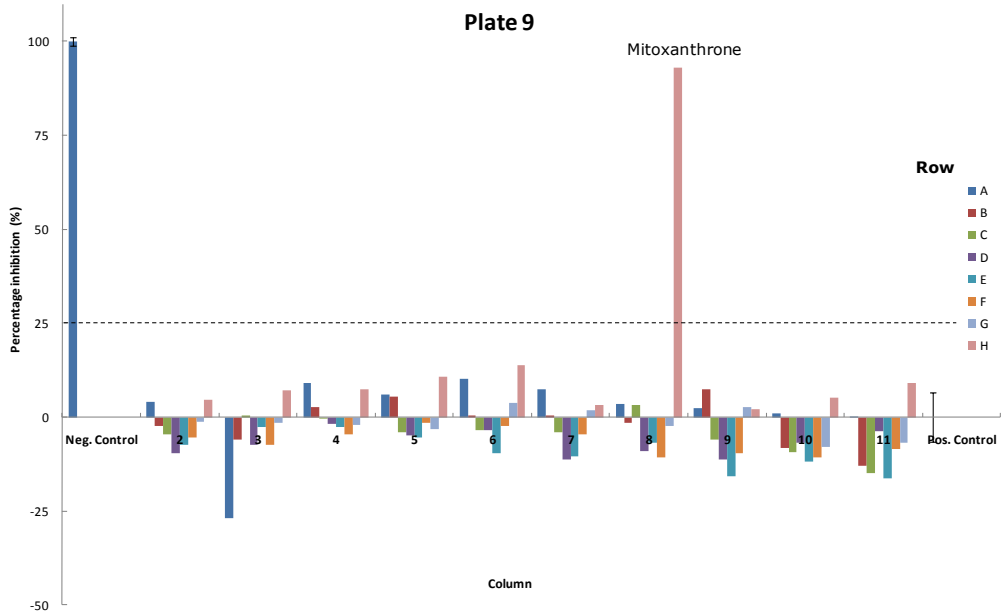
Plate 9
Mitoxanthrone
Percentage inhibition (%)
Row
Neg. Control
Pos. Control
Column

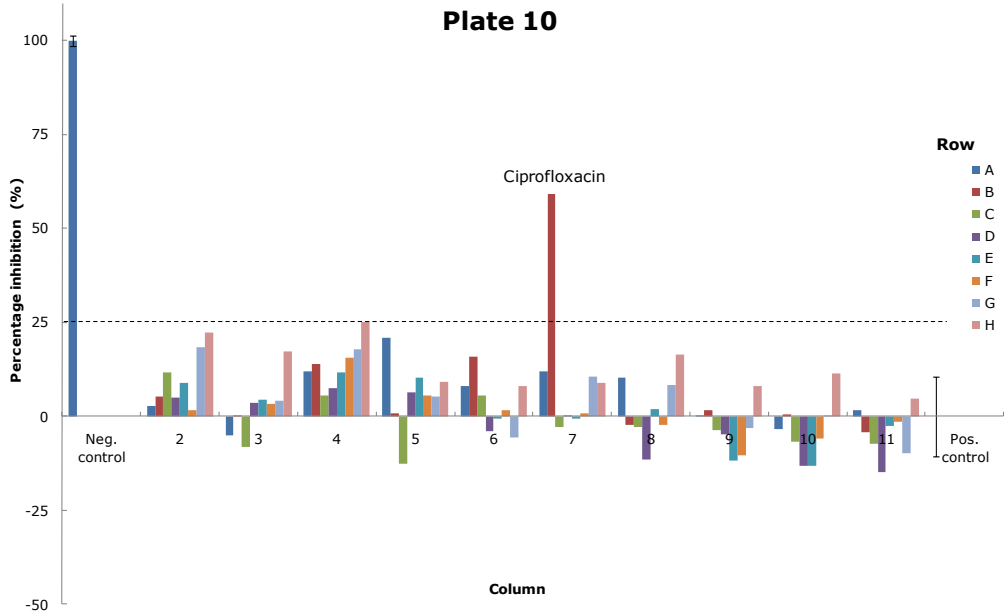
Plate 10
Ciprofloxacin
Percentage inhibition (%)
Row
Neg. control
Pos. control
Column

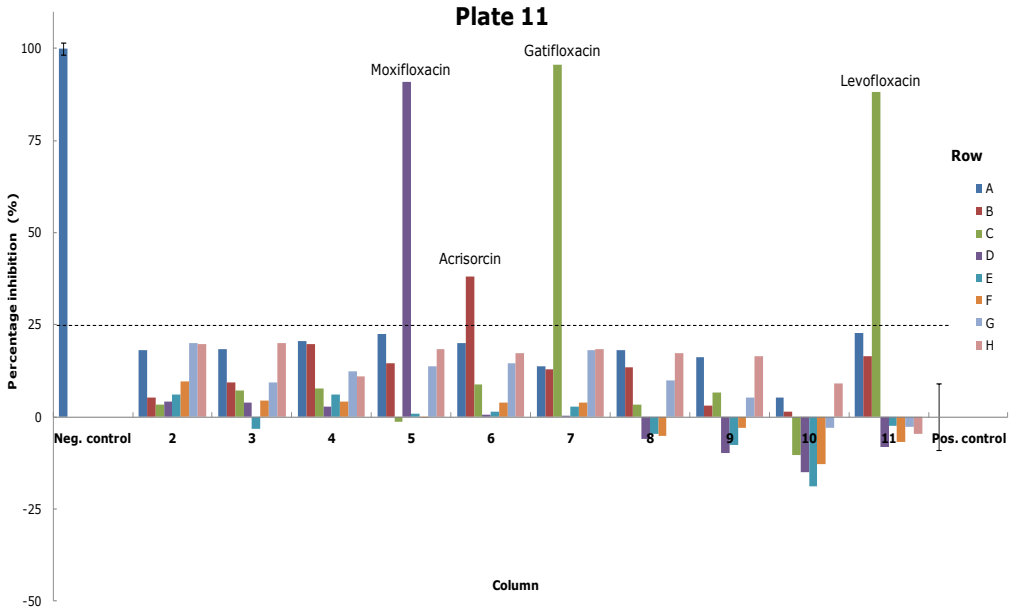
Plate 11
Moxifloxacin
Gatifloxacin
Levofloxacin
Acrisorcin
Row
A
B
C
D
E
F
G
H
Percentage inhibition (%)
100
75
50
25
0
-25
-50
Neg. control
2
3
4
5
6
7
8
9
10
11
Pos. control
Column

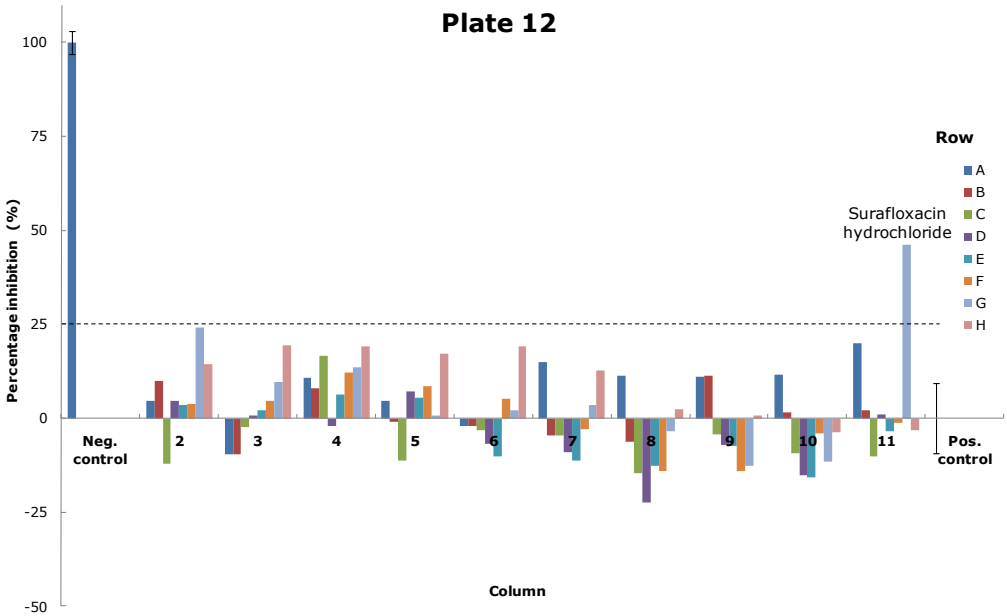
Plate 12
Row
A
B
C
D
E
F
G
H
Surafloxacin hydrochloride
Percentage inhibition (%)
100
75
50
25
0
-25
-50
Neg. control
2
3
4
5
6
7
8
9
10
11
Pos. control
Column

7.2.2 *M. mazei* topoisomerase VI screen

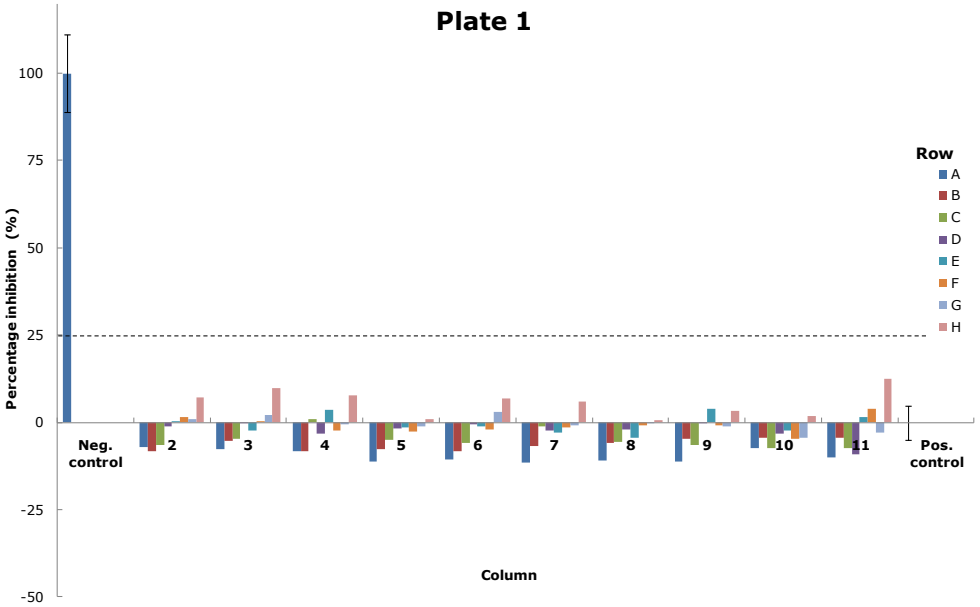

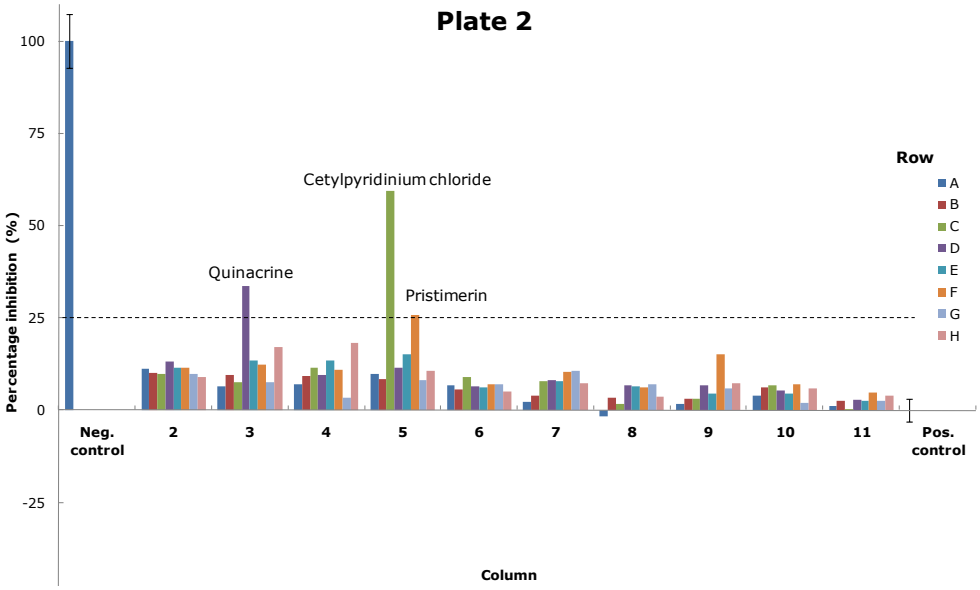

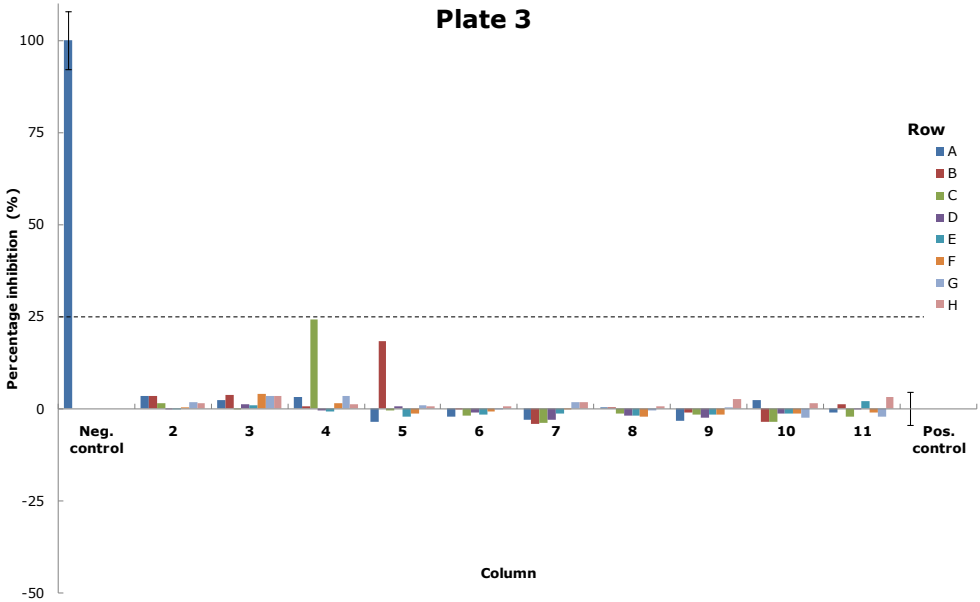

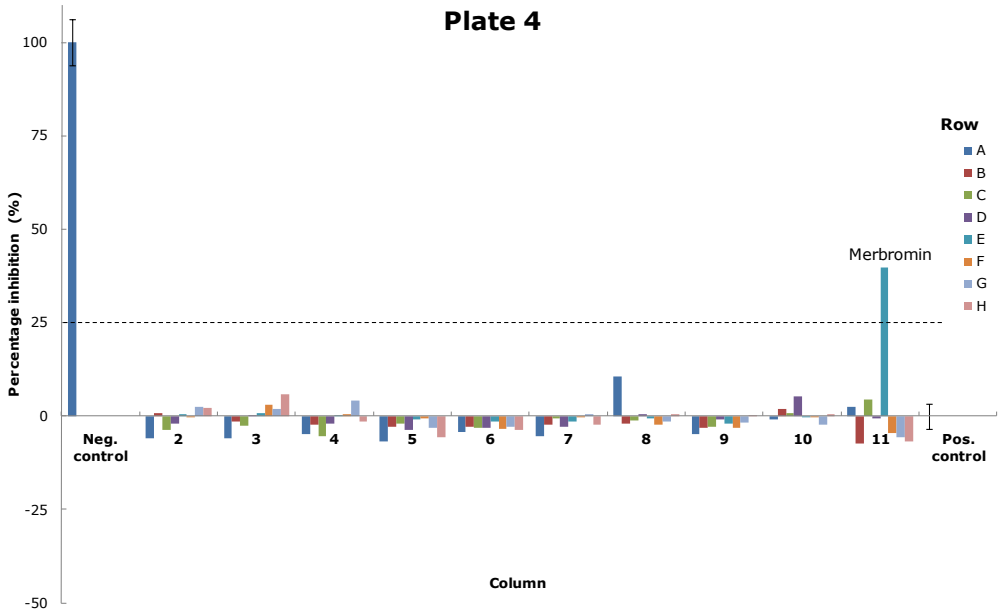
Plate 4
Percentage inhibition (%)
100
75
50
25
0
-25
-50
Merbromin
Row
A
B
C
D
E
F
G
H
Neg. control
2
3
4
5
6
7
8
9
10
11
Pos. control
Column

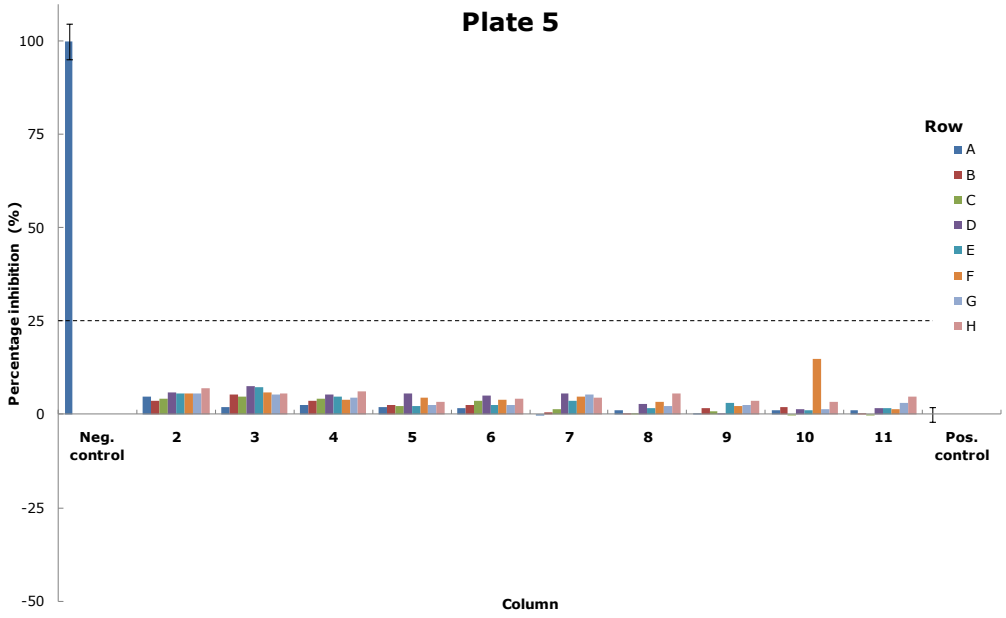
Plate 5
Percentage inhibition (%)
100
75
50
25
0
-25
-50
Row
A
B
C
D
E
F
G
H
Neg. control
2
3
4
5
6
7
8
9
10
11
Pos. control
Column

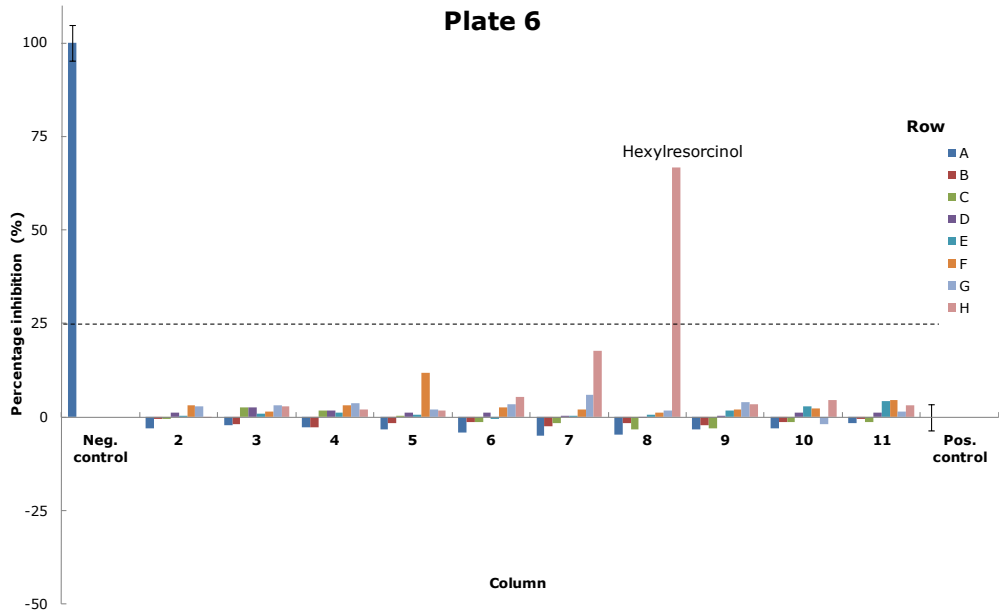
Plate 6
Percentage inhibition (%)
100
75
50
25
0
-25
-50
Hexylresorcinol
Row
A
B
C
D
E
F
G
H
Neg. control
2
3
4
5
6
7
8
9
10
11
Pos. control
Column

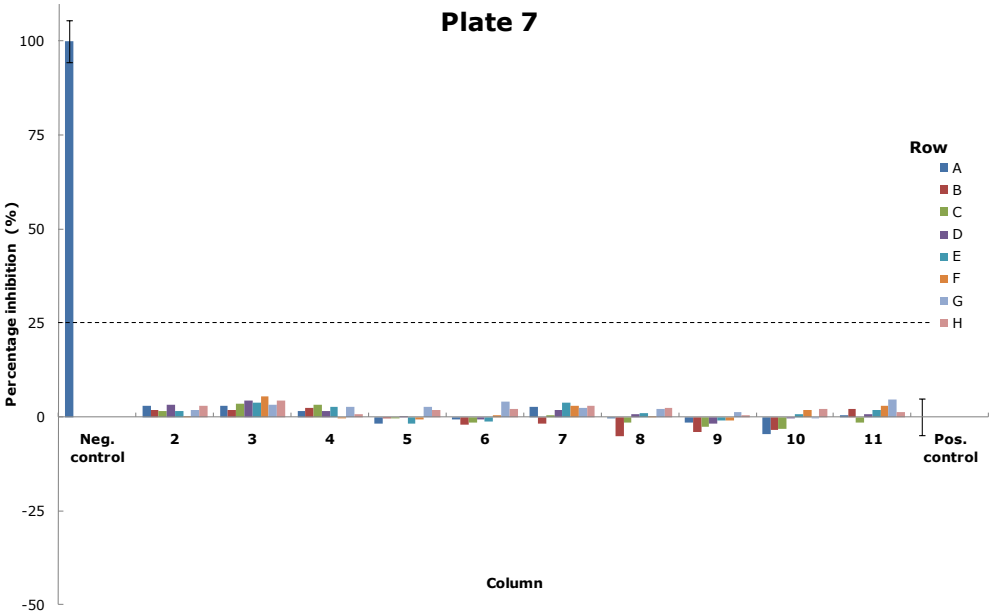
Plate 7
Percentage inhibition (%)
100
75
50
25
0
-25
-50
Row
A
B
C
D
E
F
G
H
Neg. control
2
3
4
5
6
7
8
9
10
11
Pos. control
Column

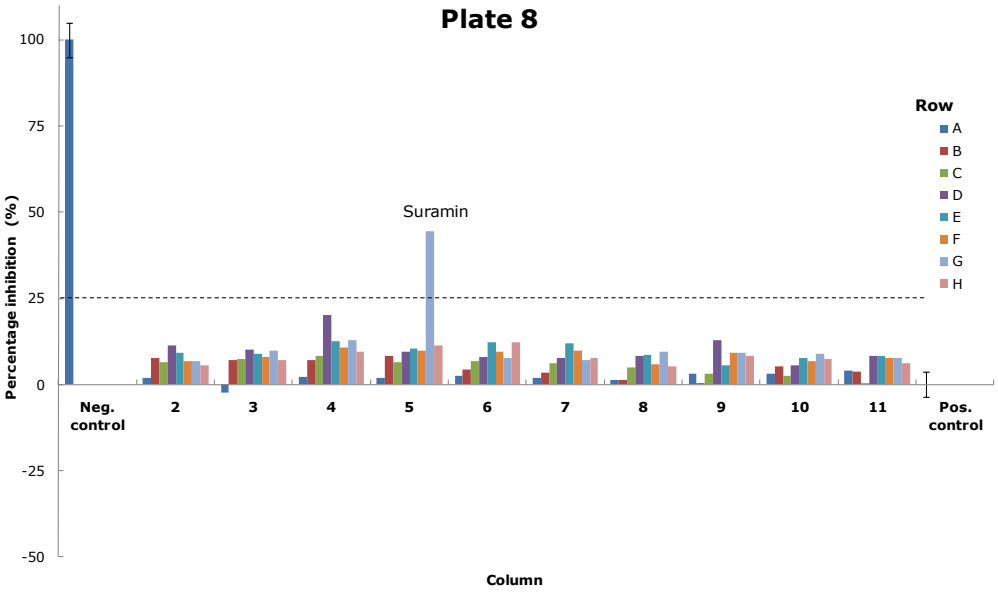
Plate 8
Percentage inhibition (%)
100
75
50
25
0
-25
-50
Suramin
Row
A
B
C
D
E
F
G
H
Neg. control
2
3
4
5
6
7
8
9
10
11
Pos. control
Column

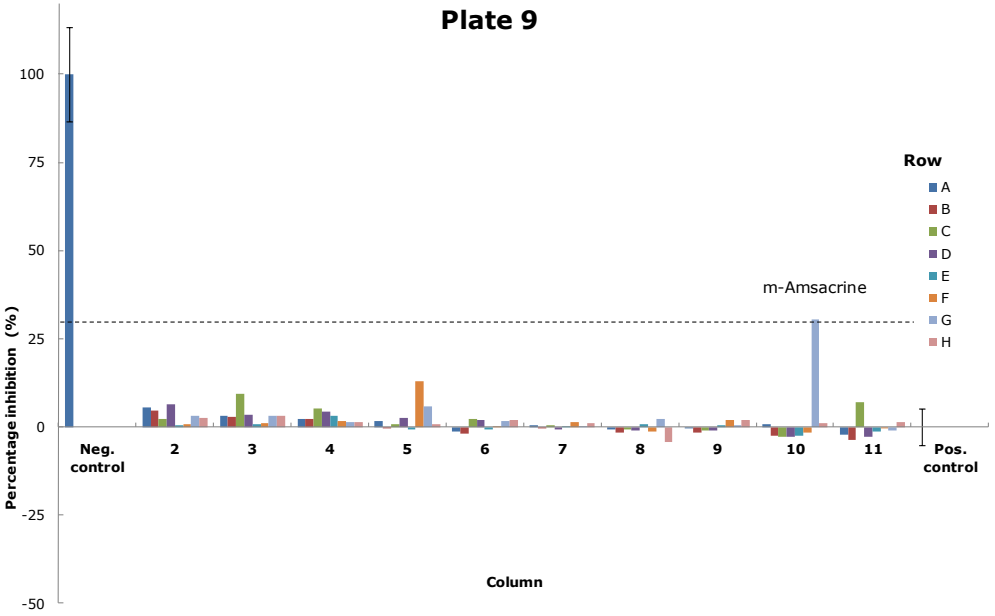
Plate 9
Percentage inhibition (%)
100
75
50
25
0
-25
-50
m-Amsacrine
Row
A
B
C
D
E
F
G
H
Neg. control
2
3
4
5
6
7
8
9
10
11
Pos. control
Column

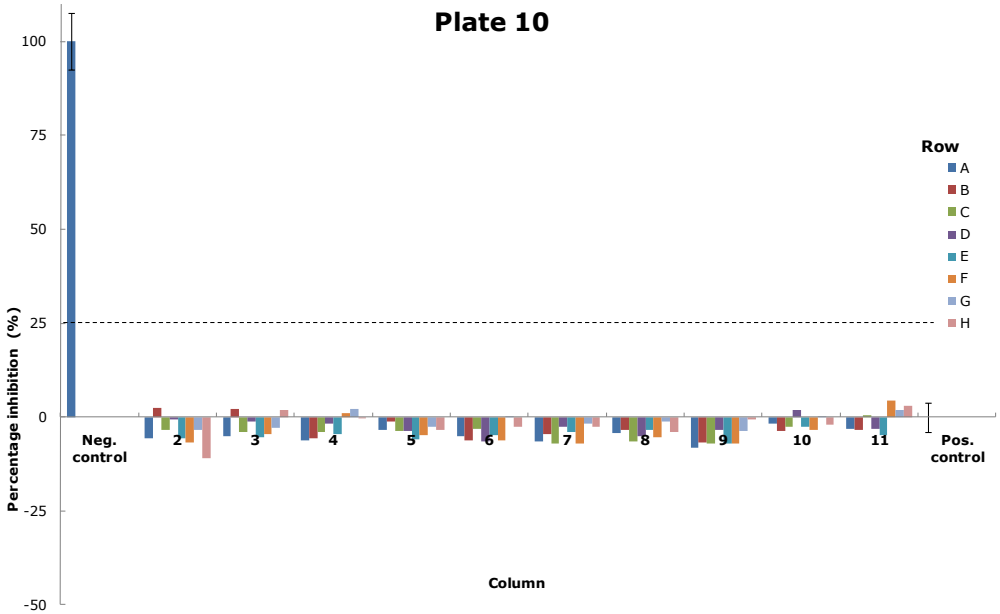
Plate 10
Percentage inhibition (%)
100
75
50
25
0
-25
-50
Neg. control
2
3
4
5
6
7
8
9
10
11
Pos. control
Column
Row
A
B
C
D
E
F
G
H

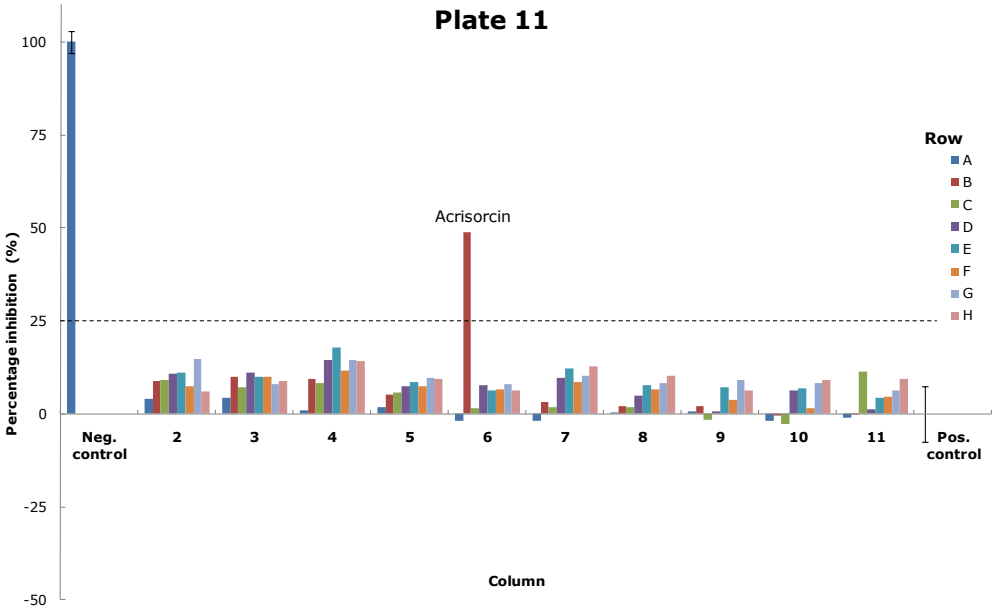
Plate 11
Percentage inhibition (%)
100
75
50
25
0
-25
-50
Acrisorcin
Neg. control
2
3
4
5
6
7
8
9
10
11
Pos. control
Column
Row
A
B
C
D
E
F
G
H

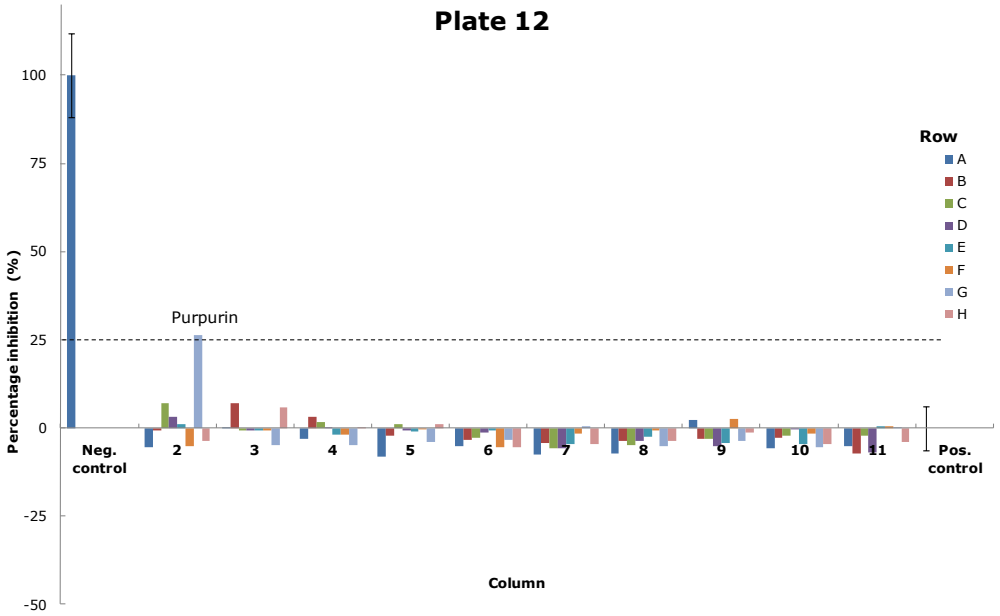
Plate 12
Percentage inhibition (%)
100
75
50
25
0
-25
-50
Purpurin
Neg. control
2
3
4
5
6
7
8
9
10
11
Pos. control
Column
Row
A
B
C
D
E
F
G
H

References

Abbracchio MP, Burnstock G, Boeynaems JM, Barnard EA, Boyer JL, Kennedy C, Knight GE, Fumagalli M, Gachet C, Jacobson KA, Weisman GA (2006) International Union of Pharmacology LVIII: update on the P2Y G protein-coupled nucleotide receptors: from molecular mechanisms and pathophysiology to therapy. *Pharmacol Rev* **58:** 281-341

Adams DE, Shekhtman EM, Zechiedrich EL, Schmid MB, Cozzarelli NR (1992) The role of topoisomerase IV in partitioning bacterial replicons and the structure of catenated intermediates in DNA replication. *Cell* **71:** 277-288

Ali JA, Jackson AP, Howells AJ, Maxwell A (1993) The 43-kilodalton N-terminal fragment of the DNA gyrase B protein hydrolyzes ATP and binds coumarin drugs. *Biochemistry* **32:** 2717-2724

Ali JA, Orphanides G, Maxwell A (1995) Nucleotide binding to the 43-kilodalton N-terminal fragment of the DNA gyrase B protein. *Biochemistry* **34:** 9801-9808

Anderle C, Stieger M, Burrell M, Reinelt S, Maxwell A, Page M, Heide L (2008) Biological activities of novel gyrase inhibitors of the aminocoumarin class. *Antimicrob Agents Ch* **52:** 1982-1990

Andersson DI (2003) Persistence of antibiotic resistant bacteria. *Curr Opin Microbiol* **6:** 452-456

Angehrn P, Buchmann S, Funk C, Goetschi E, Gmuender H, Hebeisen P, Kostrewa D, Link H, Luebbers T, Masciadri R, Nielsen J, Reindl P, Ricklin F, Schmitt-Hoffmann A, Theil FP (2004) New antibacterial agents derived from the DNA gyrase inhibitor cyclothialidine. *J Med Chem* **47:** 1487-1513

Aravind L, Iyer LM, Wellems TE, Miller LH (2003) Plasmodium biology: genomic gleanings. *Cell* **115:** 771-785

Aravind L, Leipe DD, Koonin EV (1998) Toprim--a conserved catalytic domain in type IA and II topoisomerases, DnaG-type primases, OLD family nucleases and RecR proteins. *Nucleic Acids Res* **26:** 4205-4213

Asensio JL, Lane AN, Dhesi J, Bergqvist S, Brown T (1998) The contribution of cytosine protonation to the stability of parallel DNA triple helices. *J Mol Biol* **275:** 811-822

Bateman A, Murzin AG, Teichmann SA (1998) Structure and distribution of pentapeptide repeats in bacteria. *Protein Sci* **7:** 1477-1480

Bates AD, Berger JM, Maxwell A (2011) The ancestral role of ATP hydrolysis in type II topoisomerases: prevention of DNA double-strand breaks. *Nucleic Acids Res* **39:** 6327-6339

Bates AD, Maxwell A (1997) DNA topology: Topoisomerases keep it simple. *Curr Biol* **7:** R778-R781

Bates AD, Maxwell A (2005) *DNA Topology*, 2nd edn. Oxford: Oxford University Press.

Bates AD, O'Dea MH, Gellert M (1996) Energy coupling in Escherichia coli DNA gyrase: the relationship between nucleotide binding, strand passage, and DNA supercoiling. *Biochemistry* **35:** 1408-1416

Bax BD, Chan PF, Eggleston DS, Fosberry A, Gentry DR, Gorrec F, Giordano I, Hann MM, Hennessy A, Hibbs M, Huang J, Jones E, Jones J, Brown KK, Lewis CJ, May EW, Saunders MR, Singh O, Spitzfaden CE, Shen C, Shillings A, Theobald AJ, Wohlkonig A, Pearson ND, Gwynn MN (2010) Type IIA topoisomerase inhibition by a new class of antibacterial agents. *Nature* **466:** 935-940

Beal PA, Dervan PB (1991) Second structural motif for recognition of DNA by oligonucleotide-directed triple-helix formation. *Science* **251:** 1360-1363

Belay N, Johnson R, Rajagopal BS, Conway de Macario E, Daniels L (1988) Methanogenic bacteria from human dental plaque. *Appl Environ Microbiol* **54:** 600-603

Belay N, Mukhopadhyay B, Conway de Macario E, Galask R, Daniels L (1990) Methanogenic bacteria in human vaginal samples. *J Clin Microbiol* **28:** 1666-1668

Belova GI, Prasad R, Kozyavkin SA, Lake JA, Wilson SH, Slesarev AI (2001) A type IB topoisomerase with DNA repair activities. *Proc Natl Acad Sci U S A* **98:** 6015-6020

Berger JM (1998) Structure of DNA topoisomerases. *Biochim Biophys Acta* **1400:** 3-18

Berger JM, Gamblin SJ, Harrison SC, Wang JC (1996) Structure and mechanism of DNA topoisomerase II. *Nature* **379:** 225-232

Bergerat A, de Massy B, Gadelle D, Varoutas P-C, Nicolas A, Forterre P (1997) An atypical topoisomerase II from archaea with implications for meiotic recombination. *Nature* **386:** 414-417

Bergerat A, Gadelle D, Forterre P (1994) Purification of a DNA topoisomerase II from the hyperthermophilic archaeon Sulfolobus shibatae. A thermostable enzyme with both bacterial and eucaryal features. *J Biol Chem* **269:** 27663-27669

Bernues J, Beltran R, Casasnovas JM, Azorin F (1989) Structural polymorphism of homopurine--homopyrimidine sequences: the secondary DNA structure adopted by a d(GA.CT)22 sequence in the presence of zinc ions. *EMBO J* **8:** 2087-2094

Blattner FR, Plunkett G, 3rd, Bloch CA, Perna NT, Burland V, Riley M, Collado-Vides J, Glasner JD, Rode CK, Mayhew GF, Gregor J, Davis NW, Kirkpatrick HA, Goeden MA, Rose DJ, Mau B, Shao Y (1997) The complete genome sequence of Escherichia coli K-12. *Science* **277:** 1453-1462

Bojanowski K, Lelievre S, Markovits J, Couprie J, Jacquemin-Sablon A, Larsen AK (1992) Suramin is an inhibitor of DNA topoisomerase II in vitro and in Chinese hamster fibrosarcoma cells. *Proc Natl Acad Sci U S A* **89:** 3025-3029

Boros I, Pósfai G, Venetianer P (1984) High-copy-number derivatives of the plasmid cloning vector pBR322. *Gene* **30:** 257-260

Bradford MM (1976) Rapid and Sensitive Method for Quantitation of Microgram Quantities of Protein Utilizing Principle of Protein-Dye Binding. *Anal Biochem* **72:** 248-254

Breuer C, Stacey NJ, West CE, Zhao Y, Chory J, Tsukaya H, Azumi Y, Maxwell A, Roberts K, Sugimoto-Shirasu K (2007) BIN4, a novel component of the plant DNA topoisomerase VI complex, is required for endoreduplication in Arabidopsis. *Plant Cell* **19:** 3655-3668

Brino L, Urzhumtsev A, Mousli M, Bronner C, Mitschler A, Oudet P, Moras D (2000) Dimerization of Escherichia coli DNA-gyrase B provides a structural mechanism for activating the ATPase catalytic center. *J Biol Chem* **275:** 9468-9475

Brody JR, Calhoun ES, Gallmeier E, Creavalle TD, Kern SE (2004) Ultra-fast high-resolution agarose electrophoresis of DNA and RNA using low-molarity conductive media. *BioTechniques* **37:** 598-602

Brody JR, Kern SE (2004) History and principles of conductive media for standard DNA electrophoresis. *Anal Biochem* **333:** 1-13

Buhler C, Lebbink JH, Bocs C, Ladenstein R, Forterre P (2001) DNA topoisomerase VI generates ATP-dependent double-strand breaks with two-nucleotide overhangs. *J Biol Chem* **276:** 37215-37222

Bumann D (2008) Has nature already identified all useful antibacterial targets? *Curr Opin Microbiol* **11:** 387-392

Burckhardt G, Walter A, Triebel H, Storl K, Simon H, Storl J, Opitz A, Roemer E, Zimmer C (1998) Binding of 2-azaanthraquinone derivatives to DNA and their interference with the activity of DNA topoisomerases in vitro. *Biochemistry* **37:** 4703-4711

Champoux JJ (2001) DNA topoisomerases: Structure, function, and mechanism. *Annu Rev Biochem* **70:** 369-413

Chauhan PM, Srivastava SK (2001) Present trends and future strategy in chemotherapy of malaria. *Curr Med Chem* **8:** 1535-1542

Chavalitshewinkoon P, Wilairat P, Gamage S, Denny W, Figgitt D, Ralph R (1993) Structure-activity relationships and modes of action of 9-anilinoacridines against chloroquine-resistant Plasmodium falciparum in vitro. *Antimicrob Agents Chemother* **37:** 403-406

Chen FM (1991) Intramolecular triplex formation of the purine.purine.pyrimidine type. *Biochemistry* **30:** 4472-4479

Chong CR, Sullivan DJ (2007) New uses for old drugs. *Nature* **448:** 645-646

Contreras A, Maxwell A (1992) gyrB mutations which confer coumarin resistance also affect DNA supercoiling and ATP hydrolysis by Escherichia coli DNA gyrase. *Mol Microbiol* **6:** 1617-1624

Corbett KD, Benedetti P, Berger JM (2007) Holoenzyme assembly and ATP-mediated conformational dynamics of topoisomerase VI. *Nat Struct Mol Biol* **14:** 611-619

Corbett KD, Berger JM (2003a) Emerging Roles for Plant Topoisomerase VI. *Chem Biol* **10:** 107-111

Corbett KD, Berger JM (2003b) Structure of the topoisomerase VI-B subunit: implications for type II topoisomerase mechanism and evolution. *EMBO J* **22:** 151-163

Corbett KD, Berger JM (2004) Structure, molecular mechanisms, and evolutionary relationships in DNA topoisomerases. *Annu Rev Biophys Biomol Struct* **33:** 95-118

Corbett KD, Berger JM (2006) Structural basis for topoisomerase VI inhibition by the anti-Hsp90 drug radicicol. *Nucleic Acids Res* **34:** 4269-4277

Corbett KD, Shultzaberger RK, Berger JM (2004) The C-terminal domain of DNA gyrase A adopts a DNA-bending beta-pinwheel fold. *Proc Natl Acad Sci U S A* **101:** 7293-7298

Costenaro L, Grossmann JG, Ebel C, Maxwell A (2007) Modular structure of the full-length DNA gyrase B subunit revealed by small-angle X-ray scattering. *Structure* **15:** 329-339

Courey AJ (1999) Analysis of altered DNA structures: cruciform DNA. *Methods Mol Biol* **94:** 29-40

Crick FHC (1976) Linking numbers and nucleosomes. *Proc Natl Acad Sci U S A* **73:** 2639–2643

Danquaha MK, Fordea GM (2007) Growth Medium Selection and Its Economic Impact on Plasmid DNA Production. *J Biosci Bioeng* **104:** 490-497

del Castillo I, Vizan JL, Rodriguez-Sainz MC, Moreno F (1991) An unusual mechanism for resistance to the antibiotic coumermycin A1. *Proc Natl Acad Sci U S A* **88:** 8860-8864

DiMasi JA, Hansen RW, Grabowski HG (2003) The price of innovation: new estimates of drug development costs. *J Health Econ* **22:** 151-185

Domagala JM, Hanna LD, Heifetz CL, Hutt MP, Mich TF, Sanchez JP, Solomon M (1986) New structure-activity relationships of the quinolone antibacterials using the target enzyme. The development and application of a DNA gyrase assay. *J Med Chem* **29:** 394-404

Domanico PL, Tse-Dinh YC (1991) Mechanistic studies on E. coli DNA topoisomerase I: Divalent ion effects. *J Inorg Biochem* **42:** 87-96

Dong KC, Berger JM (2007) Structural basis for gate-DNA recognition and bending by type IIA topoisomerases. *Nature* **450:** 1201-1205

Drlica K, Malik M, Kerns RJ, Zhao X (2008) Quinolone-mediated bacterial death. *Antimicrob Agents Chemother* **52:** 385-392

Drlica K, Zhao X (1997) DNA gyrase, topoisomerase IV, and the 4-quinolones. *Microbiol Mol Biol Rev* **61:** 377-392

Dutta R, Inouye M (2000) GHKL, an emergent ATPase/kinase superfamily. *Trends Biochem Sci* **25:** 24-28

Eckburg PB, Bik EM, Bernstein CN, Purdom E, Dethlefsen L, Sargent M, Gill SR, Nelson KE, Relman DA (2005) Diversity of the human intestinal microbial flora. *Science* **308:** 1635-1638

Edwards MJ, Flatman RH, Mitchenall LA, Stevenson CE, Le TB, Clarke TA, McKay AR, Fiedler HP, Buttner MJ, Lawson DM, Maxwell A (2009) A crystal structure of the bifunctional antibiotic simocyclinone D8, bound to DNA gyrase. *Science* **326:** 1415-1418

Edwards MJ, Williams MA, Maxwell A, McKay AR (2011) Mass spectrometry reveals that the antibiotic simocyclinone D8 binds to DNA gyrase in a "bent-over" conformation: evidence of positive cooperativity in binding. *Biochemistry* **50:** 3432-3440

Emmerson AM, Jones AM (2003) The quinolones: decades of development and use. *J Antimicrob Chemother* **51 Suppl 1:** 13-20

Eriksen KR (1961) "Celbenin"-resistant staphylococci. *Ugeskr Laeger* **123:** 384-386

Farooq U, Mahajan RC (2004) Drug resistance in malaria. *J Vector Borne Dis* **41:** 45-53

Felsenfeld G, Davies DR, Rich A (1957) Formation of a three-stranded polynucleotide molecule. *J Am Chem Soc* **79:** 2023-2024

Figgitt D, Denny W, Chavalitshewinkoon P, Wilairat P, Ralph R (1992) In vitro study of anticancer acridines as potential antitrypanosomal and antimalarial agents. *Antimicrob Agents Chemother* **36:** 1644-1647

Finlay GJ, Atwell GJ, Baguley BC (1999) Inhibition of the action of the topoisomerase II poison amsacrine by simple aniline derivatives: evidence for drug-protein interactions. *Oncol Res* **11:** 249-254

Finlay GJ, Wilson WR, Baguley BC (1989) Chemoprotection by 9-aminoacridine derivatives against the cytotoxicity of topoisomerase II-directed drugs. *Eur J Cancer Clin Oncol* **25:** 1695-1701

Fischer PM (2007) Analytical techniques Smarter ways to screen for drug leads. *Curr Opin Chem Biol* **11:** 477-479

Flatman RH, Eustaquio A, Li SM, Heide L, Maxwell A (2006) Structure-activity relationships of aminocoumarin-type gyrase and topoisomerase IV inhibitors obtained by combinatorial biosynthesis. *Antimicrob Agents Ch* **50:** 1136-1142

Flatman RH, Howells AJ, Heide L, Fiedler HP, Maxwell A (2005) Simocyclinone D8, an inhibitor of DNA gyrase with a novel mode of action. *Antimicrob Agents Chemother* **49:** 1093-1100

Fleck SL, Birdsall B, Babon J, Dluzewski AR, Martin SR, Morgan WD, Angov E, Kettleborough CA, Feeney J, Blackman MJ, Holder AA (2003) Suramin and suramin analogues inhibit merozoite surface protein-1 secondary processing and erythrocyte invasion by the malaria parasite Plasmodium falciparum. *J Biol Chem* **278:** 47670-47677

Flick K, Ahuja S, Chene A, Bejarano MT, Chen Q (2004) Optimized expression of Plasmodium falciparum erythrocyte membrane protein 1 domains in Escherichia coli. *Malar J* **3:** 50

Forterre P, Mirambeau G, Jaxel C, Nadal M, Duguet M (1985) High positive supercoiling in vitro catalyzed by an ATP and polyethylene glycol-stimulated topoisomerase from Sulfolobus acidocaldarius. *EMBO J* **4:** 2123-2128

Fox JL (2006) The business of developing antibacterials. *Nat Biotechnol* **24:** 1521-1528

Fox KR (2000) Targeting DNA with triplexes. *Curr Med Chem* **7:** 17-37

Froelich-Ammon SJ, Osheroff N (1995) Topoisomerase Poisons: Harnessing the Dark Side of Enzyme Mechanism. *J Biol Chem* **270:** 21429-21432

Fromme JC, Verdine GL (2002) Structural insights into lesion recognition and repair by the bacterial 8-oxoguanine DNA glycosylase MutM. *Nat Struct Biol* **9:** 544-552

Fu G, Wu J, Zhu D, Hu Y, Bi L, Zhang XE, Wang da C (2009) Crystallization and preliminary crystallographic studies of Mycobacterium tuberculosis DNA gyrase B C-terminal domain, part of the enzyme reaction core. *Acta Crystallogr Sect F Struct Biol Cryst Commun* **65:** 350-352

Fujimoto-Nakamura M, Ito H, Oyamada Y, Nishino T, Yamagishi J (2005) Accumulation of mutations in both gyrB and parE genes is associated with high-level resistance to novobiocin in Staphylococcus aureus. *Antimicrob Agents Chemother* **49:** 3810-3815

Fuller F (1971) The Writhing Number of a Space Curve. *Proc Natl Acad Sci U S A* **68:** 815–819.

Gadelle D, Bocs C, Graille M, Forterre P (2005) Inhibition of archaeal growth and DNA topoisomerase VI activities by the Hsp90 inhibitor radicicol. *Nucleic Acids Res* **33:** 2310-2317

Gadelle D, Filee J, Buhler C, Forterre P (2003) Phylogenomics of type II DNA topoisomerases. *Bioessays* **25:** 232-242

Gadelle D, Graille M, Forterre P (2006) The HSP90 and DNA topoisomerase VI inhibitor radicicol also inhibits human type II DNA topoisomerase. *Biochem Pharmacol* **72:** 1207-1216

Gantt SM, Myung JM, Briones MR, Li WD, Corey EJ, Omura S, Nussenzweig V, Sinnis P (1998) Proteasome inhibitors block development of Plasmodium spp. *Antimicrob Agents Chemother* **42:** 2731-2738

Garcia-Estrada C, Prada CF, Fernandez-Rubio C, Rojo-Vazquez F, Balana-Fouce R (2010) DNA topoisomerases in apicomplexan parasites: promising targets for drug discovery. *Proc Biol Sci* **277:** 1777-1787

Geck P, Nasz I (1983) Concentrated, digestible DNA after hydroxylapatite chromatography with cetylpyridinium bromide precipitation. *Anal Biochem* **135:** 264-268

Gellert M, Fisher LM, O'Dea MH (1979) DNA gyrase: purification and catalytic properties of a fragment of gyrase B protein. *Proc Natl Acad Sci U S A* **76:** 6289-6293

Gellert M, Mizuuchi K, O'Dea MH, Itoh T, Tomizawa JI (1977) Nalidixic acid resistance: a second genetic character involved in DNA gyrase activity. *Proc Natl Acad Sci U S A* **74:** 4772-4776

Gellert M, Mizuuchi K, O'Dea MH, Nash HA (1976) DNA gyrase: an enzyme that introduces superhelical turns into DNA. *Proc Natl Acad Sci U S A* **73:** 3872-3876

Gilbert EJ, Maxwell A (1994) The 24 kDa N-terminal sub-domain of the DNA gyrase B protein binds coumarin drugs. *Mol Microbiol* **12:** 365-373

Gilboa R, Zharkov DO, Golan G, Fernandes AS, Gerchman SE, Matz E, Kycia JH, Grollman AP, Shoham G (2002) Structure of formamidopyrimidine-DNA glycosylase covalently complexed to DNA. *J Biol Chem* **277:** 19811-19816

Goetschi E, Angehrn P, Gmuender H, Hebeisen P, Link H, Masciadri R, Nielsen J (1993) Cyclothialidine and its congeners: a new class of DNA gyrase inhibitors. *Pharmacol Ther* **60:** 367-380

Graille M, Cladiere L, Durand D, Lecointe F, Gadelle D, Quevillon-Cheruel S, Vachette P, Forterre P, van Tilbeurgh H (2008) Crystal structure of an intact type II DNA topoisomerase: insights into DNA transfer mechanisms. *Structure* **16:** 360-370

Greenstein M, Speth JL, Maiese WM (1981) Mechanism of action of cinodine, a glycocinnamoylspermidine antibiotic. *Antimicrob Agents Chemother* **20:** 425-432

Gross CH, Parsons JD, Grossman TH, Charifson PS, Bellon S, Jernee J, Dwyer M, Chambers SP, Markland W, Botfield M, Raybuck SA (2003) Active-site residues of Escherichia coli DNA gyrase required in coupling ATP hydrolysis to DNA supercoiling and amino acid substitutions leading to novobiocin resistance. *Antimicrob Agents Chemother* **47:** 1037-1046

Grote M, Fromme HG (1984) Ultrastructural demonstration of a glycoproteinic surface coat in allergenic pollen grains by combined cetylpyridinium chloride precipitation and silver proteinate staining. *Histochemistry* **81:** 171-176

Grundmann H, Aires-de-Sousa M, Boyce J, Tiemersma E (2006) Emergence and resurgence of meticillin-resistant Staphylococcus aureus as a public-health threat. *Lancet* **368:** 874-885

Hallett P, Grimshaw AJ, Wigley DB, Maxwell A (1990) Cloning of the DNA gyrase genes under tac promoter control: overproduction of the gyrase A and B proteins. *Gene* **93:** 139-142

Hampel KJ, Crosson P, Lee JS (1991) Polyamines favor DNA triplex formation at neutral pH. *Biochemistry* **30:** 4455-4459

Hanvey JC, Shimizu M, Wells RD (1988) Intramolecular DNA triplexes in supercoiled plasmids. *Proc Natl Acad Sci USA* **85:** 6292-6296

Hartung F, Angelis KJ, Meister A, Schubert I, Melzer M, Puchta H (2002a) An archaebacterial topoisomerase homolog not present in other eukaryotes is indispensable for cell proliferation of plants. *Curr Biol* **12:** 1787-1791

Hartung F, Puchta H (2000) Molecular characterisation of two paralogous SPO11 homologues in Arabidopsis thaliana. *Nucleic Acids Res* **28:** 1548-1554

Hartung HP, Gonsette R, Konig N, Kwiecinski H, Guseo A, Morrissey SP, Krapf H, Zwingers T (2002b) Mitoxantrone in progressive multiple sclerosis: a placebo-controlled, double-blind, randomised, multicentre trial. *Lancet* **360:** 2018-2025

Harvey AL (2007) Natural products as a screening resource. *Curr Opin Chem Biol* **11:** 480-484

Heddle JG, Barnard FM, Wentzell LM, Maxwell A (2000) The interaction of drugs with DNA gyrase: A model for the molecular basis of quinolone action. *Nucleos Nucleot Nucl* **19:** 1249-1264

Hegde SS, Vetting MW, Roderick SL, Mitchenall LA, Maxwell A, Takiff HE, Blanchard JS (2005) A fluoroquinolone resistance protein from Mycobacterium tuberculosis that mimics DNA. *Science* **308:** 1480-1483

Higgins NP, Peebles CL, Sugino A, Cozzarelli NR (1978) Purification of subunits of Escherichia coli DNA gyrase and reconstitution of enzymatic activity. *Proc Natl Acad Sci U S A* **75:** 1773-1777

Holdgate GA, Tunnicliffe A, Ward WH, Weston SA, Rosenbrock G, Barth PT, Taylor IW, Pauptit RA, Timms D (1997) The entropic penalty of ordered water accounts for weaker binding of the antibiotic novobiocin to a resistant mutant of DNA gyrase: a thermodynamic and crystallographic study. *Biochemistry* **36:** 9663-9673

Hooper DC (1999) Mechanisms of fluoroquinolone resistance. *Drug Resist Updat* **2:** 38-55

Horowitz DS, Wang JC (1987) Mapping the active site tyrosine of Escherichia coli DNA gyrase. *J Biol Chem* **262:** 5339-5344

Horstmann MA, Hassenpflug WA, zur Stadt U, Escherich G, Janka G, Kabisch H (2005) Amsacrine combined with etoposide and high-dose methylprednisolone as salvage therapy in acute lymphoblastic leukemia in children. *Haematologica* **90:** 1701-1703

Hosoi Y, Matsumoto Y, Enomoto A, Morita A, Green J, Nakagawa K, Naruse K, Suzuki N (2004) Suramin sensitizing cells to ionizing radiation by inactivating DNA-dependent protein kinase. *Radiat Res* **162:** 308-314

Hsiang YH, Lihou MG, Liu LF (1989) Arrest of replication forks by drug-stabilized topoisomerase I-DNA cleavable complexes as a mechanism of cell killing by camptothecin. *Cancer Res* **49:** 5077-5082

Jacoby GA, Chow N, Waites KB (2003) Prevalence of plasmid-mediated quinolone resistance. *Antimicrob Agents Chemother* **47:** 559-562

Johnson PH, Grossman LI (1977) Electrophoresis of DNA in agarose gels. Optimizing separations of conformational isomers of double- and single-stranded DNAs. *Biochemistry* **16:** 4217-4225

Jordan KL, Evans DL, Hall DJ (1999) Purification of supercoiled plasmid DNA. *Method Mol Biol* **94:** 41-49

Kampranis SC, Gormley NA, Tranter R, Orphanides G, Maxwell A (1999) Probing the binding of coumarins and cyclothialidines to DNA gyrase. *Biochemistry* **38:** 1967-1976

Kampranis SC, Maxwell A (1996) Conversion of DNA gyrase into a conventional type II topoisomerase. *Proc Natl Acad Sci U S A* **93:** 14416-14421

Kampranis SC, Maxwell A (1998) Conformational changes in DNA gyrase revealed by limited proteolysis. *J Biol Chem* **273:** 22606-22614

Kikuchi A, Asai K (1984) Reverse gyrase--a topoisomerase which introduces positive superhelical turns into DNA. *Nature* **309:** 677-681

King DE, Malone R, Lilley SH (2000) New classification and update on the quinolone antibiotics. *Am Fam Physician* **61:** 2741-2748

Kirik V, Schrader A, Uhrig JF, Hulskamp M (2007) MIDGET unravels functions of the Arabidopsis topoisomerase VI complex in DNA endoreduplication, chromatin condensation, and transcriptional silencing. *Plant Cell* **19:** 3100-3110

Kirkegaard K, Wang JC (1985) Bacterial DNA topoisomerase I can relax positively supercoiled DNA containing a single-stranded loop. *J Mol Biol* **185:** 625-637

Kock R, Becker K, Cookson B, van Gemert-Pijnen JE, Harbarth S, Kluytmans J, Mielke M, Peters G, Skov RL, Struelens MJ, Tacconelli E, Navarro Torne A, Witte W, Friedrich AW (2010) Methicillin-resistant Staphylococcus aureus (MRSA): burden of disease and control challenges in Europe. *Euro Surveill* **15:** 19688

Kola I, Landis J (2004) Can the pharmaceutical industry reduce attrition rates? *Nat Rev Drug Discov* **3:** 711-715

Korbie DJ, Mattick JS (2008) Touchdown PCR for increased specificity and sensitivity in PCR amplification. *Nat Protoc* **3:** 1452-1456

Kraal JH, Hussain AA, Gregorio SB, Akaho E (1979) Exposure time and the effect of hexylresorcinol on bacterial aggregates. *J Dent Res* **58:** 2125-2131

Krah R, Kozyavkin SA, Slesarev AI, Gellert M (1996) A two-subunit type I DNA topoisomerase (reverse gyrase) from an extreme hyperthermophile. *Proc Natl Acad Sci U S A* **93:** 106-110

Kreuzer KN, Cozzarelli NR (1979) Escherichia-Coli Mutants Thermosensitive for Deoxyribonucleic-Acid Gyrase Subunit-a - Effects on Deoxyribonucleic-

Acid Replication, Transcription, and Bacteriophage Growth. *J Bacteriol* **140:** 424-435

Kreuzer KN, Cozzarelli NR (1980) Formation and resolution of DNA catenanes by DNA gyrase. *Cell* **20:** 245-254

Lam KS (2007) New aspects of natural products in drug discovery. *Trends Microbiol* **15:** 279-289

Laponogov I, Pan XS, Veselkov DA, McAuley KE, Fisher LM, Sanderson MR (2010) Structural basis of gate-DNA breakage and resealing by type II topoisomerases. *PLoS One* **5:** e11338

Laponogov I, Sohi MK, Veselkov DA, Pan XS, Sawhney R, Thompson AW, McAuley KE, Fisher LM, Sanderson MR (2009) Structural insight into the quinolone-DNA cleavage complex of type IIA topoisomerases. *Nat Struct Mol Biol* **16:** 667-669

Le Doan T, Perrouault L, Praseuth D, Habhoub N, Decout JL, Thuong NT, Lhomme J, Helene C (1987) Sequence-specific recognition, photocrosslinking and cleavage of the DNA double helix by an oligo-[alpha]-thymidylate covalently linked to an azidoproflavine derivative. *Nucleic Acids Res* **15:** 7749-7760

Le Page E, Leray E, Edan G (2011) Long-term safety profile of mitoxantrone in a French cohort of 802 multiple sclerosis patients: a 5-year prospective study. *Mult Scler* **17:** 867-875

Lee JS, Johnson DA, Morgan AR (1979) Complexes formed by (pyrimidine)n . (purine)n DNAs on lowering the pH are three-stranded. *Nucleic Acids Res* **6:** 3073-3091

Lepp PW, Brinig MM, Ouverney CC, Palm K, Armitage GC, Relman DA (2004) Methanogenic Archaea and human periodontal disease. *Proc Natl Acad Sci U S A* **101:** 6176-6181

Lesher GY, Froelich EJ, Gruett MD, Bailey JH, Brundage RP (1962) 1,8-Naphthyridine Derivatives. A New Class of Chemotherapeutic Agents. *J Med Pharm Chem* **91:** 1063-1065

Levy SB (1998) The challenge of antibiotic resistance. *Sci Am* **278:** 46-53

Lewis RJ, Singh OM, Smith CV, Skarzynski T, Maxwell A, Wonacott AJ, Wigley DB (1996a) The nature of inhibition of DNA gyrase by the coumarins and the cyclothialidines revealed by X-ray crystallography. *EMBO J* **15:** 1412-1420

Lewis RJ, Tsai FT, Wigley DB (1996b) Molecular mechanisms of drug inhibition of DNA gyrase. *Bioessays* **18:** 661-671

Lilley DM, Chen D, Bowater RP (1996) DNA supercoiling and transcription: topological coupling of promoters. *Q Rev Biophys* **29:** 203-225

Lindsley JE, Wang JC (1993) On the coupling between ATP usage and DNA transport by yeast DNA topoisomerase II. *J Biol Chem* **268:** 8096-8104

Liu LF, Liu CC, Alberts BM (1980) Type II DNA topoisomerases: enzymes that can unknot a topologically knotted DNA molecule via a reversible double-strand break. *Cell* **19:** 697-707

Liu LF, Wang JC (1987) Supercoiling of the DNA template during transcription. *Proc Natl Acad Sci U S A* **84:** 7024-7027

Lockshon D, Morris DR (1983) Positively supercoiled plasmid DNA is produced by treatment of Escherichia coli with DNA gyrase inhibitors. *Nucleic Acids Res* **11:** 2999-3017

Lopez-Lopez R, Langeveld CH, Pizao PE, van Rijswijk RE, Wagstaff J, Pinedo HM, Peters GJ (1994) Effect of suramin on adenylate cyclase and protein kinase C. *Anticancer Drug Des* **9:** 279-290

Lopez SN, Ramallo IA, Sierra MG, Zacchino SA, Furlan RL (2007) Chemically engineered extracts as an alternative source of bioactive natural product-like compounds. *Proc Natl Acad Sci U S A* **104:** 441-444

Mah TF, O'Toole GA (2001) Mechanisms of biofilm resistance to antimicrobial agents. *Trends Microbiol* **9:** 34-39

Martin JH, Kunstmann MP, Barbatschi F, Hertz M, Ellestad GA, Dann M, Redin GS, Dornbush AC, Kuck NA (1978) Glycocinnamoylspermidines, a new class of antibiotics. II. Isolation, physiocochemical and biological properties of LL-BM123beta, gamma1 and gamma2. *J Antibiot (Tokyo)* **31:** 398-404

Maxwell A, Burton NP, O'Hagan N (2006) High-throughput assays for DNA gyrase and other topoisomerases. *Nucleic Acids Res* **34:** e104

Maxwell A, Howells AJ (1999) Overexpression and purification of bacterial DNA gyrase. In *DNA Topoisomerase Protocols I. DNA Topology and Enzymes*, Bjornsti M-A, Osheroff N (eds), pp 135-144. Totowa, New Jersey: Humana Press

Maxwell A, Lawson DM (2003) The ATP-binding site of type II topoisomerases as a target for antibacterial drugs. *Curr Top Med Chem* **3:** 283-303

Mehlin C, Boni E, Buckner FS, Engel L, Feist T, Gelb MH, Haji L, Kim D, Liu C, Mueller N, Myler PJ, Reddy JT, Sampson JN, Subramanian E, Van Voorhis WC, Worthey E, Zucker F, Hol WG (2006) Heterologous expression of proteins from Plasmodium falciparum: results from 1000 genes. *Mol Biochem Parasitol* **148:** 144-160

Mizuuchi K, Fisher LM, O'Dea MH, Gellert M (1980) DNA gyrase action involves the introduction of transient double-strand breaks into DNA. *Proc Natl Acad Sci U S A* **77:** 1847-1851

Mizuuchi K, O'Dea MH, Gellert M (1978) DNA gyrase: subunit structure and ATPase activity of the purified enzyme. *Proc Natl Acad Sci U S A* **75:** 5960-5963

Moore K, Rees S (2001) Cell-based versus isolated target screening: how lucky do you feel? *J Biomol Screen* **6:** 69-74

Morais Cabral JH, Jackson AP, Smith CV, Shikotra N, Maxwell A, Liddington RC (1997) Crystal structure of the breakage-reunion domain of DNA gyrase. *Nature* **388:** 903-906

Moser HE, Dervan PB (1987) Sequence-specific cleavage of double helical DNA by triple helix formation. *Science* **238:** 645-650

Murashige T, Skoog F (1962) A Revised Medium for Rapid Growth and Bio Assays with Tobacco Tissue Cultures. *Physiol Plantarum* **15:** 473-&

Nakada N, Gmunder H, Hirata T, Arisawa M (1994) Mechanism of inhibition of DNA gyrase by cyclothialidine, a novel DNA gyrase inhibitor. *Antimicrob Agents Chemother* **38:** 1966-1973

Nakada N, Gmunder H, Hirata T, Arisawa M (1995) Characterization of the binding site for cyclothialidine on the B subunit of DNA gyrase. *J Biol Chem* **270:** 14286-14291

Nakada N, Shimada H, Hirata T, Aoki Y, Kamiyama T, Watanabe J, Arisawa M (1993) Biological characterization of cyclothialidine, a new DNA gyrase inhibitor. *Antimicrob Agents Chemother* **37:** 2656-2661

Nakamura N, Lin HC, McSweeney CS, Mackie RI, Gaskins HR (2010) Mechanisms of Microbial Hydrogen Disposal in the Human Colon and Implications for Health and Disease. *Annu Rev Food Sci T* **1:** 363-395

Nakasu S, Kikuchi A (1985) Reverse gyrase; ATP-dependent type I topoisomerase from Sulfolobus. *EMBO J* **4:** 2705-2710

Nelson EM, Tewey KM, Liu LF (1984) Mechanism of antitumor drug action: poisoning of mammalian DNA topoisomerase II on DNA by 4'-(9-acridinylamino)-methanesulfon-m-anisidide. *Proc Natl Acad Sci U S A* **81:** 1361-1365

Nichols MD, DeAngelis K, Keck JL, Berger JM (1999) Structure and function of an archaeal topoisomerase VI subunit with homology to the meiotic recombination factor Spo11. *EMBO J* **18:** 6177-6188

Nierman MM (1961) Akrinol, a new topical anti-infective agent. *J Indiana State Med Assoc* **54:** 614-617

Noble CG, Maxwell A (2002) The role of GyrB in the DNA cleavage-religation reaction of DNA gyrase: a proposed two metal-ion mechanism. *J Mol Biol* **318:** 361-371

Nollmann M, Crisona NJ, Arimondo PB (2007) Thirty years of Escherichia coli DNA gyrase: from in vivo function to single-molecule mechanism. *Biochimie* **89:** 490-499

Oram M, Dosanjh B, Gormley NA, Smith CV, Fisher LM, Maxwell A, Duncan K (1996) Mode of action of GR122222X, a novel inhibitor of bacterial DNA gyrase. *Antimicrob Agents Chemother* **40:** 473-476

Osburne MS (1995) Characterization of a cinodine-resistant mutant of Escherichia coli. *J Antibiot (Tokyo)* **48:** 1359-1361

Osburne MS, Maiese WM, Greenstein M (1990) In vitro inhibition of bacterial DNA gyrase by cinodine, a glycocinnamoylspermidine antibiotic. *Antimicrob Agents Chemother* **34:** 1450-1452

Owen MD, Zelaya IA (2005) Herbicide-resistant crops and weed resistance to herbicides. *Pest Manag Sci* **61:** 301-311

Payne DJ, Gwynn MN, Holmes DJ, Pompliano DL (2007) Drugs for bad bugs: confronting the challenges of antibacterial discovery. *Nat Rev Drug Discov* **6:** 29-40

Pelish HE, Westwood NJ, Feng Y, Kirchhausen T, Shair MD (2001) Use of biomimetic diversity-oriented synthesis to discover galanthamine-like molecules with biological properties beyond those of the natural product. *J Am Chem Soc* **123:** 6740-6741

Pierrat OA, Maxwell A (2005) Evidence for the role of DNA strand passage in the mechanism of action of microcin B17 on DNA gyrase. *Biochemistry* **44:** 4204-4215

Postow L, Crisona NJ, Peter BJ, Hardy CD, Cozzarelli NR (2001) Topological challenges to DNA replication: conformations at the fork. *Proc Natl Acad Sci U S A* **98:** 8219-8226

Preet R, Mohapatra P, Mohanty S, Sahu SK, Choudhuri T, Wyatt MD, Kundu CN (2011) Quinacrine has anti-cancer activity in breast cancer cells through inhibition of topoisomerase activity. *Int J Cancer*

Projan SJ (2007) (Genome) Size Matters. *Antimicrob Agents Chemother* **51:** 1133-1134

Pruss GJ, Drlica K (1986) Topoisomerase I mutants: the gene on pBR322 that encodes resistance to tetracycline affects plasmid DNA supercoiling. *Proc Natl Acad Sci U S A* **83:** 8952-8956

Raghu Ram EV, Kumar A, Biswas S, Chaubey S, Siddiqi MI, Habib S (2007) Nuclear gyrB encodes a functional subunit of the Plasmodium falciparum

gyrase that is involved in apicoplast DNA replication. *Mol Biochem Parasitol* **154:** 30-39

Reece RJ, Maxwell A (1989) Tryptic fragments of the Escherichia coli DNA gyrase A protein. *J Biol Chem* **264:** 19648-19653

Rice LB (2003) Do we really need new anti-infective drugs? *Curr Opin Pharmacol* **3:** 459-463

Richter SN, Frasson I, Palumbo M, Sissi C, Palu G (2010) Simocyclinone D8 turns on against Gram-negative bacteria in a clinical setting. *Bioorg Med Chem Lett* **20:** 1202-1204

Ripley LS (1994) Deletion and duplication sequences induced in CHO cells by teniposide (VM-26), a topoisomerase II targeting drug, can be explained by the processing of DNA nicks produced by the drug-topoisomerase interaction. *Mutat Res* **312:** 67-78

Roca J, Berger JM, Harrison SC, Wang JC (1996) DNA transport by a type II topoisomerase: direct evidence for a two-gate mechanism. *Proc Natl Acad Sci U S A* **93:** 4057-4062

Roca J, Wang JC (1992) The capture of a DNA double helix by an ATP-dependent protein clamp: a key step in DNA transport by type II DNA topoisomerases. *Cell* **71:** 833-840

Roca J, Wang JC (1994) DNA transport by a type II DNA topoisomerase: Evidence in favor of a two-gate mechanism. *Cell* **77:** 609-616

Roccarina D, Lauritano EC, Gabrielli M, Franceschi F, Ojetti V, Gasbarrini A (2010) The role of methane in intestinal diseases. *Am J Gastroenterol* **105:** 1250-1256

Rodriguez AC (2003) Investigating the role of the latch in the positive supercoiling mechanism of reverse gyrase. *Biochemistry* **42:** 5993-6004

Rougee M, Faucon B, Mergny JL, Barcelo F, Giovannangeli C, Garestier T, Helene C (1992) Kinetics and thermodynamics of triple-helix formation: effects of ionic strength and mismatches. *Biochemistry* **31:** 9269-9278

Ruiz N, Falcone B, Kahne D, Silhavy TJ (2005) Chemical conditionality: A genetic strategy to probe organelle assembly. *Cell* **121:** 307-317

Ruiz N, Kahne D, Silhavy TJ (2006) Advances in understanding bacterial outer-membrane biogenesis. *Nat Rev Microbiol* **4:** 57-66

Ruthenburg AJ, Graybosch DM, Huetsch JC, Verdine GL (2005) A superhelical spiral in the Escherichia coli DNA gyrase A C-terminal domain imparts unidirectional supercoiling bias. *J Biol Chem* **280:** 26177-26184

Sadiq AA, Patel MR, Jacobson BA, Escobedo M, Ellis K, Oppegard LM, Hiasa H, Kratzke RA (2010) Anti-proliferative effects of simocyclinone D8 (SD8), a novel catalytic inhibitor of topoisomerase II. *Invest New Drugs* **28:** 20-25

Sakamoto N, Akasaka K, Yamamoto T, Shimada H (1996) A triplex DNA structure of the polypyrimidine:polypurine stretch in the 5′ flanking region of the sea urchin arylsulfatase gene. *Zoolog Sci* **13:** 105-109

Sander M, Hsieh T (1983) Double strand DNA cleavage by type II DNA topoisomerase from Drosophila melanogaster. *J Biol Chem* **258:** 8421-8428

Saravolatz LD, Leggett J (2003) Gatifloxacin, gemifloxacin, and moxifloxacin: the role of 3 newer fluoroquinolones. *Clin Infect Dis* **37:** 1210-1215

Sawitzke JA, Austin S (2000) Suppression of chromosome segregation defects of Escherichia coli muk mutants by mutations in topoisomerase I. *Proc Natl Acad Sci U S A* **97:** 1671-1676

Schimana J, Fiedler HP, Groth I, Sussmuth R, Beil W, Walker M, Zeeck A (2000) Simocyclinones, novel cytostatic angucyclinone antibiotics produced by Streptomyces antibioticus Tu 6040. I. Taxonomy, fermentation, isolation and biological activities. *J Antibiot (Tokyo)* **53:** 779-787

Schluep T, Cooney CL (1998) Purification of plasmids by triplex affinity interaction. *Nucleic Acids Res* **26:** 4524-4528

Schluep T, Cooney CL (1999) Immobilization of oligonucleotides on a large pore support for plasmid purification by triplex affinity interaction. *Bioseparation* **7:** 317-326

Schoeffler AJ, Berger JM (2008) DNA topoisomerases: harnessing and constraining energy to govern chromosome topology. *Q Rev Biophys* **41:** 41-101

Schrappe M (2010) Mitoxantrone in first-relapse paediatric ALL: the ALL R3 trial. *Lancet* **376:** 1968-1970

Schvartzman JB, Stasiak A (2004) A topological view of the replicon. *EMBO Rep* **5:** 256-261

Serre L, Pereira de Jesus K, Boiteux S, Zelwer C, Castaing B (2002) Crystal structure of the Lactococcus lactis formamidopyrimidine-DNA glycosylase bound to an abasic site analogue-containing DNA. *EMBO J* **21:** 2854-2865

Shaner DL, Lindenmeyer RB, Ostlie MH (2011) What have the mechanisms of resistance to glyphosate taught us? *Pest Manag Sci*

Shibata T, Nakasu S, Yasui K, Kikuchi A (1987) Intrinsic DNA-dependent ATPase activity of reverse gyrase. *J Biol Chem* **262:** 10419-10421

Singleton SF, Dervan PB (1992) Influence of pH on the equilibrium association constants for oligodeoxyribonucleotide-directed triple helix formation at single DNA sites. *Biochemistry* **31:** 10995-11003

Singleton SF, Dervan PB (1993) Equilibrium association constants for oligonucleotide-directed triple helix formation at single DNA sites: linkage to cation valence and concentration. *Biochemistry* **32:** 13171-13179

Sittie AA, Lemmich E, Olsen CE, Hviid L, Kharazmi A, Nkrumah FK, Christensen SB (1999) Structure-activity studies: in vitro antileishmanial and antimalarial activities of anthraquinones from Morinda lucida. *Planta Med* **65:** 259-261

Slesarev AI, Stetter KO, Lake JA, Gellert M, Krah R, Kozyavkin SA (1993) DNA topoisomerase V is a relative of eukaryotic topoisomerase I from a hyperthermophilic prokaryote. *Nature* **364:** 735-737

Smith PJ, Morgan SA, Fox ME, Watson JV (1990) Mitoxantrone-DNA binding and the induction of topoisomerase II associated DNA damage in multi-drug resistant small cell lung cancer cells. *Biochem Pharmacol* **40:** 2069-2078

Spellberg B (2008) Dr. William H. Stewart: mistaken or maligned? *Clin Infect Dis* **47:** 294

Spellberg B, Powers JH, Brass EP, Miller LG, Edwards JE, Jr. (2004) Trends in antimicrobial drug development: implications for the future. *Clin Infect Dis* **38:** 1279-1286

Stein CA (1993) Suramin: a novel antineoplastic agent with multiple potential mechanisms of action. *Cancer Res* **53:** 2239-2248

Stettler UH, Weber H, Koller T, Weissmann C (1979) Preparation and characterization of form V DNA, the duplex DNA resulting from association of complementary, circular single-stranded DNA. *J Mol Biol* **131:** 21-40

Stewart L, Redinbo MR, Qiu X, Hol WG, nbsp, J, Champoux JJ (1998) A Model for the Mechanism of Human Topoisomerase I. *Science* **279:** 1534-1541

Stuchinskaya T, Mitchenall LA, Schoeffler AJ, Corbett KD, Berger JM, Bates AD, Maxwell A (2009) How do type II topoisomerases use ATP hydrolysis to simplify DNA topology beyond equilibrium? Investigating the relaxation reaction of nonsupercoiling type II topoisomerases. *J Mol Biol* **385:** 1397-1408

Studier FW, Moffatt BA (1986) Use of bacteriophage T7 RNA polymerase to direct selective high-level expression of cloned genes. *J Mol Biol* **189:** 113-130

Stupina VA, Wang JC (2005) Viability of Escherichia coli topA mutants lacking DNA topoisomerase I. *J Biol Chem* **280:** 355-360

Sturm A, Heussler V (2007) Live and let die: manipulation of host hepatocytes by exoerythrocytic Plasmodium parasites. *Med Microbiol Immunol* **196:** 127-133

Sugimoto-Shirasu K, Roberts GR, Stacey NJ, McCann MC, Maxwell A, Roberts K (2005) RHL1 is an essential component of the plant DNA topoisomerase VI complex and is required for ploidy-dependent cell growth. *Proc Natl Acad Sci U S A* **102:** 18736-18741

Sugimoto-Shirasu K, Roberts K (2003) "Big it up": endoreduplication and cell-size control in plants. *Curr Opin Plant Biol* **6:** 544-553

Sugimoto-Shirasu K, Stacey NJ, Corsar J, Roberts K, McCann MC (2002) DNA topoisomerase VI is essential for endoreduplication in Arabidopsis. *Curr Biol* **12:** 1782-1786

Sugino A, Cozzarelli NR (1980) The intrinsic ATPase of DNA gyrase. *J Biol Chem* **255:** 6299-6306

Sugino A, Higgins NP, Brown PO, Peebles CL, Cozzarelli NR (1978) Energy coupling in DNA gyrase and the mechanism of action of novobiocin. *Proc Natl Acad Sci U S A* **75:** 4838-4842

Sugino A, Peebles CL, Kreuzer KN, Cozzarelli NR (1977) Mechanism of action of nalidixic acid: purification of Escherichia coli nalA gene product and its relationship to DNA gyrase and a novel nicking-closing enzyme. *Proc Natl Acad Sci U S A* **74:** 4767-4771

Sui Y, Wu Z (2007) Alternative statistical parameter for high-throughput screening assay quality assessment. *J Biomol Screen* **12:** 229-234

Sundar S, Jha TK, Thakur CP, Engel J, Sindermann H, Fischer C, Junge K, Bryceson A, Berman J (2002) Oral miltefosine for Indian visceral leishmaniasis. *New Eng J Med* **347:** 1739-1746

Swift LP, Cutts SM, Nudelman A, Levovich I, Rephaeli A, Phillips DR (2008) The cardio-protecting agent and topoisomerase II catalytic inhibitor sobuzoxane enhances doxorubicin-DNA adduct mediated cytotoxicity. *Cancer Chemoth Pharm* **61:** 739-749

Tanaka K, Yamada Y, Shionoya M (2002) Formation of silver(I)-mediated DNA duplex and triplex through an alternative base pair of pyridine nucleobases. *J Am Chem Soc* **124:** 8802-8803

Thadepalli H, Bansal MB, Rao B, See R, Chuah SK, Marshall R, Dhawan VK (1988) Ciprofloxacin: in vitro, experimental, and clinical evaluation. *Rev Infect Dis* **10:** 505-515

Theobald U, Schimana J, Fiedler HP (2000) Microbial growth and production kinetics of Streptomyces antibioticus Tu 6040. *Antonie Van Leeuwenhoek* **78:** 307-313

Thielmann HW, Popanda O, Edler L (1991) The effects of inhibitors of topoisomerase II and quinacrine on ultraviolet-light-induced DNA incision in normal and xeroderma pigmentosum fibroblasts. *J Cancer Res Clin Oncol* **117:** 19-26

Thompson MJ, Louth JC, Little SM, Chen B, Coldham I (2011) 2,4-diarylthiazole antiprion compounds as a novel structural class of antimalarial leads. *Bioorg Med Chem Lett* **21:** 3644-3647

Trefzer A, Pelzer S, Schimana J, Stockert S, Bihlmaier C, Fiedler HP, Welzel K, Vente A, Bechthold A (2002) Biosynthetic gene cluster of simocyclinone, a natural multihybrid antibiotic. *Antimicrob Agents Chemother* **46:** 1174-1182

Tresner HD, Korshalla JH, Fantini AA, Korshalla JD, Kirby JP, Goodman JJ, Kele RA, Shay AJ, Borders DB (1978) Glycocinnamoylspermidines, a new class of antibiotics. I. Description and fermentation of the organism producing the LL-BM123 antibiotics. *J Antibiot (Tokyo)* **31:** 394-397

Tricoli JV, Kowalski D (1983) Topoisomerase I from chicken erythrocytes: purification, characterization, and detection by a deoxyribonucleic acid binding assay. *Biochemistry* **22:** 2025-2031

Tsai FT, Singh OM, Skarzynski T, Wonacott AJ, Weston S, Tucker A, Pauptit RA, Breeze AL, Poyser JP, O'Brien R, Ladbury JE, Wigley DB (1997) The high-resolution crystal structure of a 24-kDa gyrase B fragment from E. coli complexed with one of the most potent coumarin inhibitors, clorobiocin. *Proteins* **28:** 41-52

Tse-Dinh YC (2009) Bacterial topoisomerase I as a target for discovery of antibacterial compounds. *Nucleic Acids Res* **37:** 731-737

Tuteja R (2007) Malaria - an overview. *FEBS J* **274:** 4670-4679

Ulukan H, Swaan PW (2002) Camptothecins: a review of their chemotherapeutic potential. *Drugs* **62:** 2039-2057

Vasquez KM, Glazer PM (2002) Triplex-forming oligonucleotides: principles and applications. *Q Rev Biophys* **35:** 89-107

Wall MK, Mitchenall LA, Maxwell A (2004) Arabidopsis thaliana DNA gyrase is targeted to chloroplasts and mitochondria. *Proc Natl Acad Sci U S A* **101:** 7821-7826

Wang JC (1996) DNA Topoisomerases. *Annu Rev Biochem* **65:** 635-692

Wang JC (1998) Moving one DNA double helix through another by a type II DNA topoisomerase: the story of a simple molecular machine. *Q Rev Biophys* **31:** 107-144

Wang JC (2002) Cellular roles of DNA topoisomerases: a molecular perspective. *Nat Rev Mol Cell Biol* **3:** 430-440

Wethington SL, Wright JD, Herzog TJ (2008) Key role of topoisomerase I inhibitors in the treatment of recurrent and refractory epithelial ovarian carcinoma. *Expert Rev Anticancer Ther* **8:** 819-831

Widdowson K, Hennessy A (2010) Advances in structure-based drug design of novel bacterial topoisomerase inhibitors. *Future Med Chem* **2:** 1619-1622

Wigley DB, Davies GJ, Dodson EJ, Maxwell A, Dodson G (1991) Crystal structure of an N-terminal fragment of the DNA gyrase B protein. *Nature* **351:** 624-629

Wilken A, Janzen R, Holtkamp M, Nowak S, Sperling M, Vogel M, Karst U (2010) Investigation of the interaction of Mercurochrome constituents with proteins using liquid chromatography/mass spectrometry. *Anal Bioanal Chem* **397:** 3525-3532

Williams NL, Maxwell A (1999a) Locking the DNA gate of DNA gyrase: investigating the effects on DNA cleavage and ATP hydrolysis. *Biochemistry* **38:** 14157-14164

Williams NL, Maxwell A (1999b) Probing the two-gate mechanism of DNA gyrase using cysteine cross-linking. *Biochemistry* **38:** 13502-13511

Willmott CJ, Maxwell A (1993) A single point mutation in the DNA gyrase A protein greatly reduces binding of fluoroquinolones to the gyrase-DNA complex. *Antimicrob Agents Chemother* **37:** 126-127

Winter RW, Cornell KA, Johnson LL, Isabelle LM, Hinrichs DJ, Riscoe MK (1995) Hydroxy-Anthraquinones as Antimalarial Agents. *Bioorg Med Chem Lett* **5:** 1927-1932

Wispelwey B, Schafer KR (2010) Fluoroquinolones in the management of community-acquired pneumonia in primary care. *Expert Rev Anti Infect Ther* **8:** 1259-1271

Wohlkonig A, Chan PF, Fosberry AP, Homes P, Huang J, Kranz M, Leydon VR, Miles TJ, Pearson ND, Perera RL, Shillings AJ, Gwynn MN, Bax BD (2010) Structural basis of quinolone inhibition of type IIA topoisomerases and target-mediated resistance. *Nat Struct Mol Biol* **17:** 1152-1153

Worcel A, Burgi E (1972) On the structure of the folded chromosome of Escherichia coli. *J Mol Biol* **71:** 127-147

Yanisch-Perron C, Vieira J, Messing J (1985) Improved M13 phage cloning vectors and host strains: nucleotide sequences of the M13mp18 and pUC19 vectors. *Gene* **33:** 103-119

Yin Y, Cheong H, Friedrichsen D, Zhao Y, Hu J, Mora-Garcia S, Chory J (2002) A crucial role for the putative Arabidopsis topoisomerase VI in plant growth and development. *Proc Natl Acad Sci U S A* **99:** 10191-10196

Yoshida H, Bogaki M, Nakamura M, Nakamura S (1990) Quinolone resistance-determining region in the DNA gyrase gyrA gene of Escherichia coli. *Antimicrob Agents Chemother* **34:** 1271-1272

Zechiedrich EL, Cozzarelli NR (1995) Roles of topoisomerase IV and DNA gyrase in DNA unlinking during replication in Escherichia coli. *Gene Dev* **9:** 2859-2869

Zeugin JA, Hartley JL (1985) Ethanol precipitation of DNA. *Focus* **7:** 1-2

Zhang JH, Chung TD, Oldenburg KR (1999) A simple statistical parameter for use in evaluation and validation of high throughput screening assays. *J Biomol Screen* **4:** 67-73

Zhang Z, Cheng B, Tse-Dinh YC (2011) Crystal structure of a covalent intermediate in DNA cleavage and rejoining by Escherichia coli DNA topoisomerase I. *Proc Natl Acad Sci U S A* **108:** 6939-6944

Zharkov DO, Golan G, Gilboa R, Fernandes AS, Gerchman SE, Kycia JH, Rieger RA, Grollman AP, Shoham G (2002) Structural analysis of an Escherichia coli endonuclease VIII covalent reaction intermediate. *EMBO J* **21:** 789-800

Zhivotovsky B, Kroemer G (2004) Apoptosis and genomic instability. *Nat Rev Mol Cell Biol* **5:** 752-762

Zimmerman SB (2006) Shape and compaction of Escherichia coli nucleoids. *J Struct Biol* **156:** 255-261